

This file is part of the following work:

Yaseen, Madyan Adnan (2019) *Photochemical transformations of quinones under batch and continuous-flow conditions*. PhD Thesis, James Cook University.

Access to this file is available from:

<https://doi.org/10.25903/7785%2Dkx53>

Copyright © 2019 Madyan Adnan Yaseen.

The author has certified to JCU that they have made a reasonable effort to gain permission and acknowledge the owners of any third party copyright material included in this document. If you believe that this is not the case, please email

researchonline@jcu.edu.au

Photochemical Transformations of Quinones under Batch and Continuous– Flow Conditions

PhD Thesis

Madyan Adnan Yaseen (M.Sc.)

December 2019

College of Science and Engineering

James Cook University



Supervisor:

Associate Professor Michael Oelgemöller

Dedicated to my Family & Teachers

Abstract

This thesis aimed to investigate photochemical transformations and to establish flow photochemical operations involving naphthoquinones.

Advancements in drug discovery rely on rapid synthesis tools for initial screening and lead finding. Continuous-flow operations enable rapid optimization of reaction conditions and synthesis of target compounds on site and on demand. Recently, continuous-flow photochemistry has emerged as an advantageous combination of flow operation and light activation. The decrease in path lengths enables efficient penetration of light even for high concentrations of reagents. In addition, the removal of products from the irradiated zone reduces photo-decompositions and improves yields, product qualities and selectivity. By adopting green chemistry principles, this thesis has investigated photoacylations and photocycloadditions of 1,4-naphthoquinones under conventional batch and advanced continuous-flow conditions. The optimized conditions developed offered substantial improvements: they utilized a more selective and practical light source, acetone as a green and low-cost solvent and significantly reduced reaction times. Natural sunlight was likewise investigated as an eco-friendly and sustainable energy source for photochemical activation.

Declaration

I hereby certify that this material, which I now submit for assessment on the program of study leading to the award of Doctor of Philosophy is entirely my own work, that I have exercised reasonable care to ensure that the work is original, and does not to the best of my knowledge breach any law of copyright, and has not been taken from the work of others save and to the extent that such work has been cited and acknowledged within the text of my work.

Signed:

ID No.:

Date: _____

Acknowledgements

This thesis represents the most substantial scientific contribution for me personally. I would thus like to acknowledge and thank the team at JCU for their continuous support throughout my project.

Firstly, I would like to express my sincere gratitude to my incredible supervisor, Associate Professor Michael Oelgemöller. Without his constant inspiring supervision, encouragement and assistance, I would have not been able to complete my work. A simple ‘thank you’ is barely enough to acknowledge his precious time and valuable expertise. Michael feedback and constructive criticism of my work taught me to think more logically. Even when I stumbled across unexpected results, his meaningful feedback was proof of his scientific enthusiasm and professional commitment. The same can be said about his criticism of previously published data. His help and advice was not just beneficial for my current study, but it will be of utmost value in my future research and work in general. I also consider him as a role model when it comes to his academic conscientiousness and professional commitment. Michael’s help was not solely limited to scientific and academic matters, it also extended to private, emotional and even financial levels. During my journey, I faced significant challenges on a personal level and Michael repeatedly presented my case to James Cook University. After the end of my scholarship, JCU was thus very kind to continue to fund my research as well as providing me with the financial assistance necessary to complete my studies. I was blessed having Michael supporting me personally during those difficult times.

Special thanks also goes to my secondary supervisor Dr Mark Robertson for providing me access and assistance in collecting MS- and NMR-data. I also thank Dr Jun Wang and Prof Peter Junk for the X-ray structure analyses.

Warm thanks furthermore go to the College of Science and Engineering, especially Melissa Norton and Rebecca Steele for supporting and assisting with my applications for financial support. The same goes to the helpful staff at the Graduate Research School and the International Office.

I have been very fortunate to experience a diverse, multicultural and friendly lab group with lovely fellows from around the globe. I am thankful to all of them for making my stay enjoyable and I wish them all the best in their future lives. I am especially thankful to Dr Saira Mumtaz, Dr Padmakana Malakar and Hossein Mkhani.

I am also grateful to my homeland and Tikrit University for sponsoring my initial grant and scholarship for advanced studies.

This acknowledgement would be certainly incomplete without showing my sincere gratitude to my family, especially my parents, my lovely wife NuNu and my baby Madyan Junior with their unconditional love and ongoing motivation in order reach this level of achievement. I am glad in meeting their expectations in me and making them proud of me.

List of Abbreviations

^{13}C -NMR	carbon nuclear magnetic resonance
^1H -NMR	proton nuclear magnetic resonance
acetone- d_6	deuterated acetone
CDCl_3	deuterated chloroform
CO_2	carbon dioxide
DCM	dichloromethane
dd	doublet of a doublet
ddd	doublet of a doublet of a doublet
DMSO- d_6	deuterated dimethyl sulfoxide
eq.	equivalents
<i>et al.</i>	et alia (and others)
g	gram
H_2O	distilled water
$\text{H}_{\text{arom.}}$	aromatic proton
hr	hour(s)
$h\nu$	light photon
<i>i</i> -butyl / ^iBu	iso butyl group
IUPAC	Internal Union of Pure and Applied Chemistry
J	coupling constant
m	multiplet
mmol	millimole(s)
nm	nanometres
NMR	nuclear magnetic resonance
$^{\circ}\text{C}$	degrees Celsius
PET	photoinduced electron transfer
Ph	phenyl
ppm	parts per million
s	singlet
t	triplet

<i>t</i> -butyl / ^t Bu	tertiary butyl group
TFT	trifluorotoluene
TLC	thin layer chromatography
UV	ultraviolet
π	pi
σ	sigma

Publication

1. Oelgemöeller, M.; Malakar, P.; Yaseen, M.; Pace, K.; Hunter, R.; Robertson, M., Applied and green photochemical synthesis at James Cook University in Townsville, Australia. *EPA Newsletters* **2017**, 93, 35-41.

Presentations

1. **Oral presentation presentation** “Photo-Friedel-Crafts acylation of 1,4-naphthoquinone under batch and continuous-flow conditions” **M. Yaseen**, M. Oelgemöller *Biology in the tropics - Postgraduate Student Conference 2016, James cook university, Townsville, Australia*.28.-29. September 2016.
2. **Oral and Poster presentation:** “Photochemical transformation of quinones under batch and continuous-flow conditions: A green access to acylated naphtho(hydro)quinones” **M. Yaseen**, M. Oelgemöller, M. Robertson *RACI centenary congress 2017, Melbourne (Australia)*, 23.-28. July 2017.

Curriculum Vitae

Personal data:

Name: Madyan Adnan Yaseen

Date of birth: 26-11-1987

Place of birth: Tikrit (Iraq)

Academic qualifications:

2015-2019 PhD (Organic Chemistry), James Cook University, College of Science and Engineering, Discipline of Chemistry, Townsville, Australia, with Associate Prof. Michael Oelgemöller

Title: Photochemical Transformation of Quinones under Batch and Continuous – Flow Conditions.

2010-2012 M.Sc. (Chemistry), Tikrit University, Department of Chemistry, Tikrit, Iraq

Title: Determination of Atrazine, phenyl urea and 2, 4 -Dichlorophenoxy acetic acid Herbicides by flow Injection Chemiluminescence Technique.

Professional activities:

2015-2019 Laboratory demonstrator, James Cook University, College of Science and Engineering, Discipline of Chemistry, Townsville, Australia

2012-2013 Guest lecturer, University of Tikrit College of education, Department of Chemistry, Tikrit, Iraq

Table of Contents

Abstract	i
Declaration	ii
Acknowledgements	iii
List of Abbreviations.....	v
Publication.....	vii
Presentations.....	vii
Curriculum Vitae.....	viii
1. Introduction.....	2
1.1 Quinone Photochemistry	2
1.2 Photochemistry.....	2
1.3 Photosensitization and photoinduced electron transfer (PET).	5
1.4 Photochemistry of Quinones	6
1.4.1 Photo-Friedel-Crafts Reactions of Quinones	7
1.4.2 Photocycloaddition of Quinones	17
2. Aims.....	26
3. Results.....	28
3.1 Synthesis of starting materials.....	28
3.1.1 Synthesis of 2-acetoxy-1,4-naphthoquinone.	28
3.2 Photochemical transformations	29
3.2.1 Batch chamber reactor.....	29
3.2.2 In-house capillary reactor.....	29
3.2.3 In-house tandem photochemical-thermal capillary reactor	31
3.2.4 Solar batch set-up	31
3.2.5 In-house parabolic trough concentrating solar flow reactor.....	32

3.3	Photoacylations of 1,4-naphthoquinones	33
3.3.1	Photoacylation of 1,4-naphthoquinones under batch conditions	33
3.3.2	Photoacylations of naphthoquinone under continuous flow conditions.....	36
3.3.3	Multistep one-flow reaction	41
3.3.4	Photobisacylation of monoacylated naphthohydroquinone.	43
3.3.5	Attempted synthesis of 2-dodecanoyl-3-hydroxy-1,4-naphthoquinone (DHN) ..	43
3.3.6	Photoacylation of 2-acetoxy-1,4-naphthoquinone	46
3.3.7	Solar photoacylations of 1,4-naphthoquinone.....	48
3.4	[2+2]-Photocycloadditions of 1,4-naphthoquinones	49
3.4.1	Photocycloaddition of 1,4-naphthoquinones under batch conditions	49
3.4.2	Photocycloaddition of naphthoquinone under continuous flow conditions	52
3.4.3	[2+2]-Photocycloadditions of 1,4-naphthoquinone to various alkenes.....	53
3.4.4	Photocycloaddition of 2-acetyloxy-1,4-naphthoquinone under batch conditions	66
3.4.5	Photocycloaddition of 2-acetyloxy-1,4-naphthoquinone under continuous flow conditions	67
3.4.6	Solar [2+2]-photocycloadditions of naphthoquinones	71
3.4.7	Photocycloaddition of 1,4-naphthoquinones with diphenylacetylene.....	72
4.1	Photoacylation of 1,4-naphthoquinones	77
4.1.1	Photoacylation of 1,4-naphthoquinone under batch conditions	77
4.1.2	Photoacylation of naphthoquinone under flow conditions.....	88
4.1.3	One-flow multistep synthesis of acylated 1,4-naphthoquinones.....	92
4.1.4	Attempted photoacylation of 2-hydroxy-1,4-naphthoquinone.....	92
4.1.5	Photoacylations of 2-acetoxy-1,4-naphthoquinone.....	95
4.1.6	Solar photoacylations	95
4.2	[2+2]-Photocycloaddition of naphthoquinones	98
4.2.1	Photocycloaddition of 1,4-naphthoquinones under batch conditions	98
4.2.2	Photocycloaddition of 1,4-naphthoquinone under flow conditions	105
4.2.3	Substrate scope of the photocycloaddition.....	106

4.2.4	Photocycloadditions of 2-acetoxy-1, 4-naphthoquinone.....	109
4.2.5	[2+2]-Photocycloaddition of diphenylacetylene to naphthoquinones.....	111
4.2.6	Solar photocycloaddition of naphthoquinones.....	112
5.	Summary and Outlook	116
5.1	Photo-Friedel-Crafts acylation of naphthoquinone	116
5.2	[2+2] Photocycloaddition of naphthoquinone.....	117
5.3	Outlook.....	118
6.	Experimental.....	121
6.1	General methods.....	121
6.1.1	Solvents and reagents	121
6.1.2	Photochemical equipment	121
6.1.3	Analytical methods.....	121
6.1.4	Chromatographic methods	122
6.2	Synthesis of starting materials.....	122
6.3	Photoacylations of 1,4-naphthoquinones	123
6.3.1	Photoacylations of 1,4-naphthoquinones under batch conditions.....	123
6.3.2	Photoacylations of 1,4-naphthoquinones under continuous-flow conditions	123
6.3.3	Solar photoacylations of 1,4-naphthoquinones under batch conditions.....	123
6.3.4	Solar photoacylations of 1,4-naphthoquinones under continuous-flow conditions 123	
6.3.5	Photochemical transformations	124
6.3.5.1	Synthesis of 1-(1,4-dihydroxynaphthalen-2-yl) propan-1-one (6a)	124
6.3.5.2	Synthesis of 1-(1,4-dihydroxynaphthalen-2-yl) butan-1-one (6b)	124
6.3.5.3	Synthesis of 1-(1,4-dihydroxynaphthalen-2-yl) heptan-1-one (6c).....	126
6.3.5.4	Synthesis of 1-(1,4-dihydroxynaphthalen-2-yl)dodecan-1-one (6d).....	126
6.3.5.5	Synthesis of 1-(1,4-dihydroxynaphthalen-2-yl) buten-1-one (6e)	127
6.3.5.6	Synthesis of (1,4-Dihydroxy-naphthalen-2-yl)-p-tolyl-methanone (6f)	128

6.3.5.7	Synthesis of (1,4-dihydroxy-2-naphthalenyl)bis(<i>p</i> -tolylmethanone) 8f.....	129
6.3.5.8	Synthesis of (4-chlorophenyl)-(1,4-dihydroxynaphthalen-2-yl)-methanone (6g).	131
6.3.5.9	Synthesis of (1,4-dihydroxy-2-naphthalenyl) (furan-2-yl) methanone (6h) ..	132
6.3.5.10	Attempted synthesis of 1-(1, 3, 4-trihydroxyaphthalen-2-yl)butan-1-one (10)	132
6.3.5.11	Synthesis of 7, 7'-dihydroxy-[2, 2'-binaphthalene]-5, 5', 8, 8'tetraone (11)	133
6.3.5.12	Synthesis of 3-butyryl-1,4-dihydroxynaphthalen-2-yl acetate (12)	133
6.3.6	Multistep one-flow reactions.....	134
6.3.6.1	Synthesis of 2-Butyryl-1,4-naphthoquinone (9b).....	135
6.3.6.2	Synthesis of 2-Propionyl-1,4-naphthoquinone (9a)	135
6.3.6.3	Synthesis of 2-undecanoyl-1,4-naphthoquinone (9d)	136
6.3.6.4	Synthesis of 2-crotonyl-1,4-naphthoquinone (9e).....	136
6.4	[2+2]-Photocycloadditions of naphthoquinones	136
6.4.1.	Photocycloadditions of naphthoquinones under batch conditions	136
6.4.2.	Photocycloadditions of naphthoquinones under continuous-flow conditions....	137
6.4.3.	Solar photocycloadditions of naphthoquinones under batch conditions.....	137
6.4.4.	Solar photocycloadditions of naphthoquinones under continuous-flow conditions	137
6.4.5.	Photochemical transformations	137
6.4.5.1.	Synthesis of 1-phenyl-1, 2, 2a, 8a-tetrahydrocyclobuta[b]naphthal-ene-3,8-dione (15a)	137
6.4.5.2.	Synthesis of 2,3,3a,3b,9a,9b-hexahydro-1H-cyclopenta[3,4]cyclobuta[1,2-b]naphthaaalene-4,9-dione (15b).....	139
6.4.5.3.	Synthesis of 1, 1-diphenyl-1, 2, 2a, 8a-tetrahydrocyclobuta[b]naphthalene-3, 8-dione (15c).....	140
6.4.5.4.	Synthesis of 1,2,3,4,4a,4b,10a,10b-octahydrobenzo[b]biphenylene-5,10-dione (15d)	141

6.4.5.5.	Synthesis of 3',4'-diphenyl-4H-spiro[naphthalene-1,2'-oxetan]-4-one (16e)	142
6.4.5.6.	Synthesis of 3,8-dioxo-2-phenyl-1,3,8,8a tetrahydrocyclobuta [b]naphthalene-2a(2H)-yl acetate (17a).....	143
6.4.5.7.	Synthesis of 4,9-dioxo-1,2,3,3a,4,9,9a,9b-octahydro-3bH-cyclopenta-[3,4]cyclobuta[1,2-b]naphthalen-3b-yl acetate (17b).....	144
6.4.5.8.	Synthesis of 3,8-dioxo-2,2-diphenyl-1,3,8,8a-tetrahydrocyclobuta[b]-naphthalen-2a(2H)-yl acetate (17c).	145
6.4.5.9.	Synthesis of 7-benzoyl-4H-benzo[de]anthracen-4-one (19a)	146
6.4.5.10.	Synthesis of 1, 2-diphenylcyclobuta[b]naphthalene-3, 8(2aH, 8aH)-dione (20a). 147	
6.4.5.11.	Synthesis of 7-benzoyl-4-oxo-4H-benzo[de]anthracen-6-yl-acetate (19b)....	148
6.4.5.12.	Synthesis of 3,8-dioxo-1,2-diphenyl-8,8a dihydrocyclobuta[b]naphthalen-2a(3H)-yl acetate (20b).....	149
6.5	X-ray crystallographic data	150
6.6	References	153

Chapter 1: Introduction

1. Introduction

1.1 Quinone Photochemistry

Quinones and their derivative compounds possess electron transfer and hydrogen acceptor properties; in addition the structure of quinones contain cyclic dione system along with two carbonyl groups.¹ Hence, these particular features permit quinones to play an important role in different scopes. For example, in the biologically active series, a large number of derivative quinones contribute to eminent pharmacological advancements, such as antibiotic, antitumor, antimalarial, antineoplastic, anticoagulant, herbicidal activity, and anticancer agents.^{2,3} Many classes of quinones are ubiquitous in nature and found in bacteria, fungi, plants, and even the human body, where they act as an electron transport chain in photosynthesis and protein carboxylation, such as vitamin K, coenzyme, plastoquinones, and the tocopherylquinone group.^{4,5,6} The objective of the present work is to highlight the quinone properties and the phototransformation of quinones (**Figure1.1**).

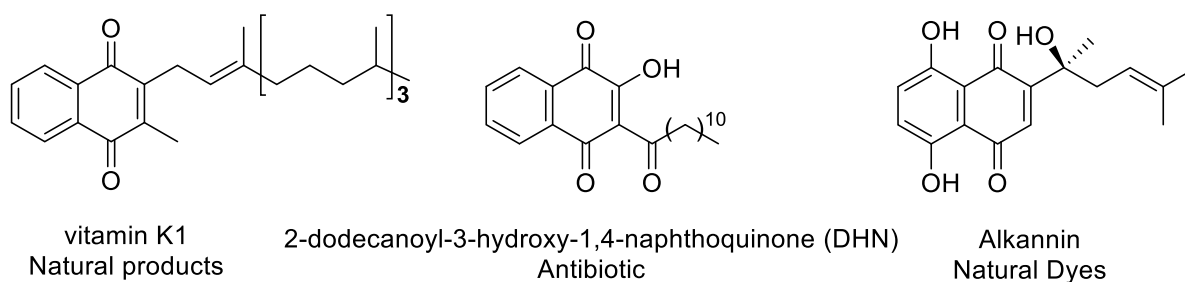


Figure1.1: Examples of quinones.

1.2 Photochemistry

In the mid-19th century, the products of dyes attracted considerable attention in the chemical industry after early endeavours to understand the relationship between the colour and structure of organic compounds.⁷ This led to the concept of *chromophore* and *auxochrome* presented by Witt in 1876.⁸ The last century has seen the emergence of many theories and basic models, such as the conjugation of molecules, colour, and molecular orbital. Forster, Kasha et al delineated the concept of excited states and electronic structure in photochemistry.⁹ Thus, the rapid development of the above considerations led to the IUPAC Recommendations in 1996, defining photochemistry as ‘the discipline of chemistry concerned with the chemical effects of light’.¹⁰ Two laws were adopted in the principles of photochemistry in terms of light change. At the beginning of the nineteenth century, Grotthus and Draper formulated the first law in the quantitative concept in photochemistry; a photochemical change occurs by only a photon that

is absorbed by a molecule.¹¹ Therefore, an effective change generates an electronically excited state (**Figure 1.2**). Stark and Einstein proposed the second law of photochemistry, concerning the photo-equivalence approach between 1908 and 1912. The Stark-Einstein law proclaims that one quantum of a photon is absorbed per molecule of absorbing and reacting substance that disappears.¹¹

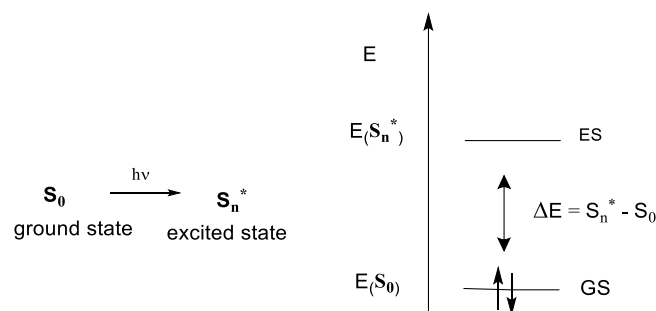


Figure 1.2: Electronic states in a photochemical reaction.

The rate or probability of absorption is expressed by the Lambert-Beer law, which states that there is a linear relationship between the absorbance, path length, and concentration of an absorbing species, which is defined as **Equation 1.1**.¹²

$$A = \epsilon Cl$$

- Molar absorption coefficient, ϵ , in units of $\text{l mol}^{-1} \text{cm}^{-1}$
- Concentration, c , in units of moles per litre, mol l^{-1} .
- Path length, l , in units of centimetres, cm .
- Absorbance, A , has no units because it is a logarithmic quantity.

Equation 1.1: Beer-Lambert law.

The ground state of a molecule is its lowest energy state before excitation. Couples of electrons occupy the lower (bonding) orbitals completely, and the upper (anti-bonding) orbitals remain unoccupied. To excite an electron to a higher energy orbital, a molecule must absorb a photon with sufficient energy, which then excites an electron from the highest occupied molecular orbital (HOMO) to the lowest unoccupied molecular orbital (LUMO) of the ground state.¹²

During the absorption of energy by a molecule, electrons can transfer to the singlet or triplet state. If the two unpaired electrons have opposite spin directions, it is denoted as a singlet state (S_1). On the other hand, if the unpaired electrons have the same spin direction, it is called a triplet state (T_1). Direct electronic transmission between an excited singlet (S_1) to an excited triplet state (T_1) is energetically preferred but forbidden by Wigner's rule. The excited triplet

state can be produced by intersystem crossing (ISC), which allows the excited singlet state to arrive at the lower energy triplet state (**Figure 1.3**).¹³

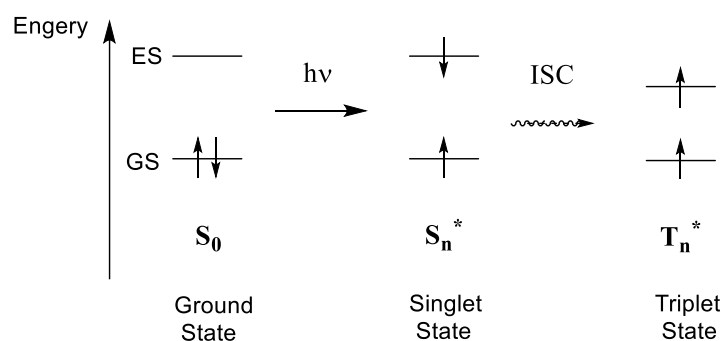


Figure 1.3: Triplet excited state.

As a molecule excited to a higher energy state returns to the ground state, it dissipates the energy acquired through paths other than those of a photochemical reaction. The Jablonski diagram illustrates the different radiative and non-radiative processes in electronically excited molecules (**Figure 1.4**).⁹

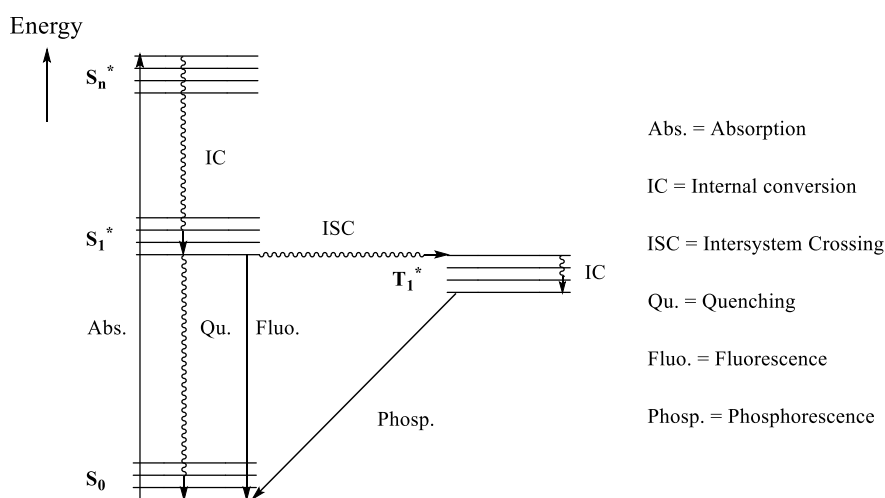


Figure 1.4: Jablonski diagram.

In general, the quenching of excited states decreases rapidly to the lowest lying S_1 or T_1 states. This occurs through non-radiative transmissions known as internal conversion (without a change of spin: $S_n \rightarrow S_1$ or $T_n \rightarrow T_1$) or intersystem crossing (involving a change of spin: $S_1 \rightarrow T_1$). Therefore, the S_1 and T_1 excited states have special significance in photochemical reactions. As the energy difference between S_1 or T_1 and the ground state S_0 is large, they have a longer

lifetime. In contrast, the dissipation of excited energy competes with radiative decay to the ground states, known as luminescent deactivation, i.e., fluorescence (no change of spin: $S_1 \rightarrow S_0 + h\nu$) or phosphorescence (change of spin: $T_1 \rightarrow S_0 + h\nu$).⁸

1.3 Photosensitization and photoinduced electron transfer (PET).

The excitation energy of a molecule in the triplet state (Donor, D) can be transferred to a neighbouring molecule in the ground state (Acceptor, A). This process is known as photosensitization and plays a very important role in organic photochemistry. Such dissipation of donors allows for the effective generation of triplet states that may not be accessible by the direct excitation of an acceptor (**Figure 1.5**)¹⁴ The triplet energy of the donor should overcome that of the acceptor.

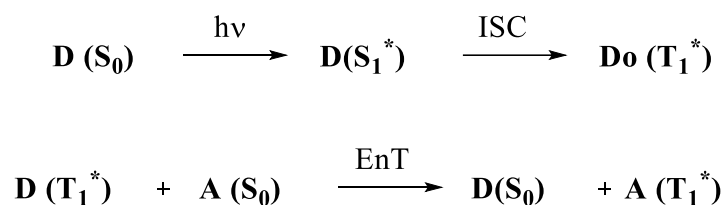


Figure 1.5: Triplet sensitization.

Another intramolecular process is called photoinduced electron transfer (PET), which is the transfer of an electron from an electron donor (D) to an electron acceptor (A).¹⁵ Therefore, radical ion pairs are generated, which can undergo additional transformations (**Figure 1.6**).

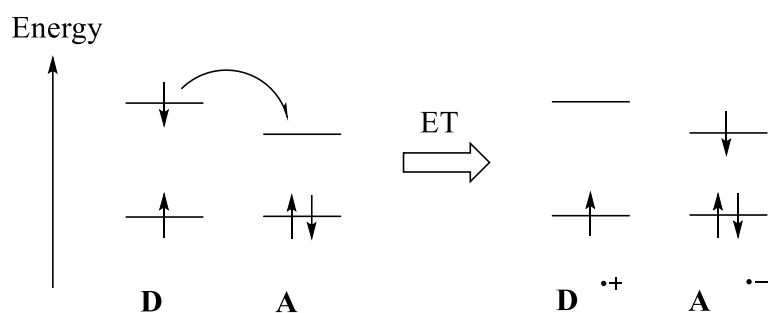


Figure 1.6: Photoinduced electron transfer.

The possibility of a photoinduced electron-transfer step can be predicted using the Rehm-Weller equation (**Equation 1.2**), where E_{ox} (D) and E_{red} (A) denote the oxidation and reduction potentials of the donor and acceptor molecule, respectively. E_{∞}^* represents the electronic excitation energy and E_{coul} is the coulombic interaction energy of the products.¹⁵

$$\Delta G = F(E_{\text{ox}}(D) - E_{\text{red}}(A)) + E_{\text{coul}} - E^*_{\infty}$$

Equation 1.2: Rehm-Weller equation.

1.4 Photochemistry of Quinones

The spectroscopic and photophysical characteristics of quinones generally show different light absorption depending on the features of the substrate and solvent. Several reports on the photophysical properties of quinones have been published. This review elucidates some of these properties and the techniques utilised.

In 2000, Mukherjee¹⁶ reviewed the available literature on the photophysical properties of 1,4-naphthoquinone (NQ) and 9,10-anthraquinone (AQ). NQ in hexane solvent shows λ_{max} at 246, 330, and 425 nm,¹⁷ and the extinction coefficients were 24×10^3 , 3.2×10^3 , and $50 \text{ dm}^3 \text{ mol}^{-1} \text{ cm}^{-1}$, respectively. The first two wavelengths can be assigned to the (π, π^*) transitions, whereas the last one can be attributed to an (n, π^*) transition (all singlet-singlet state). In heptane, however, the (n, π^*) absorption at 491 nm for the singlet-triplet transition is weak. In contrast, AQ shows a weak transition starting at 424 nm due to the excitation of two closely spaced (n, π^*) states. Three (π, π^*) transitions at 325, 252, and 272 nm have also been observed.

Based on the Φ results for both quinones, the intersystem crossing efficiency $\Phi (S_1 \rightarrow T_n)$ was very high because NQ was $\Phi_{\text{ISO}} = 0.8$ and 0.9 AQ.^{1,7} Therefore, the Φ_P for AQ was 0.44 in EPA at 77K , with Φ_{FL} being close to zero. Moreover, the triplet T_1 energies for NQ and AQ at 58 and 63 Kcal mol^{-1} respectively,¹⁷ showed strict conduct towards the solvents.¹⁶

In 2008, Barbafina et al.¹ highlighted the properties of the triplet state of tetramethyl-1,4-benzoquinone (TMBQ) and 2,6-dimethoxy-1,4-benzoquinone (DMOBQ) in acetonitrile, benzene, and water, using laser flash photolysis. First, the $(T_1 \rightarrow T_n)$ absorption spectra of DMOBQ showed the longest wavelengths in water (500 nm), followed by the triplet lifetime in benzene ($3 \mu\text{s}$). The wavelengths were shorter in acetone and benzene ($1 \mu\text{s}$). The triplet interacted with molecular oxygen, which trailed off at a constant rate of approximately $109 \text{ M}^{-1} \text{ s}^{-1}$ in acetonitrile and benzene. Second, the TMBQ characteristics were similar to the DMOBQ properties. The broadband exhibited an absorption at approximately 490 nm , and the triplet lifetime was approximately 6 and $14 \mu\text{s}$ in acetonitrile and benzene, respectively.

The most striking observations for these two benzoquinone derivatives are that the triplet quantum yields, Φ_T , approach unity, as did the triplet absorption coefficients, ϵ_T ($7200 \text{ M}^{-1} \text{ cm}^{-1}$ for DMOBQ and TMBQ).¹

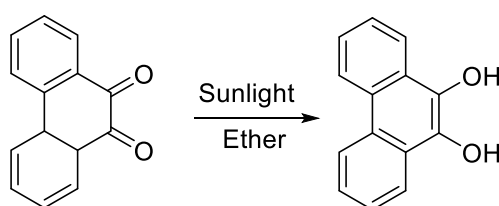
The optical absorption of 2-methyl-1,4-naphthoquinone (MeNQ), known as vitamin K3, has been reported. MeNQ exhibited a broad band centred at approximately 331 nm with $\epsilon = 2190 \text{ M}^{-1} \text{ cm}^{-1}$ in polar solvents. When the polarity of the solvent is increased, the high-intensity (π, π^*) band, which is a bathochromic shift, hides the (n, π^*) transition, which undergoes a hypsochromic shift. Therefore, a weak (n, π^*) transition is observed at approximately 267 nm with an absorbance of less than 2.5. In addition, the highest fluorescence quantum yield, Φ_{FL} , of MeNQ was recorded (3.78×10^{-3}) in isopropanol when the study was carried out in different organic solvents.¹⁸ However, the quantum yield of intersystem crossing, Φ_{ISO} , and the triplet lifetimes (τ_{T}) showed marked contrast between water and acetonitrile. For example, acetonitrile showed values of $\phi_{\text{ISO}} = 0.86$ and $\tau_{\text{T}} = 3 \text{ (}\mu\text{s)}$, whereas water showed 0.66 and 1.5 (s), respectively.^{19,20}

1.4.1 Photo-Friedel-Crafts Reactions of Quinones

A considerable volume of literature on quinone photochemistry, both experimental and theoretical, has been published.²¹ In the 20th century, several studies focused on photo-Friedel-Crafts reactions, particularly acylation reactions.⁶ During this period, reactions, such as the use of sunlight as a radiation source, were conducted using simple equipment mounted on the roofs of chemical laboratories in southern European countries (for example Giacomo Clinician's laboratory roof in Bologna, Italy).²² This process produced a viable, 'environmentally benign' alternative approach²³ because the classic Friedel-Crafts acylation reaction has many limitations. For example, the researchers noted the negative effects of using strong Lewis acids (AlCl_3 , TiCl_4 , etc.), including the production of undesirable side products (particularly volatile hydrochloric acid), and certain restrictions on the capabilities the reacting materials.^{22,23}

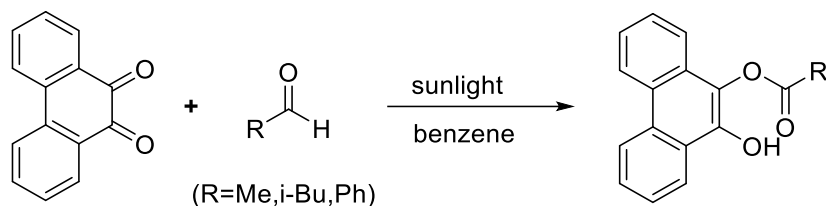
1.4.1.1 History of Photo-Friedel-Crafts Reactions

In 1886, Heinrich Klinger (Bonn, Germany) reported the first systematic photochemistry experiment. He investigated the photoreduction of 9,10-phenanthrenequinone to both its analogous dihydroquinone and acetaldehyde (**Scheme 1.1**).²⁴

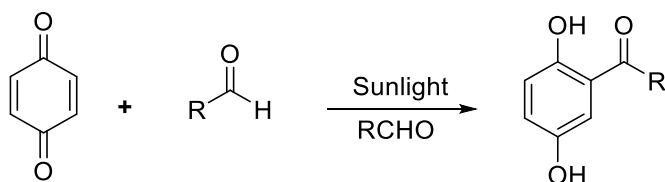


Scheme1.1: Photoreduction of 9,10-phenanthrenequinone

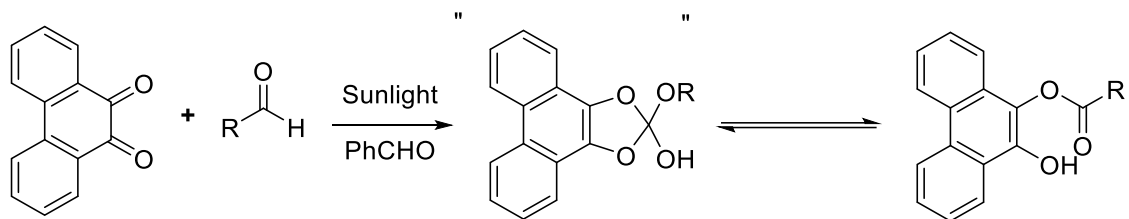
Coincidentally, he observed diketone benzyl photoreduction to hydrobezoin. In addition, during his research, he examined the solvent effect in the photoreaction, which led him to discover a new step in photosynthesis utilizing acetaldehyde and other aldehydes rather than ether (**scheme 1.2**).²⁴

**Scheme 1.2:** Solar reaction of 9,10-phenanthrenequinone in benzene

In 1891, Klinger reported the first Photo-Friedel-Crafts acylation of 1,4-benzoquinones by preparing the corresponding hydroquinone and exposing the reaction to sunlight directly for several months (**Scheme1.3**). He also mentioned the experimental obstacles encountered with the photoreaction at that time. For example, he apologized for presenting older results because of the forfeiture of his reaction flask during a storm.²²

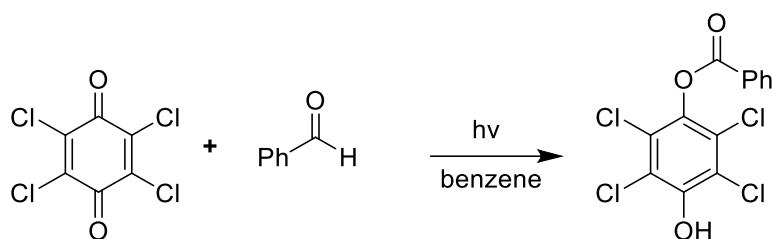
**Scheme1.3:** Photo-Friedel-Crafts acylation of 1, 4-benzoquinones.

In 1939, Alexander Schönberg, who is generally recognized as a pioneer in preparative photochemistry²⁵, observed a substitutional photoproduct resulting from a reaction between phenanthrenequinone and aromatic aldehydes (**Scheme 1.4**).²⁶ He preferred the cyclic ether instead of the ether used in Klinger's study.²⁴



Scheme 1.4: Photoacylation of 9,10- phenanthrenequinone with aromatic aldehydes.

Although Schönberg and co-workers remained adamant about their scenario, there were rewarding reinvestigations that corroborated Klinger's photoproduct conducted by Moore and Waters, then Rubin, using IR and NMR – spectroscopy, respectively.^{24,27} For example, Moore and Waters carried out the photo-acylation of chloranil with benzaldehyde in benzene, obtaining the monobenzoate in 35 % yield (**Scheme 1.5**).



Scheme 1.5: Photoacylation of chloranil with benzaldehyde.

1.4.1.2 Mechanism of Photo-Friedel-Crafts Acylation

Over the past two decades, several studies have been undertaken to elucidate the mechanism of photoacylation involving two scenarios, in-cage and out-cage. Both scenarios occur jointly and are dependent on the experimental conditions of the photoreactions, such as temperature, solvent, and type of quinone.²⁸ As a rule, the mechanism of quinone photoreaction takes place in the triplet excited state, except in very rare cases, where it is conducted in the single excited state.²⁹ According to Bruce and Maruyama³⁰⁻³¹, the phototransition was launched via an abstracted aldehyde hydrogen to the triplet excited state of the quinone because the C-H bond of the aldehyde group was weak H-abstraction led to a radical pair, followed by ionization, a process known as a proton transfer scenario (**Figure 1.7** path A). However, another likely mechanism was proposed through electron transfer in two steps, which is rounded off by proton transfer via the radical ion pair state (path B).²⁹

Despite the extensive studies of quinone photoreactions, the major mechanism of the quinone triplet state remains controversial. Maruyama and Otsuki ended this longstanding debate,

demonstrating an in-cage mechanism of pair radicals to be the main pathway to the final photoproduct.

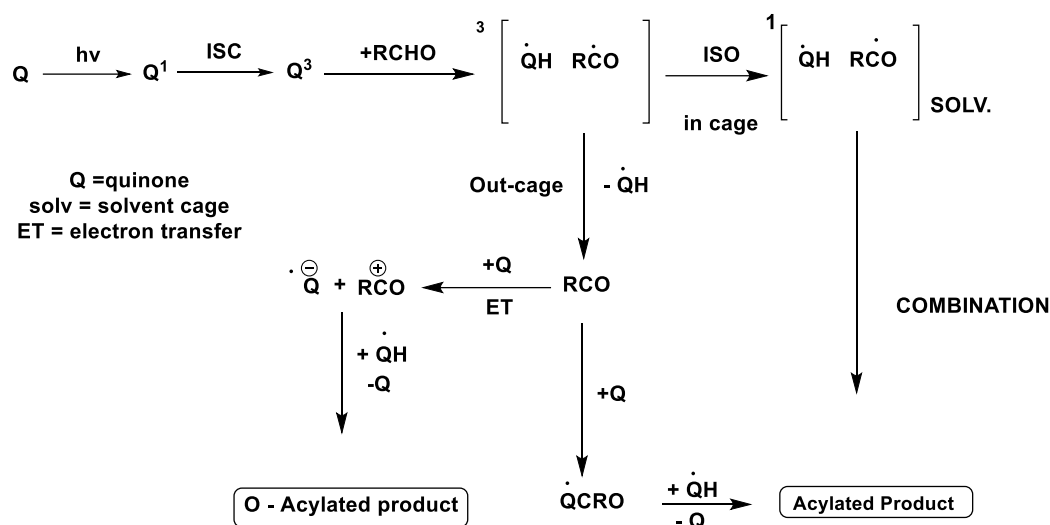
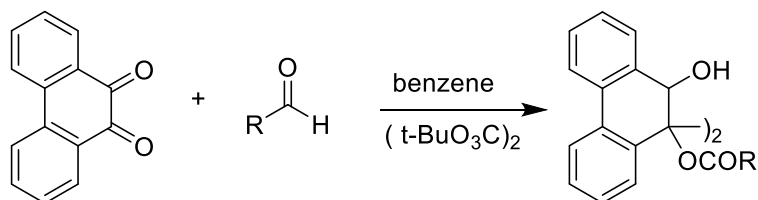


Figure 1.7: Mechanism of Photo-Friedel-Crafts Acylation.

Therefore, Maruyama and Otsuki traced the approach of radicals in the photoreaction of 9,10-phenanthrenequinone with hydrogen donors (e.g., xanthene, alkyl benzenes, ethers) using the chemically induced dynamic nuclear polarization (CIDNP) and ESR spectroscopy, and confirmed that in-cage coupling products are generally observed.³² Moreover, a comparison of the results obtained from the thermal reaction and photoreaction provided further evidence. Thus, the thermal products of an acyl radical were the dimeric isomers of the aryloxy radical in the ground state (**Scheme 1.6**), whereas photoacylation resulted in a completely different product (**Scheme 1.2**).³³ Therefore, this is another repudiation of the out-cage scenario for the quinone photoreaction.²⁴



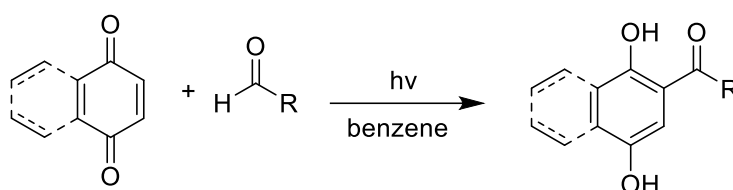
Scheme 1.6: Thermal reactions of several acyl radicals with ground state 9,10-phenanthrenequinone.

1.4.1.3 Photo-Friedel-Crafts Acylation Reactions in a laboratory framework

The past 30 years have seen rapid advances in the photochemistry of quinones with the evolution of analytical techniques leading to independence from changing weather and

radiation sources. To elucidate the synthetic conditions, the present study will examine the effects of artificial light sources, solvent, substrate, and reactor design.

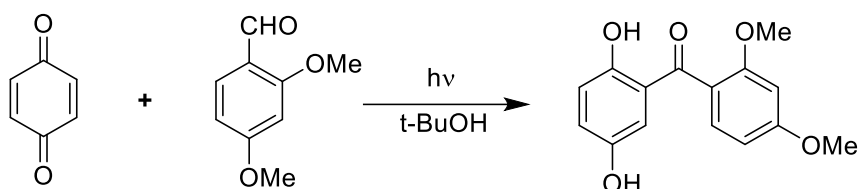
Kraus and Karawara examined quinone photoacylation with a larger scale of chemicals. The photoreaction conducted via benzoquinone and 1,4-naphthoquinone reacted with a group of aliphatic and aromatic aldehydes in benzene, employing a high-pressure Hg-vapour lamp for five days with a Pyrex filter (**Scheme 1.7**). This reaction resulted in modest yields. For example, the reaction with butyraldehyde was 88%, whereas it was 82% with benzaldehyde.³⁴



Scheme 1.7: Photoreactions of 1,4-quinones and aldehydes.

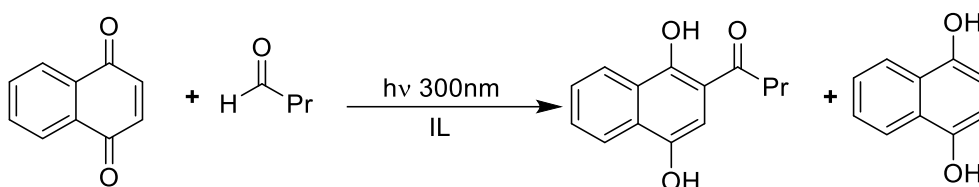
From a green photochemistry perspective, Christian et al. traced the development of quinone photoacylation incorporated in Kraus' original procedure, while also trying to search for alternative conditions and on a commercial scale. The photoreaction was performed on two models: 1,4-quinones with aldehydes, leading to acylated hydroquinones as the sole products. The first model reaction of the photoacylation of 1,4-naphthoquinone with butyraldehyde examined alternative solvents and concluded that a mixture of *tert*-butyl alcohol with acetone (3:1) was an acceptable alternative solvent with the photoproduct 12 isolated in 84% yield in a laboratory experiment. The researchers also assessed toluene as a green solvent, but the reaction was sluggish, and the yield of acylated hydroquinones was only 35 % because of radical side reactions with the solvent.^{22, 35}

The second model reaction was between 1,4-benzoquinone and 2,4-dimethoxybenzaldehyde using an artificial light source and pure *tert*-butyl alcohol as the solvent; the corresponding product was obtained easily in 66% yield (**Scheme 1.8**). This study included three different sunlight-collecting systems: CPC, PROPHIS, and a flatbed reactor. The solar reaction took place on a large scale. For example, the starting material of the first model was 500 g of 1,4-naphthoquinone and 80 L of a mixture solvent. Consequently, the yield was 90 % for three days in the CPC reactor case.²²



Scheme 1.8: Photoacylation of 1,4-benzoquinone and 2,4-dimethoxybenzaldehyde.

In other solvent investigations, Oelgemöller et al. attempted a photo-Friedel–Crafts acylation of 1,4-naphthoquinone in ionic liquids at room temperature, seeking an unconventional solvent and green chemistry. After optimising the photoacylations in different ionic liquids (cation /anion), the reaction was conducted with a series of aliphatic aldehydes. The highest yield of photoproduct was obtained as the sole product in 91% yield in [C₂mim][OTf], and 81% yield in [C₂mim][NTf₂] with the photoreduction product (**Scheme 1.9**).²⁸

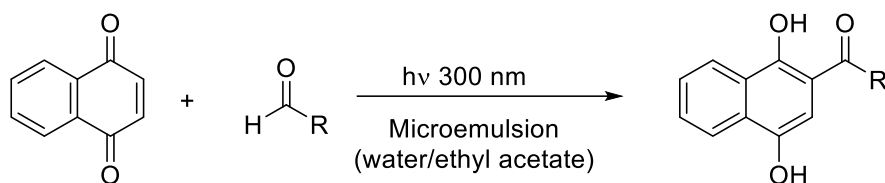


Scheme 1.9: Photoacylation of 1,4-naphthoquinone in ionic liquid.

Tanko and co-workers applied supercritical carbon dioxide as an alternative solvent and reported the photosynthesis of 1,4-hydroquinone and 1,4-diketones. The researchers studied the optimal conditions of the photoreaction, which included suitable pressure, irradiation sources, and the presence and concentration of benzophenone as the mediated reactions. The study also examined the poor solubility of the starting materials in the non-polar SC-CO₂ solvent and resolved this obstacle by testing a series of alcoholic co-solvents. Accordingly, the photoacylation of 1,4-benzoquinone with butyraldehyde in the presence of a benzophenone-mediated reaction and 5% t-BuOH in SC-CO₂ at 5735 (psi) under mild pressure resulted in 81% yield, which was the best outcome (**Scheme 1.7**).²³

In a further attempt to seek an alternative solvent, Brian³⁶ investigated the use of a microemulsion (water/ethyl acetate) as a solvent for the photo-Friedel–Crafts acylation of 1,4-naphthoquinone with a short and long chain of aldehydes. These reactions, which were irradiated for 16 hours in a Rayonet Photochemical Reactor (RPR-200; Southern New England Ultraviolet Company), produced a poor yield and inefficient purification. Nevertheless,

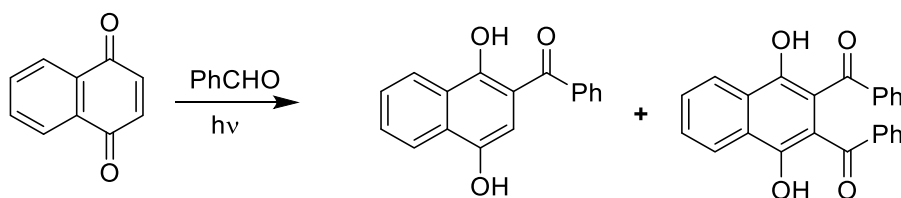
microemulsion offers some potential as a green organic solvent for this class of reaction owing to the low toxicity of their components (**Scheme 1.10**).³⁶



Scheme 1.10: photoacylation of 1,4-naphthoquinone in microemulsion solvent

Similarly, Kraus et al. also used benzophenone as a mediated conjugate addition to quinone photoacylation. The photoreaction conducted through 1,4-benzoquinone and 1,4-naphthoquinone reacted with ortho- and para-substituted benzaldehydes (**Scheme 1.7**). They concluded that the presence of benzophenone in this photoacylation might improve the yield by approximately 15–20% compared to that in the absence of benzophenone.³⁷

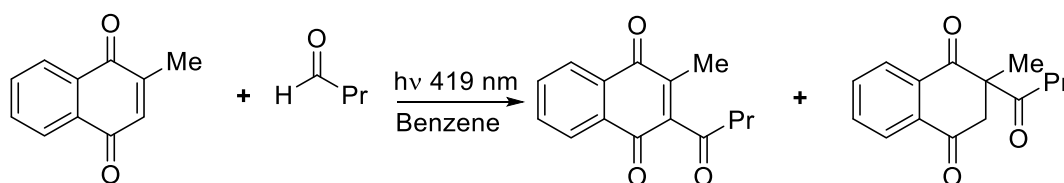
However, this is in contrast to Oelgemöller et al., who examined the photoacylation of 1,4-naphthoquinone with 1-propionaldehyde and benzaldehyde in the presence of benzophenone, and reported that the corresponding acylated product was in lower yield (**Scheme 1.11**).^{35,38} Benites suggested that this compound does not influence the yield of photoacylation.³⁹ Oelgemöller et al. improved the Kraus procedure by increasing the percentage yield of photoproduct with a shorter irradiation time. The protocol developed included the replacement of a medium-pressure lamp with RPR-3000 Å lamps (max = 300±25 nm) equipped in a Rayonet photochemical chamber reactor. For example, the photoreaction of 1,4-naphthoquinone with 1-propionaldehyde in benzene performed with a medium-pressure lamp for five days afforded the photoproduct at 79 % yield (original procedure); nevertheless, the latter reaction irradiated at 300±25 nm, attained the desired yield at 82 % after a much shorter reaction time of 40 hours.



Scheme 1.11: Photoacylation of 1,4-naphthoquinone in Rayonet reactor

In a different study, Oelgemöller and co-workers presented the results of comprehensive research on the photo Friedel–Crafts acylation of naphthoquinones, taking into consideration most outcomes previously reported. The study focused on three frameworks. First, the photoreaction was carried out using several artificial light sources with the results showing that using hydrargyrum quartz iodide (HQI), high-intensity discharge (HID) lamps, and UV sunlamp as a sun-mimicking source achieves significant conversion with a moderate yield of the photoproduct of 72 % and 55%, respectively. The second significant achievement was the utilization of trifluorotoluene as a green alternative solvent. Performing the photoacylation of naphthoquinone in trifluorotoluene resulted in complete conversion in 14.5 hours with a good yield of the corresponding product (62%). The use of trifluorotoluene, although expensive, has been demonstrated to be less hazardous and more selective than other solvents.⁴⁰ After commissioning these optimised conditions, the photoreaction was conducted with a variety of aldehydes, investigating them with further substitute (ether, alkene, or halide), so that they may offer the desired acylated quinone derivatives in reasonable to high yield (17–81%), matching, or superior to, those reported previously.^{35,38}

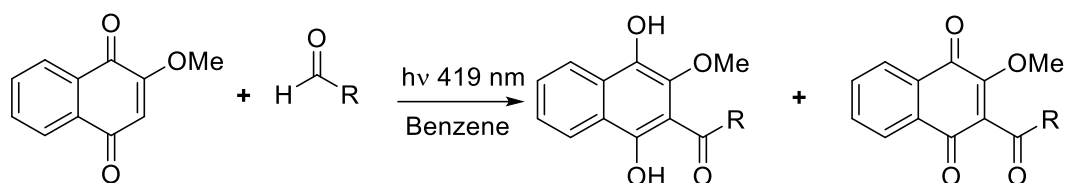
However, employing substituted and heteroaromatic substrates has attracted little attention in photochemical acylation reactions, despite their acylated quinone derivatives varying in biological implementation.⁴¹ In recent years, this type of photoreaction has been in the spotlight to fill this significant gap. For example, Oelgemöller and co-workers presented two patterns of 2-substituted 1,4-naphthoquinones photoacylation, which are 2-methyl-1,4-naphthoquinone and 2-methoxy-1,4-naphthoquinone. 2-Methyl-1,4-naphthoquinone was carried out with several aliphatic and aromatic aldehydes furnishing the analogous acylated quinones in moderate yields of 23–49%. The photoacylation of 2-methyl-1,4-naphthoquinone with butyraldehyde synthesized the tri- keto compound in 10 % yield along with an additional 49 % of the acylated quinone (**Scheme 1.12**).



Scheme 1.12: Photoacylation of 2-methyl-1,4-naphthoquinone in benzene.

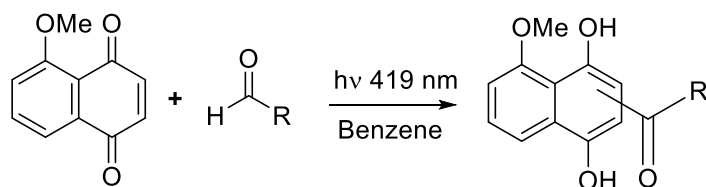
The second photoacylation of 2-methoxy-1,4-naphthoquinone with butyraldehyde produced a mixture of the monoacylated hydroquinone and acylated quinone (**Scheme 1.13**), but repeating

the photoreaction via dodecyl aldehyde yielded a solo acylated quinone, representing a significant key intermediate for the synthesis of the antibiotic.⁴²



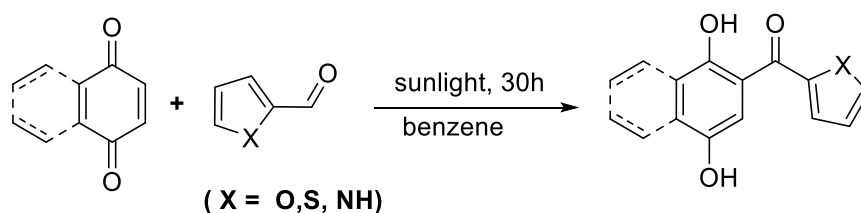
Scheme 1.13: Photoacylation of 2-methoxy-1,4-naphthoquinone in benzene

Similarly, Waske examined the photoacylation of 5-methoxy-1,4-naphthoquinone (methyl juglone) with a range of aliphatic and aromatic aldehydes, which were irradiated in benzene at 419 nm, and resulted in low to modest yields (**Scheme 1.14**). The regioselectivity and regioisomer of the acylated products have been observed with some exceptions; for example, only one regioisomer and hydroquinone were produced when 4-cyanobenzaldehyde was employed in the reaction. Where the reaction was involved with 4-chlorobenzaldehyde, a mixture of the products resulted in several pathways, including mono-acylation, bis-acylation, and *O*-acylation, as well as photoreduction.⁴³



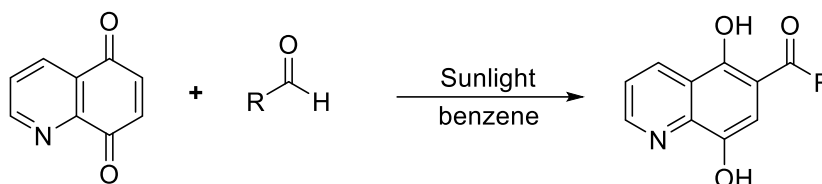
Scheme 1.14: Photoacylation of 5-methoxy-1,4-naphthoquinone in benzene

In the heteroacylation scenario, Benites investigated the synthesis of heteroacylhydroquinones from 1,4-benzoquinone and 1,4-naphthoquinone, reacting with different heteroaromatic aldehydes in various solvent media. The photoheteroacylations were performed via solar irradiation for 30 h (six days) in benzene, affording the sole heteroacylhydroquinones in 71–92 % yield (**Scheme 1.15**).^{39,44}



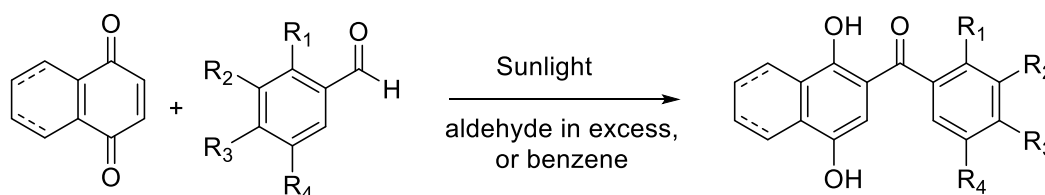
Scheme 1.15: Synthesis of heteroacylhydroquinones in benzene

With the same objective, the Shizue Mito group reported the solar acylation of quinoline-5,8-dione, as a hetero-substrate, with various aromatic and aliphatic aldehydes. The photoreaction took place in a Pyrex sealable reaction tube, which was placed on the roof of a research building for exposure to direct sunlight, producing the corresponding 6-acyl-5,8-quinolinediols in moderate to good yield (**Scheme 1.16**).⁴⁵



Scheme 1.16: Photoacylation of quinoline-5, 8-dione in benzene

More recently, Arenas and co-workers presented a significant and eco-friendly approach to constructing oxygen - substituting diaryl ketones through the photoacylation of 1,4-quinones. The synthesis of diaryl keto carried out by solar irradiation for 1,4-benzoquinone and 1,4-naphthoquinone with multi-substituted benzaldehyde gave the corresponding photoproduct in moderate to excellent yield.⁴⁶ The experiment was performed using one of two parallel paths, benzene or an excess of aldehyde as the solvent. The study outcomes indicate that the yield of the target product in benzene achieved a higher percentage than excessive aldehyde (**Scheme 1.17**).



Scheme 1.17: Photoacylation of 1,4-quinones and with substituted benzaldehydes

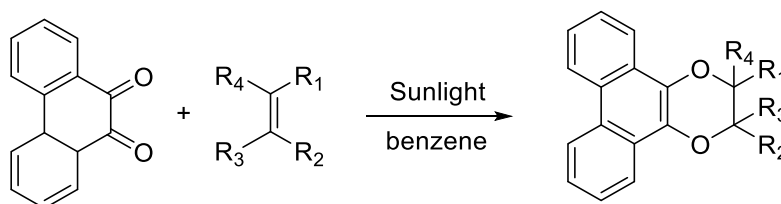
The generalisability of these studies is subject to certain limitations. For example, photoacylations have only been realized in batch reactors, where the products compete for light and require exhaustive irradiation times. Although solvent optimization has been reported, the results have largely been unsatisfactory, especially for outdoor applications in sunlight. Benzene and acetonitrile are both toxic and cannot be used on a large scale outdoors. Ionic liquids, supercritical CO₂, microemulsion, and trifluorotoluene (TFT) have been assessed as alternative ‘green’ solvents, but they are expensive or impracticable for large-scale processes.

Historically, photoacylations have been performed with natural sunlight, but the early setups were improvised. Modern solar acylations have been reported, but with varying successes.

1.4.2 Photocycloaddition of Quinones

Quinone cycloadditions have attracted considerable attention from the chemical and biological communities owing to their initial adducts being natural products or serving as a pathway to a broad range of biological activities.^{47,48,49} Schönberg and Mustafa reported the first photocycloaddition of quinone in 1944 when they exposed a solution 9,10-phenanthraquinone with several aromatic alkenes in benzene to natural sunlight and isolated the photoproducts (**Scheme 1.18**).^{50,51}

However, the photoaddition of 1,4-naphthoquinone to alkenes, alkynes, and their derivatives has received little attention in recent years, and as an extension of the work, an additional, [2+2] cycloaddition of 1,4-quinone to alkenes will be subject to review, focusing on the mechanistic aspects and experimental conditions.

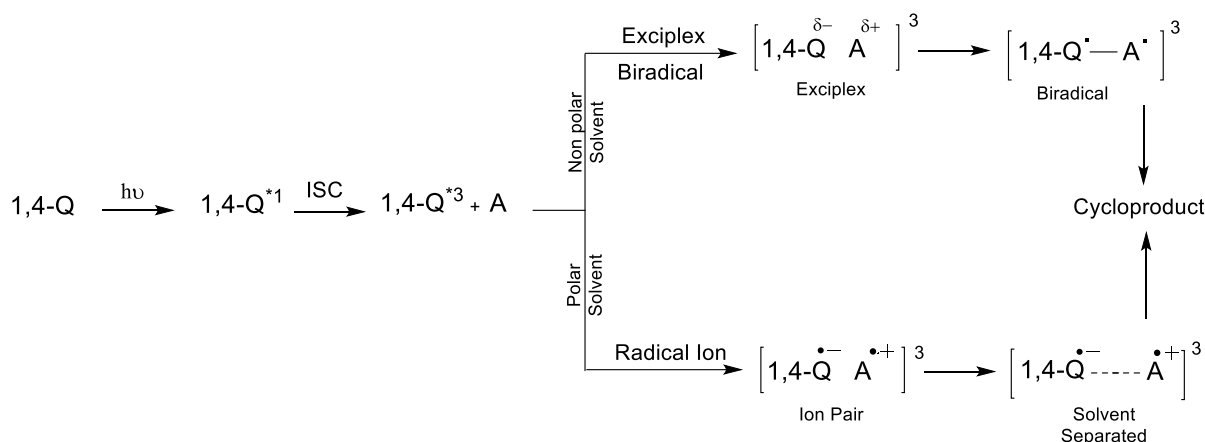


Scheme 1.18: Photocycloadditions of 9,10-phenanthraquinone to alkenes

1.4.2.1 Mechanism of [2+2] Photocycloaddition of 1,4-naphthoquinone

Several empirical studies have been conducted on the mechanism of 1,4-quinone additions to alkenes or alkynes, which proposed two pathways to the cycloadducts. However, all these studies have been dominated by the photochemistry of 1,4-quinones arising from the lowest excited triplet state, and the singlet lifetimes being very short, thereby preventing the participation of any singlet state in the media of photoreaction.⁵² Early investigations adopted a procedure whereby the cycloaddition reactions of triplet-excited 1,4-quinones to ground-state alkenes occurred by a triplet exciplex intermediate, to form a triplet biradical.⁵³⁻⁵⁶ In contrast, the second pathway suggested that the reaction occurred through radical ion formation and a solvent-separated radical ion intermediate followed by coupling processes, which are favoured in polar solvents (**Scheme 1.19**).⁵⁷⁻⁵⁹ Thus, both approaches are accepted widely as the

mechanism of this photoreaction, depending on the substrate and the experimental conditions of the particular reaction.

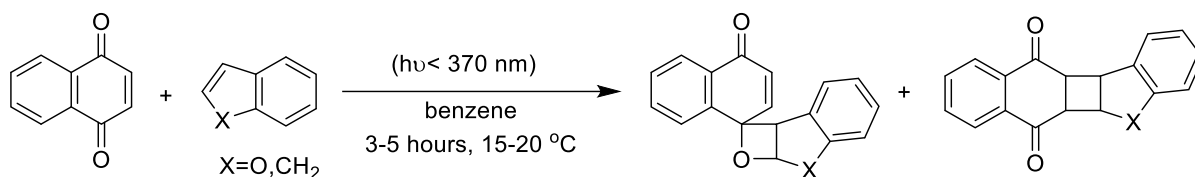


Scheme 1.19: Exciplex and radical ion mechanism for the photoaddition of *p*-quinones to alkenes (A).

The trend of alkene addition to 1,4-quinone counted on the tendency of the lowest-lying triplet state (n,π^* versus π,π^*). Consequently, the cycloadduct is produced from the carbonyl group (Paternò–Buchi reaction) or the ethene moiety ([2+2]-photocycloaddition), or both processes simultaneously. Theoretical calculations for different 1,4-quinones proposed that oxetane formation is associated with those quinones with the lowest (n,π^*) triplet states, such as 1,4-benzoquinone, whereas quinones with the lowest (π,π^*) triplets afforded cyclobutane by the addition of the alkene to the quinone C=C bond. 1,4-naphthoquinone produces both spiro-oxetanes and cyclobutanes because the energies of the (n,π^*) and (π,π^*) states are close.⁶⁰ In general, the substituents on the quinone and alkene also play a role in the selectivity of the final product. For example, the formation of spiro-oxetanes became more preferable with the increased electron-donating ability of the alkene, whereas the electron-accepting alkenes produced only cyclobutane adducts. Therefore, electronically-donor substituted quinone debilitates the (n,π^*) state and can increase its energy over that of the (π,π^*); hence, the site of ethene addition would be favored.^{61,62}

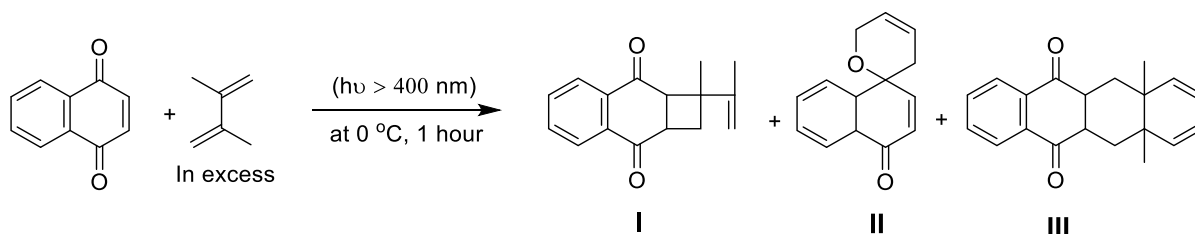
1.4.2.2 [2+2] Photocycloaddition of 1,4-naphthoquinon

Fifty years later, Krauch (1966) reported the first photocycloaddition of 1,4-naphthoquinone with alkenes. The reaction examined six benzocyclic olefins as the alkene, and both the oxetane and cyclobutane were obtained in moderate to low yield. The reaction run in benzene was irradiated (3-5 hours, at 15-20 °C) through a filter glass, offering wavelengths less than 370 nm, using a 125 W high-pressure Hg lamp (**Scheme 1.20**).⁶³



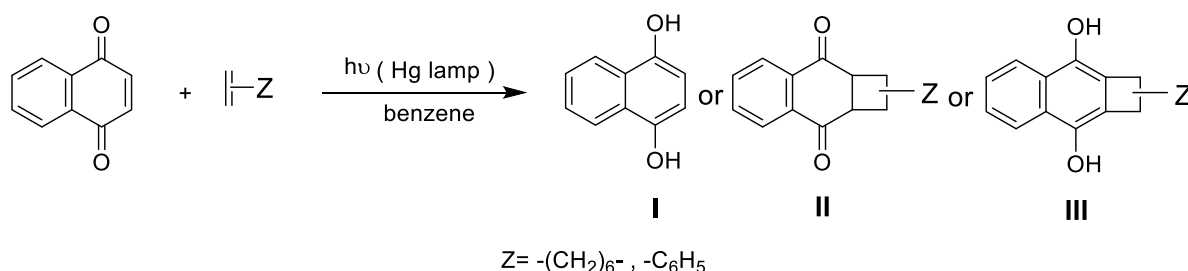
Scheme 1.20: Photocycloaddition of 1,4-naphthoquinone with benzocyclic olefins.

One year later, Barltrop et al. began studying the photocycloaddition of 1,4-naphthoquinone with an excess of 2,3-dimethylbutadiene as a solvent, giving bicyclo-octane (I) as the major product, spiropyran (II), and two isomers of the adduct (III), (2: 1). The reaction mixture in a Pyrex annular vessel was irradiated with light ($h\nu > 400$ nm) for 1 hour at 0 °C, which was filtered via a solution of ethanol-carbon dioxide (**Scheme 1.21**).⁶⁴



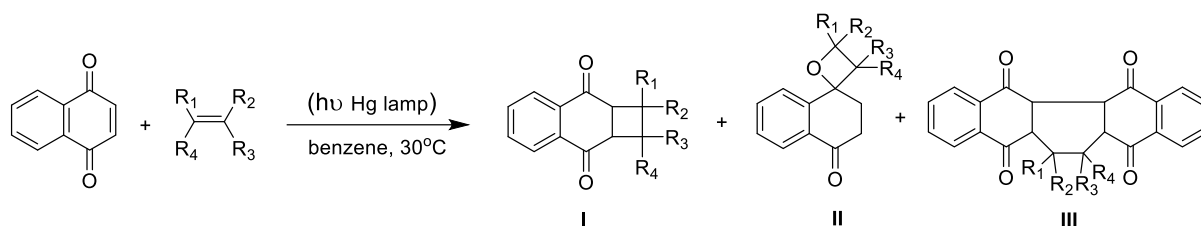
Scheme 1.21: Photocycloaddition of 1,4-naphthoquinone with 2,3-dimethylbutadiene

In addition, Maruyama et al. carried out comprehensive investigations into the photoaddition of parent and substituted 1,4-naphthoquinones to a wide range of alkene types. First, Maruyama irradiated one mole of 1,4-naphthoquinone with two mole of alkene in benzene for 20-40 hours, using a high-pressure Hg lamp (400 W). The alkenes examined afforded three types of products. 1,4-naphthoquinone was reduced readily to 1,4-naphthohydroquinone (I) by α -pinene, cyclopentene, and cyclohexene. The photoaddition of 1,4-naphthoquinone with indene and styrene yielded the cyclobutene (II) while cyclooctene and acenaphthylene produced dihydrocyclobutane (III). (**Scheme 1.22**).⁶⁵



Scheme 1.22: Photocycloaddition of 1,4-naphthoquinone with alkenes.

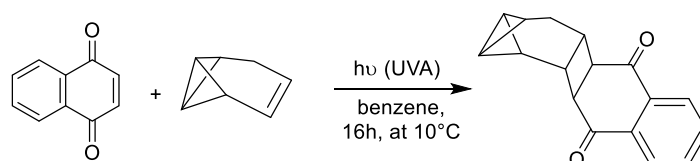
In a different experimental procedure, Maruyama et al. studied the irradiation of two molecules of 1,4-naphthoquinone with one molecule of the alkene. The cycloadducts observed in this study were classified into three structural types: cyclobutane (I), spiro-oxetane (II) through a [2+2]cycloaddition process, and cyclohexane (III) via a [2+2+2] cycloaddition process (Scheme 1.23). The reactants were dissolved in benzene, placed in a glass tube, and irradiated with a high-pressure Hg lamp (300 W) through a 5 cm thick water layer. However, the yields of the products were very low and the other products were difficult to identify.⁶⁶⁻⁶⁷



Scheme 1.23: Photocycloaddition of 1,4-naphthoquinone with alkenes (2:1).

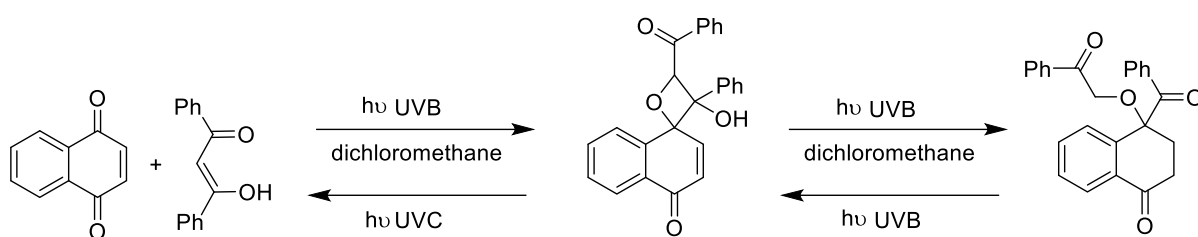
In the 1990s, a number of researchers examined the 1,4-naphthoquinone / alkene system. Bryce and co-workers investigated the photocycloaddition of 1,4-naphthoquinone to a variety of electron donor and electron acceptor alkenes. The study resulted in two types of photo-products, spirooxetanes and/or cyclobutane derivatives. In addition, an acyclic addition product was obtained by a photoreaction between 1,4-naphthoquinone and 2,3-dimethylbutadiene. The irradiations were performed on 1,4-naphthoquinone and an alkene (1:1) in benzene. The reaction was carried out using a Pyrex immersion well reactor comprised of a 125 W medium-pressure mercury lamp, and wavelengths longer than 400 nm were achieved when recirculated cooling water was replaced with a nitrite-bipthalate filter solution (**Scheme 1.23**).⁶⁸

Remarkably, Christl et al. conducted the first photocycloaddition of 1,4-naphthoquinone in a Rayonet reactor using homobenzvalene as the alkene irradiated in benzene ($\lambda = 350$ nm) at 10°C for 16 hours; the corresponding adduct was obtained as the sole product in 21% yield (**Scheme 1.24**).⁶⁹

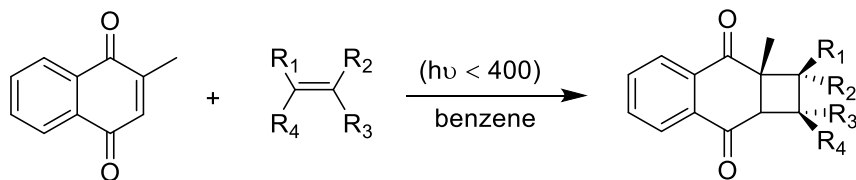


Scheme 1.24: Photocycloaddition of 1,4-naphthoquinone with homobenzvalene.

Kim *et al.* described the de Mayo-type photoaddition of dibenzoylmethane to the carbonyl group of 1,4-naphthoquinone, giving hydroxyoxetanes. Upon further irradiation, the reaction afforded 1,5-diketones via a retro-Aldol method in moderate yield. The study also showed that the hydroxyoxetane began to reverse to the reactants when irradiated with 254-nm radiation. In another experiment, irradiating the 1,5-diketone with 300-nm light converted it to hydroxyoxetane (**Scheme 1.25**). The reaction was carried out in dichloromethane using a Rayonet reactor equipped with 300 nm UV lamps and irradiated for 110 hours in a Pyrex flask.⁷⁰

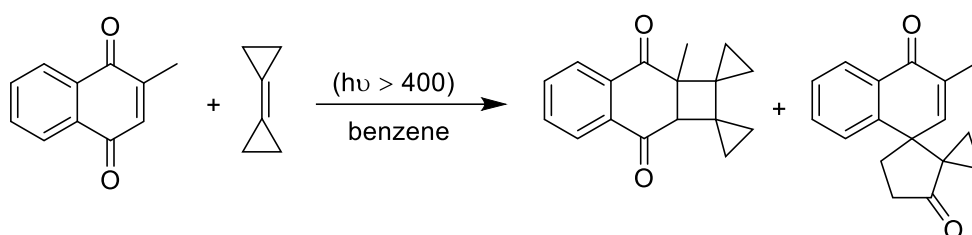
**Scheme 1.25:** Photoaddition of 1,4-naphthoquinone to dibenzoylmethane.

Over the past 30 years, the photocycloadditions of substituted 1,4-naphthoquinone with substituted alkenes have attracted considerable attention and revealed a significant effect on the photoreaction procedure. For example, Liu *et al.* and Maruyama *et al.* examined the photoaddition of 2-methyl-1,4-naphthoquinone to various olefins in several studies.⁷¹⁻⁷³ The reactions were conducted in benzene and irradiated at room temperature with a high-pressure Hg lamp through a Pyrex filter, giving an isomer mixture of cyclobutane products only in excellent yield (**Scheme 1.26**).

**Scheme 1.26:** Photoaddition of 2-methyl-1,4-naphthoquinone to an alkene.

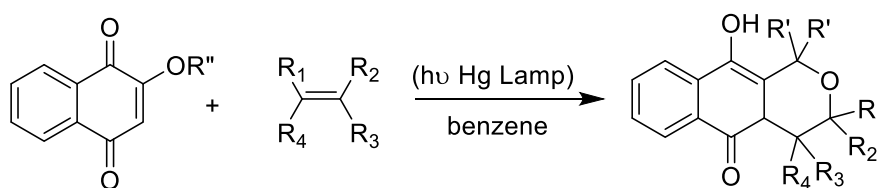
Therefore, the experimental findings showed that the photocycloadditions of 2-substituted-1,4-naphthoquinone with the alkene proceeds from the lowest (π, π^*) singlet excited state band and was observed at 300 nm, which overlapped with the (n, π^*) band. Accordingly, Maruyama *et*

al. reported that no adducts were observed when the reaction mixture was exposed to wavelengths longer than 400 nm.⁷² In contrast, Wang et al. reported the significant photocycloaddition of *p*-quinones with light of $\lambda > 400$ nm in benzene. For example, 2-methyl-1,4-naphthoquinone with bicyclopropylidene (BCP) were irradiated with a 500 W medium-pressure mercury lamp filtered through a solution of 20% aqueous sodium nitrite to cut off light with wavelengths shorter than 400 nm. In this case, the corresponding products were obtained in two forms: cyclobutane derivative, as the main adduct, along with the primary spirooxetane product (**Scheme 1.27**).⁷⁴



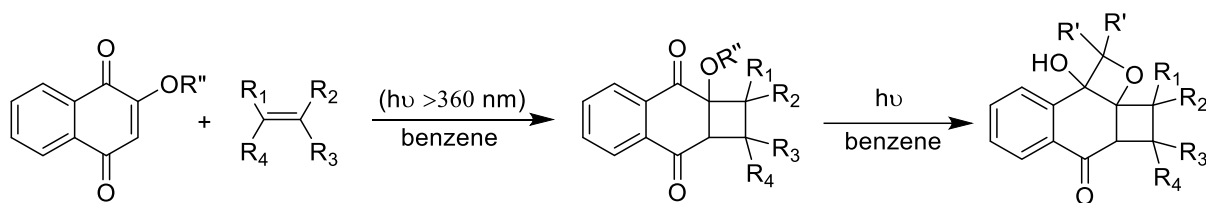
Scheme 1.27: Photoaddition of 2-methyl-1,4-naphthoquinone to (BCP).

The photoreactions of 2-alkoxy-1,4-naphthoquinone with various alkenes were a subject of many early examinations and continue to attract appreciable attention. The first studies of this type of photocycloaddition were performed by Maruyama *et al.* followed by Otsuki, who concluded that the product structure of photoaddition was a tetrahydropyran derivative.⁷⁵⁻⁷⁶ The photoreactions were carried out in benzene and irradiated in a glass tube by a high-pressure mercury lamp (300W) through a 5 cm thick water layer (**Scheme 1.28**).



Scheme 1.28: Formation of tetrahydropyran-ring Compounds.

Two years later, Otsuki revised the previous report, proving that the photocycloaddition of 2-alkoxy-1,4-naphthoquinone to a variety of alkenes offer the spirooxetane and cyclobutane adducts;⁷⁷ this correction was supported by the following research (**Scheme 1.29**).^{73,74, 78,79}



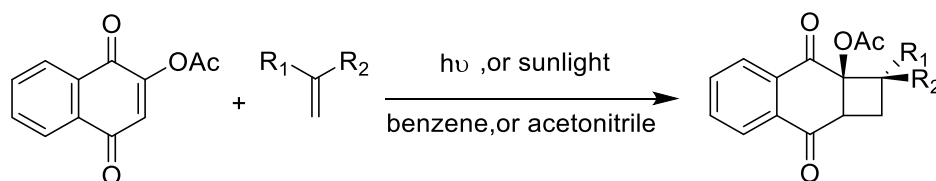
Scheme 1.29: Photoaddition of 2-alkoxy-1,4-naphthoquinone to alkenes.

Most examples showed that cyclobutane is generated first, where its stability relied on the substituents of the reactants and the wavelength of light. When unstable cyclobutane was already produced, the secondary intramolecular hydrogen abstraction took place with further irradiation, resulting in the corresponding hydroxyoxetane. To achieve the sole product in high yield, the irradiation period should be very short, and a cut-off filter at 360 nm should be used.^{74, 77-78}

2-Acetoxy-1,4-naphthoquinone similarly underwent $[2\pi+2\pi]$ -photocycloaddition to alkenes, which yielded cyclobutane exclusively, emerging from regio- and stereo-specific chemistry to give a head-to-head structure with styrene and 1,1-diphenylmethane. In contrast, both *trans* and *cis*-stilbene yielded spiro-oxetane preferentially, and the stereochemistry of adduct was observed with *trans*-stilbene. In general, the irradiations were conducted in benzene or acetonitrile using the Pyrex-filtered light from a high or medium mercury arc lamp.^{78, 80}

In the same vein, Covell et al. investigated the solar irradiation of the artificial procedure reaction when an acetonitrile solution of 2-acetoxy-1,4-naphthoquinone with styrene or 1,1-diphenylmethane were irradiated with sunlight for six hours using a CPC reactor. The corresponding cyclobutane adducts were obtained in quantitative yield. The reaction could also be scaled-up easily with the efficient a photoreaction up to 60 °C (**Scheme 1.30**).⁸¹

Therefore, 2-electron donor substituted-1,4-naphthoquinone increases the energy of the ($^3n,\pi^*$) excited state. Moreover, the site of quinone carbon-carbon double bond addition is the most preferable for particular quinones with ethenes, but the orientation of the reaction is not straightforward.



Scheme 1.30: Photocycloaddition of 2-acetoxy-1,4-naphthoquinone with arylenes

From the photoreactions mentioned above, several experimental parameters are subject to at least three limitations. First, the photocycloaddition of 1,4-naphthoquinone to alkenes have been conducted in batch mode using a medium or high-pressure mercury lamp. This avoids over-irradiation of the photoproduct, which may absorb the UV strongly. Therefore, attached light filters are needed to suppress their secondary photochemical reactions. Second, most conventional quinone [2+2]-photocycloadditions are performed in benzene with a few exceptions, which is a known hazard and carcinogen. Thus far, no attempt has been made to explore the photocycloaddition of quinone in a sustainable chemistry approach. Third, although an early examination of the quinone photocycloaddition used natural sunlight, only one example of solar cycloaddition has been described thus far.

Chapter 2:

Aims

2. Aims

The main objectives of this research project were to establish and validate a new technology in organic photosynthesis and offer a promising green alternative to existing methodologies. The project combined organic synthesis, synthetic photochemistry, continuous-flow operation, and analytical techniques. Hence, it represents a novel and innovative approach to synthetic organic photochemistry in continuous-flow.

The main objectives of the present study were as follows:

- evaluate the potential for improving the synthetically important photo-Friedel-Crafts acylation and photocycloaddition of quinones under traditional batch conditions that circumvent the disadvantages of the currently established protocols (e.g., irradiation wavelength, solvent, etc.),
- develop new methodologies for the photochemical transformation of quinones in continuous-flow operation,
- utilize sunlight as a sustainable and natural light source that can replace energy-intensive and hazardous artificial lamps,
- conduct multistep reactions in a single run using in-series flow protocols, and
- evaluate the flow reactor performance in comparison with that of a batch reactor.

Chapter 3:

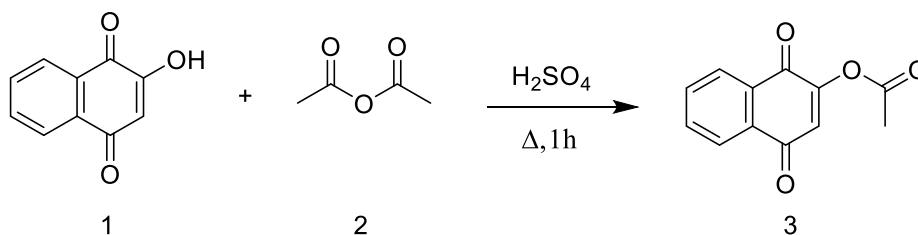
Results

3. Results

3.1 Synthesis of starting materials

3.1.1 Synthesis of 2-acetoxy-1,4-naphthoquinone.

The preparation of 2-acetoxy-1,4-naphthoquinone (**3**) was achieved following a procedure described by Nigel by refluxing 2-hydroxy-1,4-naphthoquinone (**1**) with acetic anhydride (**2**) in the presence of catalytic amounts of concentrated sulfuric acid (**Scheme 3.1**).⁸² The reaction mixture was heated in the steam bath and subsequently poured into cold water. After recrystallization from ethanol or aqueous methanol, the desired product **3** was obtained in a good yield of 80% as yellow prisms. The 2-acetoxy-1,4-naphthoquinone structure was confirmed by ¹H-NMR spectroscopy. The full ¹H-NMR spectrum of **3** is shown in **Figure 3.1**. The aromatic signals are found at 8.12 and 7.77 ppm and the quinonoid signal at 6.76 ppm, respectively. The newly formed acetoxy-group gave a characteristic singlet at 2.39 ppm.



Scheme 3.1: Synthesis of 2-acetoxy-1,4-naphthoquinone (**3**).

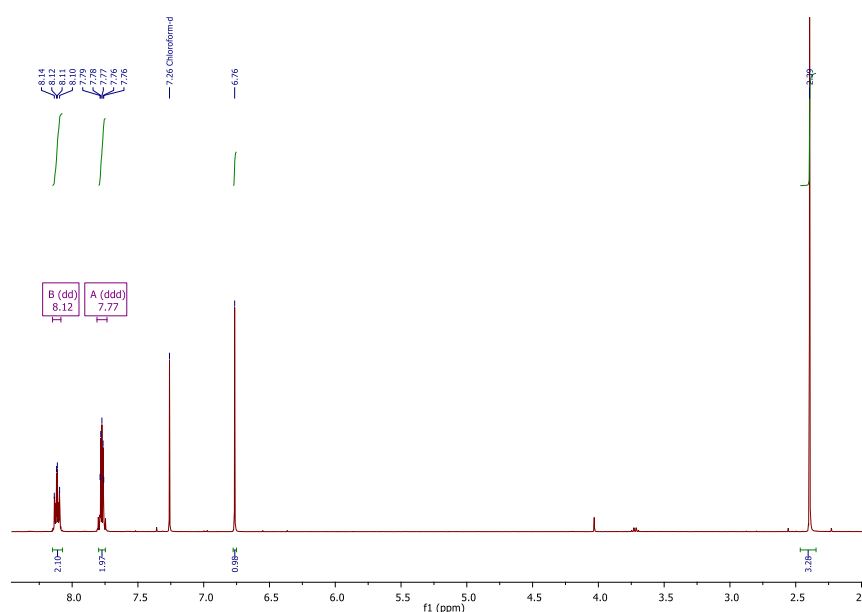


Figure 3.1: ¹H-NMR spectrum of a 2-acetoxy-1, 4-naphthoquinone (**3**) (in CDCl₃).

3.2 Photochemical transformations

3.2.1 Batch chamber reactor

Batch experiments were performed in a Rayonet photochemical chamber reactor (RPR-200; Southern New England Ultraviolet Company, USA) equipped with 16 × 8 W UVA (350 ± 25 nm), UVB (300 ± 25 nm), UVC (254 ± 25 nm) or visible light (400–700 nm) fluorescent tubes and a cooling fan. Pyrex (transmission >300 nm) or quartz (transmission >200 nm) Schlenk flasks with capacities of 60–180 mL were used as reaction vessels. A cold finger was inserted into the flask to maintain the reaction temperature below 25 °C (**Figure 3.2**). The reaction mixtures were degassed with N₂ through a sidearm for approx. 5 min before capping the reaction vessel. All other photoreactions were monitored by TLC or by ¹H-NMR spectroscopy.

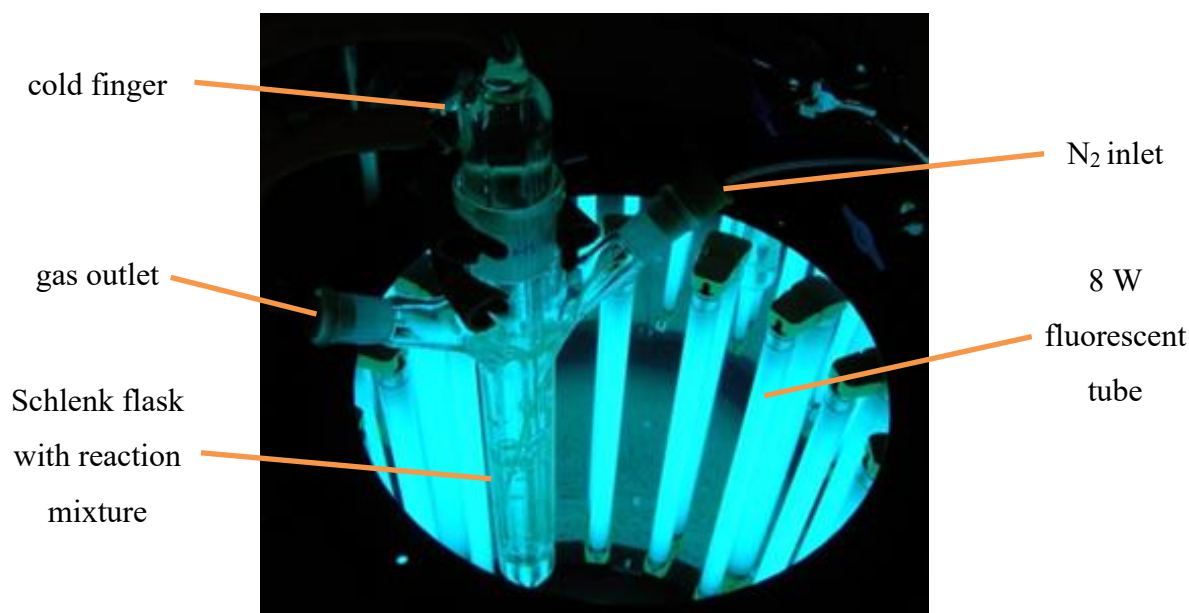


Figure 3.2: Batch chamber photoreactor (Rayonet) with inserted Schlenk flask.

3.2.2 In-house capillary reactor

Photoacylation reactions and photocycloadditions in continuous flow mode were mainly investigated using a laboratory built capillary reactor (**Figure 3.3** and **Table 3.1**). The reactor used a fluorinated ethylene propylene (FEP) capillary with an exposed length of 10 m, an inner diameter of 0.8 mm and an internal volume of 5 mL. The capillary was wrapped around a Pyrex body with an outer diameter of 6.5 cm (48 windings covering 7.8 cm). At its center, the reactor contained a single 8 W UV fluorescence tube. A small fan was mounted into the base of the reactor column. The whole setup was kept in a light-tight box. An additional cooling fan was

mounted on the left side of the reactor box. A hanging thermometer allowed for temperature monitoring during operation. A syringe pump was used to transfer the reaction mixture through the capillary tubing. The product solution was collected outside the reactor box in an amber flask.

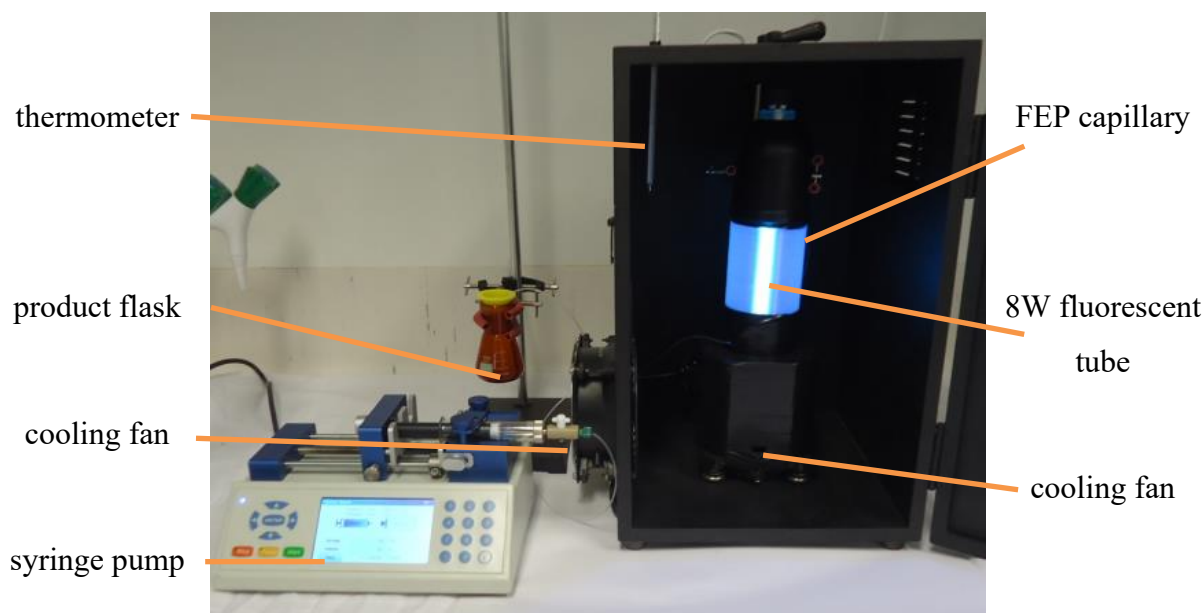


Figure 3.3: In-house capillary reactor.

Table 3.1: Technical data of the in-house capillary reactor.

Tube material	Fluorinated ethylene propylene (FEP)
External diameter	1.58 mm
Internal diameter	0.8 mm
Length of tube	10 m
Volume of tube	5 mL (exposed)
Pump	Chemyx syringe pump (Model: Fusion 200)
Light source	UVB (300 ± 25 nm) ^a or UVA (350 ± 25 nm) ^b , 8 W each

^a Used for 1,4-naphthoquinone photocycloadditions. ^b Used for 2-acetyloxy-1,4-naphthoquinone photocycloadditions.

3.2.3 In-house tandem photochemical-thermal capillary reactor

The capillary reactor was subsequently modified for in-flow oxidation (**Figure 3.4**). The effluent stream from the photoreactor loop entered a syringe cartridge (ca. 50 mL) against gravity from the bottom. The product mixture was collected external in an amber flask.

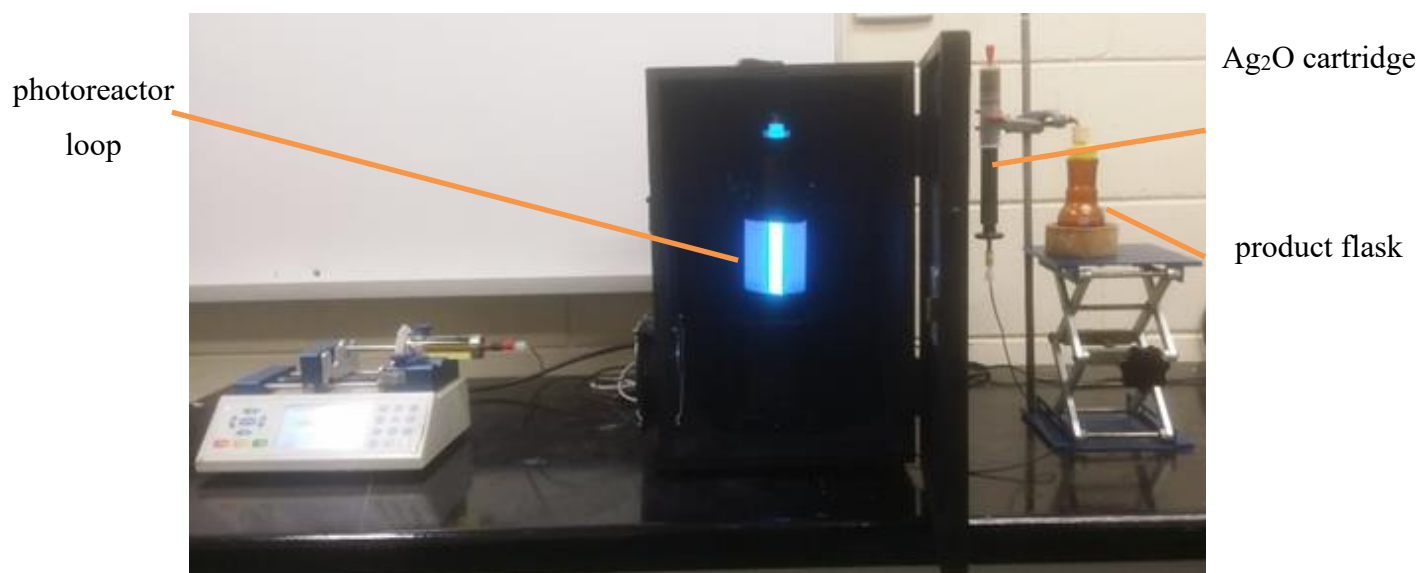


Figure 3.4: Tandem photochemical-thermal capillary reactor.

3.2.4 Solar batch set-up

A series of illumination experiments in direct sunlight were performed by placing capped Pyrex test tubes (25 mL) inside an opening in a small boogie board (Figure 3.5). The exposed test tubes were held in place by a plastic frame inside the solar float.

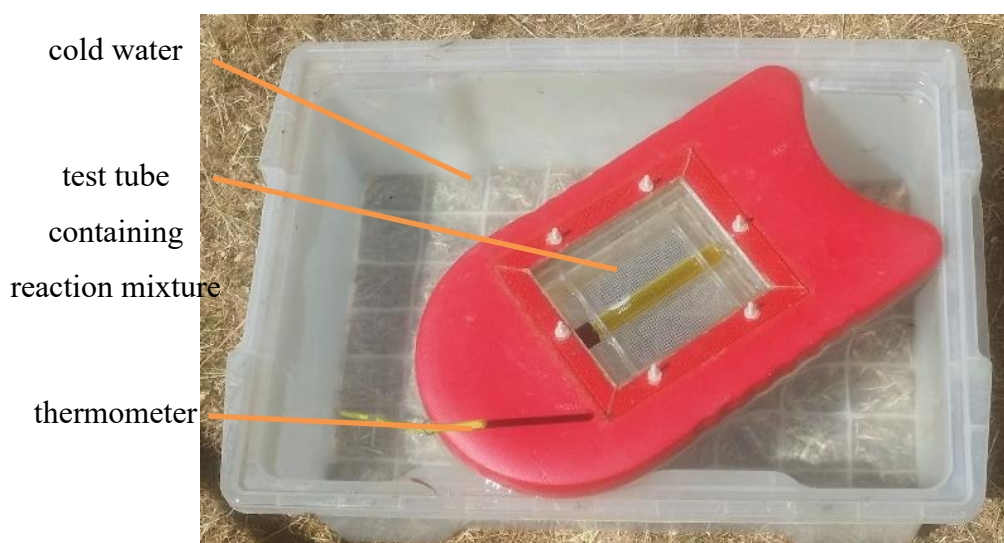


Figure 3.5: Direct illumination using a solar float.

Illumination data for the days of operations were collected from the photovoltaic station at James Cook University in Townsville.

3.2.5 In-house parabolic trough concentrating solar flow reactor

Outdoor transformations under flow conditions were studied using an in-house built parabolic trough concentrating solar reactor (**Figure 3.6** and **Table 3.2**). The trough was made from a polished aluminum sheet supported in a stainless steel metal frame. A Pyrex glass tube, which was covered by the reaction capillary, was positioned in its focal line with ring clamps. The FEP capillary tube had an inner diameter of 1.6 mm, a length of 27 m and an internal volume of 53 mL. The temperature of the reaction mixture was controlled by flowing chilled tap water through the center of the glass tube. A piston pump was attached to push the reaction mixture through the capillary. A back pressure regulator was used at the outlet to maintain a smooth flow pattern. Reaction and product mixtures were kept in amber flasks underneath the reflector to minimise any reaction outside the capillary. Likewise, the non-exposed connecting tubing was covered with black shrink tube. Illumination data for the days of operations were collected from the photovoltaic station at James Cook University in Townsville.



Figure 3.6: Parabolic trough concentrating solar flow reactor.

Table 3.2: Technical data of the in-house parabolic trough concentrating solar flow reactor.

Length of the internal glass tube	1.2 m
Inner diameter of the glass tube	3 cm
Capillary tube material	Fluorinated ethylene propylene (FEP)
External diameter	3.2 mm
Internal diameter	1.6 mm
Length of tube	27 m
Volume of tube	53 mL
Pump	Ismatec piston pump
Position to sun	manually
Concentrator material	polished aluminum
Concentration factor	3 measured (theoretical= 13)

3.3 Photoacylations of 1,4-naphthoquinones

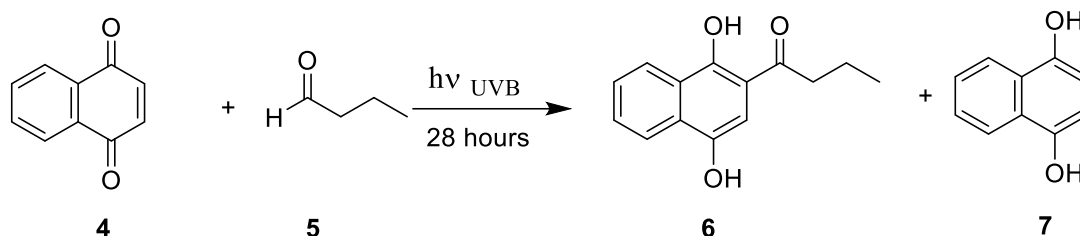
3.3.1 Photoacylation of 1,4-naphthoquinones under batch conditions

To improve the currently known reaction protocol in terms of their environmental impact, the photoacylations of naphthoquinone were carried out following a procedure described by Oelgemöller *et al.* by irradiating 1,4-naphthoquinone with excess amounts of aldehyde in an organic solvent in a Rayonet photochemical chamber reactor (**Figure 3.2**).⁸³ All photoreactions were monitored by TLC and the conversions were determined by integration of characteristic signals in the coresponding ¹H-NMR spectra of the crude products. The photocycloaddition of 1,4-naphthoquinone (**4**) with butyraldehyde (**5**) to the corresponding adduct was used as a model system. A number of parameters, *i.e.* choice of organic solvent, wavelength, glass type and light sources, were optimised experimentally. The reaction protocol was subsequently applied to other photoacylations with 1,4-naphthoquinone, 2-hydroxy-1,4-naphthoquinone and 2-acetyloxy-1,4-naphthoquinone.

3.3.1.1 Solvent optimisation

To identify the ideal solvent, a series of photoreactions of 1,4-naphthoquinone (**4**) (1 mmol) and butyraldehyde (**5**) (5 mmol) in different organic solvents (50 mL) were conducted with UVB light (300 ± 25 nm) in a Pyrex Schlenk flask (transmission >300 nm) for 28 hours under batch conditions (**Scheme 3.4**). The corresponding acylated naphthohydroquinone **6** was readily obtained in yields of 51-76% by washing the crude product twice with hot water

(~55°C). The experimental results revealed a dependency of the chemoselectivity, *i.e.* photoacylation to **6** *vs.* photoreduction to **7**, on the organic solvent used. The photochemical activation mode, *i.e.* direct excitation *vs.* photosensitization, also differed depending on the solvent system. The outcomes are summarised in **Table 3.3**.



Scheme 3.2: Photoacylation of 1,4-naphthoquinone (**4**) and butyraldehyde (**5**) under batch condition.

Table 3.3: Experimental results from the solvent study.

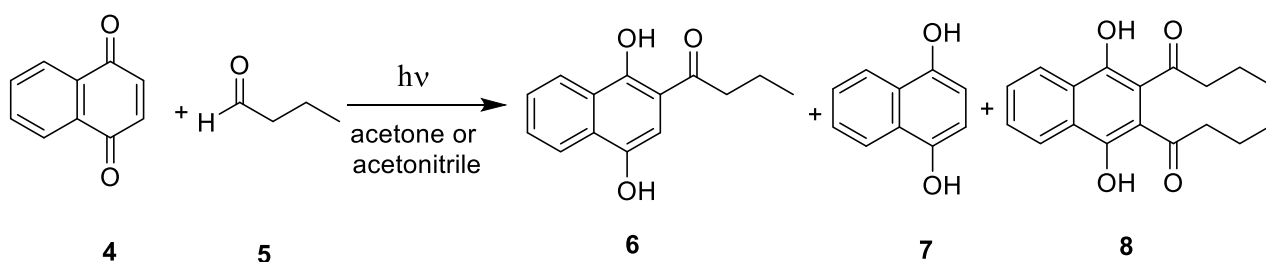
Entry	Solvent	Conversion (%) ^a (7 ^b)	Yield (%) ^c (6)
1	acetone	95	76
2	acetonitrile	94	75
3	trifluorotoluene	100	62
4	xylene	64	51
5	<i>tert</i> -amyl alcohol	86 (30)	n.d. ^d
6	<i>tert</i> -butyl alcohol	87 (4)	67
7	isopropanol	73 (46)	n.d. ^d

^a Determined by ¹H-NMR analysis (±3%). ^b Amount of photoreduction product **7**. ^c Isolated yield of **6**. ^d n.d. = not determined.

The results show that the most selective conversions occurred in acetone, acetonitrile and trifluorotoluene (TFT). In contrast, photoreduction of naphthoquinone to **7** was observed in alcoholic solvents.⁸⁴ The polar photoacylation product **6** precipitated during irradiation in TFT. This strongly within the UVB range absorbing product was thus removed from the reaction mixture, reducing light filtering effects and causing complete conversion. However, since precipitation is undesired in flow operation due to potential clogging, TFT was found not suitable as a solvent.

3.3.1.2 Wavelength study

In order to find the optimum wavelength for irradiation, the emission of the light sources and the glass type of the reaction vessel were investigated. Glass has a profound impact on light transmission.⁸⁵ The study was conducted in acetone and acetonitrile to further explore photoexcitation under direct or sensitised conditions. Therefore, a series of photoacylations involving the **4/5** model system were conducted under batch conditions for 28 hours in a Pyrex ($\lambda \geq 300$ nm) or quartz ($\lambda \geq 200$ nm) vessel with different UV as well as visible light (**Scheme 3.3**). The experimental results obtained are compared in **Table 3.4**.



Scheme 3.3: Photoacylation of 1,4-naphthoquinone (**4**) with butyraldehyde (**5**) under different light conditions.

The reaction was further repeated with eight different irradiation conditions in different organic solvents. ¹H-NMR spectra were recorded after regular intervals to determine conversions and product compositions. No reaction was observed by visible light irradiation in TFT, whereas UVC irradiations furnished by-products **7** and **8** in both acetone and acetonitrile. Quartz-filtered UVB light in acetone also showed photoreduction to **7**. However, the optimal preparative irradiation of 1,4-naphthoquinone was achieved using acetone, UVB light and a Pyrex vessel.

Table 3.4: Experimental results from the wavelength study.

Entry	Irradiation conditions	Solvent	Conversion (%) ^a		Yield (%) ^d (6)
			(7 ^b)	(8 ^c)	
1	Visible light, Pyrex	TFT	trace		n.d. ^f
2	Visible light, Pyrex	acetone	54		n.d. ^f
3	419 ± 25 nm, Pyrex	acetone	66		56
4	350 ± 25 nm, Pyrex	acetone	80		60
5	300 ± 25 nm, Pyrex	acetone	95		76

Entry	Irradiation conditions	Solvent	Conversion (%) ^a	Yield (%) ^d (6)
			(7 ^b) (8 ^c)	
6	300 ± 25 nm, Pyrex	acetonitrile	94	75
7	300 ± 25 nm, Quartz	acetone	74 (22)	50
8	254 ± 25 nm, Quartz	acetone	96 (35), (28)	30
9	254 ± 25 nm, Quartz	acetonitrile	89 (8), (38)	40

^a Determined by ¹H-NMR analysis (±3%). ^b Amount of photoreduction product 7. ^c Amount of bisacylation product 8. ^d Isolated yield of 6. ^e no reaction. ^f not determined.

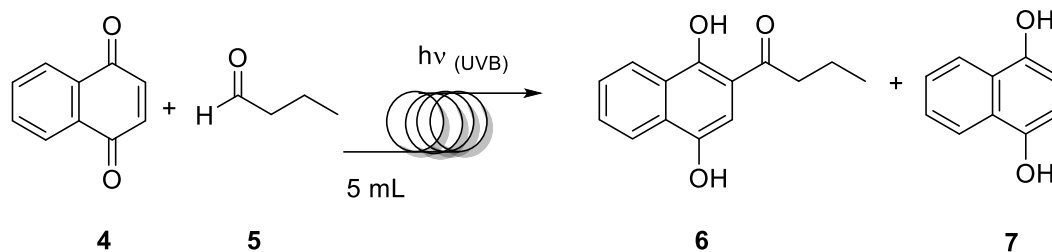
3.3.2 Photoacylations of naphthoquinone under continuous flow conditions

After optimizing the conditions in the batch system with respect to solvent, wavelengths and glass type, a series of photoacylations was carried out in the in-house continuous flow reactor (**Figure 3.3**) using the same reagents and concentrations. The available reactor coil has an internal volume of 5 mL. The residence and thus irradiation time within the reactor coil can be simply controlled by the flow rate of the pump (**Equation 3.1**). Although extensive research has been carried out on the quinone photoacylation, no single study exists which employs continuous flow techniques.

$$\text{residence time (min)} = \frac{\text{reactor volume (mL)}}{\text{flow rate (mL/min)}} \quad (\text{Equation 3.1})$$

3.3.2.1 Residence time and flow rate study

A series of photoacylations was performed with the 1,4-naphthoquinone / butyraldehyde pair in the in-house reactor using selected solvents and Pyrex-filtered light from a UVB lamp. The residence time and flow rate were investigated to achieve high and selective conversions. The general scheme of the reaction is shown in **Scheme 3.4**. The conversion rates were determined by integration of baseline-separated signals in the ¹H-NMR spectra and the results are summarized in **Table 3.5**. The obtained results show that the reaction time can be significantly reduced from 28 hours to 70 minutes by transferring the reaction procedure from batch to flow conditions. Flow operation was also found to be more economical in terms of the light source applied. In particular, the flow reactor utilized a single 8 W fluorescent tube. In contrast, the much larger Rayonet reactor employed 16 × 8 W tubes instead.



Scheme 3.4: Photoacylation of **4** with **5** under continuous flow conditions.

Table 3.5: Experimental results from the continuous flow study.

Entry	Solvent	Resident time (min)	Flow rate (mL/min)	Conversion (%) ^a (7 ^b)	Yield (%) ^c
1	acetonitrile	25	0.2	82	70
2	acetonitrile	50	0.1	87	78
3	acetonitrile	70	0.071	90	86
4	acetonitrile	100	0.05	92	90
5	acetone	70	0.071	96	88
6	<i>tert</i> -butyl alcohol	70	0.071	92 (22)	55
7	ethyl acetate	70	0.071	91 (16)	53
8	chloroform	70	0.071	95	90

^a Determined by ¹H-NMR analysis (±3%). ^b Amount of photoreduction product **7**. ^c Isolated yield after washing with hot water.

Initially, the resident time was investigated for direct excitation in acetonitrile. High conversions are readily achieved with residence times of 25 to 70 minutes, but only marginally increase further by 2% with a residence time of 100 minutes. This is due to the strong light-filtering effect of the acylated hydroquinone **6**, which becomes dominant at high conversions. Additional experiments were thus conducted in other solvent. For example, the reaction proceeded in excellent yields of 88% and 90% with a residence time of 70 minutes in acetone and chloroform. Triplet sensitisation by acetone was found competitive to direct excitation in acetonitrile and chloroform. The formation of the photoreduced naphthohydroquinone **7** was also noted in *tert*-butyl alcohol and ethyl acetate. Trifluorotoluene was not selected for flow operation because of the precipitation of **6** which may lead to blocking of the capillary tube inside the reactor.

Using residence times of 70 min, the less hazardous solvent acetone and Pyrex-filtered light from a UVB lamp selectively furnished the desired acylated naphthohydroquinone **6** in an excellent isolated yield of 88%. Acetone was thus chosen for further studies due to its low toxicity and role as a triplet sensitizer.⁸⁶ The ¹H-NMR spectra of the crude mixture (A) and pure

(B) product **6** are shown in (Figure 3.7). The A spectrum confirmed the high conversion of the reaction to the acylated hydroquinone **6**. Upon close inspection, trace amounts of residual 1,4-naphthoquinone (**4**) may be indicated by a weak singlet at 6.99 ppm, representing the two quinonoid protons in **4**. Pure product **6** can be obtained by simple washing with hot water, as visible from the ^1H -NMR spectrum (B). Two triplets and one quartet were observed for the $(-\text{COCH}_2\text{CH}_2\text{CH}_3)$ group in the aliphatic range. The signals of the aromatic protons appear between 7.03 and 8.78 ppm. The signal for the HO-groups emerge at very different position. Intramolecular hydrogen-bonding causes a strong and sharp singlet at 13.77 ppm, whereas the unbonded HO-group appears as a broad singlet at 4.91 ppm instead.

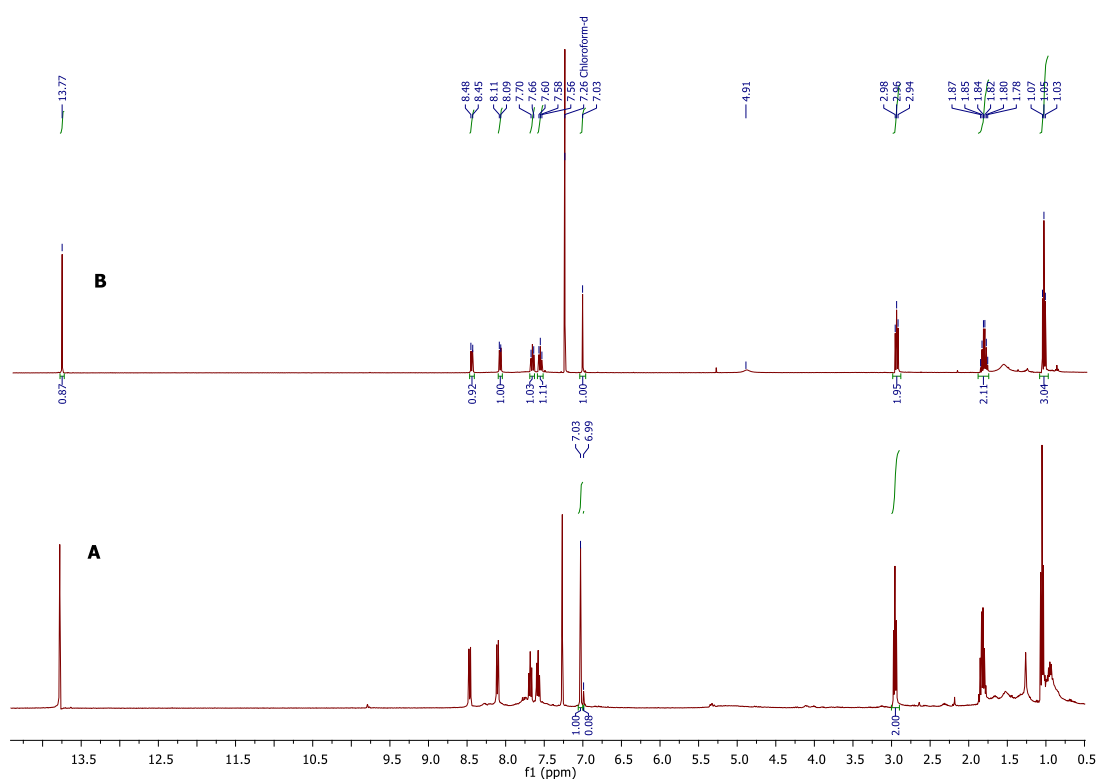
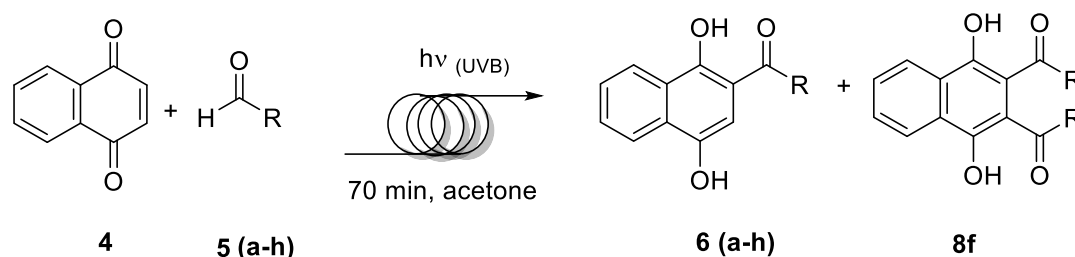


Figure 3.7: ^1H -NMR spectra (in CDCl_3) of the crude product mixture (A) and pure acylated hydroquinone product **6** (B).

3.3.2.2 Flow photoacylation of naphthoquinone with different aldehydes

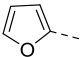
In order to expand the reaction scope, the irradiation protocol in acetone was subsequently applied to a series of aldehydes. Examples included aliphatic, unsaturated, aromatic and heteroaromatic aldehydes. The general scheme of the reaction is shown in Scheme 3.5 and the experimental results are summarized in Table 3.6. With one exception (entry h), the isolated

yields of the acylated hydroquinones **6a-h** were superior or comparable to previously conducted studies.^{34, 42, 87-89}



Scheme 3.5: Photoacylation of naphthoquinone under continuous flow condition.

Table 3.6: Experimental results from the continuous flow study with different aldehydes.

Entry	Aldehyde	R	Yield (%) (8 ^a)
a	propionaldehyde	C ₂ H ₅	70 ^b
b	butyraldehyde	C ₃ H ₇	90 ^b
c	heptaldehyde	C ₆ H ₁₃	75 ^b
d	dodecylaldehyde	C ₁₁ H ₂₃	34 ^c
e	crotonaldehyde	CH ₃ CH=CH	72 ^d
f	<i>p</i> -tolualdehyde	<i>p</i> -CH ₃ C ₆ H ₄	66 ^c (14)
g	<i>p</i> -chlorobenzaldehyde	<i>p</i> -ClC ₆ H ₄	80 ^d
h	furfural aldehyde		20 ^c

^a Amount of bisacylation product **8**. ^b Isolated yield of **6** after washing with hot water. ^c After column chromatography. ^d Precipitated from cold chloroform.

Overall, the photoproducts were obtained using greener alternative conditions along with shorter irradiation times. The experimental results furthermore indicate that continuous flow conditions can be successfully applied to other aldehydes. With the exception of dodecylaldehyde, the linear aliphatic aldehydes furnished the desired acylated naphthohydroquinones selectively in good to excellent yields. This may be attributed to the necessary purification technique. For instance, the photoproducts obtained from short chain aldehydes [entries a-c] can be easily purified by evaporating the excess aldehyde under low pressure, followed by washing with hot water to remove the remaining starting material and polymeric byproducts. As dodecylaldehyde possess a very high boiling point of 185 °C (100 mm Hg), simple evaporation became impractical without risking thermal decomposition.

Consequently, column chromatography was necessary to purify the crude product. Although the obtained yield of acylated hydroquinone **6d** was low with 34%, the conversion was determined at 64% by ^1H -NMR analysis. Likewise, product **7h** was obtained in just 20% after column chromatographic workup. In contrast, the unsaturated aldehyde [entry e] gave the desired acylated product in good yield and using simple workup. In the case of aromatic aldehydes, *p*-tolualdehyde [entry f] showed the formation of diacylated photoproduct **8f** which was isolated along with the mono-acylated quinone **6f**, while *p*-chlorobenzaldehyde [entry g] furnished only the corresponding mono-acylated product **6g** in a high yield of 80%. The ^1H -NMR spectra of the main product **6f** and the bisacylated by-product **8f** are displayed in **Figure 3.8**.

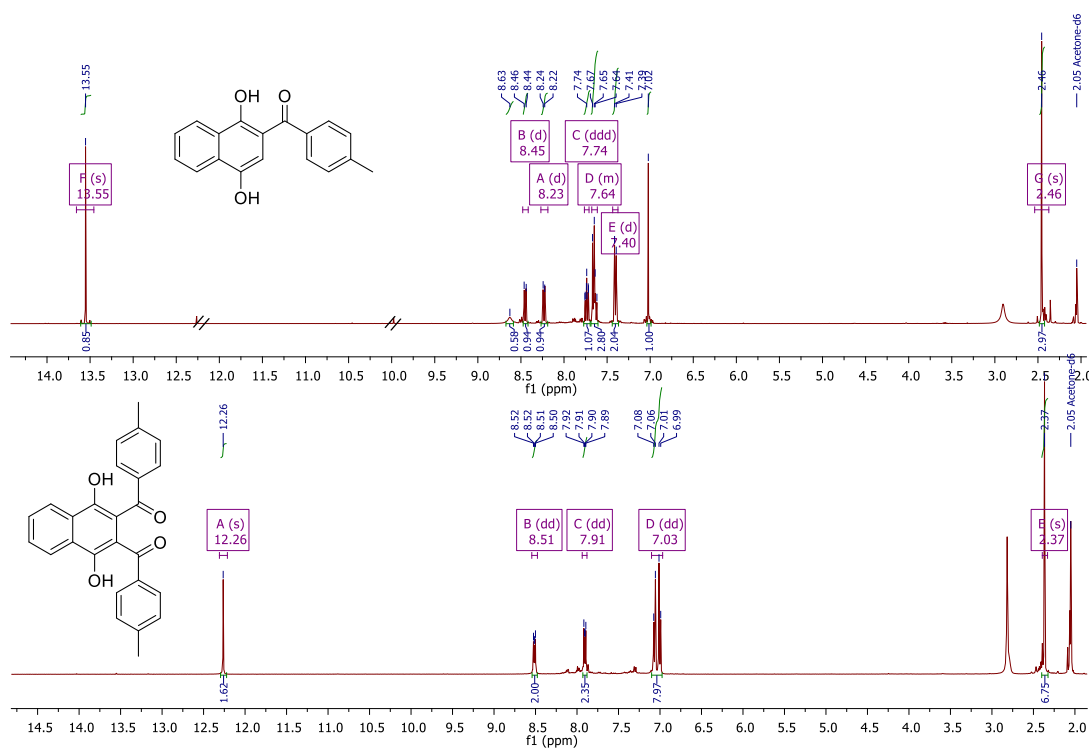


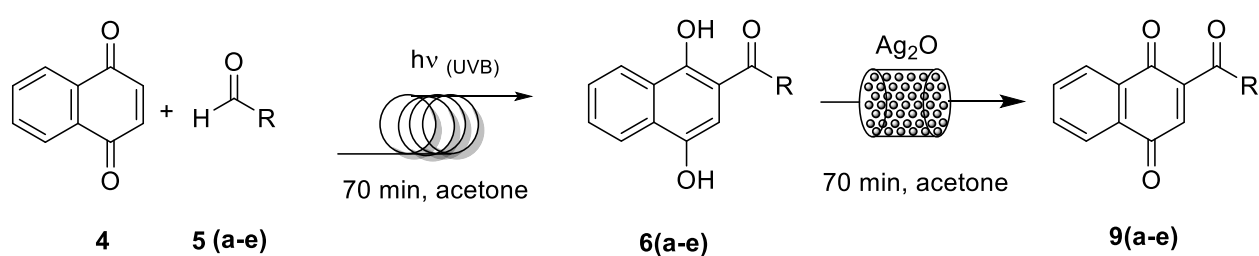
Figure 3.8: ^1H -NMR spectra of products **6f** and **8f** (in acetone- d_6).

The spectrum of the monoacylated **6f** shows three sharp singlets at 2.46, 7.02 and 13.55 ppm for the methyl group ($-\text{CH}_3$), the aromatic proton originating from the quinonoid proton and the hydrogen-bonded HO-group, respectively. A broad singlet at 8.63 ppm was found for the second, non-hydrogen-bonded hydroxyl group. The aromatic protons furnished five signals which appeared as three doublets of 7.40, 8.23 and 8.45 ppm, multiplets at 7.64 ppm and a doublet of a doublet of a doubled at 7.74 ppm. In contrast, the ^1H -NMR spectrum of the symmetrical biacylated product **8f** gave three pairs of doublets of doublets (dd) for all aromatic

protons at 7.03, 7.91 and 8.51 ppm, respectively. Also, two sharp signals were observed at 2.37 ppm and 12.26 ppm, respectively, representing the CH₃- and HO-groups at. Noteworthy, the HO-groups appeared at a lower chemical shift when compared to the monoacylated compound, suggesting a somewhat weaker intramolecular hydrogen-bond.

3.3.3 Multistep one-flow reaction

Continuous-flow operations can be easily combined in series, thus enabling multistep one-flow operations.⁹⁰ The photochemical-thermal tandem synthesis of a model acylated naphthoquinone was thus investigated by combining the photoacylation with a thermal oxidation step (**Scheme 3.6**). The oxidation was carried out *in-line* using a plunger cartridge loaded loosely with 10 g of solid Ag₂O. Selecting a flow-rate of 0.071 mL/min and thus a residence time of 70 min for both photoacylation step and oxidation step, the integrated assembly rapidly provided the target compounds with conversion rates of 15-94% over both steps (**Table 3.7**).



Scheme 3.6: Multistep one-flow reaction.

Table 3.7: Experimental results from the multistep one-flow reaction.

Entry	Aldehyde	R	Conversion (%) ^a
a	propionaldehyde	C ₂ H ₅	76
b	butyraldehyde	C ₃ H ₇	94
d	dodecylaldehyde	C ₁₁ H ₂₃	15
e	crotonaldehyde	CH ₃ CH=CH	75

^a determined by ¹H-NMR analysis (±3%).

As a typical example, the ¹H-NMR and ¹³C-NMR spectra of the desired acylated naphthoquinone **9b** are displayed in **Figure 3.9** and **Figure 3.10**.

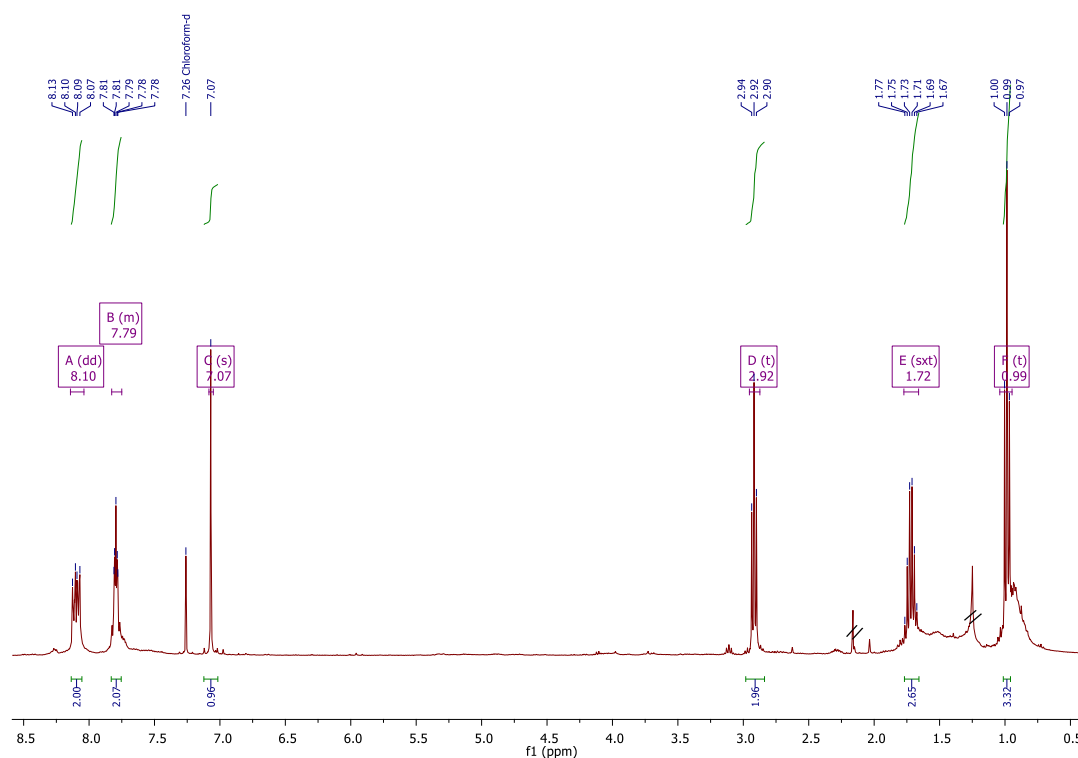


Figure 3.9: ^1H -NMR spectrum of acylated quinone **9b** (in CDCl_3).

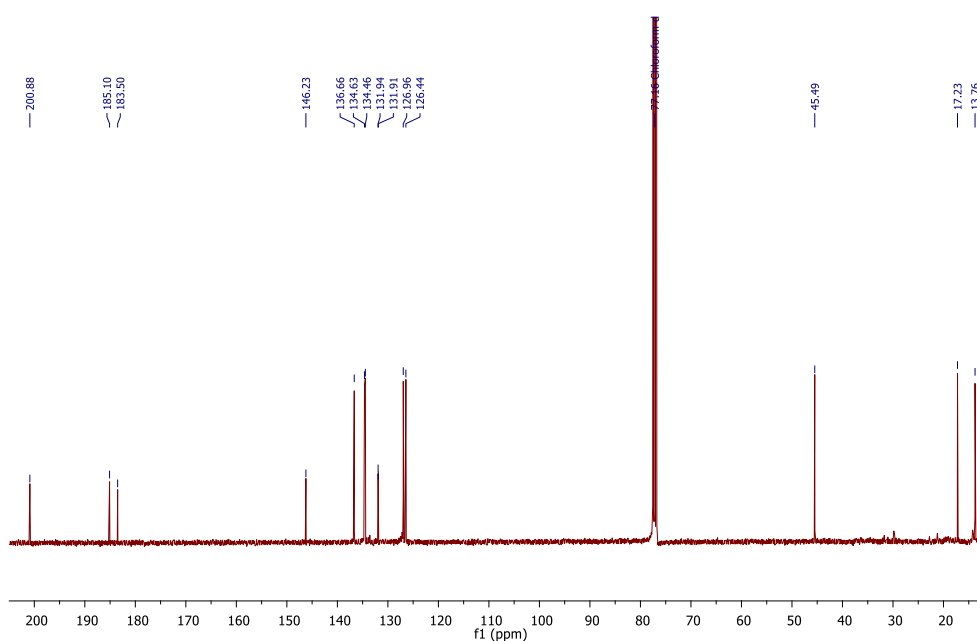


Figure 3.10: ^{13}C -NMR spectrum of acylated quinone **9b** (in CDCl_3).

In the ^1H -NMR spectrum, the aromatic signals appeared as a doublet of doublet at 8.10 ppm and a multiplet at 7.79 ppm, whereas the quinonoid signal showed a sharp singlet at 7.07 ppm. The $\text{CH}_3\text{CH}_2\text{CH}_2$ -group was found as two triplets at 0.99 ppm and 2.92 ppm and a sextet at

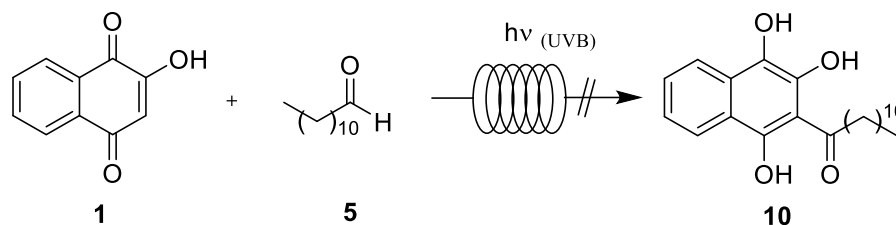
As the bisacylation of 1,4-naphthoquinone (**4**) was observed at UVC irradiation, directed photobisacylation of monoacylated product was furthermore investigated. Thus, irradiations of 2-acylated naphthohydroquinone (**6a**) with propionaldehyde (**5a**) and butyraldehyde (**5b**) were conducted with 419 nm light in acetonitrile for 5 hours (**Scheme 3.7**). Under these conditions, the ¹H-NMR spectrum of the crude product showed a symmetrical and unsymmetrical biacylation product along with undefined polymeric by-products (**Table 3.8**). Also, the conversion rates of these two reaction were low with 30 and 39%, respectively.



Entry	R	Conversion ^a	¹ H-NMR (ppm) ^b
a	CH ₂ CH ₃	30%	(CO <u>H</u>) 12.21
b	CH ₂ CH ₂ CH ₃	39%	(CO <u>H</u>) 12.21, 12.29

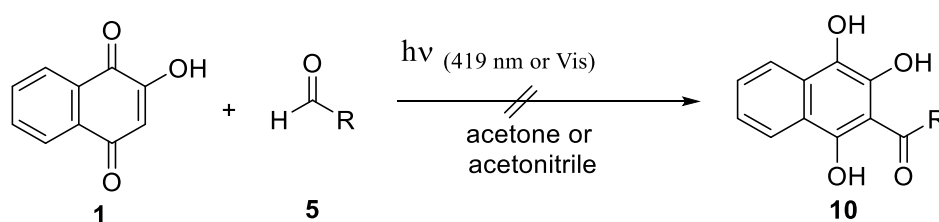
The successful outcomes of the in series multistep flow reactions encouraged us to investigate the synthesis of 2-dodecanoyl-3-hydroxy-1,4-naphthoquinone (DHN) with antibiotic

properties.⁹¹ Thus, 2-hydroxy-1,4-naphthoquinone (**1**) and dodecyl aldehyde (**5**) were first subjected to photoacylation under continuous flow conditions (**Scheme 3.8**). Unfortunately, no reaction towards the acylated hydroquinone **10** was observed.



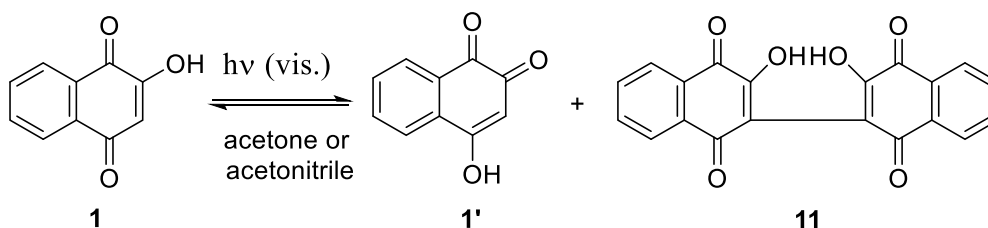
Scheme 3.8: Attempted synthesis of DHN in multistep one-flow reaction.

In order to probe for the general photoreactivity, the photoacylation of 2-hydroxy-1,4-naphthoquinone (**1**) was repeated under batch conditions in acetone or acetonitrile with the shorter propionaldehyde and butyraldehyde using a Rayonet reactor equipped with 419 nm or visible light (**Scheme 3.9**).



Scheme 3.9: attempted photoacylation of **1**.

Under all conditions, the photoirradiation of **1** with aldehydes did not show even trace amounts of the corresponding acylated hydronaphthoquinones **10**. Instead, photodimerisation and phototautomerization of 2-hydroxy-1,4-naphthoquinone **1** to **11** and **1'** was observed with visible light (**Scheme 3.10**).



Scheme 3.10: Photodimerization and tautomerism of 2-hydroxy-1,4-naphthoquinone (**11**).

The ^1H -NMR spectrum of the crude product showed a mixture of the two tautomeric forms of the starting material and the photodimer (**Figure 3.11**).

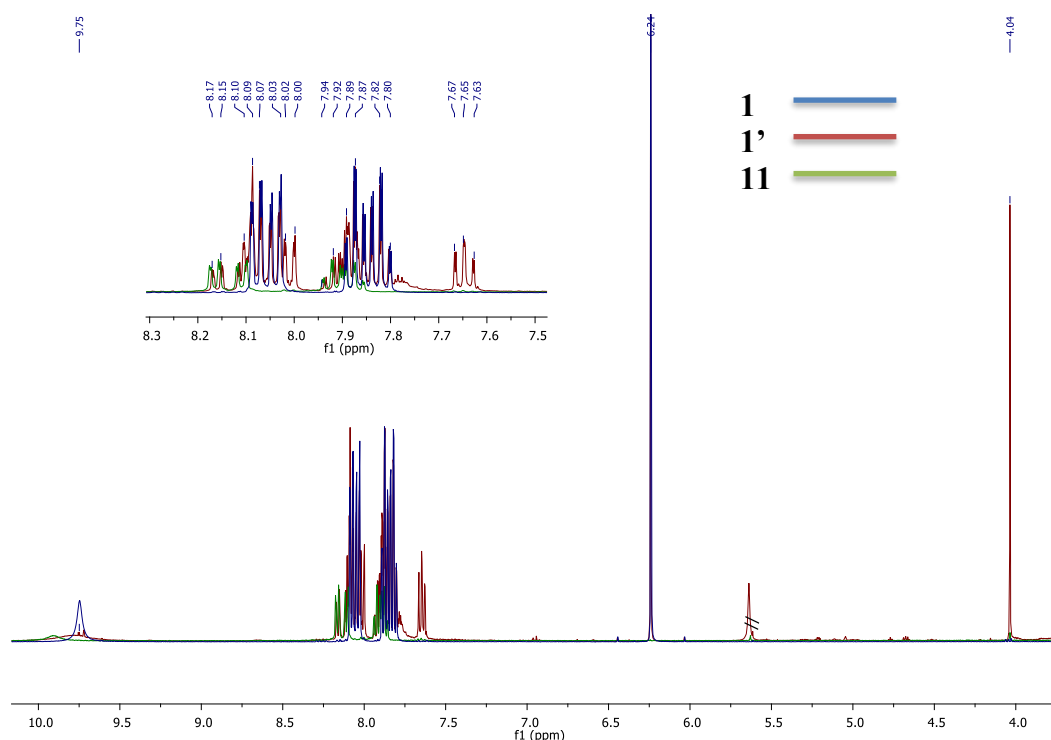


Figure 3.11: ^1H -NMR spectrum of photodimer and -tautomers of **1** (in acetone- d_6).

The β -hydrogen atoms of the tautomeric 2-hydroxy-1,4-naphthoquinone (**1**) and 4-hydroxy-1,2-naphthoquinone (**1'**) furnished sharp singlets at 6.24 ppm and 4.04 ppm, whereas their two hydroxyl protons appeared as a broad singlet at 9.78 ppm and 5.64 ppm, respectively. The downfield shift of the HO-proton at 9.78 ppm for the 1,4-isomer (**1**) is caused by an intramolecular hydrogen bond.⁹² The ratio of the tautomeric forms was determined by integration as 1:1.5 in favor of **1'**. A double of a doublet of a doublet (ddd) appeared at 7.65 ppm, representing the aromatic proton at C6 in the 1,2-tautomer **1'**. In contrast, the dimer **11** showed a characteristic doublet of a doublet at 8.16 ppm, while all other signals of the three compounds overlapped strongly between 7.80-8.12 ppm.

The photodimer (**11**) was subsequently precipitated with diethyl ether and was isolated as a fine yellow powder in a yield of 17% (m.p 280-282 $^{\circ}\text{C}$).⁹³ The identity of **11** was again confirmed by ^1H -NMR and ^{13}C -NMR spectroscopy (**Figure 3.12**). TLC- and ^1H -NMR analyses of the filtrate only indicated the presence of the tautomeric forms. Although column chromatographic

separation was subsequently attempted, 4-hydroxy-1,2-naphthoquinone (**1'**) was converted back to 2-hydroxy-1,4-naphthoquinone (**1**) due to its improved stability.⁹²

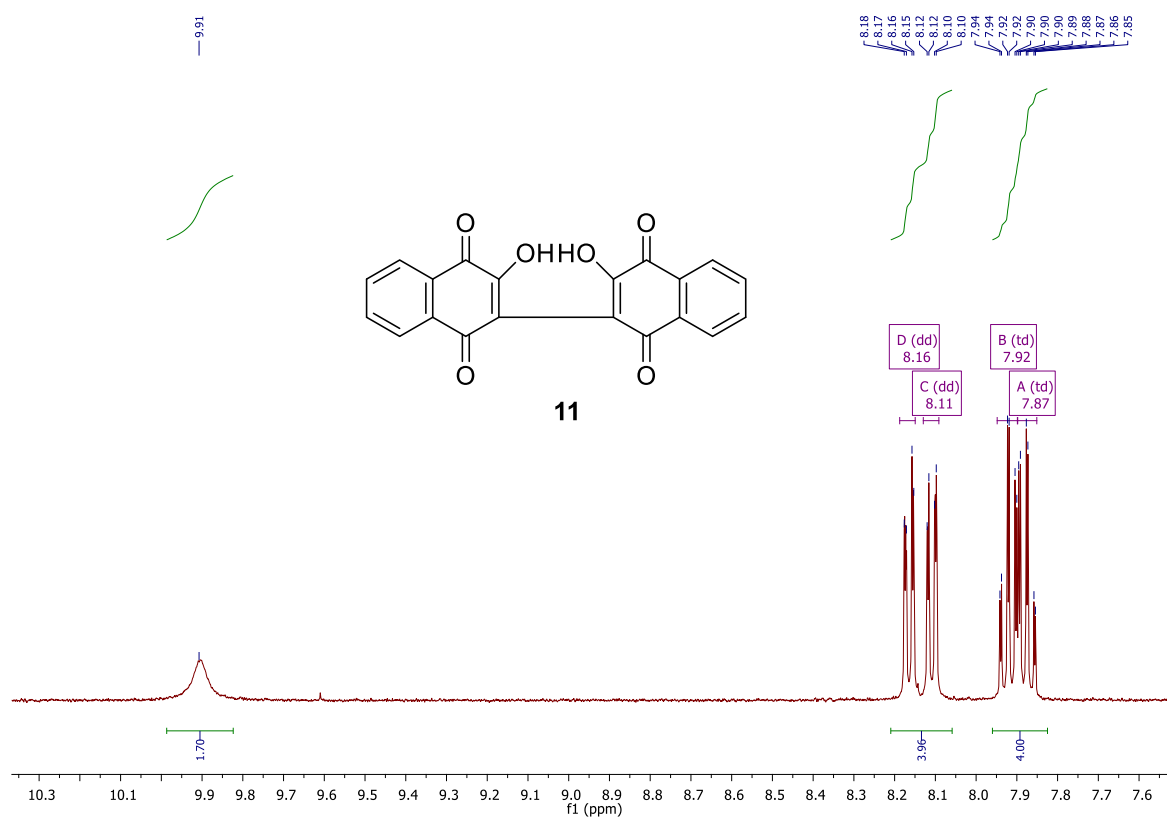
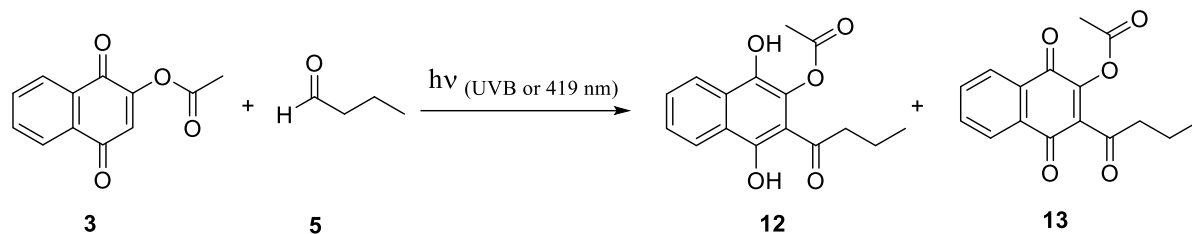


Figure 3.12: ¹H-NMR spectrum of **11** (in acetone-d₆).

3.3.6 Photoacylation of 2-acetoxy-1,4-naphthoquinone

Since 2-hydroxy-1,4-naphthoquinone did not undergo the desired photoacylation, its derivative 2-acetoxy-1,4-naphthoquinone (**3**) was investigated as an alternative access to the DHN target compound **10**. As the photochemical acylation of 2-acetoxy-1,4-naphthoquinone has not been reported yet, its photoacylation with butyraldehyde (**5**) was investigated under batch conditions in different organic solvents and with different lamps (**Scheme 3.11**). The results are shown in **Table 3.9**.



Scheme 3.11: Photoacylation of 2-acetoxy-1,4-naphthoquinone.

Table 3.9: Experimental results of the photoacylation of **14** with **5** under batch conditions.

Entry	Irradiation conditions	Solvent	Yield (%) ^a (12)
1	UVB, 28 hours	acetone	20
2	UVB, 28 hours	acetonitrile	48
3	419 nm, 28 hours	acetone	n.r. ^b
4	419 nm, 28 hours	acetonitrile	20
5	419 nm, 7 hours	trifluorotoluene	18 ^c (15 ^d)

^a Isolated yield of **12** after washing with hot water. ^b no reaction. ^c Precipitated in cold TFT. ^d Product **13** precipitated in cold ethanol.

For all irradiation conditions, the ¹H-NMR spectrum of the crude product showed the formation of the oxidized product **13** and undefined compounds as well. The desired acylated hydroquinone (**12**) was only formed in low yields. Due to the poor selectivity and the formation of numerous unknown photoproducts, the in-series synthesis was abandoned.

A representative ¹H-NMR spectrum for compound **12** is shown in **Figure 3.13**. The two broad singlets for the -OH group appear at 6.10 and 14.93 ppm, respectively. Characteristic peaks within the aromatic region were present as two pairs of doublets and doublets of doublets. The doublets were found at 8.40 ppm and 7.48 ppm, whereas the doublet of doublets showed at 7.60 ppm and 7.38 ppm. A sharp singlet at 2.50 ppm represents the three methyl protons of the ester group. The seven protons for the CH₃CH₂CH₂-group were observed as a sextet at 1.79 ppm and two triplets at 3.20 ppm and 1.02 ppm, respectively.

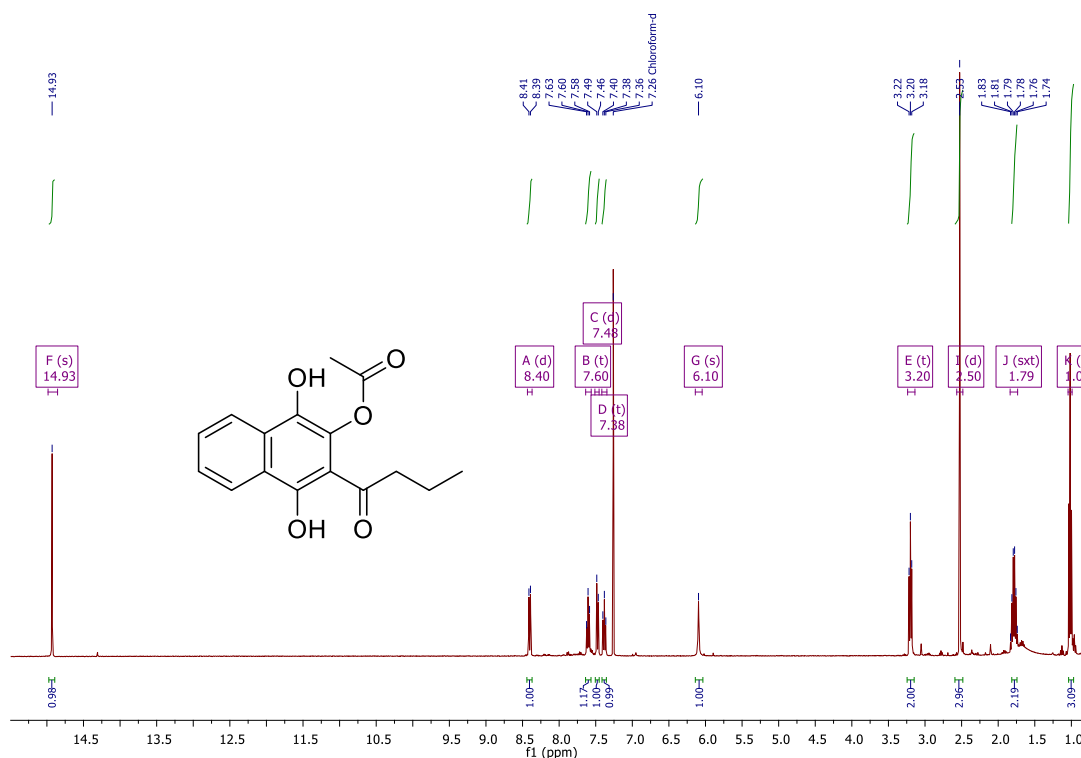
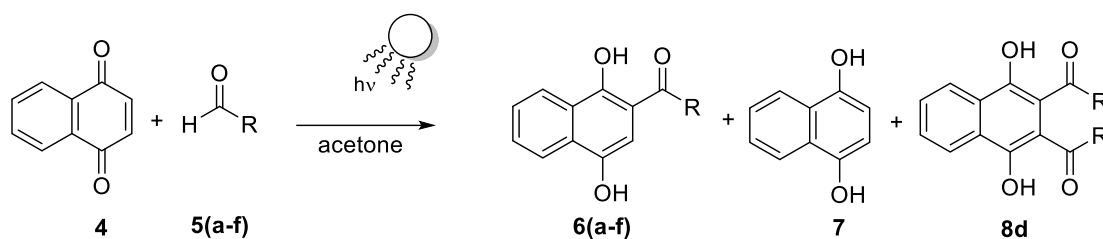


Figure 3.13: ¹H-NMR spectrum of 12 (in CDCl₃).

3.3.7 Solar photoacylations of 1,4-naphthoquinone

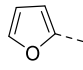
A series of illumination experiments of 1,4-naphthoquinone (**4**) with various aldehydes in acetone (**Scheme 3.12**), using the same concentrations as used for irradiations with artificial UVB light, were conducted in parallel in the solar float reactor (**Figure 3.5**) and the parabolic trough concentrating solar reactor (**Figure 3.6**). For comparison, each solarchemical reaction was executed under solar-batch and solar-flow conditions on the same day and during the same time period.

Batch reactions were carried out by placing reaction mixtures of 1,4-naphthoquinone (**4**) and aldehyde under direct sunlight for 200 min in test tubes inside a floating reactor. The exposed test tubes were fixed in a frame inside the solar float. Water from the surrounding pool entered the holding frame through a mesh on the bottom. Solar flow reactions used the same residence time of the indoor reactions of 70 minutes. The results of the solar illuminations are compiled in **Table 3.10**.



Scheme 3.12: Solar photoacylations of 1,4-naphthoquinone.

Table 3.10: Experimental results of photoacylation of 1,4-naphthoquinone with aldehydes in sunlight.

Entry	R	Reactor	Illumination time	Conversion ^a (%)	Yield (%)
a	C ₃ H ₇	Batch	200 min	68 (17)	60 ^b
		Flow	70 min	90 (7)	88 ^b
b	C ₁₁ H ₂₃	Batch	200 min	54 (10)	17 ^c
		Flow	70 min	66 (7)	22 ^c
c	CH ₃ CH=CH	Batch	200 min	41	40 ^d
		Flow	70 min	66	52 ^d
d	<i>p</i> -CH ₃ C ₆ H ₄	Batch	200 min	48	25 ^c
		Flow	70 min	58	44 ^c (5) ^e
e	<i>p</i> -ClC ₆ H ₄	Batch	200 min	63	34 ^d
		Flow	70 min	86	52 ^d
f		Batch	200 min	20	16 ^c
		Flow	70 min	80	n.d. ^f

^a Based on the ¹H-NMR analysis (±3%), bracketed conversions represent compound (7). ^b Isolated yield after washing by hot water. ^c After column chromatography. ^d Precipitated in cold chloroform. ^e Amount of bisacylation product **8**. ^f not determined.

Although the illumination periods were very short, conversion rates were between 41–90%. In comparison with the direct exposure in partially submerged test tubes, the flow process gave higher yields in shorter illumination times in all cases. Aliphatic aldehydes showed the formation of 1,4-hydronaphthoquinone (**7**) as a byproduct, while unsaturated and (hetero)aromatic aldehydes selectively furnished the acylated hydronaphthoquinones **6**.

3.4 [2+2]-Photocycloadditions of 1,4-naphthoquinones

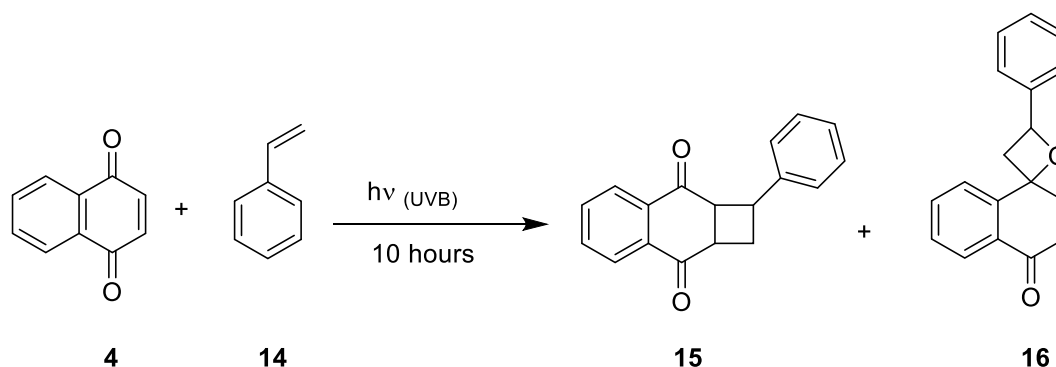
3.4.1 Photocycloaddition of 1,4-naphthoquinones under batch conditions

[2+2]-Photocycloadditions were carried out following a modified procedure described by Maruyama et al. by irradiating 1,4-naphthoquinone with excess alkene in an organic solvent in

a Rayonet photochemical chamber reactor (**Figure 3.2**).⁹⁴ The reaction mixtures were degassed with N₂ for approx. 5 min before capping of the reaction vessel. All photoreactions were monitored by TLC or by ¹H-NMR spectroscopy. The photocycloaddition of 1,4-naphthoquinone (**4**) with styrene (**14**) to the corresponding cycloadduct was initially used as a model system to investigate the reaction conditions. A number of parameters, *i.e.* the choice of solvent, wavelength, glass type and light source were optimized. The reaction protocols were subsequently extended to other [2+2] photocycloadditions of 1,4-naphthoquinone and 2-acetyloxy-1,4-naphthoquinones with a range of alkenes.

3.4.1.1 Solvent optimization

To optimize the reaction medium, solutions of 1,4-naphthoquinone (**4**, 1 mmol) and styrene (**14**, 5 mmol) in different organic solvents (50 mL) were irradiated with UVB light (300 ± 25 nm) in a Pyrex Schlenk flask (transmission >300 nm) for 10 hours. The general scheme of the reaction is shown in **Scheme 3.13** and the results are summarized in **Table 3.11**.



Scheme 3.13: Photocycloaddition of 1,4-naphthoquinone to styrene.

The photocycloaddition of 1,4-naphthoquinone with styrene showed two reaction pathways: cyclobutane vs. oxetane formation. The chemoselectivity depended on the solvent applied. For example, photoreactions by direct excitation of **4** in acetonitrile, trifluorotoluene and chloroform produced mixtures of the cyclobutane and spiro-oxetane. In contrast, potential triplet sensitization by acetone solely yielded 69% of the cyclobutane adduct. The photoreaction in methanol underwent rapid photoreduction instead.⁹⁵

Table 3.11: Experimental results of the solvent study

Entry	Solvent	Conversion ^a	Composition ^a		Yield ^b
			spiro-oxetanes	cyclobutane	
a	acetonitrile	88%	7%	93%	51%
b	trifluorotoluene	87%	6%	94%	58%
c	chloroform	100%	22%	78%	55%
d	acetone	96%	0%	100%	69%
e	methanol	photoreduction	-	-	n.d. ^c

^a Determined by ¹H-NMR analysis (±3%). ^b After automated flash chromatography. ^c not determined.

3.4.1.2 Light source and glass type study

In order to find the optimum procedure in terms of selectivity and yields, the impact of the wavelength of the lamps and the glass type of the reaction vessel was examined. Thus, a series of photocycloadditions in a Pyrex ($\lambda \geq 300$ nm) or quartz ($\lambda \geq 200$ nm) vessel was conducted with different UV light as well as visible light for 10 hours in different organic solvents (**Scheme 3.13**). The results are summarized in **Table 3.12**.

Table 3.12: Experimental results of the solvent and glass type study

Entry	Irradiation conditions	Solvent	Conversion ^a	Composition	
				Oxetane	Cyclobutane
a	visible light, Pyrex	acetone	73%	37%	63%
b	419±25 nm, Pyrex	acetone	89%	18%	82%
c	419±25 nm, Pyrex	trifluorotoluene	74%	19%	81%
d	419±25 nm, Pyrex	acetonitrile	69%	10%	90%
e	350 ± 25 nm, Pyrex	acetone	93%	5%	95%
f	300 ± 25 nm, Pyrex	acetone	96%	0%	100%
g	300 ± 25 nm, Quartz	acetone	96%	0%	100%
h	254 ± 25 nm, Quartz	acetone	91%	0%	100%
i	254 ± 25 nm, Quartz	acetonitrile	65%	0%	100%

^a Determined by ¹H-NMR analysis (±3%).

The experimental results again reveal the superiority of acetone as a solvent in terms of high conversion rates and selectivity. The combination of Pyrex-filtered light emitted from a UVB

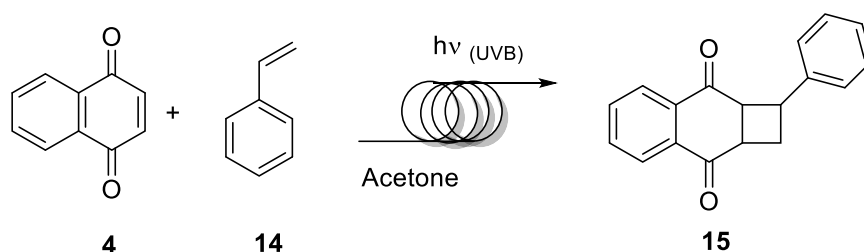
lamp and acetone as a solvent were found as ideal irradiation conditions for photocycloadditions. Therefore, this procedure was subsequently applied to other alkenes.

3.4.2 Photocycloaddition of naphthoquinone under continuous flow conditions

After optimizing the conditions in the batch system in terms of solvent, wavelength and glass type, a series of photoreactions were performed in the in-house continuous flow reactor (**Figure 3.3**) using the same reagents and concentrations. Although the photocycloaddition of para-quinones has been studied intensively, no reports of quinone photochemistry in continuous flow have been reported yet.

3.4.2.1 Residence time and flow rate study

Adopting acetone as a common solvent, a series of flow reactions of the model pair 1,4-naphthoquinone and styrene were carried out the in-house reactor equipped with a UVB lamp. The residence time and flow rate were optimized to achieve high conversions. The general scheme of the reaction is shown in **Scheme 3.14**. The conversion rates were determined by ^1H -NMR analysis, and the results are set out in **Figure 3.14**.



Scheme 3.14: Photocycloaddition of 1,4-naphthoquinone to styrene under continuous flow conditions.

As expected, increasing the residence time resulted in a higher conversion. Initial irradiation with a residence time of 15 minutes gave a conversion of 83%, which gradually increased by around 2% for every 5 minutes increase in residence time until the conversion rate reached 97%. Full conversion was not achieved even with prolonged residence times. As a result, the resident time of 45 minutes, achieved with a flow rate of 0.11 mL/min, was chosen as optimal. From this experiment, the corresponding adduct **15** was obtained in a high yield of 80%.

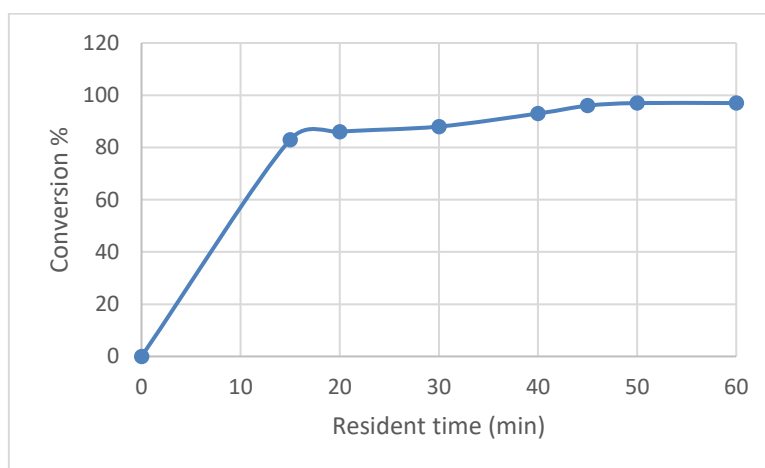


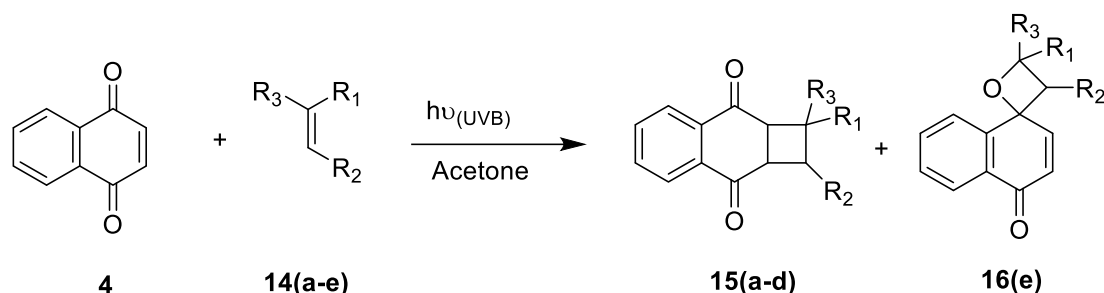
Figure 3.14: Conversion rate vs. resident time.

By transferring the reaction protocol from batch to flow conditions, a significant reduction in reaction times from 10 hours to 45 minutes was achieved in order to reach the same conversion rate. Flow operation was also found to be more economical in terms of the light source applied. In particular, the flow reactor utilized a single 8 W fluorescent tube. In contrast, the much larger Rayonet chamber reactor employed 16×8 W tubes.

Subsequently, additional [2+2] photocycloadditions of 1,4-naphthoquinone with different alkenes were conducted under continuous flow conditions in acetone to expand the product scope. To achieve high conversions and at the same time minimize any photodegradation, a residence time of 60 minutes, delivered with a flow rate of 0.083 mL/min, was furthermore chosen.

3.4.3 [2+2]-Photocycloadditions of 1,4-naphthoquinone to various alkenes

The irradiation procedures from the batch and continuous flow processes were consequently applied to a series of photocycloaddition reactions involving 1,4-naphthoquinone (**4**) with a range of alkenes. The general scheme of the photoreaction is shown in **Scheme 3.15**. A wide selection of alkenes was chosen to examine the chemoselectivity, *i.e.* spiro-oxetane vs. cyclobutane/cyclobutene formation. Examples selected included diarylethenes, cyclic alkenes, and aromatic alkenes. The corresponding photoadducts were obtained in low to medium yields after automated flash chromatography. The experimental findings obtained are shown in **Table 3.13**.



Scheme 3.15: Photocycloaddition of 1,4-naphthoquinone to alkenes.

Table 3.13: Experimental results of the reagent study.

Entry	Alkene	Reactor	Irradiation time	Conversion ^a	Yield ^b
a	styrene	batch	10 hours	96 %	69%(15a)
		flow	45 min	96%	84% ^c (15a)
b	cyclopentene	batch	13 hours	67%	50%(15b)
		flow	60 min	88%	73%(15b)
c	1,1-diphenylethylene	batch	12 hours	78%	42%(15c)
		flow	60 min	86%	60%(15c)
d	cyclohexane	batch	12 hours	84%	25%(15d)
e	<i>trans</i> -stilbene	batch	13 hours	40%	27%(16e)
		batch	6 hours	93%	78%(16e)
		flow	60 min	50%	47%(16e)

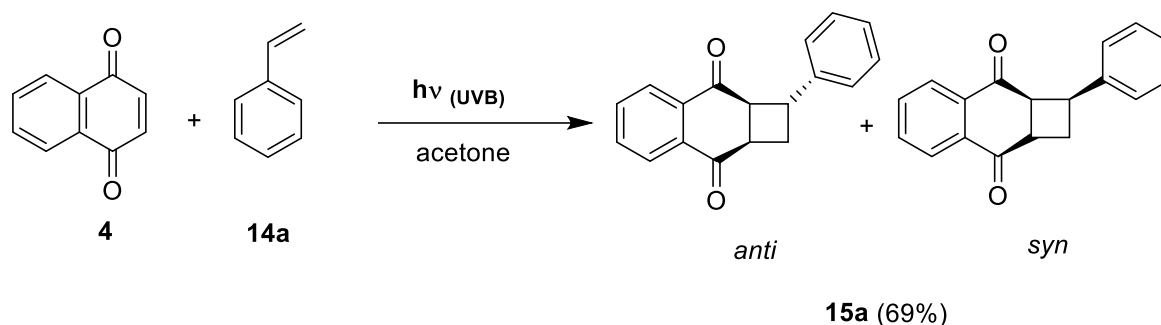
^a Based on ¹H-NMR analysis (±3%). ^b After automated flash chromatography. ^c After washing with hot water.

As can be seen in **Table 3.13**, the reaction of 1,4-naphthoquinone with styrene, cyclopentene, cyclohexane and 1,1-diphenylethylene resulted in cyclobutane formation, while *trans*-stilbene gave the spiro-oxetane exclusively.

3.4.3.1 Photocycloadditions of 1,4-naphthoquinone to styrene

1,4-naphthoquinone (**4**) was irradiated with styrene (**14a**) for 10 hours in acetone using Pyrex-filtered light from a UVB light (**Scheme 3.16**). The photoreaction gave a 2.8 : 1 mixture of the anti : syn isomers of the cyclobutane photoproduct **15a** in a combined yield of 69%. Bryce-Smith et al. reported a similar reaction in benzene using a medium-pressure mercury arc lamp and obtained cyclobutane at 40% with a stereoisomeric ratio of 2 : 1 instead.⁹⁶

Transfer of the reaction protocol from batch to flow conditions caused a significant reduction in reaction times from 10 hours to 45 min.



Scheme 3.16: Photocycloaddition of 1,4-naphthoquinone to styrene.

The ^1H -NMR spectrum of the crude photoproduct **15a** is depicted in **Figure 3.15**. The presence of the two isomeric products is evident from two complete sets of signals. The ratio of the isomers was determined by integration of the baseline-separated β -hydrogen atoms (labelled 25) in the cyclobutane ring for both isomers and was found to be 2.8 : 1 in favor of the *anti* isomer. The selected signal appeared at 3.46 ppm for the major stereoisomer, whereas the minor isomer occurred in the range of 3.63–3.69 ppm.

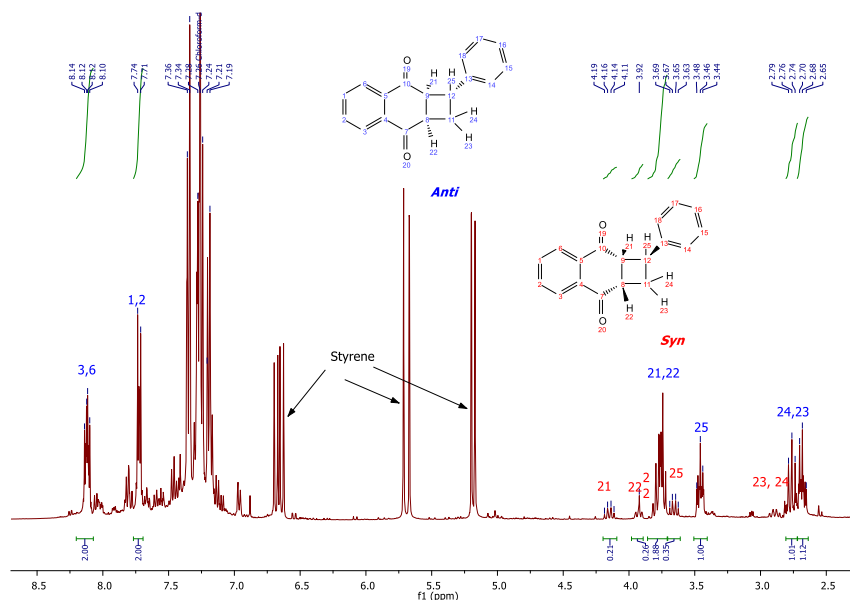


Figure 3.15: ^1H -NMR spectrum of a crude product **15a** (in CDCl_3).

The crude product was subsequently purified by column chromatography to obtain the pure isomeric mixture. The *anti*-isomer was subsequently crystallized from methanol while the *syn*-isomer was precipitated with TFT. The preference for the *anti*-isomer can be attributed to the

addition of the excited 1,4-naphthoquinone to the sterically most accessible face of styrene. The syn-isomer, which displays steric clashing between the phenyl group of styrene and the dihydronaphthoquinone ring system, would result from the approach to the more hindered face of styrene.

The structures of isolated isomers were unambiguously confirmed by NMR spectroscopy in comparison with literature data. The ^1H -NMR spectrum of anti-**15a** is shown in **Figure 3.16**. The five protons of the cyclobutane ring appear as four individual signals between 2.73–3.89 ppm. One doublet of a doublet of a doublet (ddd) at 2.76 ppm and a doublet of a doublet at 2.85 ppm with a germinal coupling of $^2J = 12$ Hz corresponded to the cyclic methylene group (CH_2). The third signal appeared as a doublet of a doublet of a doublet at 3.54 ppm while one multiplet at 3.85 ppm represented the two α -hydrogens on the dihydroquinonoid ring. Four separate signals were observed for the aromatic protons, two multiplets at approx. 7.25 ppm and between 7.31–7.37 ppm (phenyl protons), and two doublet of doublets at 7.81 ppm and 8.18 ppm, respectively.

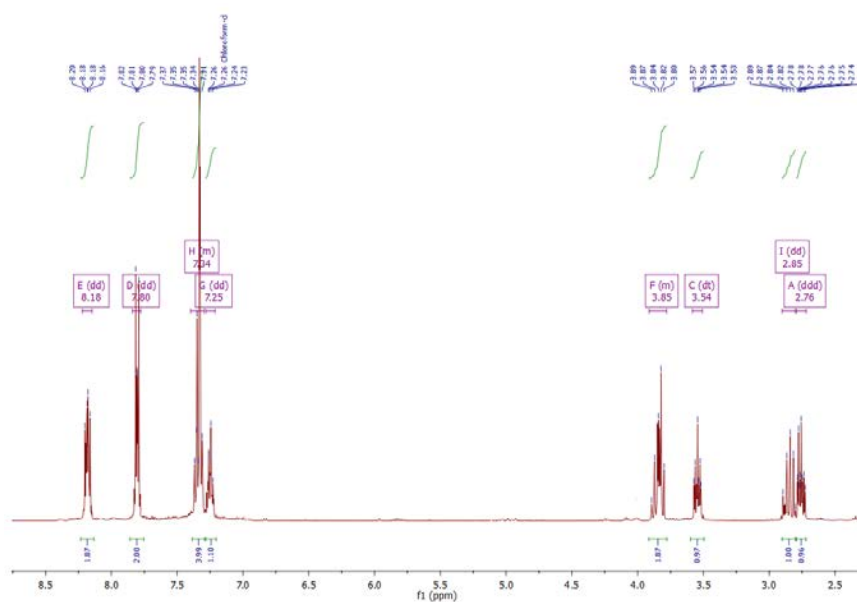


Figure 3.16: ^1H -NMR spectrum of an *anti*-**15a** on (in CDCl_3).

The structure of the major anti-isomer was furthermore established by X-ray crystallography (**Figure 3.17**). The conformation of the cyclobutane was puckered with bond angles between 87° and 88° . The five hydrogen atoms along the cyclobutane ring were not quite eclipsed, whereas the phenyl substituent occupied a pseudo-equatorial position.⁹⁷

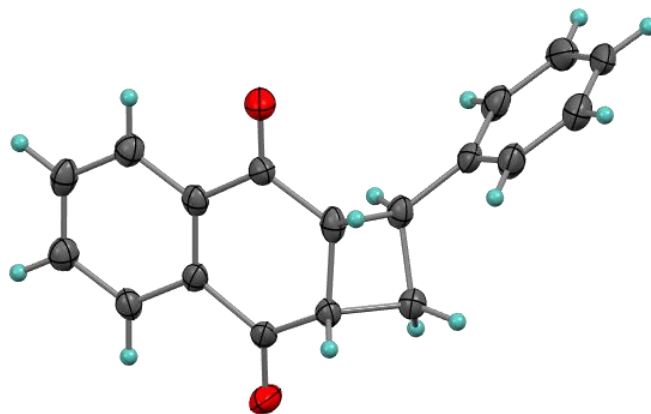


Figure 3.17: Crystal structure of *anti*-**15a**.

As the crystal structure of the *syn* isomer was not obtained, its ^1H -NMR spectrum was closely analyzed with respect to the coupling constants (J) of the cyclobutane system (**Figures 3.18 and 3.19**). The phenyl substituent and proton H^e occupied pseudo-equatorial positions while the protons H^a , H^b , H^d and H^c were placed in pseudo-axial positions. The cyclobutane system in the *syn* compound presumably adopted a more shallow conformation than its *anti*-counterpart as noticeable from the coupling constants of the ring protons. In particular, the $^3J_{\text{cis}}$ coupling constants were determined in the range of 8–10 Hz, corresponding to a dihedral angle close to 0° . The coupling constant of the trans-protons with $^3J_{\text{ec}} = 10$ Hz was larger than that of the cis-protons with $^3J_{\text{ed}} = 8$ Hz. The germinal coupling was determined from a pair of doublets of doublets (ddd) at 2.80 ppm and 2.92 ppm as $^2J = 12$ Hz, representing both protons of the methylene group (H^c , H^d). However, the ^1H -NMR spectrum showed two broad signals with a poor resolution for H^a at 4.24 ppm and H^b at 4.02 ppm.

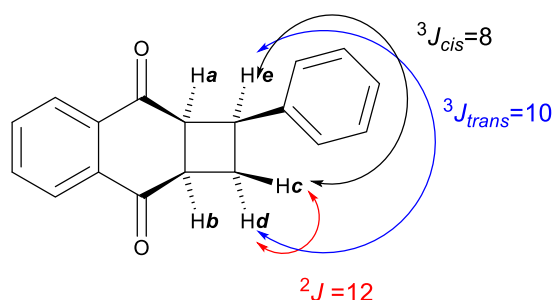


Figure 3.18: structure of *syn*-**15** isomer.

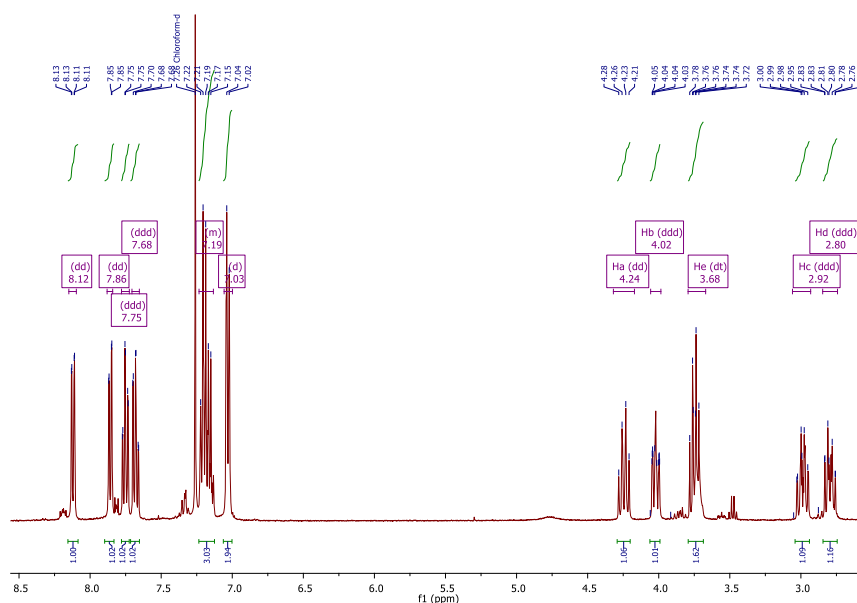
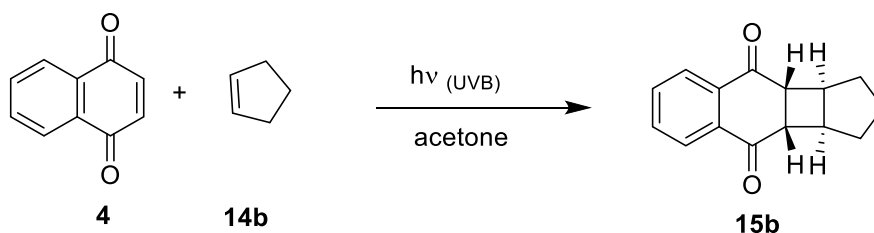


Figure 3.19: ¹H-NMR spectrum of *syn*-**15a** (in CDCl₃).

3.4.3.2 Photocycloadditions of 1,4-naphthoquinone to cyclopentene

Solutions of 1,4-naphthoquinone (**4**) with cyclopentene (**14b**) in acetone were irradiated in Pyrex Schlenk flasks in the Rayonet chamber reactor for 13 hours with UVB light, yielding predominantly a *cis* ring product **15b** in a yield of 50% after purification by column chromatography (Scheme 3.17).



Scheme 3.17: Photocycloaddition of 1,4-naphthoquinone to cyclopentene.

When operating this photocycloaddition in the in-house capillary reactor under the same reaction conditions, cyclobutane **15b** was obtained in an improved yield of 70% despite a reduced irradiation time of just one hour. The photoreaction was previously reported in benzene and produced the same isomer **15b** in a yield of just 10%.⁹⁶

The ¹H-NMR spectrum of the pure product **15b** in CDCl₃ is shown in Figure 3.20. The three bridging -CH₂-protons appear as unresolved multiplets at 1.62 ppm and 1.92 ppm, respectively.

The protons of the cyclobutane ring gave two doublets at 2.90 ppm and 3.08 ppm with $^3J_{\text{cis}}$ couplings of 4.4 Hz and 3.3 Hz, respectively. A pair of doublet to doublets at 7.77 ppm and 8.12 ppm represented the four aromatic protons.

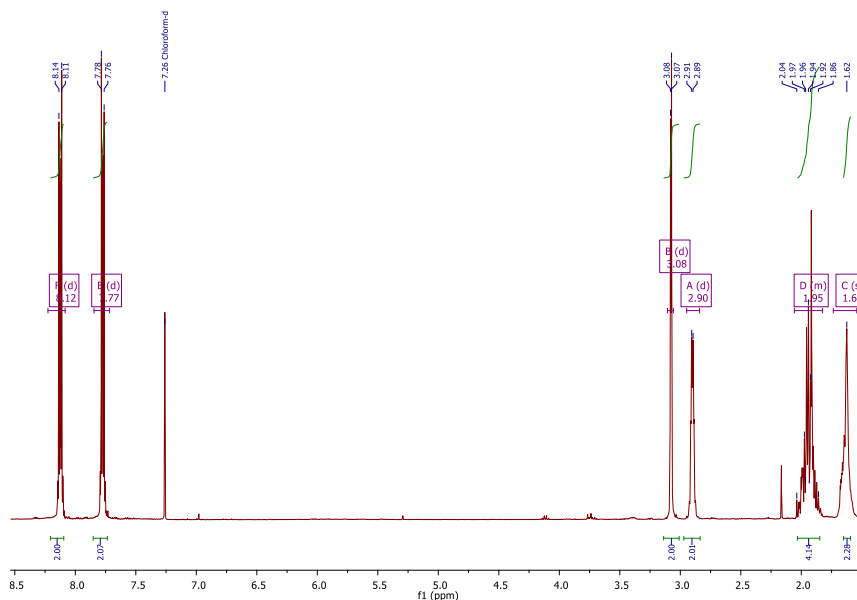


Figure 3.20: ^1H -NMR spectrum of **15b** (in CDCl_3).

The crystal structure of **15b** is shown in **Figure 3.21**. The cyclobutane adopted a more shallow conformation with all bond angles $>89^\circ$. The *cis*-protons appeared not completely eclipsed with dihedral angles of 7° and 6° , respectively. In contrast, the bond angles in a typical puckered structure have been determined to 88° and the dihedral angles to 28° .⁹⁷⁻⁹⁸ The cyclopentane ring adopted an envelope conformation with its ring protons in a skew conformation. The C–C–C bond angles varied from 103 – 106° , resulting in an asymmetrical envelope conformation.

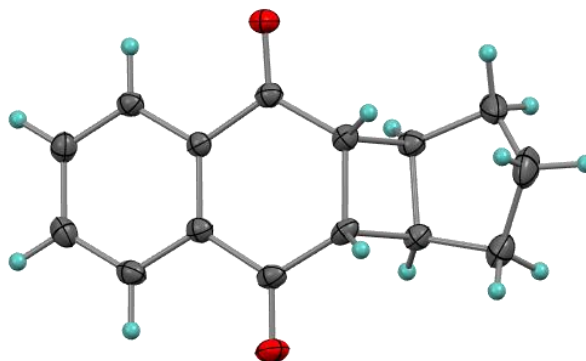
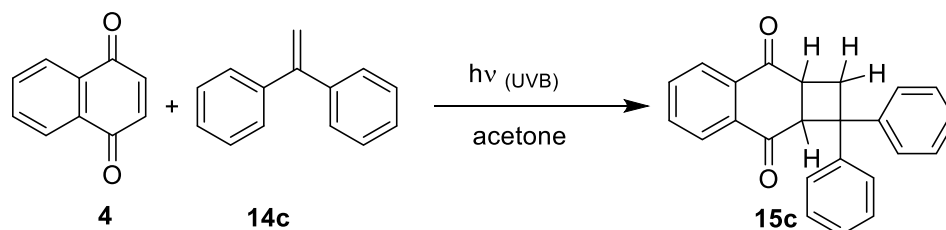


Figure 3.21: Crystal structure of **15b**.

3.4.3.3 Photocycloadditions of 1,4-naphthoquinone to 1,1-diphenyl ethylene

The photocycloaddition of 1,4-naphthoquinone (**4**) with 1,1-diphenyl ethylene (**14c**) was likewise carried out under batch and flow conditions in acetone using UVB light (**Scheme 3.18**). The reaction in the Rayonet chamber reactor required 12 hours and yielded the corresponding adduct **15c** in 42%. In contrast, **15c** was obtained in a superior yield of 60% with a residence time of 60 min under continuous flow conditions.



Scheme 3.18: Photocycloaddition 1,4-naphthoquinone to 1,1diphenyl ethylene.

The ^1H -NMR couplings and spectra of the pure adduct **15c** are shown in **Figure 3.22** and **Figure 3.23**. The four protons of the cyclobutane system displayed four signals between 3.10 ppm and 4.63 ppm. In particular, two doublets of doublets were observed for the methylene protons (H^a and H^b) at 3.13 ppm and 3.68 ppm with a germinal coupling of $^2J = 12.5$ Hz. A doublet of doublet of doublet at 3.56 ppm represented proton H^c with two cis couplings ($^3J_{cb}$ and $^3J_{ce}$) of 10.5 Hz and 8.8 Hz and one trans coupling ($^3J_{ca}$) of 2.9 Hz, respectively. Proton H^e appeared as a doublet at 4.62 ppm and the aromatic protons were present between 6.82 ppm and 7.98 ppm.

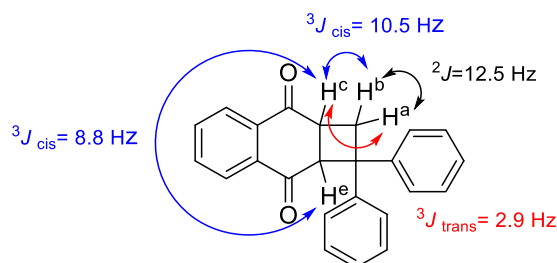


Figure 3.22: ^1H -NMR couplings in compound **15c**.

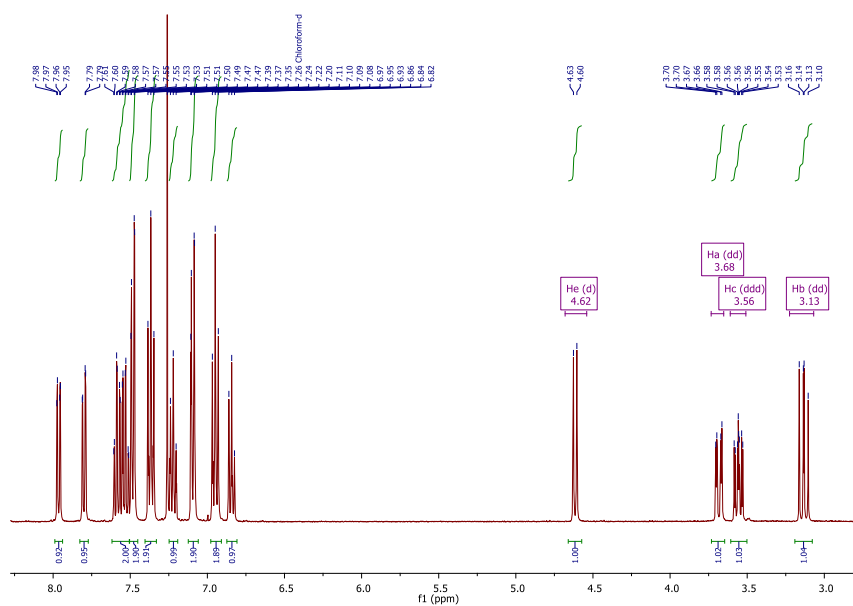


Figure 3.23: ^1H -NMR spectrum of **15c** (in CDCl_3).

The structure of product **15c** was furthermore confirmed by X-ray crystallography (**Figure 3.24**). The cyclobutane ring possessed a puckered structure with a dihedral angle of *ca* 14° . Four hydrogen atoms and one phenyl substituent were placed in pseudo-equatorial positions while the second phenyl ring occupied a pseudo-axial position. The bond angles were found between $87\text{--}90^\circ$, with the lowest one around the CPh_2 -carbon. The hydrogen atoms along the cyclobutane ring were not completely eclipsed. Overall, the data obtained from the X-ray analysis corresponded well with the NMR-data.

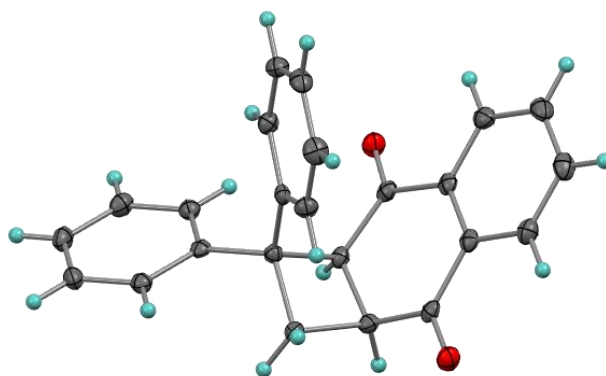
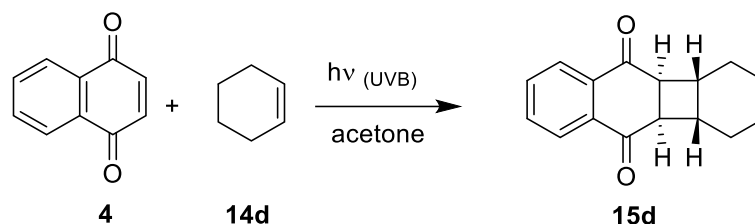


Figure 3.24: Crystal structure of **15c**.

3.4.3.4 Photocycloadditions of 1,4-naphthoquinone to cyclohexane

The photocycloaddition of 1,4-naphthoquinone (**4**) to cyclohexane (**14d**) was furthermore conducted in the Rayonet reactor with Pyrex-filtered UVB light (**Scheme 3.19**). After 12 hours of irradiation in acetone, cyclobutane adduct **15d** was obtained in a yield of 25 % after repeated purification. In contrast, NMR-analysis of the crude product revealed a good conversion of 84%.



Scheme 3.19: Photocycloaddition 1,4-naphthoquinone to cyclohexene.

The ^1H -NMR spectrum of **15d** is shown in **Figure 3.25**. Three broad signals with a poor resolution were observed between 1.61-2.69 ppm for the cyclohexane protons. The two *cis* protons of the cyclobutane revealed a narrowly spaced doublet of doublet at 3.35 ppm, whereas the four aromatic protons occurred at 7.76 and 8.14 ppm, respectively.

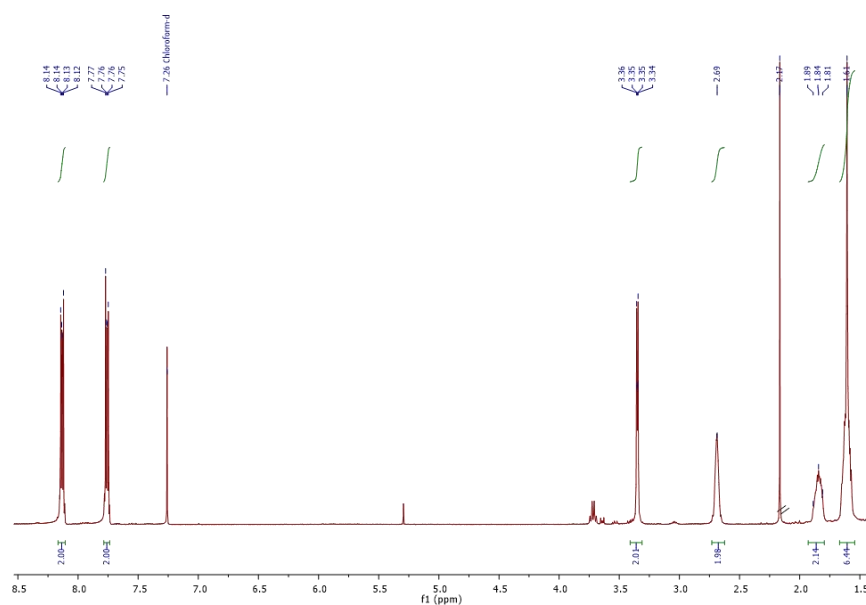


Figure 3.25: ^1H -NMR spectrum of **15d** (in CDCl_3).

The ^{13}C -NMR spectrum of **15d** in CDCl_3 is likewise shown in **Figure 3.26**. Overall, eight signals are observed owing to its symmetrical structure. The two ethylene bridges of the cyclohexane ring gave two peaks at 22.3 and 27.5 ppm, respectively. The aromatic CH-carbons furnished two signals at 127.4 and 134.4 ppm, whereas the quaternary carbons were found at 135.3 ppm. The remaining intact $\text{C}=\text{O}$ groups gave a signal at 197.8 ppm.

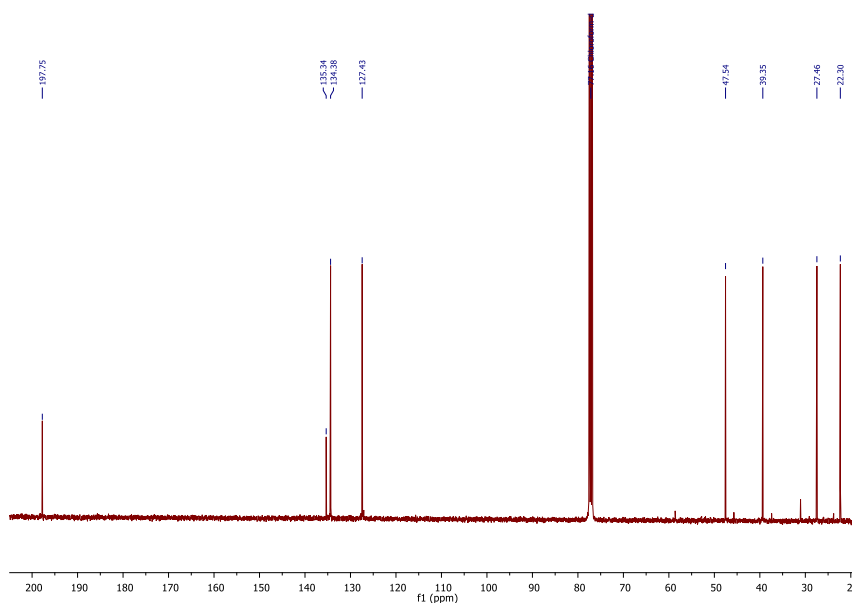


Figure 3.26: ^{13}C -NMR spectrum of **15d** (in CDCl_3).

The crystal structure of photoadduct **15b** is furthermore shown in **Figure 3.27**. The cyclobutane ring is somewhat less puckered with a dihedral angle of 22° , whereas the cyclohexane ring adopts a highly desirable chair conformation.

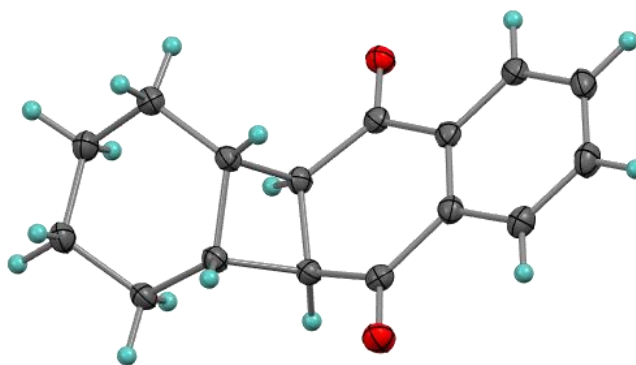
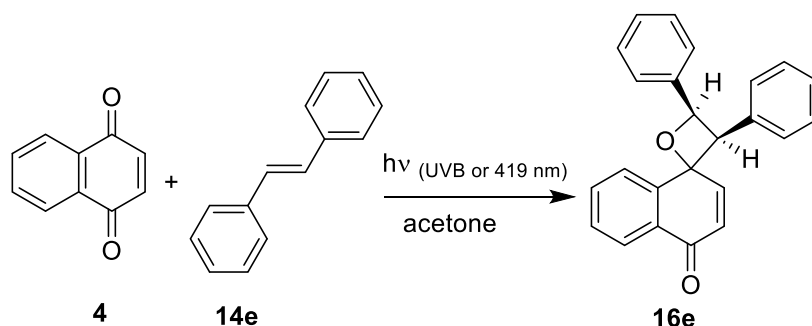


Figure 3.27: Crystal structure of **15d**.

The H⁷- and H⁸-atoms are placed in angular positions on the same side between cyclobutane and cyclohexane. In the cyclobutane, two types of C–H bonds were identified, pseudoaxial (H², H⁷) and pseudoequatorial (H⁸, H³). The puckered conformation of cyclobutane exhibited bond angles of 87–88°. The constraint imposed by the cis-fusion of the rings forced the cyclohexane ring to adopt a slightly distorted and flattened chair conformation. As a result, the bond angles are found in the range of 110–119°.

3.4.3.5 Photocycloadditions of 1,4-naphthoquinone with stilbene

The cycloaddition reaction of 1,4-naphthoquinone (**4**) with *trans*-stilbene (**14e**) in acetone was investigated using UVB and 419 nm light and exclusively gave the spirooxetane adduct **16e** in varying yields (**Scheme 3.20**).



Scheme 3.20: Photocycloaddition 1,4-naphthoquinone to stilbene.

When the photoreaction was initially carried out using Pyrex-filtered light from a UVB lamp, the crude product revealed the formation of phenanthrene as a result of an oxidative photocyclization of stilbene.⁹⁹ The spirooxetane product **16e** was nevertheless obtained in a yield of 27% under batch and 47% under flow continuous after column chromatography. When 1,4-naphthoquinone (**4**) was irradiated with 419 nm light in the presence of *trans*-stilbene (**14e**) in the Rayonet reactor, the photoreaction required a shorter reaction time and afforded a cleaner reactions.¹⁰⁰ Consequently, the photoproduct **16e** was obtained in a higher yield of 78% after purification by column chromatography.

The structure of the spirooxetane compound **16e** was confirmed by ¹H-NMR spectroscopy (**Figures 3.28**). The spectrum showed a pair of doublets for the oxetane protons at 4.64 ppm and 6.27 ppm. Likewise, the former quinonoid ring displayed a pair of doublets at 6.48 ppm

and 7.03 ppm, whereas the aromatic signals gave complex multiplets between 7.25 and 8.14 ppm.

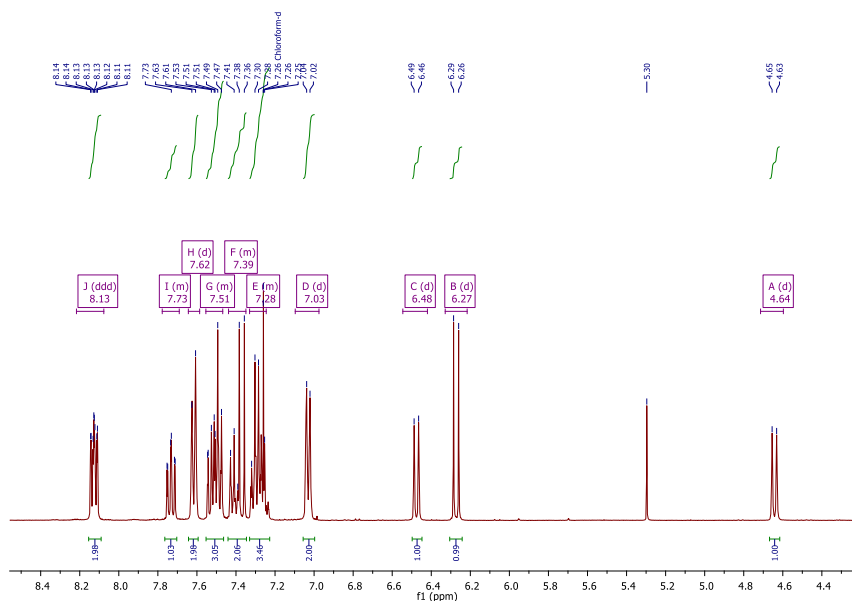


Figure 3.28: ¹H-NMR spectrum of **16e** (in CDCl₃).

In addition, the ¹³C-NMR spectrum is shown in **Figure 3.29**. The oxetane group furnished three signals at 62.5, 79.0 and 81.4 ppm, respectively. The sixteen aromatic signals were seen between 125.3 and 147.4 ppm, whereas the C=O groups gave a signal at 184.2 ppm.

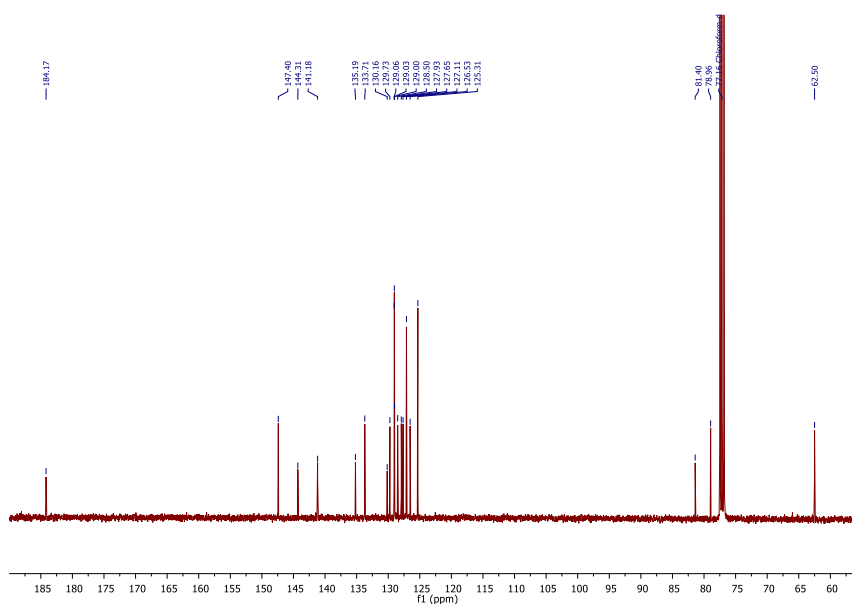


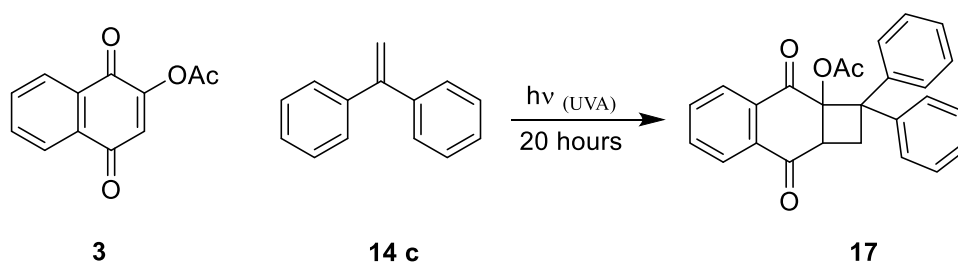
Figure 3.29: ¹³C-NMR spectrum of **16e** (in CDCl₃).

3.4.4 Photocycloaddition of 2-acetyloxy-1,4-naphthoquinone under batch conditions

Thus far, only three examples of [2+2]-photocycloaddition involving 2-acetyloxy-1,4-naphthoquinone (**3**) have been independently reported by Senboku,⁸⁰ Covell,⁸¹ and Cleridou.⁷⁸ To fill this gap, 2-acetyloxy-1,4-naphthoquinone (**3**) was used for selected cycloaddition reactions using the Rayonet chamber reactor.

3.4.4.1 Light and solvent optimization

The photocycloaddition of acetyloxy-1,4-naphthoquinone (**3**) with 1,1-diphenylethylene (**14c**) to the corresponding adduct was chosen as a model reaction for optimization. The general scheme reaction is shown in **Scheme 3.21**.



Scheme 3.21: Photocycloaddition of **3** with **14**.

A series of the irradiations with different UV and 419 nm light was subsequently performed in a Pyrex ($\lambda \geq 300$ nm) vessel in acetone or acetonitrile for 20 hours. The experimental results obtained are summarized in **Table 3.14**.

Table 3.14: Experimental results of photocycloaddition of **3**.

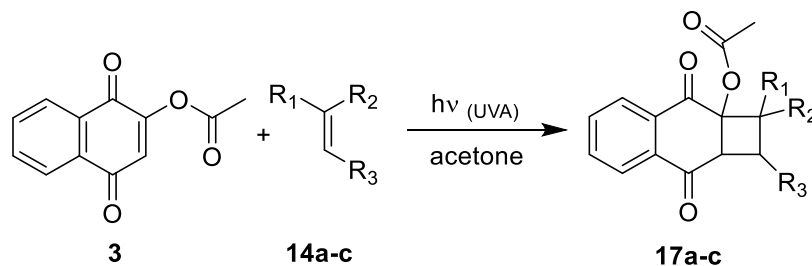
Entry	Irradiation conditions	Solvent	Conversion ^a
a	300 ± 25 nm, Pyrex	acetone	88%
b	300 ± 25 nm, Pyrex	acetonitrile	82%
c	419 ± 25 nm, Pyrex	acetone	78%
d	350 ± 25 nm, Pyrex	acetone	100%
e	350 ± 25 nm, Pyrex	acetonitrile	100%

^a Determined by ¹H-NMR analysis (±3%).

The photocycloaddition of 2-acetyloxy-1,4-naphthoquinone (**3**) to 1,1-diphenylethylene (**14c**) gave complete conversion in acetone and acetonitrile when irradiated with UVA (350 ± 25 nm). Due to its lower toxicity, the photocycloaddition of **3** in acetone was subsequently conducted with other alkenes using Pyrex-filtered light emitted from a UVA (350 ± 25 nm) lamp.

3.4.5 Photocycloaddition of 2-acetyloxy-1,4-naphthoquinone under continuous flow conditions

Using the optimized conditions developed in the batch system, photoreactions of 2-acetyloxy-1,4-naphthoquinone (**3**) with a series of alkenes were carried out in the in-house continuous flow reactor (**Figure 3.3**). The residence time and flow rate were optimized in order to achieve high conversions. The general scheme of the reaction is shown in **Scheme 3.22**. The conversion rates were determined by ^1H -NMR analysis, and the results are summarized in **Table 3.15**. The general regio- and chemoselectivity towards cyclobutane (**17**) formation was confirmed by NMR- and X-ray structural analyses.



Scheme 3.22: Photocycloaddition of acetyloxy-1,4-naphthoquinone with alkenes.

Table 3.15: Experimental results of alkene study.

Entry	Alkene	Reactor	Irradiation time	Conversion ^a	Yield ^b
a	styrene	Batch	10 hours	95%	69%
		Flow	120 min	97%	91% ^c
b	cyclopentene	Batch	12 hours	76%	21%
		Flow	100 min	36%	30%
c	1,1-diphenyl ethylene	Batch	20 hours	100%	50%
		Flow	300 min	100%	50%

^a Determined by ^1H -NMR analysis ($\pm 3\%$). ^b After automated flash chromatography. ^c After recrystallization.

The ^1H -NMR spectrum of product **17a** in CDCl_3 is shown in **Figure 3.30**. The four protons of the cyclobutane ring appeared as four individual signals, *i.e.* three doublets of doublets of doublets (ddd) at 2.59, 3.11, and 3.62 ppm and one doublet of doublet (dd) at 3.98 ppm, respectively. A sharp singlet at 2.00 ppm represented the methyl protons of the acetate group. Five separate signals were observed for the aromatic protons; two multiplets between 7.28-7.39 ppm (phenyl protons) and three doublet of doublets at 7.84, 8.21 and 8.28 ppm, respectively.

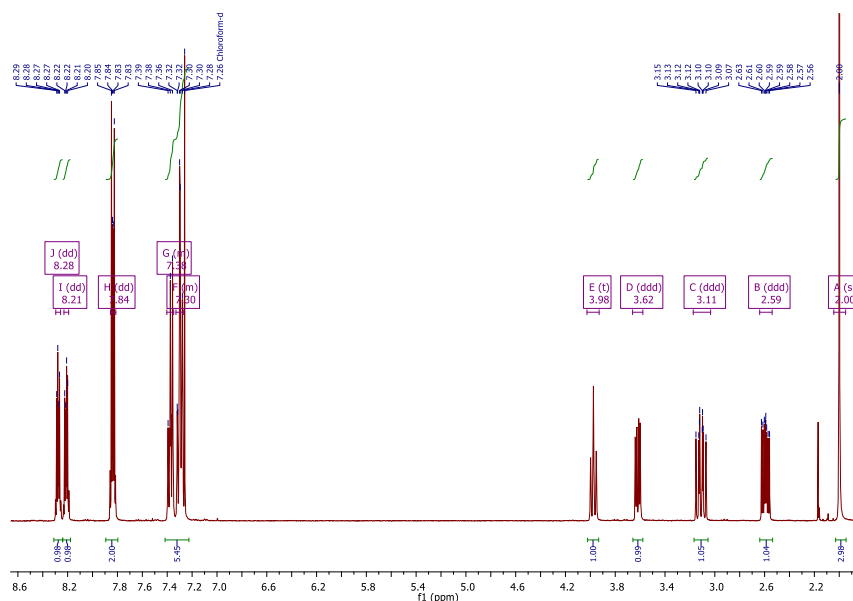


Figure 3.30: ^1H -NMR spectrum of **17a** (in CDCl_3).

The X-ray structure of the *head to head*-isomer revealed the cyclobutane as a slightly twisted ring, particularly on the side of the phenyl substituent where the bond angle was 87° . The puckered ring in **17a** led to a near eclipsed alignment between H^7 and H^{8A} with a torsion angle of around 9° (**Figure 3.31**).

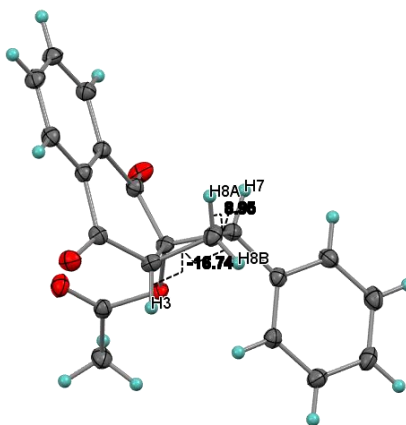


Figure 3.31: Crystal structure of **17a**.

The ^1H -NMR spectrum of **17b** is furthermore shown in **Figure 3.32**. The three bridging $-\text{CH}_2-$ protons of the cyclopentane ring appeared in poor resolution as one doublets at 2.38 ppm and two broad multiplets between 1.55 and 1.95 ppm, respectively. A sharp singlet at 2.11 ppm represented the acetate group. The protons of the cyclobutane moiety gave three signals, which appeared as doublet of doublets at 2.70 and 2.91 ppm and a doublet at 3.03 ppm, respectively. A set of three multiplets at 7.78, 8.10 and 8.17 ppm represented the four aromatic protons.

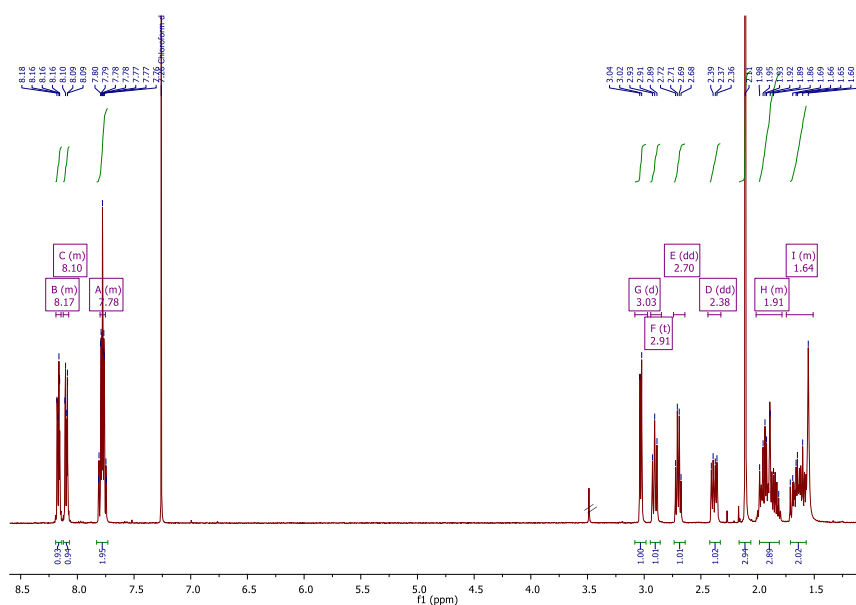


Figure 3.32: ^1H -NMR spectrum of **17b** (in CDCl_3).

The crystal structure of **17b** is depicted in **Figure 3.33**. The structure contained two different cycloalkane conformations. The cyclobutane ring remained rather shallow with bond angles of

$>89^\circ$. The *cis*-protons appeared not to be completely eclipsed with a torsion angle between H^9 and H^{10} of about 6° . The cyclopentane conformation of **17b** was similar to the one found in product **15b**.

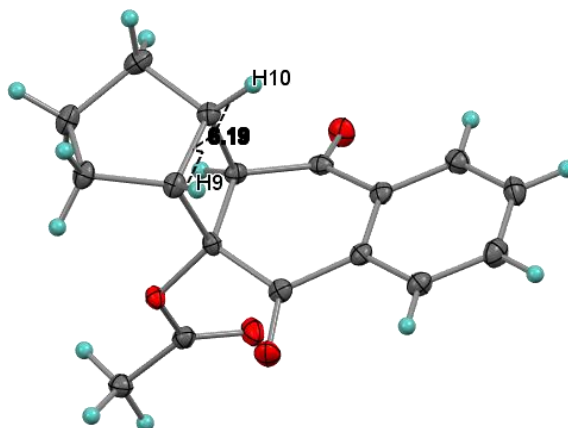


Figure 3.33: Crystal structure of **17b**.

The 1H -NMR spectrum of the pure adduct **17c** is furthermore shown in **Figure 3.34**. A sharp singlet at 2.08 ppm represented the methyl protons of the acetate group. The three protons of the cyclobutane system displayed signals between 3.10–4.63 ppm. A pair of doublet of doublets at 3.40 and 3.59 ppm with a germinal coupling of $^2J = 12.3$ Hz was observed for the methylene protons H^{10a} and H^{10b} , whereas a multiplet at 3.57 ppm represented the remaining proton. The aromatic protons appeared between 6.86 and 7.94 ppm.

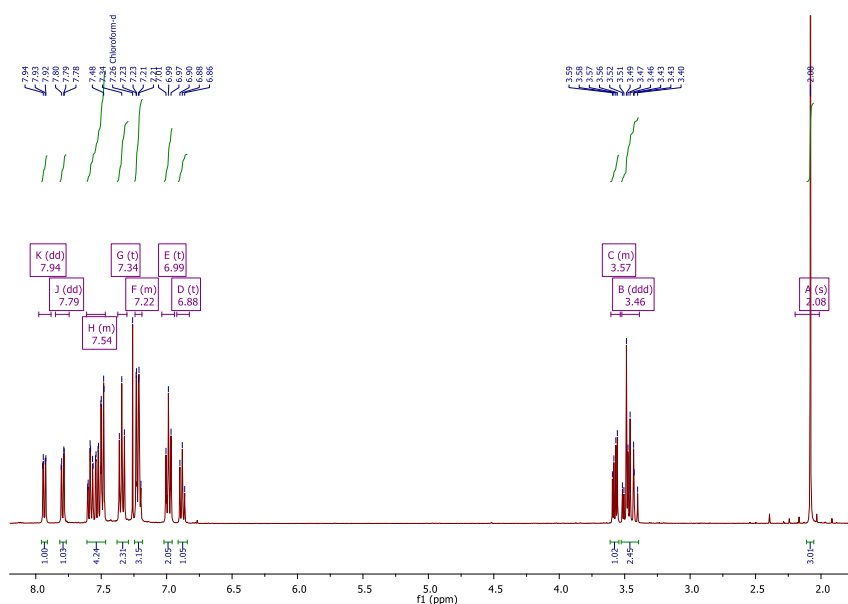


Figure 3.34: 1H -NMR spectrum of **17c** (in $CDCl_3$).

The *head to head*-structure of **17c** was additionally confirmed by X-ray crystallographic analysis (**Figure 3.35**). The puckered structure of the cyclobutane system resulted in bond angles in the range of 89-90°, except for the carbon carrying the phenyl substituents, which gave a bond angle of 87° instead. Two hydrogen atoms (H³ and H^{10a}) were placed at pseudo-equatorial positions with a dihedral angle of *ca* 14°.

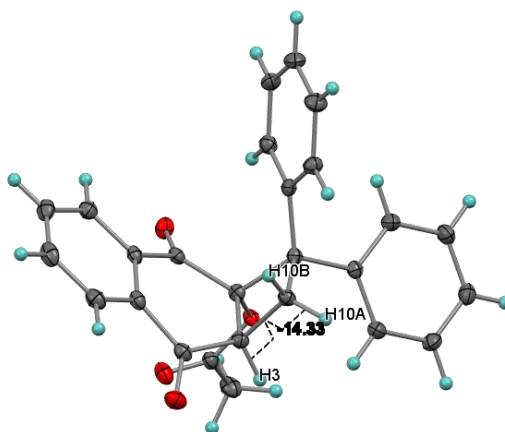
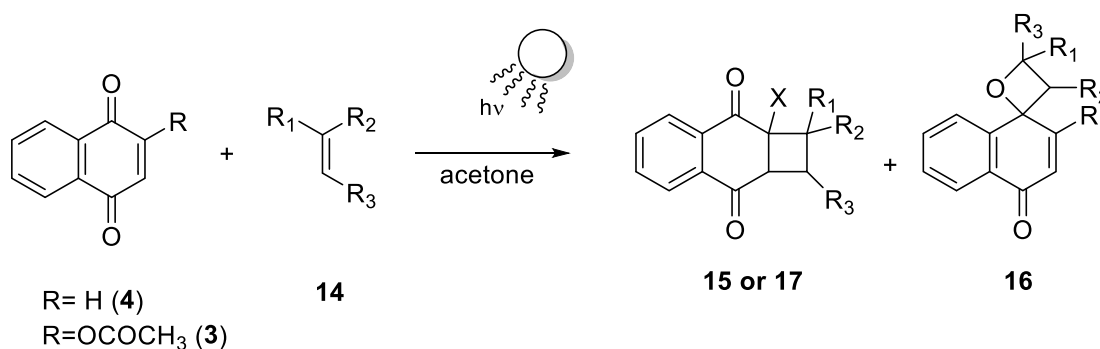


Figure 3.35: Crystal structure of **17c**.

3.4.6 Solar [2+2]-photocycloadditions of naphthoquinones

A series of illumination experiments of 1,4-naphthoquinone (**4**) or 2-acetyloxy-1,4-naphthoquinone (**3**) with alkenes in acetone (**Scheme 3.23**) were conducted simultaneously in test tubes inside the floating reactor and the parabolic trough concentrating solar reactor. The experimental results obtained are compared in **Table 3.16**.



Scheme 3.23: Solar photocycloaddition of naphthoquinone to alkenes

Table 3.16: Experimental results for solar photocycloadditions.

Date	X	Alkenes	Reactor	Illumination time	Conversion (%) ^a	Yield (%)
21/09/18	H	styrene	Batch	200 min	66	43 ^b
			Flow	70 min	79	65 ^b
24/09/18	H	1,1-diphenylethylene	Batch	200 min	46	20 ^c
			Flow	70 min	86	46 ^c
26/09/18	H	cyclopentene	Batch	200 min	71	43 ^d
			Flow	70 min	77	56 ^d
30/09/18	H	<i>trans</i> -stilbene	Batch	200 min	70	30 ^b
			Flow	70 min	78	n.d. ^c
18/12/18	OAc	styrene	Batch	200 min	35	29 ^d
			Flow	70 min	100	90 ^e
19/12/18	OAc	1,1-diphenylethylene	Batch	200 min	38	20 ^c
			Flow	70 min	83	36 ^b

^a Determined by ¹H-NMR analysis (±3%). ^b After automated flash chromatography. ^c n.d. = not determined. ^e recrystallized

3.4.7 Photocycloaddition of 1,4-naphthoquinones with diphenylacetylene

With the aim of expanding the reaction scope, the photoaddition of 1,4-naphthoquinone (**4**) and its acetoxy-derivative **3** with diphenylacetylene (**18**) was investigated. In general, the irradiations were carried out in acetone using Pyrex-filtered UVB-light for 1,4-naphthoquinone (**4**) or UVA-light for 2-acetoxy-1,4-naphthoquinone (**3**). The photocycloaddition of diphenylacetylene to naphthoquinones yielded a mixture for two types of adducts: benzoanthracenone (**19**) and cyclobutene (**20**). The general scheme of the reaction is shown in **Scheme 3.24** and the results are summarized in **Table 3.17**.

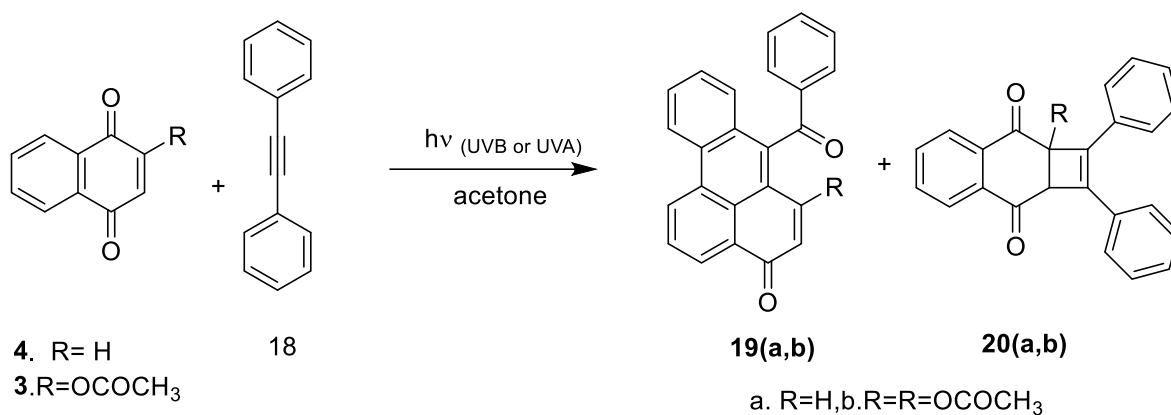
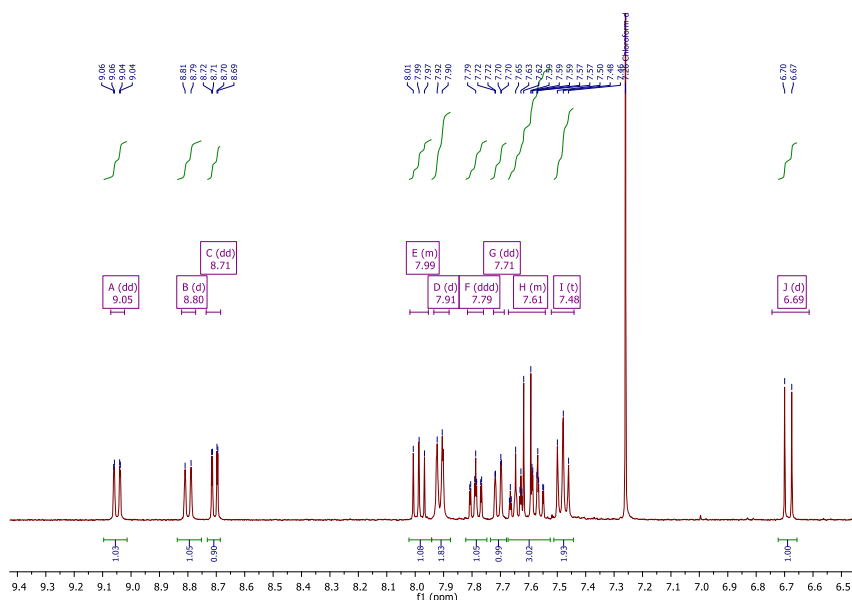
**Scheme 3.24:** Photocycloaddition of diphenylacetylene to naphthoquinones

Table 3.17: Experimental results of photocycloadditions with diphenylacetylene.

Entry	R	Time	19 [%] ^a	20 [%] ^a
a	H	12 hours	75	13
b	OCOCH ₃	10 hours	7	5

^a After automated flash chromatography.

The structure of the benzoanthracenone compound **19a** was confirmed by ¹H-NMR spectroscopy (**Figures 3.36**). The spectrum showed a pair of doublets for the olefinic protons at 6.69 ppm and 7.61 ppm. Also, the aromatic signals appeared between 7.48 and 9.05 ppm.

**Figure 3.36:** ¹H-NMR spectrum of **19a** (in CDCl₃).

The structure of product **19a** was furthermore confirmed by X-ray crystallography (**Figure 3.37**). The four aromatic rings of benzoanthracenone molecule were formed in one plane while the phenyl ring placed at a pseudo-axial position out of the plane with bond angle of *ca* 118°.

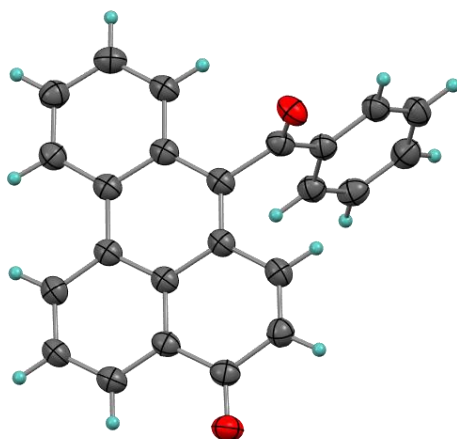


Figure 3.37: Crystal structure of **19a**.

The full ^1H -NMR spectrum of **20b** is shown in **Figure 3.38**. The five aromatic signals appeared as multiplets at 7.34, 7.58, 7.70, 7.94 and 8.12 ppm. The single cyclobutene proton showed a singlet at 4.34 ppm. A sharp singlet at 2.22 ppm represented the three methyl protons of the acetate-group. The structure of the cyclobutene adduct **20b** was furthermore confirmed by X-ray crystallographic analysis (**Figure 3.39**).

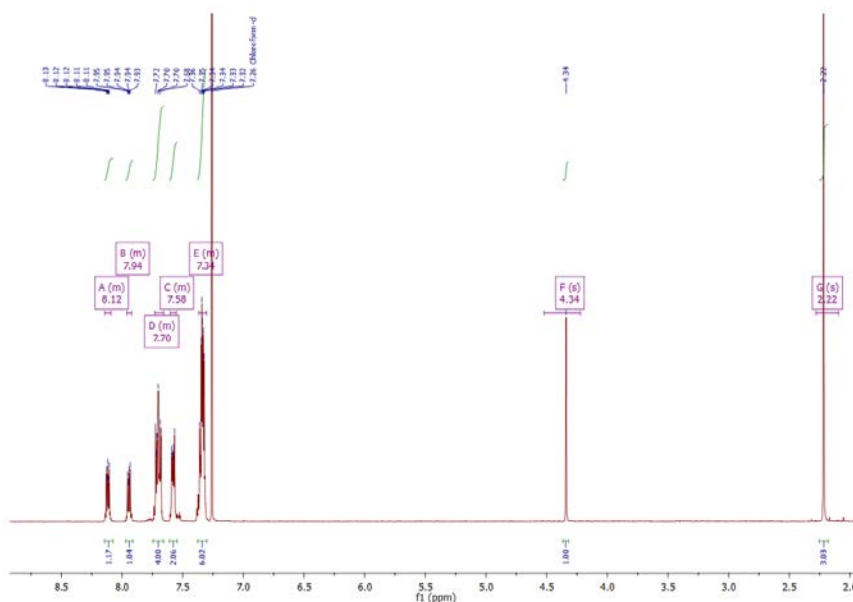


Figure 3.38: ^1H -NMR spectrum of **20b** (in CDCl_3)

The structure of **20b** was also confirmed by X-ray crystallographic analysis (**Figure 3.39**). The puckered structure of the cyclobutene system resulted in bond angles in the range of 85-92°.

Two phenyl groups were placed at pseudo-equatorial positions with a dihedral angle of *ca* 6°, while the hydrogen atom occupied a pseudo-axial position.

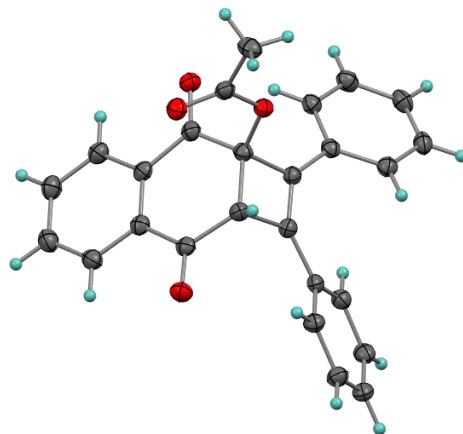


Figure 3.39: Crystal structure of **20b**.

Chapter 4: Discussion

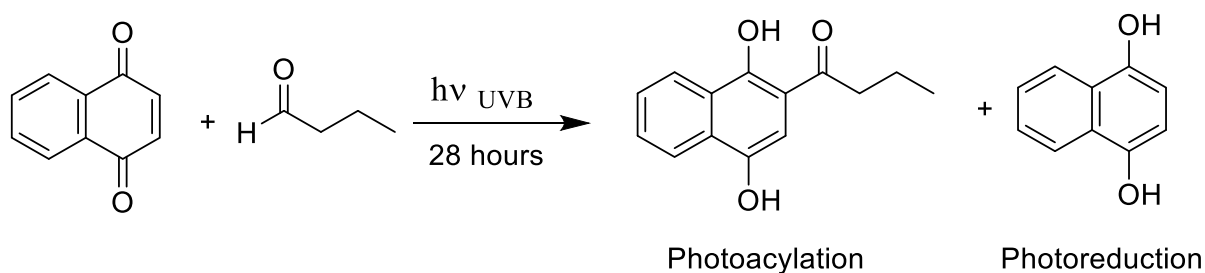
4.1 Photoacylation of 1,4-naphthoquinones

4.1.1 Photoacylation of 1,4-naphthoquinone under batch conditions

The photochemical reaction between 1,4-quinones and aldehydes has been investigated extensively due to the broad biological activity spectrum of their acylated hydroquinone products.¹⁰¹ Benzene and acetonitrile are ideal and common solvent for this photoreaction as they are chemically inert and transparent. However, both are toxic and should thus be avoided, especially for large outdoor scale. Although solvent optimization studies have been previously reported, they largely remain unsatisfactory, especially for outdoor applications in sunlight. For example, ionic liquids,¹⁰² supercritical CO₂,¹⁰³ microemulsions³⁶ and trifluorotoluene (TFT)⁸⁸ have been proposed as alternative ‘green’ solvents. Most of these alternative media are expensive or not practicable for large-scale or solar processes. Due to these limitations, a cheap, easy-to-use and environmental benign solvent for the photoacylation of naphthoquinones was still desirable.

4.1.1.1 Solvent optimization

The choice of solvent had an impact on the chemoselectivity. For the model system 1,4-naphthoquinone and butyraldehyde, the desired photoacylation was observed in all solvents. Solely alcoholic solvent additionally yielded photoreduction (**Scheme 4.1**). Photoreductions of quinones in alcohols are well known and are typically initiated by α -hydrogen-abstraction from the alcohol by the excited quinone.¹⁰⁴ Consequently, isopropanol furnished the highest degree of photoreduction. The presumed accompanying oxidation product, i.e. acetone, was not detected due to its volatility. Irradiations in both tertiary alcohols, i.e. *tert*-amyl alcohol and *tert*-butyl, also showed photoreduction, suggesting alternative hydrogen-abstractions from the β -positions in these alcohols.¹⁰⁵ Any follow-up products of these alcohols have again not been detected.



Scheme 4.1: Photoacylation of 1,4-naphthoquinone and butyraldehyde

The solvent can also impact on the photochemical activation pathway. Acetonitrile, trifluorotoluene, xylenes, *tert*-amyl alcohol, *tert*-butyl alcohol and isopropanol are photochemically inert under the given irradiation conditions. Direct excitation of naphthoquinone thus operates in these solvents. In contrast, acetone is commonly employed as a triplet sensitiser with its important n,π^* transition in the UVB-range and a high intersystem crossing quantum yield ($\Phi_{ISC}=1$).^{12,106} The triplet energy of acetone (333 kJ/mol) is greater than that of 1,4-naphthoquinone (241 kJ/mol). Thus, efficient triplet sensitisation of 1,4-naphthoquinone by acetone is energetically feasible (**Figure 4.1**).¹⁰⁷

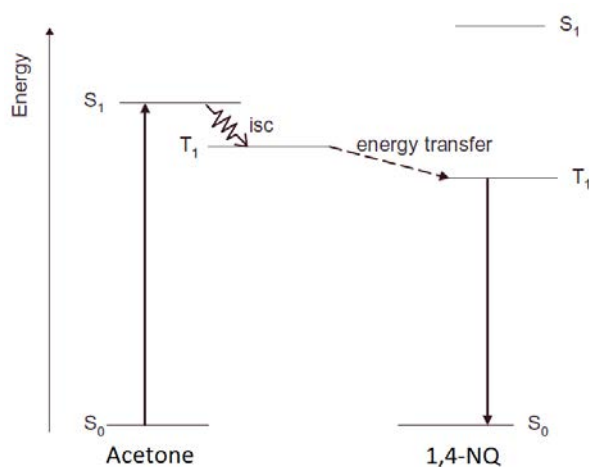


Figure 4.1: Triplet sensitization by acetone.

Lorna and co-workers suggested that acetone is unlikely to function as triplet sensitizer when the same photoacylation is conducted in a 3 : 1 mixture of *tert*-butanol and acetone, although no scientific explanation was provided. The authors simply argued that 1,4-naphthoquinone absorbs at longer wavelengths ($\lambda_{\max} = 331$ nm) than acetone ($\lambda_{\max} = 275$ nm).⁸⁸

In this study, acetone was used in without dilution by a co-solvent. Acetone is thus present in large excess compared to the 1,4-naphthoquinone reagent. Since 1,4-naphthoquinone is also consumed during the reaction, predominant light absorption by acetone can be assumed for irradiations conducted with UVB-light.^{8, 108} **Figure 4.2** shows the UV-spectra of acetone, 1,4-naphthoquinone and its photoacylation product in comparison with the emission of the UVB-fluorescent tube. The solvent shows the best and largest overlap. Acetone thus served as an effective solvent and triplet-sensitizer.

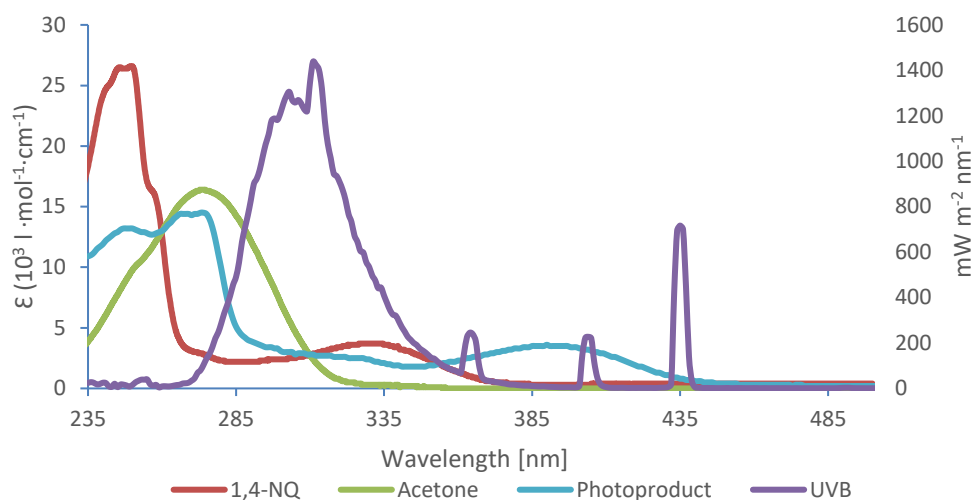
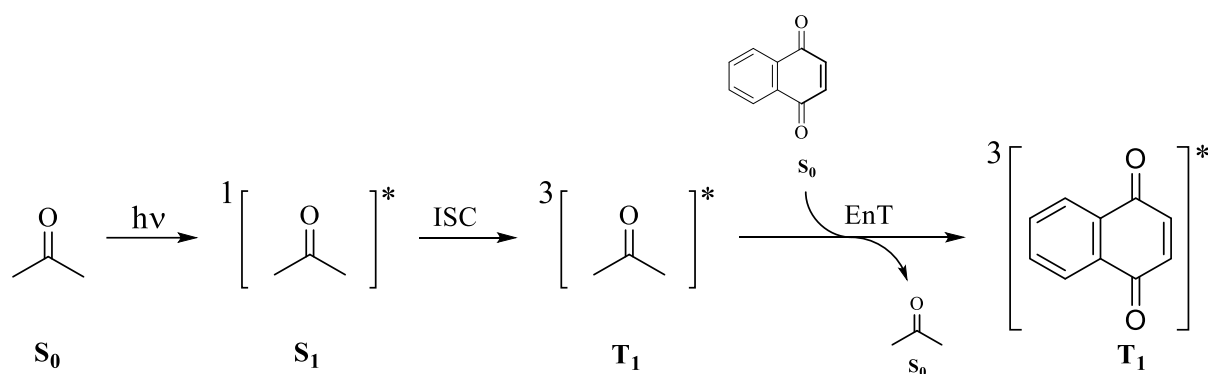


Figure 4.2: Comparison of UV-spectra (in MeCN) with emission of UVB-lamp.

The photoactivation scenario is depicted in (Scheme 4.2). The photoreaction is initiated by the absorption of light by acetone and subsequent population of its triplet excited state via intersystem crossing (ISC). Collision energy transfer (EnT) from the excited acetone to the naphthoquinone chromophore generates the corresponding triplet excited naphthoquinone.



Scheme 4.2: Photosensitization pathway.

Irradiation in trifluorotoluene and acetonitrile selectively afforded the photoproduct with complete and near complete conversion. The differences in efficiency may be best described by the solubility of the polar acylated hydronaphthoquinone photoproducts. Reagents and product remain completely dissolved in acetonitrile. Hence, the UV-active product can function as a filter agent. When comparing the UV-spectra obtained in acetonitrile shown in Figure 4.2, the absorption of the photoproduct indeed overlaps with the emission of the fluorescent tube.

Hence, the acylated hydroquinone competes for light absorption, especially at higher conversion rates. This inner filter effect may explain the incomplete reaction progress in acetonitrile. Maruyama and Miyagi determined the quantum yields for the photoacylation of 1,4-naphthoquinone with propionaldehyde with 425 nm light and noted a significant drop with increasing conversion. This decline in photon utilization was attributed to inner filter effects by the photoproduct.¹⁰⁹ Upon excitation, the photoproduct may undergo photochemical keto-enol tautomerisation, which reverts thermally. This behaviour is well known for the related 2-hydroxybenzophenones.¹¹⁰ In contrast, the photoproduct largely precipitated during the photoreaction in TFT due to its poor solubility in this solvent. Thus, light filtering by the product becomes no longer possible.

As mentioned above, alcoholic solvents furnished partial photoreduction by hydrogen-abstraction.^{84, 111} Rennert stated that photoreduction of 1,4-naphthoquinone most effectively occurs at the long-wavelength tail of the n,π^* absorption band at 436 nm, which was not covered by the emission of the UVB lamp.^{112,113} This may partially explain why photoacylation still operated as the dominant process.

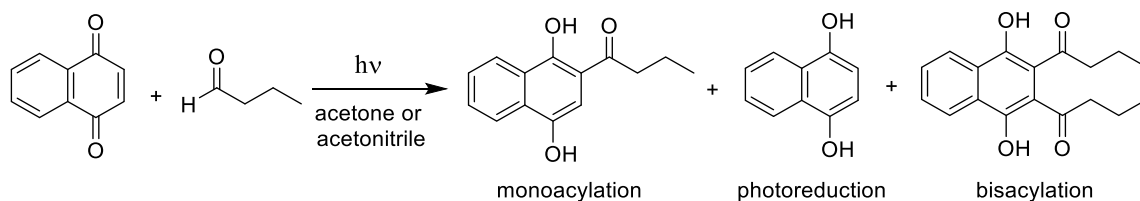
The photoreaction in xylene (mixture of isomers) proceeded surprisingly selective but only gave a moderate conversion and isolated yield. It was initially assumed that photoreduction would compete with the desired photoacylation pathway, as known for toluene.¹¹⁴ Due to its high boiling point range of 137-140°C,¹¹⁵ the complete removal of xylenes remained challenging, especially for more heat sensitive compounds.

The photochemical reaction of 1,4-naphthoquinone and aldehyde under direct excitation can proceed via two possible pathways (**Scheme 4.3**). The ‘in-cage’ scenario, which was first reported by Schenck and was later extended by Maruyama, proposed the formation of a caged triplet biradical. This is followed by the in-cage coupling of biradicals that furnish the acylated product.¹⁰⁹ An alternative ‘out-of-cage’ scenario was first suggested by Moore and later supported by Bruce and co-workers. This mechanism postulates separation of the triplet biradical pair and subsequent addition of the acyl radical to another ground state quinone.¹¹⁶

4.1.1.2 Wavelengths study

This study continued the work by Friedrichs et al. by including additional wavelengths and the glass type of the reaction vessel. Therefore, the series of photoacylations of the naphthoquinone-butyraldehyde model pair (**Scheme 4.4**) was conducted in Pyrex or quartz vessels with different wavelengths. The outcome of the reaction in terms of selectivity and conversion strongly depended on these conditions. Irradiation with visible light in TFT showed very limited photoactivity, whereas a change to acetone gave substantial photoacylation. Notably, photoreduction was observed in quartz vessels upon irradiation in acetone and

acetonitrile with UVB and in particular UVC light. In contrast, bisacylation was only observed when UVC light was utilized.



Scheme 4.4: Chemoselectivity of photoacylation of 1,4-naphthoquinone with butyraldehyde.

The general photoreactivity can be linked to the absorption spectra of the starting material, the photoproduct and the solvent as well as the emission spectrum of each fluorescent tube. Excitation is only possible if lamp emission matches the absorption of a particular compound. In acetonitrile solution, 1,4-naphthoquinone exhibited strong absorptions with λ_{max} at 246 and 331 nm and extinction coefficients (ϵ) of 26×10^3 and 3.6×10^3 L/(mol . cm), whereas a very weak absorption was noted ~ 430 nm. In *n*-hexane, the spectrum of 1,4-naphthoquinone was reported to show absorptions (λ_{max}) at 246, 330 and 425 nm with extinction coefficients of 24×10^3 , 3.2×10^3 and 50 L/(mol . cm), respectively.¹¹⁷⁻¹¹⁸ Of these, the n, π^* absorption in the visible range at 425 nm was sought to be the most important one for photochemistry. The π, π^* transition at 330 nm has been assigned to both, the quinonoid and benzenoid transition. In contrast, the π, π^* transition at 246 nm has been assigned as a combination of a quinonoid transition at 264 nm and a benzenoid transition at 241 nm, respectively.¹¹⁹ The recorded spectrum in acetonitrile largely aligned with the reported data in *n*-hexane. In contrast, the acylated naphthohydroquinone showed strong absorption bands with λ_{max} at 248, 275 and 394 nm and extinction coefficients of 13×10^3 and 14×10^3 and 3.5×10^3 L/(mol . cm), respectively. Friedrichs et al. also recorded the UV-spectrum of the related photoproduct obtained with propionaldehyde in methanol and reported a strong absorption in the 350-450 nm range with a λ_{max} at ~ 390 nm and an ϵ value of $\sim 5.9 \times 10^3$ L/(mol . cm).

4.1.1.2.1 Visible light

Although the visible lamp showed emission above 365 nm that overlapped with the n, π^* absorption of 1,4-naphthoquinone at approx. 430 nm (**Figure 4.3**), this did not result in any significant photochemical activity. In contrast, the poor overlap with the absorption of acetone did effectively initiate photoacylation. This differing behaviour suggests different photochemical activation pathways. Acetone must behave like a sensitizer for naphthoquinone,

but it may populate a higher triplet state (T_n). For TFT, direct excitation generates the lowest lying triplet T_1 state via intersystem crossing from the S_1 state. Under the given reaction conditions, this T_1 state may be deactivated prior to any subsequent (thermal) reaction step. Interactions between naphthoquinone and the aromatic TFT through π -stacking may also hinder any further reaction. As the photoproduct also strongly absorbs in the visible range (λ_{max} at ~ 390 nm, shown in **Figure 4.3**), it can act as an inner filter agent and consequently retard the reaction progress.

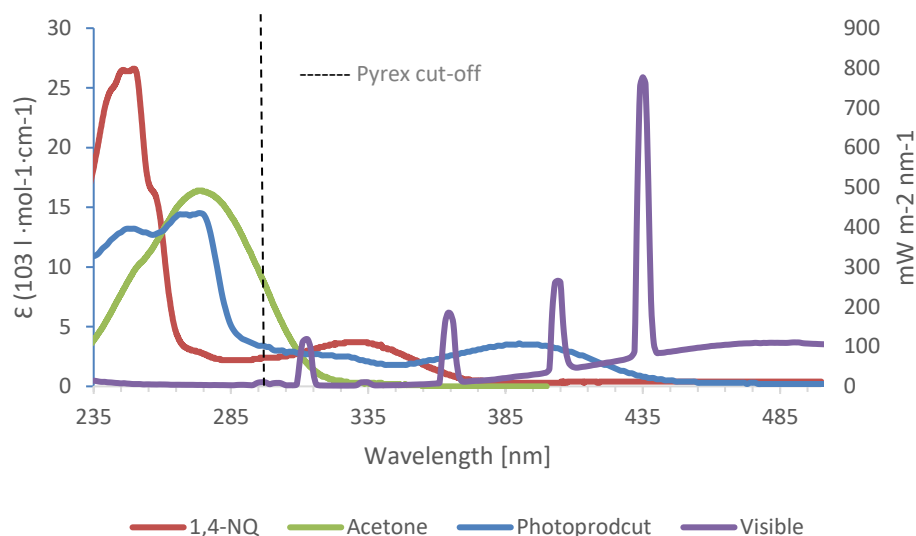


Figure 4.3: Comparison of UV-spectra (in MeCN) with emission of visible light lamp.

4.1.1.2.2 419 nm light

Photoacylation in acetone using 419 nm irradiation showed clear photoacylation, with an increased conversion by 12% compared to visible light. At this wavelength (**Figure 4.4**), acetone does no longer absorb (cut-off at approx. 330 nm) and consequently, triplet sensitization of 1,4-naphthoquinone by acetone must be ruled out. Instead, the emission spectrum of the fluorescent tube overlaps satisfactorily with the weak but important n,π^* absorption band of naphthoquinone. The photoacylation observed thus operated exclusively via direct excitation. The improved conversion was most likely caused by the increased output power of the 419 nm lamp, if compared to the much weaker and broader visible lamp. However, as the photoproduct also absorbs strongly in the 355–440 nm range (shown in **Figure 4.3**), inner filter effects retard the reaction at higher conversion rates.

The acylated naphthohydroquinone was nevertheless obtained in 56% yield, which corresponded to the reported isolated yield of 60% for the corresponding irradiation with 419 nm light in benzene by Waske.⁴²

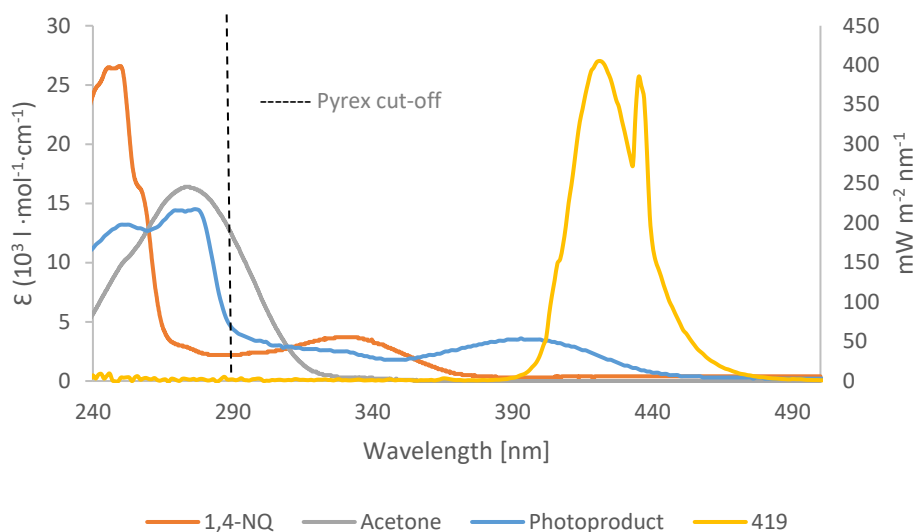


Figure 4.4: UV spectra of model reaction vs. 419 nm lamp.

4.1.1.2.3 UVA light

UVA irradiation in acetone gave a good conversion with excellent selectivity towards photoacylation. The emission spectrum of the lamp largely covers the π,π^* transition band of 1,4-naphthoquinone at 330 nm and partially the broad n,π^* transition band centered at 425 nm (**Figure 4.5**). Direct excitation is thus the dominant proposed photoactivation pathway. Due to the partial overlap with the important n,π^* absorption of acetone, however, some involvement of triplet sensitization cannot be ruled out. As the photoproduct also partially absorbs in the emission range, inner filter effects may operate at higher conversions, thus preventing completion.

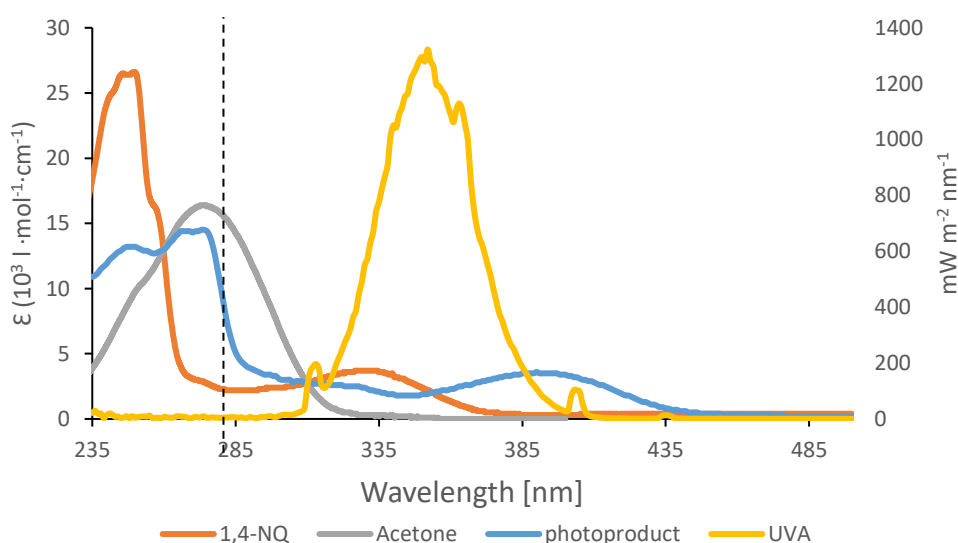


Figure 4.5: UV spectra of model reaction vs. UVA lamp.

4.1.1.2.4 UVB light

As already demonstrated by Friedrichs et al. for irradiations in benzene, the best results in terms of conversion and selectivity were obtained with Pyrex-filtered UVB light in either acetone or acetonitrile. In acetone, effective light absorption by the solvent without any light-filtering effects by the corresponding product can be assumed (**Figure 4.2**). In acetonitrile, the acylated photoproduct slightly absorbs within the lamp emission range, but this had only a marginal impact on the conversion. Isolated yields were similar for both solvent systems with 76% for acetone and 75% for acetonitrile. In contrast, Friedrichs et al. irradiated 1,4-naphthoquinone and butyraldehyde in benzene under the same conditions and obtained a lower yield of 58% for the desired acylation product.⁸³

Interestingly, irradiation in a quartz vessel with UVB light in acetone gave the corresponding acylated product in a significantly lower yield of 50% with significant amounts of the photoreduced dihydroxynaphthalene. Although photoreduction has been linked to the n,π^* transition of 1,4-naphthoquinone, the UVB emission bands clearly overlapped with the π,π^* transition band at 246 nm and especially the quinonoid transition at 264 nm within. Hydrogen-abstraction from acetone by excited naphthoquinone has been reported by Harbour and Tollins during irradiation under anaerobic conditions using a high-vacuum system.⁹⁵ Light-filtering by Pyrex completely prevents this side reaction.

4.1.1.2.5 UVC light

In both solvents, UVC irradiations in quartz vessels were characterized by poor selectivity with photoreduction as well as bisacylation operating as side-reactions. Undefined polymeric by-products were also noted by ¹H-NMR-analyses of the crude products. While photoacylation remained the dominant pathway, the desired photoproducts were isolated in poor yields of 30% and 40%, respectively. Acetone showed a higher degree of photoreduction, which may be caused by competitive absorption of UVC light by acetone and hence photosensitization. In contrast, irradiation in acetonitrile strictly followed direct excitation of the π,π^* transition of naphthoquinone. Light-absorption by the photoproduct is likely to become dominant at higher conversions of naphthoquinone (**Figure 4.6**).

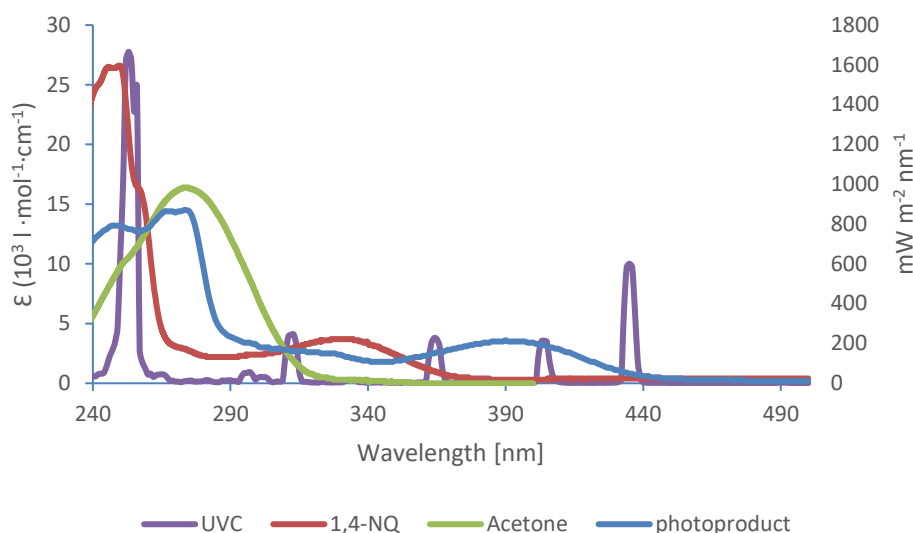


Figure 4.6: UV spectra of model reaction vs. UVC lamp.

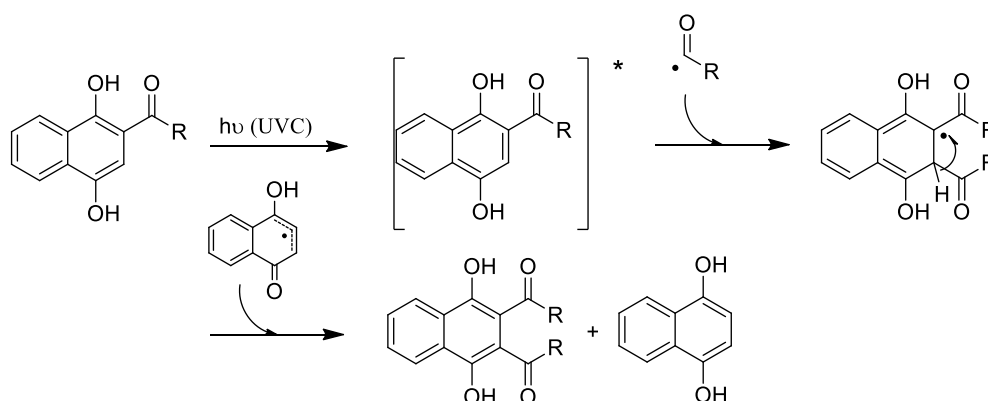
Bisacylation have been previously reported for irradiations in the presence of benzaldehyde by Oelgemöller and co-workers.¹²⁰ Several mechanistic pathways to the bisacylated compound have been proposed:

1. a thermal oxidation/reduction equilibrium followed by photoacylation of the initially formed acylated naphthoquinone,³⁰
2. Photo-Fries rearrangements of an isomeric ester¹²¹ or
3. addition of an acyl cation to a monoacylated product.¹²⁰

These pathways were subsequently ruled out experimentally. Instead, the authors demonstrated that bisacylation occurred directly from the monoacylated naphthohydroquinone, as shown by subsequent photoacylation in the presence of the corresponding aldehyde and isolation of the diacylated product in a 36% yield. However, a mechanistic explanation was not provided at the time.

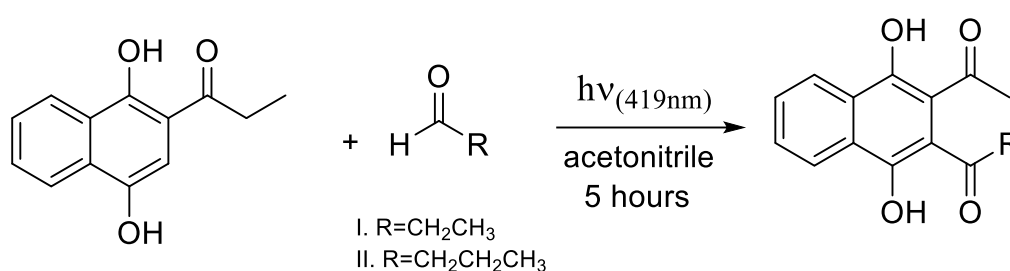
In this study, bisacylation was observed for aliphatic aldehydes and irradiation with UVC light. It is assumed that excitation of the monoacylated product operates simultaneously with monoacylation at higher conversions. This scenario would support the *out-of-cage* mechanism depicted in **Scheme 4.3**, at least in parts. The acyl radical formed reacts with the excited acylated naphthohydroquinone (**Scheme 4.5**). Subsequent hydrogen-transfer furnishes the bisacylation product as well as dihydronaphthoquinone. The latter compound would thus not be formed by conventional photoreduction involving hydrogen-abstraction from the solvent. Reasonable support for this mechanistic explanation was provided by the observation that

naphthohydroquinone and bisacylated product were indeed formed at the same time under these conditions.



Scheme 4.5: Possible bisacylation pathway.

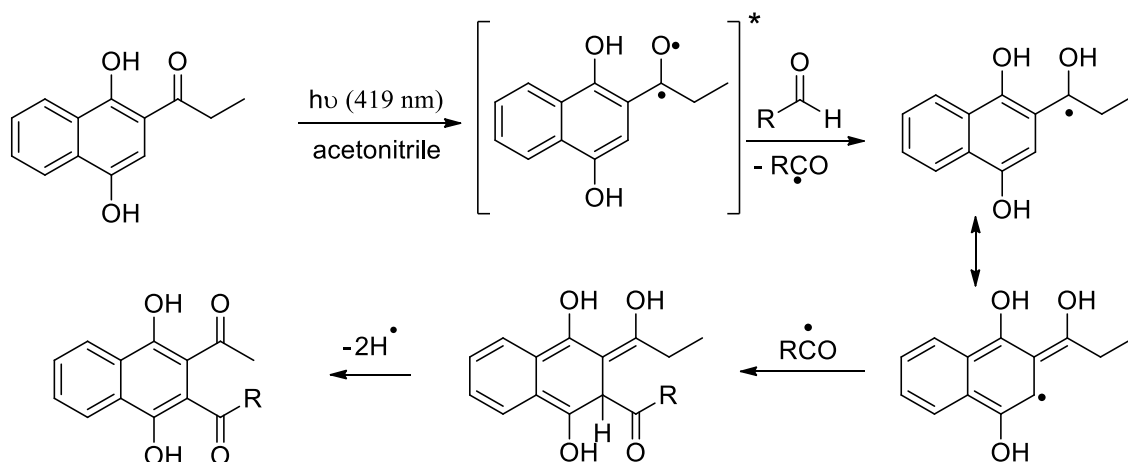
A directed photobisacylation of monoacylated product was furthermore investigated. UVC irradiation was considered to sluggish, so an alternative protocol was followed. As the 2-acylated naphthohydroquinone shows a strong n,π^* absorption at 420 nm,⁹² irradiations were conducted with 419 nm light in acetonitrile for 5 hours (**Scheme 4.6**). Under these conditions, a symmetrical as well as unsymmetrical biacylation product became available, although conversion rates were low with 30 and 39%, respectively. Undefined polymeric by-products were noted in the crude NMR-spectra.



Scheme 4.6: Photobisacylation of monoacylated naphthohydroquinone.

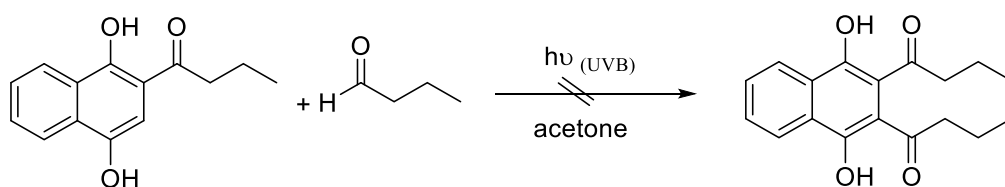
The successful bisacylation aligns with the findings reported by Oelgemöller and co-workers, and bisacylation operates from the initial monoacylated photoproduct. A possible mechanistic scenario for irradiation at 419 nm is shown in **Scheme 4.7**. Irradiation into the n,π^* absorption band initiates hydrogen-abstraction from the aldehyde. The subsequent radical intermediate can trap the acyl-radical formed. Formal loss of hydrogen yields the observed bisacylated product.

The low conversion suggest that the loss of hydrogen operates unselectively, which may cause the observed polymerizations.



Scheme 4.7: Mechanistic scenario for directed biacylation using 419 nm light.

When conducted in acetone with Pyrex-filtered UVB-light, no directed bisacylation or photodegradation was observed (**Scheme 4.8**). Excitation of the monoacylated photoproduct is thus essential for photoactivity. Likewise, acetone as the dominant light-absorbing compound is unable to sensitize bisacylation and rather acts as a protective filter agent.



Scheme 4.8: Attempted bisacylation with UVB light.

In conclusion, the solvent and irradiation wavelength has a profound impact on the photoacylation of 1,4-naphthoquinone with aldehyde. The best performance in terms of convenience, greenness, conversion, yield and selectivity was obtained in acetone using UVB lamps in combination with Pyrex glassware.

4.1.2 Photoacylation of naphthoquinone under flow conditions

The mild photoacylation process represents an attractive alternative to existing thermal Friedel-Crafts acylations.³¹ However, the developed photochemical procedures require exhaustive

irradiation to achieve high conversions and thus yields.³⁴ Recently, continuous-flow photochemistry has emerged as an advantageous combination of flow operation and light activation that can significantly accelerate the desired transformation.¹²² So far, quinone photochemistry has not been studied under continuous flow yet.

In this study, the photoacylation of 1,4-naphthoquinone with aldehyde was successfully transferred to continuous flow operation and a significant reduction in reaction time was achieved. In particular, a reasonable residence time of 70 min was determined in flow, compared to exhaustive irradiation for 28 hours in batch.

For comparison, the results obtained under flow conditions are compared with literature results in **Table 4.1**.

Table 4.1: Results of Photo-Friedel-Crafts acylation of naphthoquinone under flow conditions

Entry	Aldehyde	R	Yield (%) (bis-acylation)	literature (%) ^d
a	propionaldehyde	C ₂ H ₅	73 ^a	73
b	butyraldehyde	C ₃ H ₇	90 ^a	62
c	heptaldehyde	C ₆ H ₁₃	75 ^a	75
d	dodecylaldehyde	C ₁₁ H ₂₃	34 ^b	34
e	crotonaldehyde	CH=CHCH ₃	72 ^c	65
f	<i>p</i> -tolualdehyde	<i>p</i> -CH ₃ -C ₆ H ₄	66 ^b (14)	61
g	<i>p</i> -chlorobenzaldehyde	<i>p</i> -Cl-C ₆ H ₄	80 ^c	65
h	furfural aldehyde	C ₄ H ₃ O	20 ^b	89

^a Isolated yield after washing by hot water. ^b After column chromatography. ^c Precipitated from cold chloroform.

^d Highest isolated yield reported in the literature so far. Entries a, c: UVB lamps, Rayonet reactor, benzene, 23 h. Entry b: HQI-T metal halide bulb (400W), TFT, 12 h, Entries d, f: 419 nm lamps, Rayonet reactor, benzene, 12 h. Entry e: high-pressure Hg-vapour lamp, benzene, 5 days. Entry g: high-pressure Hg-vapour lamp, Ph₂CO, benzene, 5 days. Entry h: sunlight, 30h, benzene. not reported under artificial irradiation conditions.

Thus, the microcapillary reactor was more efficient that could be spelled out by the improvement of light penetration and irradiation area to the volume ratio (**Table 4.2**). For example, the path length of the Schlenk flask, *i.e.* the space between outer reactor wall and cooling finger, was about 4-5 mm. Whilst, the path length, *i.e.* inner diameter, of the capillary reactor was just 0.8 mm or 5-6 5 times narrower than in the batch flask.

Moreover, the flow reactor was being more economical in terms of light-consuming that was indicated by its dominant lamp power per irradiated area and lamp power over time values. The design of *inside-out* irradiation used a single 8 W fluorescent tube was surrounded by the reaction mixture (**Figure 4.7**). This construction is mimicking the geometry of immersion-well reactor which is well-known for taking full advantage of the emitted light.⁸⁵ In contrast, the larger Rayonet reactor was supplied with 16×8 W of fluorescent tubes in an *outside-in* arrangement. Although the chamber equipped reflective vest wall which may reduce light losing, most of the emitted light is lost since it does not hit the whole reaction vessel. In addition, the distance between fluorescent tube and reaction mixture is much shorter in the capillary tower, consequently reducing the decrease in light intensity reaching the reaction solution. The diameter of its Pyrex glass cylinder was 6.5 cm, whereas the inner diameter of the Rayonet chamber was 25 cm. The significance of the distance between light source and reactor has been revealed by Sugimoto and co-workers for the Barton reaction (nitrite photolysis) of a steroidal substrate.¹²³

Table 4.2: Comparison of reactor's efficiency.

Reactor parameter	Batch	Flow
Path length (mm)	4-5	0.8
Volume (mL)	60	5 ^a
Distance between light source & reactor (mm)	90	45
Irradiated area (cm ²)	102 ^b	159.3 ^c
Irradiated area/volume (cm ² /mL)	1.7	31.86
Lamp power (W)	128 (16 \times 8)	8
Lamp power/irradiated area (W/cm ²)	1.25	0.05
Luminous intensity (μ W/cm ²)	7164	264
Time (h)	28	1.1 (5.9 ^d , 14.1 ^e)
Lamp power \times time (W h)	3584	24 (47.2 ^f , 112.7 ^g)

^a Volume of exposed capillary. ^b Assuming a cyclic geometry of the Schlenk flask. ^c Covered cylinder area by capillary. ^d Operation time required to pump all 25 mL through the capillary at a flow rate of 0.071 mL/min. ^e Operation time required to pump 60 mL through the capillary at a flow rate of 0.071 mL/min. ^f Value for whole operation time and 25 mL. ^g Value for whole operation time and 60 mL.

However, a simple comparison of residence time (flow) and irradiation time (batch) is somewhat misleading as it does not consider the overall volume of the flow process. The operation time, *i.e.* time require to pump all 25 mL of solution and to pump the same batch volume of 60 mL through the reactor, are thus also provided. When comparing the same reaction volume of 60 mL, the flow reactor required approximately half of the time than the batch reactor.

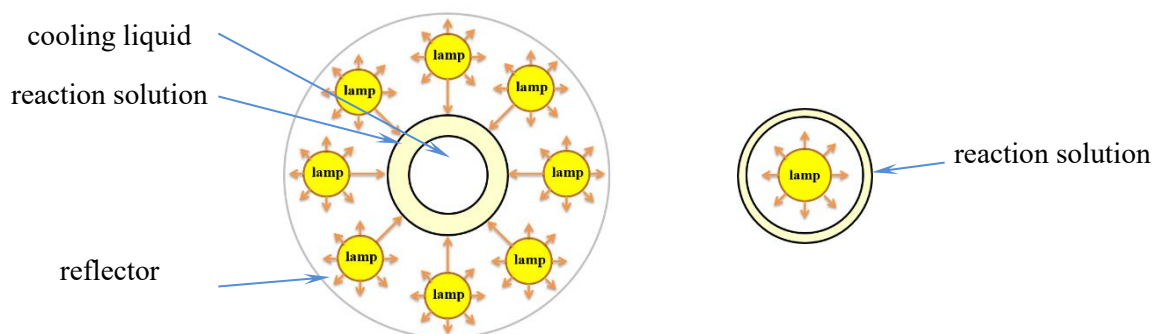


Figure 4.7: Schematics of *outside-in* and *inside-out* irradiation (not to scale).

In general, the Rayonet setup showed a better match of light source and Schlenck flask dimensions (**Figure 4.8**). The usable filling height of the Schenk flask from the bottom of the flask to the side-arms was approximately 15-18 cm. It thus does cover most of the arc length of the fluorescent tube of 23 cm. For the simple *in-house* capillary tower, only approximately $\frac{1}{3}$ of the arc length of the fluorescent tube was covered by the capillary instead, which leaves room for improvement for future flow reactors.¹²⁴

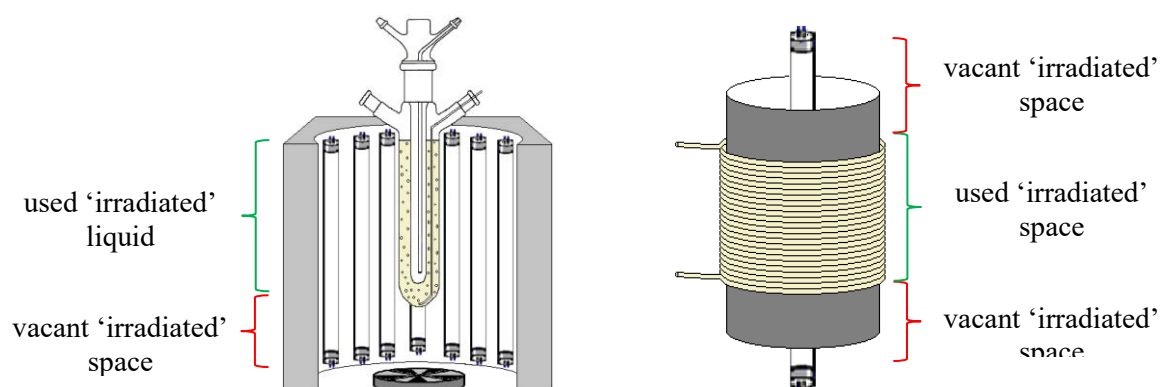
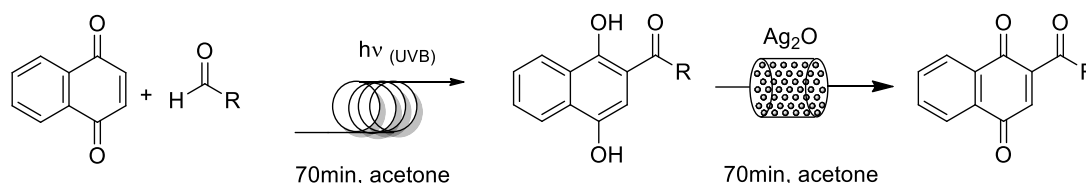


Figure 4.8: Coverage of arc lengths in Rayonet chamber reactor and in the in-house capillary reactor (not to scale).

4.1.3 One-flow multistep synthesis of acylated 1,4-naphthoquinones

Individual flow chemical steps can be easily combined into combined one-flow processes, thus realizing continuous flow multi-step organic synthesis.^{90, 125-126} Thus far, multi-step reactions involving photochemistry are rather rare.¹²⁷⁻¹²⁹ The oxidation reaction under batch conditions was carried out in dry ether after isolation of the purified acylated naphthohydroquinone, which was obtained from photoacylation in benzene.^{83, 120} To avoid a solvent switch, the photochemical-thermal tandem synthesis in one-flow was conducted in acetone and using a flow-rate of 0.071 mL/min. This again resulted in a residence time of 70 min for the photoacylation step. Although the residence time for the subsequent oxidation step has not been determined separately, it is estimated to be within minutes rather than hours. The batch procedure required stirring overnight, which corresponds to a reaction time of 10-16 hours. In comparison, the combined process furnished satisfactory to high conversion of 31-94% over both steps with a residence time of under 2 hours (**Scheme 4.9**).



Scheme 4.9: Photochemical-thermal tandem synthesis in one-flow.

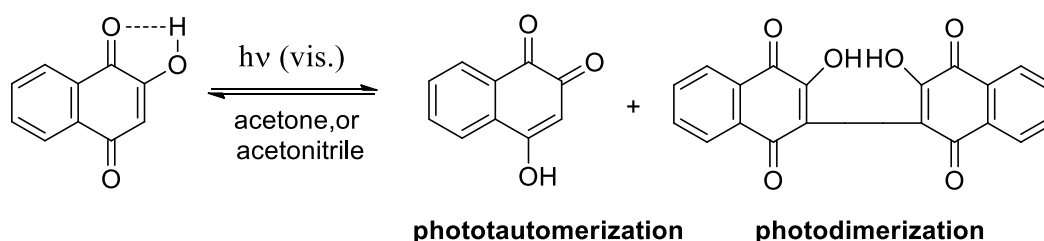
The efficient one-flow setup realized easy access to potentially important quinonoid pharmaceuticals, agrochemicals or building blocks by driving each reaction step at the same flow rate. Compared to the conventional batch processes, the one-flow system exhibited much reduced reaction times and increased overall conversions. Isolation of final products is only performed once at the end of the one-flow process. In comparison, conventional batch operation requires time- and resource-intensive isolations and purifications after each individual reaction step.

4.1.4 Attempted photoacylation of 2-hydroxy-1,4-naphthoquinone

2-Hydroxy-1,4-naphthoquinone (lawsone) and its derivatives are widely used in human medicine and natural products.^{130,131} For example, 2-dodecanoyl-3-hydroxy-1,4-naphthoquinone (DHN) is known to have antibiotic properties,⁹¹ which makes it an interesting target molecule for direct photoacylation and oxidation.

In ethanol, lawsone exhibits absorptions with λ_{max} at 287, 332 and 462 nm and molar extinction coefficients (ϵ) of 70×10^3 , 18×10^3 and 12×10^3 L/(mol . cm), respectively.¹³² The first two bands in the UV region have been assigned to π, π^* transitions within the benzenoid and quinonoid system, while the broad and weak absorption in the visible region corresponds to the n, π^* transition.¹³³ Like naphthoquinone itself, the latter absorption is important for the photochemistry of lawsone.

Irradiation of 2-hydroxy-1,4-naphthoquinone with dodecyl aldehyde did not yield any photoacylation or other photoproducts with either UVB or 419 nm light. Instead, photoirradiation of lawsone in the presence of butyraldehyde with visible light in acetone or acetonitrile solely resulted in tautomerization and photodimerization (**Scheme 4.10**).



Scheme 4.10: Photoprocesses of 2-hydroxy-1,4-naphthoquinone.

In contrast to the parent 1,4-naphthoquinone (Φ_{ISC} of 0.8),¹¹⁷ lawsone exhibits a very low quantum yield for intersystem crossing.¹¹⁸ Moreover, lawsone forms inter- and intramolecular hydrogen bonds.¹³⁴⁻¹³⁶ Intramolecular hydrogen transfer thus causes photoenolization of hydroxyl-substituted naphthoquinones.^{117, 134} Two tautomeric forms, denoted 1,4-isomer and 1,2-isomer, have been recognized for lawsone in solution (**Scheme 4.10**).^{92, 135, 137} The 1,4-isomer is more than 42 kJ/mol more stable than the 1,2-isomer due to the elimination of a dipole moment in the carbonyl groups, combined with a stabilizing intramolecular hydrogen bond.⁹² The presence of this intramolecular hydrogen bond was confirmed by Idriss et al. and Rostkowska et al. by IR- and UV-analyses of lawsone.¹³⁵

The photodimerization of lawsone was firstly described by Walsh, who observed a small quantity of redish substance in the solution of lawsone. Later, Hooker reported that the photodimer (di- β -hydroxy- α -naphthoquinone) was obtained from UV irradiation of a warm aqueous solution of lawsone in the presence of oxygen.¹³⁸⁻¹⁴⁰

In contrast, the photocyclodimerization of 1,4-quinones proceeds by addition of an excited quinone molecule to a ground state quinone, affording a cyclodimer product. The products obtained from the photodimerization of 1,4-naphthoquinone and 2-methyl-1,4-naphthoquinone

as depicted in **Figure 4.10**.¹¹⁷ This dimerization clearly differs from the dimerization of 2-hydroxy-1,4-naphthoquinone.

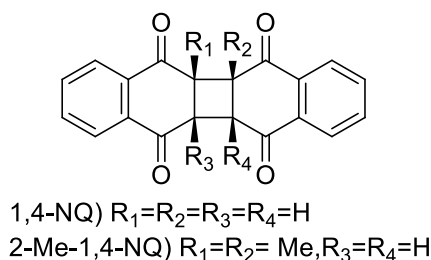
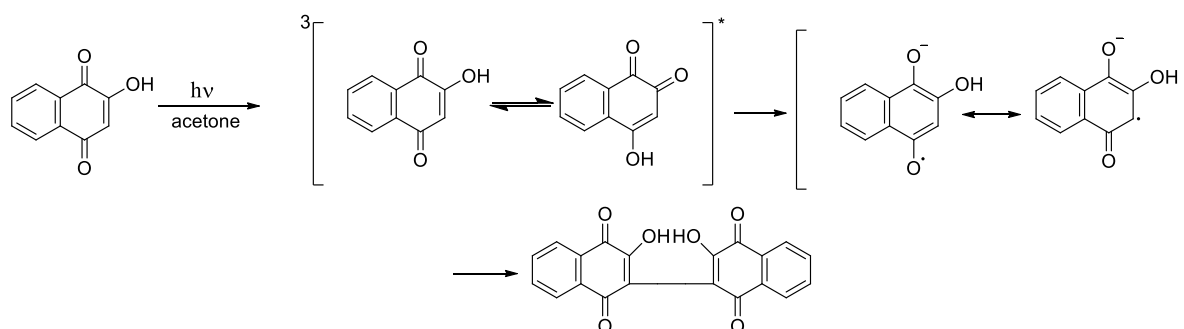


Figure 4.10: Dimerization of 1,4-naphthoquinone and 2-methyl-1,4-naphthoquinone.

Upon irradiation in the presence of air, lawsone undergoes oxidative coupling at C3 to form an open carbon-carbon dimer.¹⁴⁰⁻¹⁴¹ A possible reaction pathway for the irradiation of lawsone in acetone is shown in **Scheme 4.11**. Population of the tautomeric excited triplets, followed by the generation of radical ions and subsequent bond formation at positions 3 result in the observed dimerization.¹⁴²⁻¹⁴³

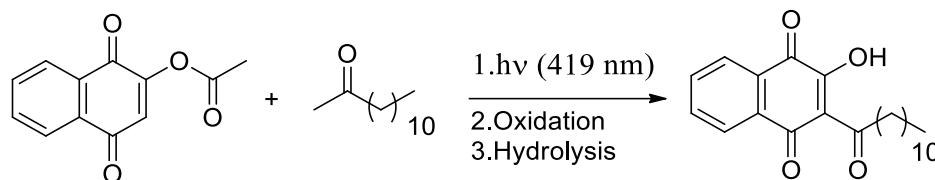


Scheme 4.11: Possible dimerization mechanism.

The lawsone dimer and its derivatives play a central role as biosynthetic precursors. For example, the lawsone dimer has been used in the synthesis of the natural biquinone aurofusarin.¹⁴¹ More recently, Sharma et al. reported that a series of dimeric naphthoquinones incorporating the natural 2-hydroxy-1,4-naphthoquinone moiety show inhibition features towards H5N1 virus neuraminidase.¹⁴⁴

4.1.5 Photoacylations of 2-acetoxy-1,4-naphthoquinone

2-Acetoxy-1,4-naphthoquinone was selected to realize an alternative access to the bioactive DHN. The subsequent one-flow three-step synthesis in series involved photoacylation, oxidation and hydrolysis (**Scheme 4.12**).



Scheme 4.12: Proposed one-flow multistep synthesis of DHN from 2-acetoxy-1,4-naphthoquinone.

The initial photoacylation of 2-acetoxy-1,4-naphthoquinone with butyraldehyde under different irradiation condition in acetone and acetonitrile resulted in the formation of acylated naphthoquinone beside the acylated hydronaphthoquinone. The photochemical reaction proceeded faster with 419 nm than UVB light, as noticeable for a higher conversion rate. This wavelength dependency can be explained by the significant absorption of 2-acetoxy-1,4-naphthoquinone at 336 nm.¹³³ The presence of a substituent in the 2-position favoured oxidation of the desired acylated hydroquinone during the work-up.¹⁴⁵⁻¹⁴⁶ This behaviour is consistent with other photoacylations at 419 nm involving 2-methoxy- and 2-methyl-1,4-naphthoquinone, respectively.⁴²

Although photoacylation of 2-acetoxy-1,4-naphthoquinone has been realized for the first time, the low yield and the poor selectivity discouraged any implementation into subsequent one-flow processes.

4.1.6 Solar photoacylations

Sunlight represents the most sustainable light source in photochemical synthesis.¹⁴⁷ The solar radiation spectrum covers a range of 300-700 nm of applicable wavelengths, which restricts the choice of photochemical transformations. In addition, solar photons at Earth's surface only consist of 3% UVA and 0.5% UVB radiation, in contrast to 42–43% of visible (400–700 nm) and 52-55% of infrared radiation.^{85,148} Naturally, solar photochemical synthesis also relies on weather conditions and is limited to daylight hours.

A modern solar acylation in an advanced circulating batch parabolic through reactor (PROPHIS) using 500 g of 1,4-naphthoquinone and 4 kg of butyraldehyde in 80 L of a *tert*-butanol-acetone mixture (3:1) has been reported by Mattay *et al.* The reaction required exposure to sunlight for 3 days and furnished the corresponding acylated naphthohydroquinone in 90% yield.¹¹⁴

In contrast, a simple concentrating flow reactor was employed in this study to realize the acetone-sensitized photoacylation under flow conditions. The transformation represents a borderline application for solar synthesis. As acetone only absorbs light below 330 nm (**Figure 4.2**),¹⁴⁹ concentrated sunlight was utilized to accelerate the reaction.¹⁵⁰

4.1.6.1 Solar continuous-flow photoacylations in concentrated sunlight

The in-house parabolic trough concentrating solar flow reactor produced the desired acylated naphthohydroquinones in low to excellent yields of 22–88% using a short residence time of 70 min. The chosen FEP capillary exhibited good transmissions of >78% above 300 nm (**Figure 4.9**). The polished aluminum mirror gave a measured concentration factor of 3 suns. Due to the simple design and optical losses, this value was considerably lower than the theoretical concentration factor of 13. Aluminum nevertheless shows a good reflectivity of >60% above 300 nm.¹² Triplet-sensitization by acetone as well as direct absorption pathways are thus likely to operate in parallel. The general design of the solar flow reactor enables complete illumination of the capillary with the front exposed to direct and the back to concentrated sunlight (**Figure 4.10**).

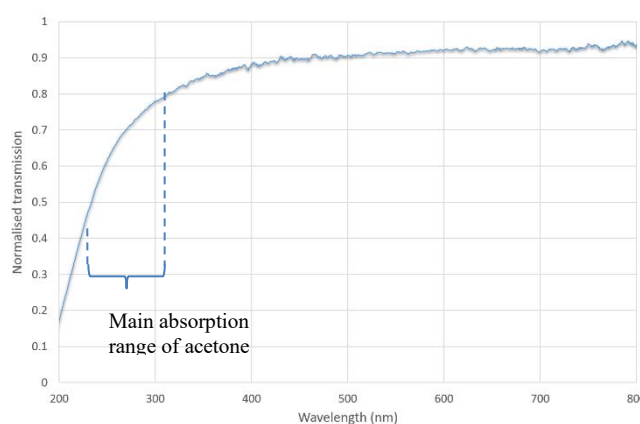


Figure 4.9: Transmission spectrum of the FEP capillary. Figure provided by Vapourtec Ltd.

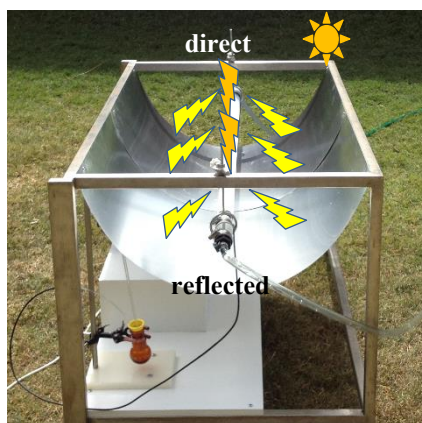
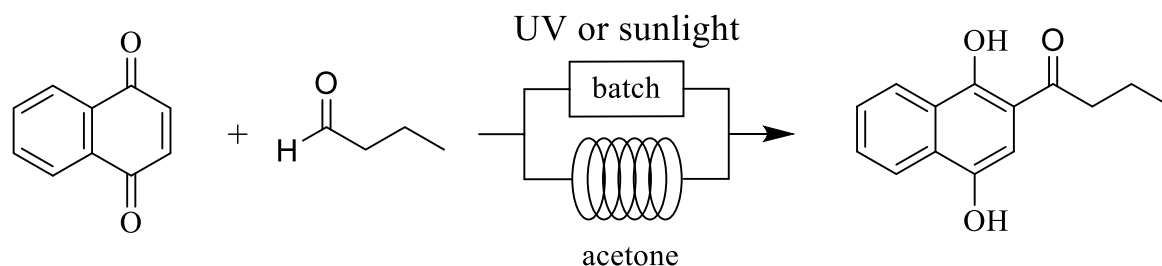


Figure 4.10: Sunlight usage of the solar flow reactor.

4.1.6.2 Solar photoacylations in direct sunlight

Simple exposure of the reaction mixtures in direct sunlight gave the desired photoacylation products in low to moderate yields of 17–60%, despite prolonged illuminations for 200 min. This modest performance is predominantly caused by the limited harvesting of solar light. The flasks only have a very small surface area that can collect sunlight directly. Due to the lack of a solar concentrator, the solar exposures depended merely on direct sunlight hitting the flasks. Likewise, the reaction mixtures remain static with no movement or mixing. Direct excitation of naphthoquinone is likely the most dominant photoactivation process. The compared to the FEP capillary reduced transmission of Pyrex glass in the important UV-range of acetone makes triplet sensitization less likely.¹² Depending on the thickness of the glass, Pyrex shows a transmission of just about 10–20% at 300 nm.

The performances of the UV-driven batch, UV-driven flow and solar-driven flow processes for the photoacylation of 1,4-naphthoquinone and butyraldehyde (**Scheme 4.13**) are compared in **Table 4.3**. In all cases, isolated yields were comparable and ranged from 76–88%. The flow processes utilizing artificial UV-light and sunlight showed the fastest reactions. A similar discrepancy in yield rate by sunlight irradiation was also reported by Christian and co-workers when they scaled up the same model reaction using PROPHIS reactor. The reaction mixture was illuminated by sunlight in a *tert*-butyl alcohol–acetone mixture for three days gave the photoproduct in 90% yield.¹¹⁴



Scheme 2.13: Photoacylation of model reaction used for process comparison.

Table 4.3: Comparison of batch, UV-driven flow, and solar-driven flow processes.

R	UV-driven				Solar Flow	
	Batch		Flow		Time	Yield
	Time	yield	Time	Yield		
C ₃ H ₇	28h	76%	70 min	88%	70 min	88%

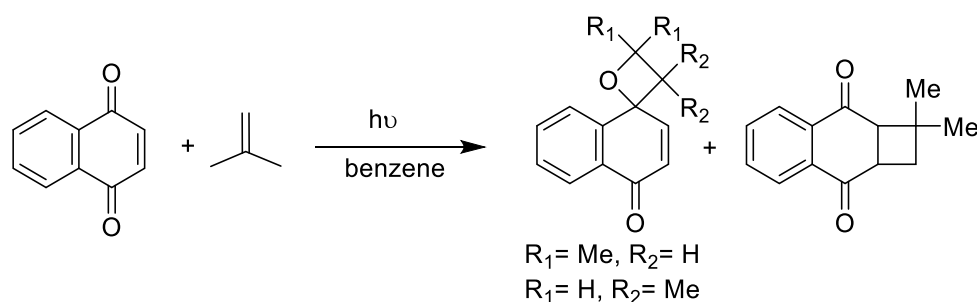
4.2 [2+2]-Photocycloaddition of naphthoquinones

4.2.1 Photocycloaddition of 1,4-naphthoquinones under batch conditions

Photocycloadditions of 1,4-quinones with olefins have been intensively studied as they furnish interesting target structures with potential bioactivities.⁴⁷ Most experimental photocycloaddition procedures are conducted in conventional immersion well reactors using benzene and Pyrex-filtered light from medium- or high-pressure mercury lamps.¹⁵¹ These conditions cause several drawbacks for effective [2+2]-photocycloaddition. For instance, medium- and high-pressure mercury lamps show broad emissions with numerous wavelengths between 253 and 579 nm,¹⁴ while photocycloadditions of quinones proceed most efficiently within 300-400 nm.¹⁵² In addition to wasting energy and generating excessive heat, optical filters must be applied to prevent photodegradation of the initial photoadducts. Most primary cycloadducts retain photochemical active chromophores, especially carbonyl groups, that easily absorb another photon under the given irradiation conditions.¹⁵³ The application of sophisticated filters reduces the energy efficiency of the lamps significantly.¹² Benzene is used as the most common solvent for this photosynthesis due to its transparency and assumed stability. However, it has been shown to quench the triplet state of *p*-quinones.^{52, 154-155} It has also been pointed out that benzene can react in some cases chemically, even when the quinonoid reagent is excited with visible light.^{30, 117} Most importantly, benzene is toxic and should thus be

replaced by other solvents. Traditional immersion well apparatuses can also cause optical losses and suffer from safety concerns regarding its overall transparent design.¹⁵⁶

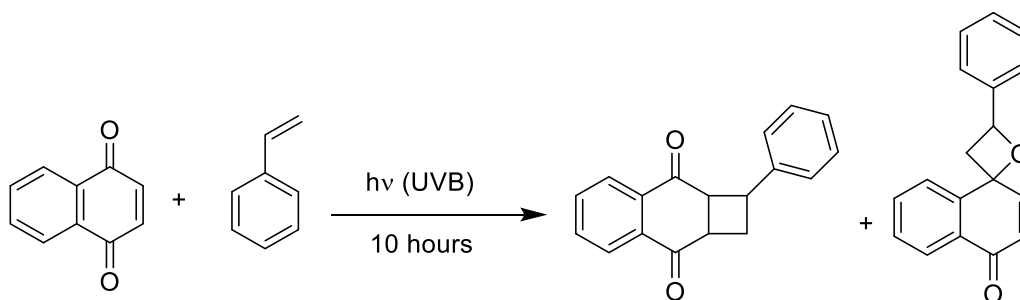
In general, the photoaddition of alkenes to 1,4-naphthoquinone delivers cyclobutenes and spiro-oxetanes due to the slight energy gap of only 25 kJ/mol between the n,π^* and π,π^* triplet states.^{30, 60} For example, photocycloaddition of 1,4-naphthoquinone to 2-methylpropene results in a cyclobutane and a 1:1 ratio of regioisomeric spiro-oxetanes in a total yield of 70% (**Scheme 4.14**).⁶⁸



Scheme 4.14: Photocycloaddition of 1,4-naphthoquinone to 2-methylpropene

4.2.1.1 Solvent study

A series of experiments of 1,4-naphthoquinone and styrene was conducted in a range of organic solvents, namely acetone, acetonitrile, methanol, chloroform and trifluorotoluene (TFT). All reactions were performed under batch conditions with UVB light (300 ± 25 nm) in a Pyrex Schlenk flask (transmission >300 nm) for 10 hours. The general scheme of the reaction is shown in **Scheme 4.15**.



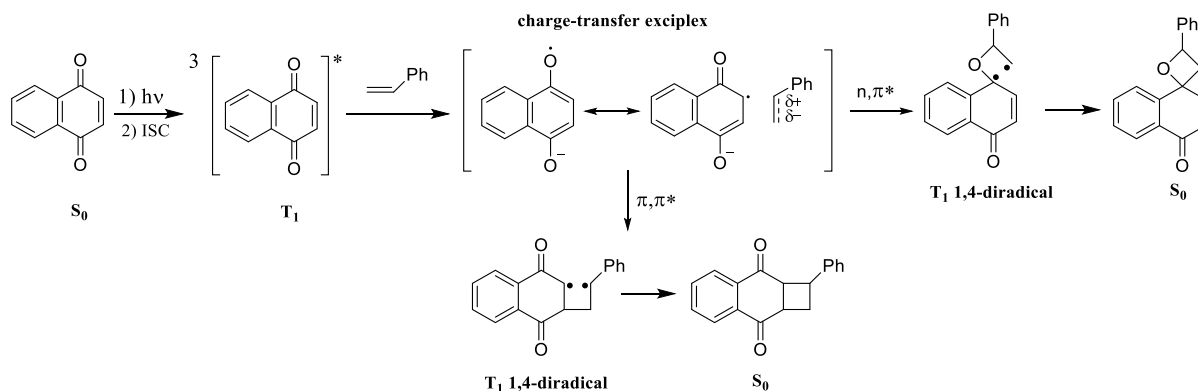
Scheme 4.15: Photocycloaddition of styrene to 1,4-naphthoquinone.

As for the photoacylation, two general pathways can be distinguished: direct excitation and sensitized photolysis by acetone, which is often utilized as a solvent and triplet sensitizer in

[2+2]-photocycloadditions.¹⁵⁷⁻¹⁵⁹ The experimental findings show a different selectivity of the reaction.

Upon direct irradiation in acetonitrile, trifluorotoluene and chloroform, the addition of styrene to the triplet state of 1,4-naphthoquinone gave both, spiro-oxetane and cyclobutane owing to the overlapping of n,π^* and π,π^* excitation band of 1,4-naphthoquinone. Of these, the n,π^* transition gives rise to spiro-oxetane formation, whereas the π,π^* transition results in cyclobutane generation.¹⁶⁰ Solvent polarity has significant effect on the energy levels of the excited states. Polar solvents also favour radical ionic mechanisms (**Scheme 4.16**).¹⁶¹

Generally, the photocycloaddition is initiated by promoting 1,4-naphthoquinone to its singlet excited state, which is extremely short-lived. Rapid intersystem crossing (ISC) generates the corresponding longer-lived triplet excited state. An electron subsequently transfers from styrene to the excited 1,4-naphthoquinone to form a radical ion pair that subsequently combines and produces triplet 1,4-diradical intermediates. After further ISC of these triplet diradicals to their singlet counterparts, ring closure yields either the spiro-oxetane or cyclobutane adduct.⁵⁹ The relative stabilities of the intermediary 1,4-diradicals is reflected in the regioisomeric ratio of spiro-oxetane and cyclobutane.¹⁵¹



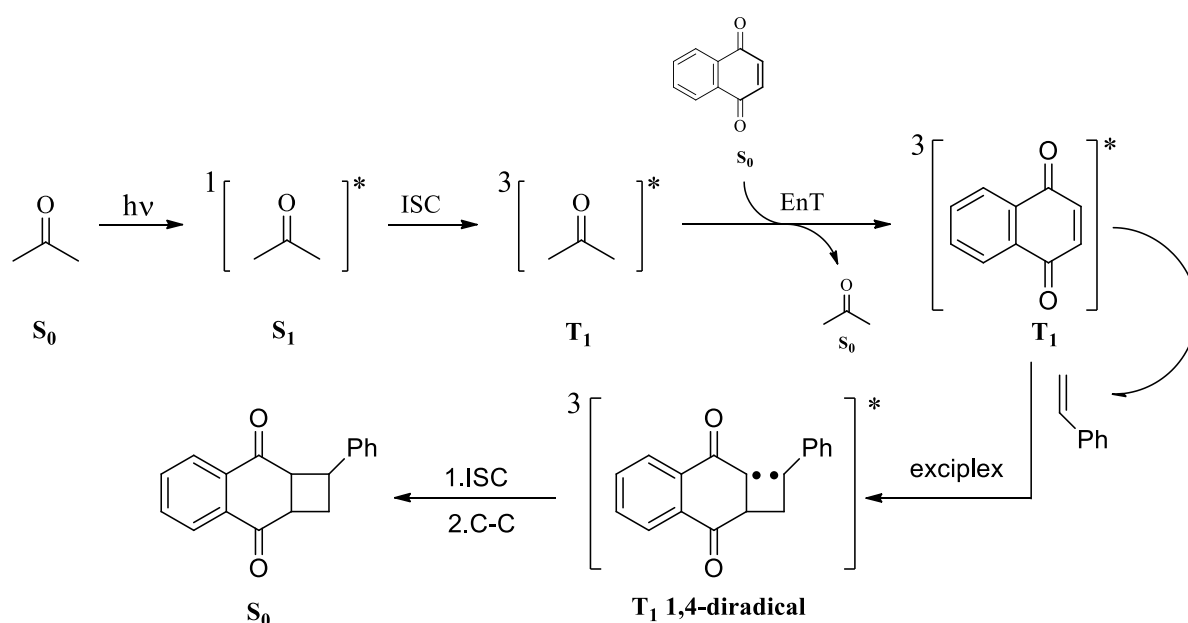
Scheme 4.16: Electron-transfer mechanism of the [2+2]-photocycloaddition.

The polarity of the reaction medium also impacted on the adduct distribution. Cyclobutane formation in acetonitrile and trifluorotoluene (more polar) was higher with 93 and 94% than in chloroform (less polar) with 78%. These deviations may be attributed to the sensitivity of the n,π^* and π,π^* energy levels to solvent polarity, which is consistent with a mechanism involving polar intermediates.^{53, 60, 151} However, the conversion in acetonitrile and trifluorotoluene slowed and nearly stopped, while the conversion in chloroform proceeded to complete consumption of 1,4-naphthoquinone.

As noted above, the solvent's polarity has an impact on the mechanistic scenario of the photocycloaddition. Acetonitrile and TFT as highly polar solvents presumably favour electron transfer steps and the formation of radical ions.¹⁵⁵ In contrast, electron transfer is unlikely in chloroform. As radical ionic intermediates can be trapped by other reagents, their existence favours the formation of byproducts.

The photoreaction of 1,4-naphthoquinone with styrene in methanol is dominated by photoreduction to 1,4-naphthohydroquinone and this undesired pathway has been described for the related photoacylations.^{65, 77, 84} Photoreductions of 1,4-quinones in the presence of alkene in alcohol have been described. For example, Buchachenko *et al.* reported that *p*-quinones reacts with alcohol by α -hydrogen abstracting in the presence of styrene.¹⁶²

In contrast, photoirradiation of 1,4-naphthoquinone with styrene in acetone proceeded through triplet sensitization when a UVB light source was applied (**Scheme 4.17**). The photoreaction is initiated by the absorption of light by acetone and subsequent population of its triplet excited state via intersystem crossing (ISC). Since $\Delta E_T = E_{T(1,4-NQ)} - E_{T(\text{acetone})} \leq 0$, energy transfer from the excited acetone ($T_1 = 332 \text{ kJ/mol}$)¹⁰⁶ to 1,4-naphthoquinone ($T_1 = 225 \text{ kJ/mol}$) is energetically favourable,⁵⁶ thereby generating the corresponding triplet excited (π, π^*) naphthoquinone. The triplet excited naphthoquinone reacts with ground state styrene via a triplet exciplex to a triplet 1,4-diradical. Following spin inversion, the cyclobutane isomer is formed.⁵²



Scheme 4.17: Triplet-sensitization mechanism of the [2+2]-photocycloaddition.

The reaction in acetone was characterized by exclusive addition towards the quinonoid C=C bond. This outcome suggests that the n,π^* triplet state of acetone selectively populates the π,π^* triplet state of 1,4-naphthoquinone. Sensitization thus avoids involvement of the n,π^* triplet state of naphthoquinone, which would result in oxetane-formation instead. The energy levels of the various triplet excited states of naphthoquinone have been calculated in the literature. In line with experimental observations, the lowest lying triplet state was assigned to a n,π^* nature. However, the calculated energy differences to other n,π^* and π,π^* states were small. Acetone may thus sensitize a higher π,π^* triplet state. Alternatively, the polar nature of acetone may alter the energy levels of the triplet states of naphthoquinone with the π,π^* triplet state being the lowest one.

Photocycloadditions in acetone were also free of any other products, thus solely forming the corresponding cyclobutane adduct in a respectable isolated yield of 69%. No degradation of the cyclobutane photoproduct was observed, which can be explained as follows:

- acetone is unable to sensitize the cyclobutane photoproduct and/or
- acetone functions as a light filter and prevents direct excitation of the cyclobutane.

In conclusion, acetone was successfully employed for the selective generation of the cyclobutane photoadduct without any noticeable by- or follow-up products. This is further supported by analysis of the UV-spectra in comparison with the emission spectrum of the UVB light source.

In acetonitrile solution, the cyclobutane adduct exhibits absorptions with λ_{max} at 227, 254 and 306 nm and extinction coefficients of 35×10^3 , 11×10^3 and 1.3×10^3 L/(mol . cm), respectively (**Figure 4.13**). In contrast to the solvent acetone, the weak cyclobutane absorption above 300 nm only partially overlaps with the emission spectrum of the UVB-lamp. Acetone is thus the predominantly absorbing species, especially at high conversions of naphthoquinone, and acts as a light-filter that protects the cyclobutane from secondary photolysis.

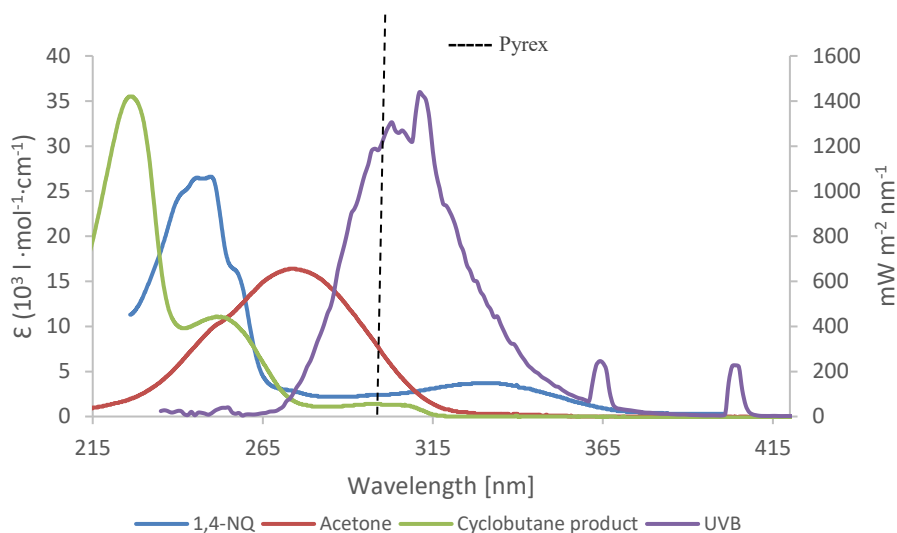
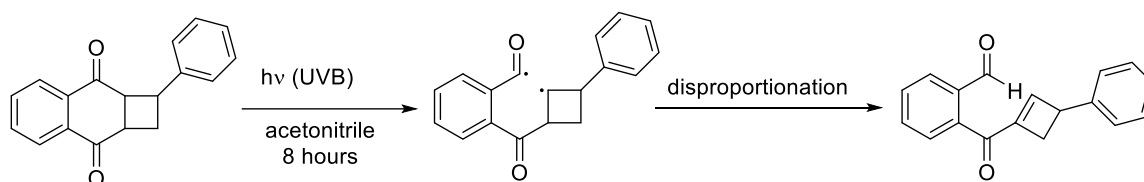


Figure 4.13: UV spectra of model reaction vs. UVB lamp.

In contrast, acetonitrile has a cut-off wavelength at 190 nm.⁸⁵ In this solvent, the cyclobutane is subsequently exposed to UVB light. Subsequent absorption of light by its carbonyl-chromophores can cause second-order cleavage reactions.¹⁵³

To support this assumption, the photostability of the cyclobutene towards Pyrex-filtered UVB-light was evaluated in acetone and acetonitrile for a period of 8 hours. No photodegradation was observed when acetone was utilized as solvent, confirming its photoprotective nature. In contrast, illumination in acetonitrile showed photodegradation of the cyclobutane. ¹H-NMR analysis suggested the formation of an aldehyde and a possible degradation pathway is outlined in **Scheme 4.18**. This compound is formed by a Norrish type I cleavage process of the excited cyclobutane adduct.¹⁶³



Scheme 4.18: Possible Norrish Type I degradation pathway of the cyclobutane.

4.2.1.2 Wavelength study

A series of photocycloadditions of the model pair were conducted for 10 hours under batch conditions with different light sources and in Pyrex ($\lambda > 300 \text{ nm}$) or quartz ($\lambda > 200 \text{ nm}$) vessels (**Scheme 4.15**). The results confirmed that the wavelength plays an important role in the

photocycloaddition of 1,4-naphthoquinone in terms of conversion efficiency and selectivity of the reaction. A comparison of the absorption spectra of important compounds with the emission spectra of the various light sources is shown in **Figure 4.14**.

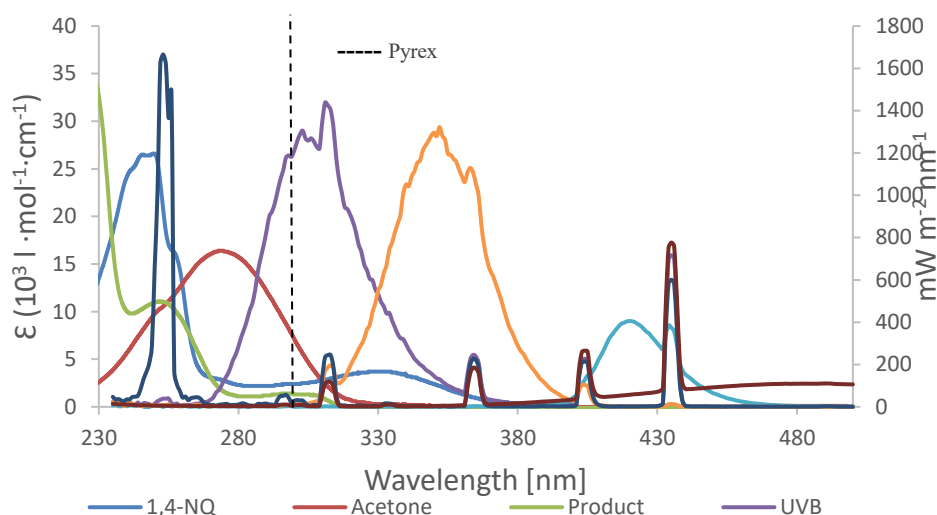


Figure 4.14: UV spectra of 1,4-naphthoquinone, acetone and cyclobutane adduct in acetonitrile vs. UV, 419 nm and visible lamps.

The absorption spectrum of 1,4-naphthoquinone shows λ_{max} at 246, 330 and 425 nm in hexane, respectively, with the first two due to π,π^* and the last due to n,π^* transition.¹¹⁸ As a result, wavelengths in the range 400–500 nm can efficiently promote the photocycloaddition of alkenes to 1,4-naphthoquinone.^{164–166} It has also been noted that the excitation of the longest wavelength transitions can prevent photodecomposition of the cycloadducts.⁵⁴

4.2.1.2.1 Visible and 419 nm light

The favoured formation of the spiro-oxetane adduct with visible and 419 nm irradiation is due to the predominant excitation of the n,π^* transition. Although the corresponding cyclobutane is formed from the π,π^* transitions of 1,4-naphthoquinone, these were not covered by neither visible nor 419 nm irradiation. However, it has been shown that the lowest excited n,π^* triplet state of 1,4-naphthoquinone can promote the formation of both, cyclobutane and spiro-oxetane.⁶⁰

4.2.1.2.2 UVA and UVB light

Irradiation with UVA light afforded near complete conversion but produced both photoproducts. The high preference for cyclobutane formation suggest a significant contribution of triplet photosensitization by acetone. As can be seen in **Figure 4.14**, 1,4-naphthoquinone predominantly and strongly absorbs within the emission band of the UVA lamp, thus suggesting direct excitation as the dominant photoactivation pathway. The photocycloaddition using Pyrex-filtered UVB light in acetone has been previously described. Interestingly, the corresponding irradiation in a quartz vessel did not show any noticeable changes in the outcome of the photoreaction. However, to prevent decomposition of the cyclobutane adducts, the usage of Pyrex vessels is recommended.¹⁶⁶

4.2.1.2.3 UVC light

The photoreactions with UVC light in quartz vessels solely yielded cyclobutanes. At this short wavelength, only the π,π^* triplet state of 1,4-naphthoquinone can be populated. The solvent, i.e. acetone vs. acetonitrile, has a notable impact on the efficiency of the photocycloaddition. Acetone generally gave a cleaner reaction and better conversion compared to acetonitrile. As the cyclobutane as well as styrene show absorption bands at 254 and 248 nm, respectively,¹⁶⁷ competing light absorption by these compounds retards the desired photocycloaddition. Excitation of styrene with wavelength shorter than 280 nm can also result in the formation of polymeric by-products, which have been indeed observed by ¹H-NMR analysis of the crude product. In contrast, acetone successfully prevented any side-reactions of either the cyclobutane photoadduct or styrene.

In conclusion, the best experimental results for cyclobutane formation under batch conditions were obtained in acetone and using Pyrex-filtered UVB-light. These conditions furnished improved conversions and selectivity, thus increasing the yield of the desired photoproduct.

4.2.2 Photocycloaddition of 1,4-naphthoquinone under flow conditions

The [2+2]-photocycloaddition of 1,4-naphthoquinone under batch conditions took 10 hours. In contrast, the corresponding transformation in the flow reactor only required a residence time of 60 minutes to achieve even higher conversions.

To illustrate the superiority of the flow protocol, the results from this study are compared with equivalent batch studies from the literature (**Table 4.4**).

Table 4.4: Comparison of selected photocycloadditions.

Entry	Alkene	Irradiation time	Conversion ^a	Yield ^b	Mode	Literature ^c
a	styrene	10 hours	96%	69%	Batch	40%
		45 min	96%	69%	Flow	
b	cyclopentene	13 hours	67%	50%	Batch	10%
		60 min	88%	73%	Flow	
c	1,1-diphenyl	12 hours	78%	42%	Batch	n.r. ^d
	ethylene	60 min	86%	60%	Flow	
d	cyclohexane	12 hours	84%	25%	Batch	n.r. ^d
e	<i>trans</i> -stilbene	13 hours	40%	27%	Batch	s.q. ^f
		6 hours	93%	78%	Batch ^e	
		60 min	50%	47%	Flow	

^a Determined by ¹H-NMR analysis ($\pm 3\%$). ^b after automated flash chromatography. ^c highest isolated yield reported in the literature so far. Literature conditions:⁹⁶ Pyrex immersion well reactor, 125 W medium-pressure mercury arc, benzene, 48 h. ^d n.r.: not reported yet. ^e irradiation with 419 nm light in acetone using a Rayonet reactor. ^f s.q.: small quantity.

Despite its simple design, the microflow photoreactor showed better performances in terms of reaction time and utilization of available light. This was again achieved by the improved light penetration within the microcapillary in combination with the superior *inside-out* reactor design. In addition, the removal of the potentially photoactive products from the irradiated zone reduced or avoided any photodecompositions and thus improved yields, product qualities and selectivity. The larger Schlenk flask had a usable filling height of 30-35 cm, which significantly exceeded the arc length of the fluorescent tube of 23 cm. A portion of the reaction mixture was thus not exposed to any light.

4.2.3 Substrate scope of the photocycloaddition

Photocycloadditions involving 1,4-naphthoquinone proceeded with excellent regioselective towards cyclobutane formation with styrene, cyclopentene, cyclohexane and 1,1-diphenylethylene. In contrast, *trans*-stilbene exclusively gave the alternative spiro-oxetane. Naturally, the diastereoselectivity of the photoaddition is particularly attractive for any synthetic applications.⁸¹ The diastereoselectivity varied with the alkene used.

For example, the addition of styrene to naphthoquinone resulted in a 3:1 mixture of the diastereoisomeric *anti:syn* cyclobutanes (**Figure 4.15**). The predominant formation of the *anti*-

isomer is caused by its higher stability. The phenyl-substituent at the cyclobutane is opposite the cyclohexene-1,4-dione moiety, thus minimizing steric clashing of these groups.

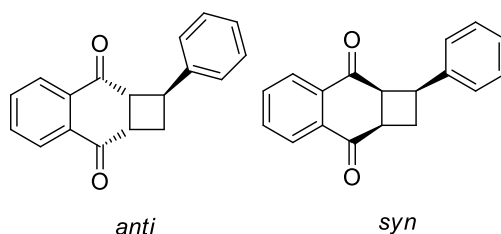
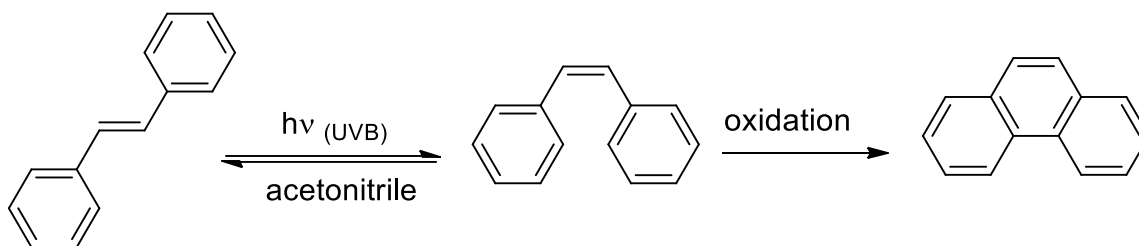


Figure 4.15: *anti:syn* cyclobutane isomers obtained from styrene and naphthoquinone.

However, solely the *anti*-diastereoisomer was obtained from the addition of cyclopentene and cyclohexene to 1,4- naphthoquinone. This may be explained by the increased steric bulk and flexibility of the corresponding cyclopentane and cyclohexane moieties. In contrast, Maruyama *et al.* reported that no cycloaddition reaction was observed when 1,4-naphthoquinone and cyclopentene or cyclohexene were irradiated in benzene solution. Instead, photoreduction to 1,4-dihydronaphthoquinone via hydrogen-abstraction from the allylic positions of the cycloalkenes was noted.⁹⁴ This somewhat contradictory literature finding again corresponds to the different triplet excited states. Photoreduction is favoured upon n,π^* transition, whereas triplet-photosensitization populates a π,π^* triplet state.

Naturally, the photocycloaddition to 1,1-diphenylethylene offered only a single isomer of the cyclobutane adduct.

The reaction scenario for *trans*-stilbene was found more complex. Photocycloaddition of 1,4-naphthoquinone with *trans*-stilbene under direct or sensitized conditions always resulted in oxetane formation with high stereospecificity. The crude product also showed the formation of phenanthrene and *cis*-stilbene beside undefined compound. The photochemical oxidative electrocyclization of stilbene to phenanthrene is well known.^{99, 168} When *trans*-stilbene was independently irradiated with UVB in acetonitrile, the formation of phenanthrene was indeed observed (**Scheme 4.19**).



Scheme 4.19: Photochemical oxidative electrocyclization of *trans*-stilbene.

A comparison of the UV-spectrum of *trans*-stilbene in acetonitrile with the emission spectra of the UVB- and 419 nm lamps is shown in **Figure 4.16**. The absorption band of stilbene strongly overlaps with the UVB emission centered at 300 nm. Consequently, the photochemistry of stilbene interferes with the desired photocycloaddition reaction in this wavelength region.

The photocycloaddition of 1,4-naphthoquinone to *trans*-stilbene was subsequently executed in acetone using 419 nm light, hence avoiding excitation of stilbene. Under these direct excitation conditions, solely the spiro-oxetane was formed. Due to the absence of competing light absorption, the irradiation time could be reduced from 13 hours to 6 hours.

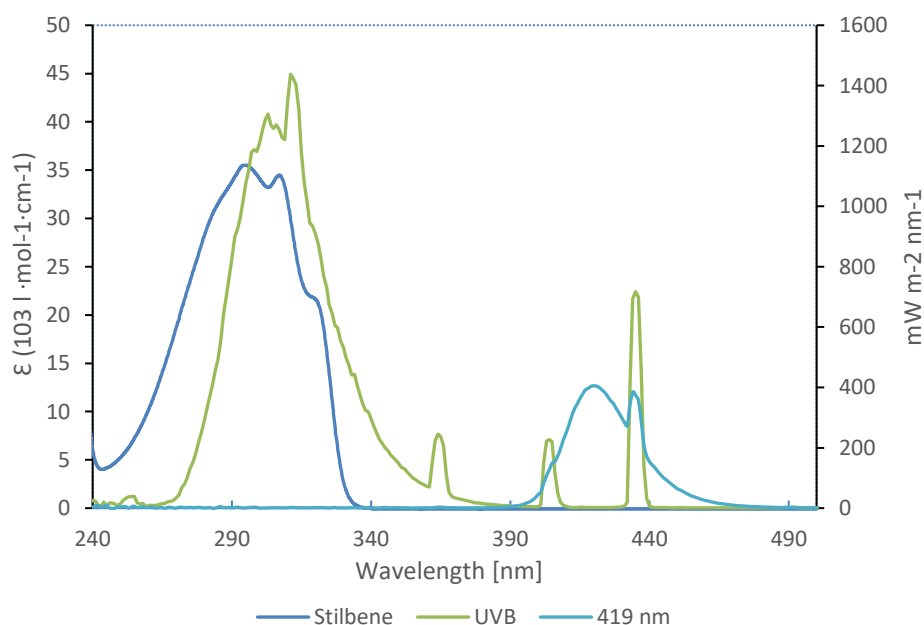


Figure 4.16: Absorption spectrum of *trans*-stilbene vs. UVB and 419 nm lamps.

The formation of the spiro-oxetane is in line with other studies.^{96, 161} The selective formation of the spiro-oxetane with 419 nm light can be explained by the exclusive excitation of the n, π^*

transition of naphthoquinone.^{52, 161} However, no notable cyclobutane product was observed during irradiation in acetone, suggesting an alternative mechanistic scenario.

Similar experimental outcomes have been reported for photocycloadditions of stilbene to chloranil,¹⁰⁰ which possesses a π,π^* state as the lowest triplet state,³¹ and anethole to 1,4-naphthoquinone,⁵⁹ respectively. The selective spiro-oxetane formation in these transformations was explained by an alternative electron-transfer pathway. Consequently, the reaction proceeds through electron transfer from the stilbene donor to the excited 1,4-quinone acceptor to form triplet ion-radical pairs. These intermediates combine to a 1,4-biradical intermediate that ultimately leads to spiro-oxetane formation (**Scheme 4.15**).¹⁰⁰ In addition, exclusive oxetane formation was rationalized by Maruyama and Otsuki in terms of dipole-dipole interactions of the reactants.³¹

Bryce-Smith and Gilbert observed the formation of the cyclobutane adduct (despite predominant spiro-oxetane formation) upon irradiation in benzene, albeit only in trace amounts.^{81, 96}

4.2.4 Photocycloadditions of 2-acetoxy-1, 4-naphthoquinone

Photocycloadditions involving 2-acetoxy-1,4-naphthoquinone are rare.^{78, 80-81} In this study, the best conditions in terms of conversion and selectivity were achieved in acetone using UVA light. As can be seen in **Figure 4.18**, the absorption of 2-acetoxy-1,4-naphthoquinone overlaps most efficiently with the emission of UVA lamp, thus enabling effective excitation.

Due to the lack of information on the excited states of 2-acetoxy-1,4-naphthoquinone, the role of acetone cannot be determined. The photocycloaddition gave the corresponding cyclobutane in excellent regioselectivity, while the formation of spiro-oxetanes was not observed. This excellent chemoselectivity is caused by the electron-donor substituent at the 2-position. The acetoxy-group increases the energy of the n,π^* triplet state above that of the corresponding π,π^* counterpart, thus favouring the addition of the alkene at the quinonoid C=C site.¹⁶¹

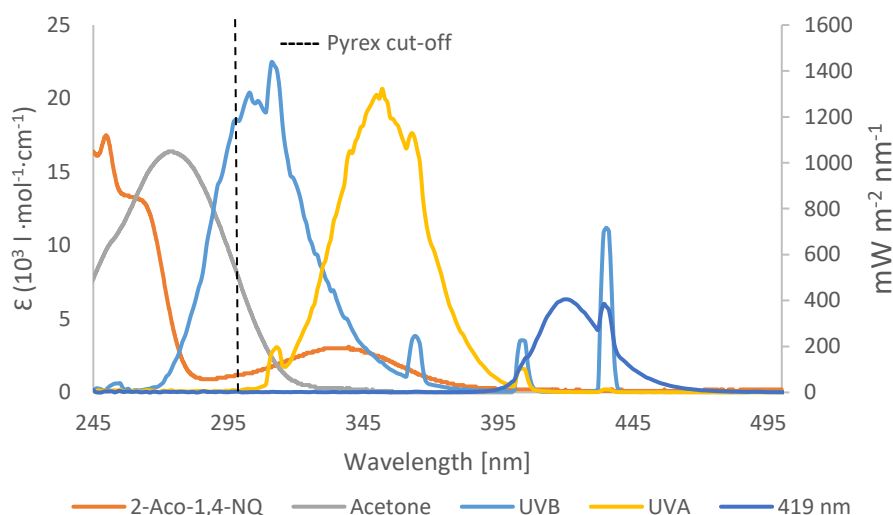
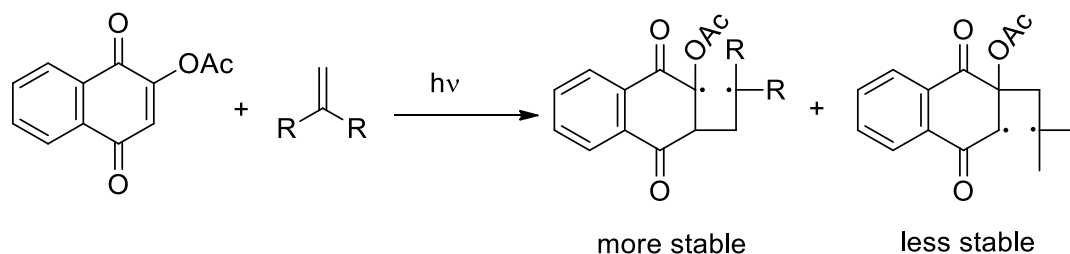


Figure 4.18: UV spectra (in MeCN) vs. UVB, UVA and 419 nm lamps.

Although photocycloadditions involved asymmetrical alkenes, the cyclobutane adduct was obtained in high regioselectivity as *head-to-head* isomer. This outcome can be attributed to differences in stability of the 1,4-diradical intermediates (**Scheme 4.20**).¹⁵³



Scheme 4.20: Possible 1,4-diradical intermediates.

As the tertiary 1,4-diradical intermediate is more stable, the *head-to-head* arrangement is preferentially adopted. Subsequent ring closure results in the formation of the corresponding cyclobutane derivatives.

The general trends obtained under batch conditions were also observed under flow conditions, although the latter achieved a reduction in irradiation time. Again, improved light penetration in combination with the somewhat superior design configuration of the flow device can explain the improved performance.

Photocycloadditions of acetyloxy-1,4-naphthoquinone have been reported by Covell and Cleridou in benzene or acetonitrile using a conventional immersion well reactor.^{78, 81} Although

these others reported similar yields for the cyclobutane adducts, the developed procedure in this study utilized non-hazardous acetone in combination with more selective UVA light instead. This protocol was furthermore successfully transferred to the *in-house* flow reactor.

4.2.5 [2+2]-Photocycloaddition of diphenylacetylene to naphthoquinones

The photocycloaddition of diphenylacetylene to 1,4-naphthoquinone and 2-acetoxy-1,4-naphthoquinone in acetone was successfully realized under batch conditions. In contrast to the corresponding alkenes, photoadditions occurred at both, the carbonyl as well as the quinonoid C=C sites.¹⁶⁹ Farid and co-workers noted that photocycloadditions involving alkynes utilize different excited states of the quinone.¹⁷⁰ Pappaasn and Portnoy furthermore suggested that the competing modes of addition were impacted by the solvent, temperature and concentration.¹⁷¹ In acetone, the 1,4-naphthoquinone-diphenylacetylene pair showed complete reaction and furnished a 4 : 1 mixture of benzoanthracenone product and cyclobutene adduct after 12 hours of UVB irradiation. In comparison, irradiation of 2-acetoxy-1,4-naphthoquinone with UVA for 10 hours yielded the corresponding products in equal amounts. The results obtained for 1,4-naphthoquinone are in agreement with those reported by Chen *et. al.*, who isolated the benzoanthracenone and cyclobutene products in yields of 37 and 24%, respectively, after 16 hours of irradiation in benzene with light >400 nm.¹⁷²

Pappaasn and co-workers studied the same transformation in acetonitrile using a black (UVA) light source.¹⁶⁹ After 9 hours, the authors obtained a 1 : 4 mixture of the cyclobutene adduct and the methide product (Figure 4.19). 2-acetoxy-1,4-naphthoquinone gave a 1 : 1 mixture of the corresponding cyclobutene adduct and methide product after 31 hours of irradiation. A related methide product was furthermore obtained during the photoreaction of 1,4-benzoquinone with diphenylacetylene.¹⁷³

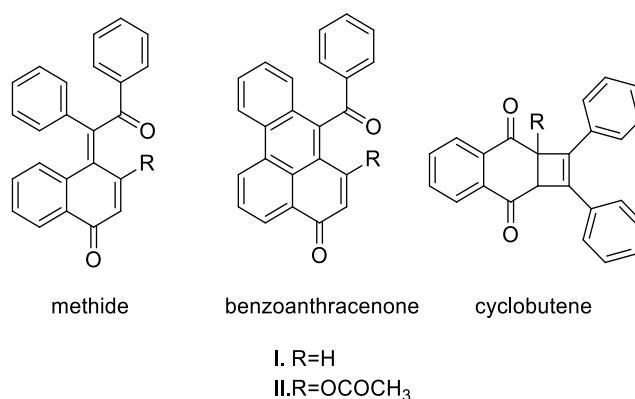
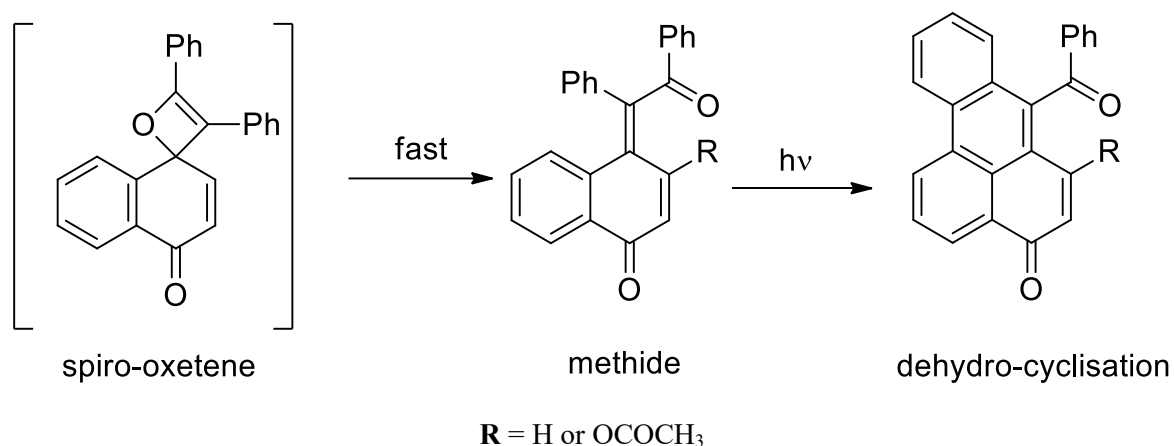


Figure 4.19: General photoadducts obtained with diphenylacetylene.

Farid suggested that the observed methides are generated by rearrangement of the initially formed spiro-oxetene. Subsequent irradiation converted the methide into the corresponding benzoanthracenone product in high yield via a dehydrocyclization route.¹⁷⁰ The same mechanistic scenario can be adopted for this study. This is supported by the successful isolation of the methide intermediate in 5% during purification (**Scheme 4.21**).



Scheme 4.21: Benzoanthracenone formation pathway.

In comparison with the related *trans*-stilbene, the mechanistic pathways towards methide or benzoanthracenone and spiro-oxetane formation appear somewhat related. Bosch and co-workers indeed revealed that quinone methide formation is initiated by either photoinduced electron transfer or direct excitation of the quinone.¹⁷³

Interestingly, Chen and co-workers examined the bioactivities of benzoanthracenones, which exhibited a universal activation on miRNAs.¹⁷² As a result, the developed procedure may offer a convenient and general access to benzoanthracenones.

4.2.6 Solar photocycloaddition of naphthoquinones

Although early examinations on the photochemistry of quinones were conducted in natural sunlight, only one example of a solar cycloaddition has been described.^{81, 174}

The solar photocycloaddition of alkenes to 1,4-naphthoquinone showed significant differences in performances. In particular, direct exposure in the solar float furnished low to moderate conversions after 200 min of illumination, while the concentrating solar flow reactor achieved excellent conversions with residence times of 70 min. The results thus mirror those obtained for the photoacylation reactions. The superior performance of the solar flow process can be again attributed to the improved harvesting of sunlight through concentration in combination

with advantageous reactor materials. The solar radiation data for the individual experimental periods is shown in **Figure 4.20**. Illuminations were launched at noon, when solar irradiation was most intense, and were typically run until 3–4 pm. As noticeable from the shape of the individual radiation curves, most experiments were conducted under largely sunny conditions. Clouds caused a reduction in solar radiation, especially noticeable for the 21st of September 2018. Ideal sunny conditions were present solely on the 30th of September 2018.

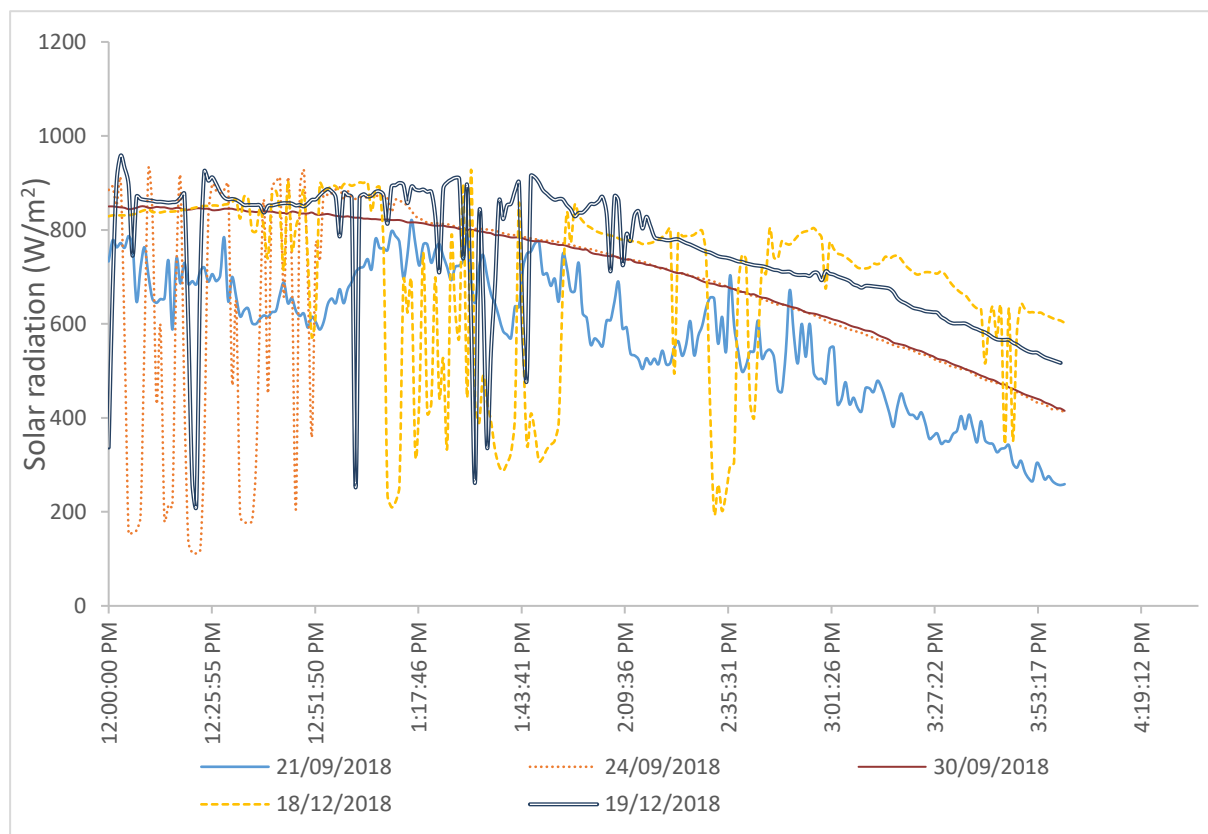
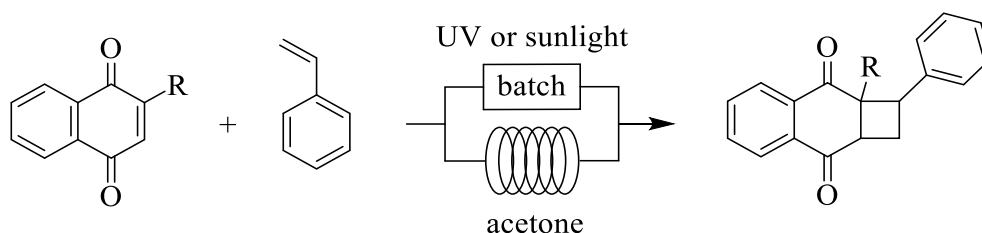


Figure 4.20: Solar radiation data for the experimental days.

Large-scale solar [2+2]-cycloadditions of 2-acetoxy-1,4-naphthoquinone with styrene and 1,1-diphenylethylene in acetonitrile were first realized by Covell and co-workers.⁸¹ The reaction mixtures were exposed for 6 hours in an advanced CPC reactor with a sun concentrating factor of 2-3, which achieved 96% conversion for both alkenes. However, the same reactions in acetone were conducted in the simple concentrating solar flow reactor with a similar concentration factor of 3 and resulted in complete conversion for styrene and 83% conversion for 1,1-diphenylethylene, respectively. The concentration of sunlight thus allows acceleration of photochemical processes due to an increase in the solar photon flux.

For both naphthoquinones, the chemoselectivity towards cyclobutane formation was largely the same with artificial and solar light, suggesting predominant sensitization by acetone.

The performances of the UV-driven batch, UV-driven flow and solar-driven flow processes for the naphthoquinone photocycloaddition reactions involving styrene (**Scheme 4.22**) are compared in **Table 4.5**. In all cases, conversions were comparable and ranged from 80-100%. The flow processes utilizing artificial UV-light showed the fastest reactions. The excellent conversions observed during the solar flow process may be attributed to the larger inner dimensions of the solar flow reactor, thus allowing the population of more excited states. Although the usable UV-range of sunlight is limited, the solar flow transformation involving 2-acetoxy-1,4-naphthoquinone showed the fastest reaction. A similar discrepancy in conversion rates between artificial and sunlight irradiation was also reported by Covell and co-workers. In particular, solar illumination achieved 96% conversion, while that with artificial light was around 80%.⁸¹



Scheme 2.22: Photocycloaddition of naphthoquinones to styrene used for process comparison.

Table 4.5: Comparison of batch, UV-driven flow, and solar-driven flow processes.

entry	R	UV-driven				Solar Flow	
		Batch		Flow		Time	Conversion
		Time	Conversion	Time	Conversion		
1	H	10 hours	96%	45 min	96%	70 min	80%
2	OCOCH ₃	10 hours	97%	120 min	97%	70 min	100%

In summary, this study has developed a sustainable protocol to conduct efficient and selective photocycloaddition reactions. It combines natural sunlight, acetone as a sustainable solvent and flow operation and provides an easy access to cyclobutane adducts

Chapter 5: Summary and Outlook

5. Summary and Outlook

5.1 Photo-Friedel-Crafts acylation of naphthoquinone

Quinone photochemistry is a key intermediate step in pharmaceuticals and a pathway to natural products. However, there are few reports of the photochemical transformations of 1,4-naphthoquinone. Thus, a series of photochemical reactions for naphthoquinone were explored.

By adopting a green chemistry approach, the conventional procedure for the Photo-Friedel-Crafts acylation of naphthoquinone was improved under batch conditions by replacing the toxic and expensive solvents commonly used, *i.e.* ionic liquids, supercritical CO₂ and trifluorotoluene (TFT), with acetone, a green and low-cost solvent. Acylated hydroquinones were also observed in higher yield and selectivity compared to those reported elsewhere due to acetone triplet sensitisation, which was first employed in naphthoquinone acylation.

Combining the advantages of acetone photochemistry with a chemical flow operation resulted in remarkable outcomes for naphthoquinone photoacylation, as illustrated by the reduced reaction time from 28 hr to 70 min.

The photochemical-thermal tandem synthesis of an acylated naphthoquinone was investigated by combining the photoacylation with a thermal oxidation step; conversions of 31-94% in both steps were achieved.

Despite the failure of the one-flow multistep scheme for the synthesis 2-dodecanoyl-3-hydroxy-1,4-naphthoquinone (DHN) from 2-substituted-1,4-naphthoquinone, the photochemical reaction of 2-hydroxy-1,4-naphthoquinone with aldehyde was first explored by the author. The failure of the acylation reaction of 2-hydroxy-1,4-naphthoquinone was discussed. The photoacylation of 2-acetoxy-1,4-naphthoquinone with an aldehyde was first performed in this research, but the yield was poor. Therefore, the electron donor substituents on naphthoquinone did not provide convenient access to the DHN compound because of their non-selectivity.

Selected examples of the photoacylation of 1,4-naphthoquinone with aldehydes were realized in a concentrated solar trough flow reactor. The reactor was designed to focus sunlight onto a reaction capillary. The initial design achieved a three-fold concentration of sunlight; the desired products were isolated in low to high yield within a short residence time of 70 min. Comparison reactions by placing a Pyrex test tube into direct sunlight produced lower yields for the same exposure.

5.2 [2+2] Photocycloaddition of naphthoquinone

The photochemistry of quinones involves cycloaddition processes that produce 4-membered rings, which are extremely difficult to synthesise by thermal reactions. However, the [2+2] photocycloaddition of naphthoquinone to an alkene is still underutilised in organic synthesis. To fill this gap, this study investigated the photocycloaddition of alkene and alkyne to naphthoquinone using green chemistry.

The conventional procedure for the photocycloaddition of naphthoquinone to an alkene under batch conditions changed to a more sustainable experimental procedure in terms of the product yield, light source, reaction time, and solvent usage. Acetone again served as an effective co-solvent and triplet-sensitizer.

The substantial improvements in the batch system were transferred successfully to the continuous flow set-up. The findings revealed a significantly reduced reaction time from 12 hr. to 60 min because of the efficient penetration of light. In addition, the removal of products from the irradiated zone reduced the rate of photodecomposition and improved the yield, product quality, and selectivity.

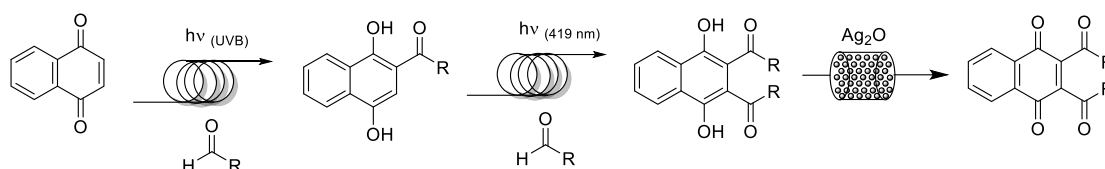
The experimental procedure with artificial UV light was then transferred outdoors using sunlight. Solar comparison studies were conducted by either placing a Pyrex test tube into direct sunlight or by utilizing a concentrated solar trough flow reactor.

The results confirmed the superiority of solar flow operations over conventional solar batch procedures. Therefore, natural sunlight is a suitable, eco-friendly, and sustainable energy source for photochemical activation.

5.3 Outlook

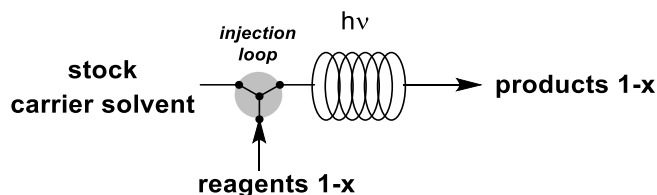
Some acylated hydroquinones and photo-adducts of quinones exhibit biological activity and resemble natural products. Selected derivatives synthesized in this project have the potential for biological screening.

Regarding synthesis in series, examining the multi-irradiation step photoacylation of 1, 4-naphthoquinone in a single flow is interesting because acylated hydroquinones are capable of secondary acylation. For example, when photoacylation is carried out using UVB light, further irradiation is required at a longer wavelength, such as 419 nm, followed by an oxidation step in one flow (**Scheme 5.1**).



Scheme 5.1: three-step synthesis in a single flow

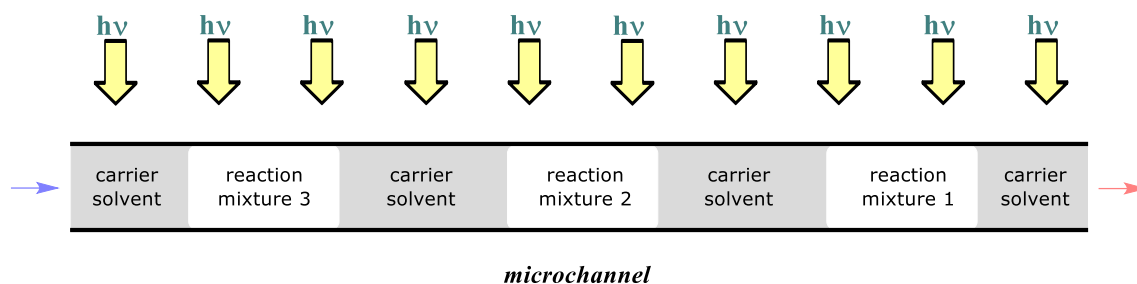
In terms of continuous flow operation, novel approaches will be investigated. For example, flow injection is an exciting approach for the space- and time-efficient production of small libraries. Conventional flow reactors only allow single reactions per run. Flow injection techniques, as commonly used for analytical and separation devices, offer an interesting modification that allows in-series synthesis. The use of a rotary pump allows a chemically inert and immiscible carrier solvent to be pumped continuously through the flow reactor from an external reservoir. The entire reaction mixture can be injected into the carrier solvent in carefully timed intervals, thereby generating segmented flow (**Scheme 5.2**).



Scheme 5.2: Flow injection techniques.

The time required for the segments to pass through the reaction channel can be calculated directly from the flow-rate and the volume of the reaction and injection channel. The departing segment flow can be collected using a fraction collector (literally ‘reaction’ collector) (**Scheme 5.3**). For this study, a manual injection option can be used for HPLC, but the flow injection

design allows for future automation using robotic syringes and fraction collectors. The injection loop can be retrofitted easily into conventional flow devices.



Scheme 5.3: The irradiation area in segment flow.

Chapter 6:

Experimental Part

6. Experimental

6.1 General methods

6.1.1 Solvents and reagents

All solvents and reagents were commercially available (Sigma-Aldrich or Alfa Aesar) and were used without purification unless otherwise noted. 1,4-Naphthoquinone was purified by sublimation.

6.1.2 Photochemical equipment

Photoreactors: Batch experiments were carried out in a Rayonet RPR-200 photochemical chamber reactor (Southern New England Ultraviolet Company, USA) equipped with 16 × 8 W fluorescent tubes. In-house setups were used for both in-door as well as outdoor flow reactions and have been described in detail in **Chapter 3.2**.

Glassware: All reactions were performed in Pyrex glassware unless otherwise specified.

6.1.3 Analytical methods

NMR: The NMR facilities at JCU and at the Biomolecular Analysis Laboratory at AIMS in Townsville were used. At JCU, NMR spectra were recorded on a Bruker 400 Ascend™ (¹H: 400 MHz and ¹³C: 100 MHz) equipped with an auto-sampler. At AIMS, NMR spectra were recorded on a Bruker Avance 300 Ultrashield™ (¹H: 300 MHz and ¹³C: 75 MHz) or Bruker 400 Ascend™ (¹H: 400 MHz and ¹³C: 100 MHz). Data was acquired using TopSpin 2.1, 3.0 or 3.5, respectively. NMR spectra were processed using the MestReNova v5.3.2-4936 software. Samples were prepared in CDCl₃ (δ = 7.26/77.3 ppm) and acetone-d₆ (δ = 2.09/30.6 ppm). TMS (δ = 0 ppm) or the residual solvent peak served as internal standards. Solvent peaks and impurities were compared with literature values.¹⁷⁵

LCMS: Mass spectra were recorded using direct injection on a Shimadzu LCMS-2020 equipped with a DUIS ion source. Ions were subsequently detected in positive mode and/or negative mode within a mass range of m/z 100-500. The mobile phase were aqueous solutions of HPLC grade methanol or acetonitrile with

- 0.1% formic acid added. All experimental event sequences were controlled and processing performed using LabSolutions for LCMS-2020 software.
- IR: Infrared spectra were recorded on a Perkin Elmer Spectrum One FT-IR Spectrometer as thin films. Spectra were recorded in the range 600-4000 cm^{-1} . IR peaks are listed in wavenumbers (ν ; in cm^{-1}).
- Melting point: Melting points were measured in open capillaries using a Tathastu or Gallenkamp melting point apparatus and are uncorrected.
- X-ray: X-ray crystallographic analyses were performed on a Bruker APEX-II CCD diffractometer.

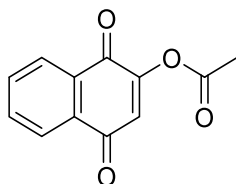
6.1.4 Chromatographic methods

- TLC: Thin layer chromatography was performed in glass jars on Macherey-Nagel polygram sil G/UV₂₅₄. Mixtures of ethyl acetate and cyclohexane or ethyl acetate and *n*-hexane were used as mobile phase.
- Separations: Column chromatography was carried out in Pyrex glass columns using Scharlau silica gel 60 (particle size 0.06-0.2 nm) 70-230 mesh ASTM. Mixtures of ethyl acetate and cyclohexane or ethyl acetate and *n*-hexane was used as mobile phase.
- Combi flash: A CombiFlash[®] Rf⁺ Lumen[™] flash chromatography system from Teledyne Isco was used to purify product mixtures. The system recorded UV spectra in real-time during peak elution. Normal phase cartridges were used. A mixture of *n*-hexane and ethyl acetate was utilized as mobile phase.

6.2 Synthesis of starting materials

6.2.1 Synthesis of 2-acetoxy-1,4-naphthoquinone

2-Hydroxy-1,4-naphthoquinone (0.05 mol), acetic anhydride (30 mL) and concentrated sulfuric acid (10 drops) were heated for 1 hour on a steam bath. The reaction mixture was subsequently poured into cold water. After complete hydrolyses of excess anhydride had taken place, the solid product was filtered and washed by cold water. Recrystallization from ethanol or aqueous methanol gave 2-acetoxy-1,4-naphthoquinone as yellow prisms in a yield of 80%.



¹H-NMR: (400 MHz, CDCl₃)

δ (ppm): 8.13 (dd, $J = 9.3$ Hz, 1H, CH_{arom}), 7.79 (m, 1H, CH_{arom}), 6.79 (s, 1H, CH_{quin}), 2.41 (s, 3H, COCH₃).

6.3 Photoacylations of 1,4-naphthoquinones

6.3.1 Photoacylations of 1,4-naphthoquinones under batch conditions

General procedure 1 (GP1): A solution of 1,4-naphthoquinone (1 mmol) and aldehydes (5 mmol) in an organic solvent (50 mL) was degassed with nitrogen for 5 minutes and irradiated in a Pyrex Schlenk flask (transmission >300 nm) for 28 hours inside a Rayonet photochemical reactor (RPR-200; Southern New England Ultraviolet Company) equipped with 16 × 8 W fluorescent tubes.

6.3.2 Photoacylations of 1,4-naphthoquinones under continuous-flow conditions

General procedure 2 (GP2): A solution of naphthoquinone (0.5 mmol) and aldehyde (2.5 mmol) in acetone (25 mL) was degassed with nitrogen for 5 minutes and placed into a syringe. The solution was pumped through the in-house flow photoreactor equipped with a single 8 W fluorescent tube. Photoacylations were conducted using a residence time of 70 min.

6.3.3 Solar photoacylations of 1,4-naphthoquinones under batch conditions

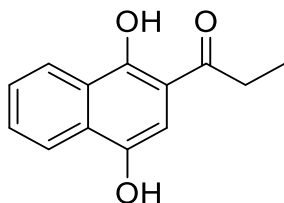
General procedure 3 (GP3): A solution of 1,4-naphthoquinone (1 mmol) and aldehyde (5 mmol) in acetone (50 mL) was degassed with nitrogen for 5 minutes and split over two test tubes. The tubes were placed in the solar float and exposed to direct sunlight for 200 min.

6.3.4 Solar photoacylations of 1,4-naphthoquinones under continuous-flow conditions

General procedure 4 (GP4): A solution of 1,4-naphthoquinone (2 mmol) and aldehyde (10 mmol) in acetone (100 mL) was degassed with nitrogen for 5 minutes and pumped through the in-house solar flow reactor. Photoacylations were conducted using a residence time of 70 min.

6.3.5 Photochemical transformations

6.3.5.1 Synthesis of 1-(1,4-dihydroxynaphthalen-2-yl) propan-1-one (6a)



General procedure **GP2** was followed using 0.079 g of 1,4-naphthoquinone, 0.145 g of propionaldehyde in 25 mL of acetone and a residence time of 70 min. Yield: 0.0756 g (70 %).

¹H-NMR: (400 MHz, acetone-d₆)

δ (ppm): 13.68 (s, 1H, OH), 8.39 (d, J = 8.4 Hz, 1H, CH_{arom}), 8.21 (dd, J = 8.3, 1.3 Hz, 1H, CH_{arom}), 7.70 (ddd, J = 8.3, 1.3 Hz, 1H, CH_{arom}), 7.60 (ddd, J = 8.3, 1.3 Hz, 1H, CH_{arom}), 7.20 (s, 1H, CH_{arom}) 3.10 (q, J = 7.2 Hz, 2H, CH₂), 1.22 (t, J = 7.2 Hz, 3H, CH₃).

¹³C NMR: (100 MHz, CDCl₃)

δ (ppm): 206.3 (s, 1C, C=O), 157.4 (s, 1C, C_{qarom}), 143.0 (s, 1C, C_{qarom}), 129.8 (d, 1C, CH), 129.4 (s, 1C, C_{qarom}), 126.7 (d, 1C, CH_{arom}), 126.4 (s, 1C, C_{qarom}), 124.8 (d, 1C, CH_{arom}), 121.6 (d, 1C, CH_{arom}), 111.7 (s, 1C, C_{qarom}), 105.5 (d, 1C, CH_{arom}), 32.1 (t, 1C, CH₂), 8.47 (q, 1C, CH₃).

MS (DUIS):

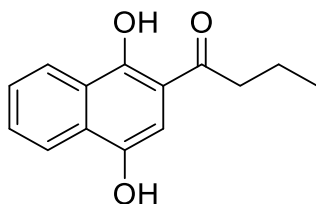
m/z: 217 [M⁺+H]; expected: 216 [M⁺].

IR (neat):

ν (cm⁻¹): 3398, 2921, 1636, 1613, 1595, 1515, 1470, 1429, 1302, 1215, 1138, 1073, 1038, 789, 758.

M.P: 175-177°C (lit.:¹⁰¹ 178-179°C).

6.3.5.2 Synthesis of 1-(1,4-dihydroxynaphthalen-2-yl) butan-1-one (6b)



General procedure **GP1** was followed using 0.158 g of 1,4-naphthoquinone, 0.36 g of butyraldehyde in 50 mL of acetone and irradiation with UVB light for 28 hours. Yield: 0.172 g (75 %).

General procedure **GP2** was followed using 0.079 g of 1,4-naphthoquinone, 0.18 g of butyraldehyde in 25 mL of acetone and a residence time of 70 min. Yield: 0.101 g (88 %).

General procedure **GP3** was followed using 0.158 g of 1,4-naphthoquinone, 0.36 g of butyraldehyde in 50 mL of acetone and illumination in sunlight for 200 min. Yield: 0.138 g (60 %).

General procedure **GP4** was followed using 0.316 g of 1,4-naphthoquinone, 0.72 g of butyraldehyde in 100 mL of acetone and a residence time of 70 min. Yield: 0.404 g (88 %).

The crude photoproduct was purified by washing with warm distilled water (~50°C) and filtration, followed by washing with cold *n*-hexane and drying in vacuum to give the title product as a yellow solid.

¹H-NMR: (400 MHz, CDCl₃)

δ (ppm): 13.78 (s, 1H, OH), 8.46 (d, *J* = 8.3 Hz, 1H, CH_{arom}), 8.10 (d, *J* = 8.2, 1H, CH_{arom}), 7.68 (ddd, *J* = 8.3, 1.4 Hz, 1H, CH_{arom}), 7.58 (ddd, *J* = 8.2, 1.3 Hz, 1H, CH_{arom}), 7.03 (s, 1H, CH_{arom}), 5.07 (s, 1H, OH), 2.96 (t, *J* = 7.5 Hz, 2H, CH₂), 1.82 (sxt, *J* = 7.2 Hz, 2H, CH₂), 1.05 (t, *J* = 7.4 Hz, 3H, CH₃).

¹³C NMR: (100 MHz, CDCl₃)

δ (ppm): 206.0 (s, 1C, C=O), 157.6 (s, 1 C, C_{qarom}), 143.0 (s, 1 C, C_{qarom}), 129.8 (d, 1C, CH_{arom}), 129.5 (d, 1 C, C_{qarom}), 126.7 (d, 1C, CH_{arom}), 126.3 (s, 1 C, C_{qarom}), 124.8 (d, 1C, CH_{arom}), 121.7 (d, 1C, CH_{arom}), 111.9 (s, 1 C, C_{qarom}), 105.6 (d, 1C, CH_{arom}), 40.8 (t, 1C, CH₂), 18.2 (t, 1C, CH₂), 14.0 (q, 1C, CH₃).

MS (DUIS):

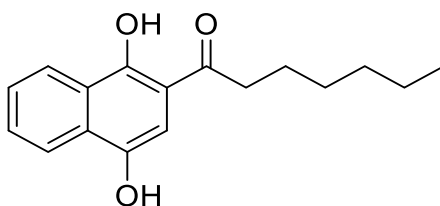
m/z: 231 [M⁺+H]; expected: 230 [M⁺].

IR (neat):

ν (cm⁻¹): 3316, 2967-2876, 1633, 1592, 1463, 1398, 1380, 1327, 1291, 1200, 1139, 1074, 1044, 765.

M.P: 144-145°C(lit.:⁸⁸ 145-146°C)

6.3.5.3 Synthesis of 1-(1,4-dihydroxynaphthalen-2-yl) heptan-1-one (6c)



General procedure **GP2** was followed using 0.079 g of 1,4-naphthoquinone, 0.285 g of heptaldehyde in 25 mL of acetone and a residence time of 70 min. Yield: 0.102 g (75 %).

¹H-NMR: (300 MHz, CDCl₃)

δ (ppm): 13.77 (s, 1H, OH), 8.45 (d, J = 8.3 Hz, 1H, CH_{arom}), 8.09 (d, J = 8.2 Hz, 1H, CH_{arom}), 7.67 (ddd, J = 8.1, 1.4 Hz, 1H, CH_{arom}), 7.57 (ddd, J = 8.2, 1.2 Hz, 1H, CH_{arom}), 7.02 (s, 1H, CH_{arom}), 5.15 (s, 1H, OH), 2.96 (t, J = 7.4 Hz, 2H, CH₂), 1.77 (quin, J = 7.5 Hz, 2H, CH₂), 1.46–1.24 (m, 6H, 3×CH₂), 0.90 (t, J = 6.9 Hz, 3H, CH₃).

¹³C NMR: (100 MHz, CDCl₃)

δ (ppm): 206.3 (s, 1C, C=O), 157.5 (s, 1 C, C_{qarom}), 143.1 (s, 1 C, C_{qarom}), 129.8 (d, 1C, CH_{arom}), 129.5 (s, 1 C, C_{qarom}), 126.6 (d, 1C, CH_{arom}), 126.3 (s, 1 C, C_{qarom}), 124.7 (d, 1C, CH_{arom}), 121.7 (d, 1C, CH_{arom}), 111.9 (s, 1 C, C_{qarom}), 105.9 (d, 1C, CH_{arom}), 38.9 (d, 1C, CH_{arom}), 31.8 (t, 1C, CH₂), 29.2 (d, 1C, CH₂), 24.7 (d, 1C, CH₂), 22.7 (d, 1C, CH₂), 14.2 (q, 1C, CH₃).

MS (DUIS):

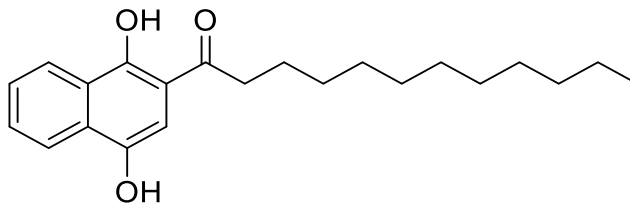
m/z : 271 [M⁺-H]; expected: 272 [M⁺].

IR (neat):

ν (cm⁻¹): 3012, 2969-2855, 1738, 1616, 1540, 1456, 1365, 1229, 1216, 1073, 762.

M.P: 133-134°C (lit.:³⁶ 135-136°C).

6.3.5.4 Synthesis of 1-(1,4-dihydroxynaphthalen-2-yl)dodecan-1-one (6d)



General procedure **GP2** was followed using 0.079 g of 1,4-naphthoquinone, 0.46 g of dodecylaldehyde in 25 mL of acetone and a residence time of 70 min. Yield: 0.058 g (34 %).

General procedure **GP3** was followed using 0.158 g of 1,4-naphthoquinone, 0.921 g of dodecylaldehyde in 50 mL of acetone and illumination in sunlight for 200 min. Yield: 0.06 g (17 %).

General procedure **GP4** was followed using 0.316 g of 1,4-naphthoquinone, 1.842 g of dodecylaldehyde in 100 mL of acetone and a residence time of 70 min. Yield: 0.150 g (22 %).

The crude photoproduct was purified by washing with warm distilled water (~50°C) and filtration, followed by column chromatography on silica gel (*n*-hexane : ethyl acetate = 4 : 1) and drying in vacuum to give the title product as a yellow solid.

¹H-NMR: (400 MHz, CDCl₃)

δ (ppm): 13.78 (s, 1H, OH), 8.46 (d, *J* = 8.7 Hz, 1H, CH_{arom}), 8.10 (d, *J* = 8.3 Hz, 1H, CH_{arom}), 7.67 (ddd, *J* = 8.3, 1.3 Hz, 1H, CH_{arom}), 7.57 (ddd, *J* = 8.2, 1.1 Hz, 1H, CH_{arom}), 7.02 (s, 1H, CH_{arom}), 5.16 (s, 1H, OH), 2.95 (t, *J* = 7.5 Hz, 2H, CH₂), 1.77 (quin, *J* = 7.6 Hz, 2H, CH₂), 1.45–1.20 (m, 16H, 8×CH₂), 0.88 (t, *J* = 6.8 Hz, 3H, CH₃).

¹³C NMR: (100 MHz, CDCl₃)

δ (ppm): 206.2 (s, 1C, C=O), 157.6 (s, 1C, C_{qarom}), 143.0 (s, 1C, C_{qarom}), 129.8 (d, 1C, CH_{arom}), 129.5 (s, 1C, C_{qarom}), 126.7 (d, 1C, CH_{arom}), 126.4 (s, 1C, C_{qarom}), 124.8 (d, 1C, CH_{arom}), 121.6 (d, 1C, CH_{arom}), 111.8 (s, 1C, C_{qarom}), 105.7 (d, 1C, CH_{arom}), 38.9 (t, 1C, CH₂), 32.1 (t, 1C, CH₂), 29.8 (t, 1C, CH₂), 29.8 (t, 1C, CH₂), 29.7 (t, 1C, CH₂), 29.6 (t, 1C, CH₂), 29.5 (t, 1C, CH₂), 29.4 (t, 1C, CH₂), 24.8 (t, 1C, CH₂), 22.8 (t, 1C, CH₂), 14.3 (q, 1C, CH₃).

MS (DUIS):

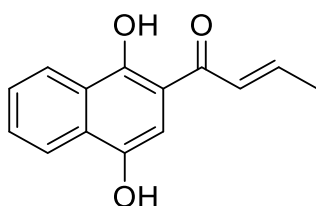
m/z: 341 [M⁺-H]; expected: 342 [M⁺].

IR (neat):

ν (cm⁻¹): 3331, 2953-2850, 1738, 1634, 1590, 1467, 1399, 1292, 1190, 1136, 1075, 1028, 879, 765.

M.P: 105-106°C(lit.:³⁶ 130-133°C).

6.3.5.5 Synthesis of 1-(1,4-dihydroxynaphthalen-2-yl) buten-1-one (6e)



General procedure **GP2** was followed using 0.079 g of 1,4-naphthoquinone, 0.175 g of crotonaldehyde in 25 mL of acetone and a residence time of 70 min. Yield: 0.08 g (72%).

General procedure **GP3** was followed using 0.158 g of 1,4-naphthoquinone, 0.35 g of crotonaldehyde in 50 mL of acetone and illumination in sunlight for 200 min. Yield: 0.091 g (40 %).

General procedure **GP4** was followed using 0.316 g of 1,4-naphthoquinone, 0.7 g of crotonaldehyde in 100 mL of acetone and a residence time of 70 min. Yield: 0.237 g (52 %).

The crude photoproduct was purified by washing with warm distilled water (~50°C) and filtration, followed by precipitation from cold chloroform and drying in vacuum to give the title product as a redish solid.

¹H-NMR: (400 MHz, DMSO-d₆)

δ (ppm): 14.13 (s, 1H, OH), 9.76 (s, 1H, OH), 8.31 (d, J = 8.2 Hz, 1H, CH_{arom}), 8.13 (d, J = 8.3 Hz, 1H, CH_{arom}), 7.72 (ddd, J = 8.3, 1.3 Hz, 1H, CH_{arom}), 7.61 (ddd, J = 8.0, 1.2 Hz, 1H, CH_{arom}), 7.20 (s, 1H, CH_{arom}), 7.18–7.15 (m, 2H, 2×CH=), 2.05 (d, J = 4.1 Hz, 3H, CH₃).

¹³C NMR: (100 MHz, acetone-d₆)

δ (ppm): 194.3 (s, 1C, C=O), 158.7 (s, 1C, C_{qarom}), 146.5 (d, 1C, =CH), 145.5 (s, 1C, C_{qarom}), 130.9 (s, 1C, C_{qarom}), 130.3 (d, 1C, =CH), 127.2 (d, 1C, CH_{arom}), 126.9 (s, 1C, C_{qarom}), 126.7 (d, 1C, CH_{arom}), 124.8 (d, 1C, CH_{arom}), 123.1 (d, 1C, CH_{arom}), 113.0 (s, 1C, C_{qarom}), 105.3 (d, 1C, CH), 18.7 (q, 1C, CH₃).

MS (DUIS):

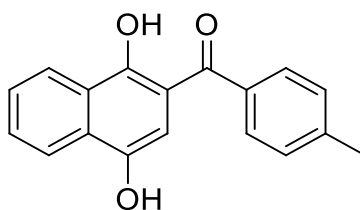
m/z: 229 [M⁺+H]; expected: 228 [M⁺].

IR (neat):

ν (cm⁻¹): 3302, 1630, 1578, 1514, 1474, 1441, 1390, 1299, 1221, 1140, 1076, 1062, 959, 893, 810, 762.

M.P: 169-170°C (lit.:¹⁰¹ 164-165°C).

6.3.5.6 Synthesis of (1,4-Dihydroxy-naphthalen-2-yl)-p-tolyl-methanone (6f)



General procedure **GP2** was followed using 0.079 g of 1,4-naphthoquinone, 0.3 g of *p*-methylbenzaldehyde in 25 mL of acetone and a residence time of 70 min. Yield: 0.092g (66%).

General procedure **GP3** was followed using 0.158 g of 1,4-naphthoquinone, 0.6 g of *p*-methylbenzaldehyde in 50 mL of acetone and illumination in sunlight for 200 min. Yield: 0.071 g (25 %).

General procedure **GP4** was followed using 0.316 g of 1,4-naphthoquinone, 1.2 g of *p*-methylbenzaldehyde in 100 mL of acetone and a residence time of 70 min. Yield: 0.245 g (44%).

The crude photoproduct was purified by column chromatography using toluene : ethyl acetate (4 : 1) and afforded the title product as a brownish solid.

¹H-NMR: (400 MHz, acetone-d₆)

δ (ppm): 13.55 (s, 1H, OH), 8.66 (broad s, 1H, OH), 8.45 (d, J = 8.4 Hz, 1H, CH_{arom}), 8.23 (d, J = 8.4 Hz, 1H, CH_{arom}), 7.74 (ddd, J = 8.3, 1.3 Hz, 1H, CH_{arom}), 7.69–7.62 (m, 3H, CH_{arom}), 7.42 (d, J = 7.8 Hz, 2H, CH_{arom}), 7.02 (s, 1H, CH_{arom}), 2.47 (s, 3H, CH₃).

¹³C NMR: (100 MHz, acetone-d₆)

δ (ppm): 201.8 (s, 1C, C=O), 158.0 (s, 1 C, C_{qarom}), 145.2 (s, 1C, C_{qarom}), 143.1 (s, 1C, C_{qarom}), 136.6 (s, 1 C, C_{qarom}), 130.5 (d, 1C, CH_{arom}), 130.0 (d, 2C, CH_{arom}), 129.8 (d, 2C, CH_{arom}), 127.3 (d, 1C, CH_{arom}), 126.8 (s, 1 C, C_{qarom}), 124.9 (d, 1C, CH_{arom}), 123.2 (d, 1C, CH_{arom}), 112.9 (d, 1C, CH_{arom}), 108.0 (d, 1C, CH_{arom}), 21.5 (q, 1C, CH₃).

MS (DUIS):

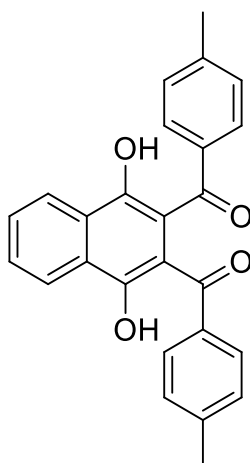
m/z: 279 [M⁺+H]; expected: 278 [M⁺].

IR (neat):

ν (cm⁻¹): 3288, 3000-2921, 1667, 1633, 1584, 1557, 1506, 1456, 1392, 1325, 1281, 1252, 1180, 1160, 1115, 1076, 999, 831, 755.

M.P: 154-155°C (lit.:¹⁰¹ 167-169°C).

6.3.5.7 Synthesis of (1,4-dihydroxy-2-naphthalenyl)bis(*p*-tolylmethanone) **8f**



General procedure **GP2** was followed using 0.079 g of 1,4-naphthoquinone, 0.3g of *p*-methylbenzaldehyde in 25 mL of acetone and a residence time of 70 min. Yield: 0.028 g (14 %).

General procedure **GP4** was followed using 0.316 g of 1,4-naphthoquinone, 1.2 g of *p*-methylbenzaldehyde in 100 mL of acetone and a residence time of 70 min. Yield: 0.039 g (5%).

The crude photoproduct was purified by column chromatography using toluene : ethyl acetate (4 : 1) and afforded the title product as a side product as an orange solid.

¹H-NMR: (400 MHz, acetone-d₆)

δ (ppm): 13.55 (s, 1H, OH), 8.66 (broad s, 1H, OH), 8.45 (d, *J* = 8.4 Hz, 1H, CH_{arom}), 8.23 (d, *J* = 8.4 Hz, 1H, CH_{arom}), 7.74 (ddd, *J* = 8.3, 1.3 Hz, 1H, CH_{arom}), 7.69–7.62 (m, 3H, CH_{arom}), 7.42 (d, *J* = 7.8 Hz, 2H, CH_{arom}), 7.02 (s, 1H, CH_{arom}), 2.47 (s, 3H, CH₃).

¹³C NMR: (100 MHz, acetone-d₆)

δ (ppm): 198.7 (s, 2C, 2×C=O), 154.2 (s, 2C, 2×C_{qarom}), 144.0 (s, 2C, 2×C_{qarom}), 138.3 (s, 2C, 2×C_{qarom}), 131.2 (d, 2C, 2×CH_{arom}), 129.7 (d, 4C, 4×CH_{arom}), 129.5 (d, 4C, 4×CH_{arom}), 129.4 (s, 2C, 2×C_{qarom}), 125.2 (d, 2C, 2×CH_{arom}), 112.6 (s, 2C, 2×C_{qarom}), 21.5 (q, 2C, CH₃).

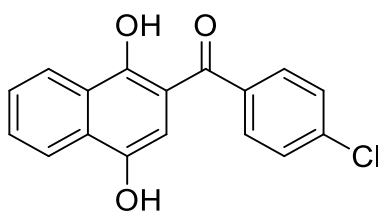
MS (DUIS):

m/z: 397 [M⁺+H]; expected: 396 [M⁺].

IR (neat):

ν (cm⁻¹): 3330, 2969-2919, 1738, 1658, 1592, 1495, 1454, 1372, 1281, 1229, 1216, 1117, 1034, 996, 901, 814, 749.

M.P: 169-170°C.

6.3.5.8 Synthesis of (4-chlorophenyl)-(1,4-dihydroxynaphthalen-2-yl)-methanone (6g).

General procedure **GP2** was followed using 0.079 g of 1,4-naphthoquinone, 0.351 g of *p*-chlorobenzaldehyde in 25 mL of acetone and a residence time of 70 min. Yield: 0.12 g (80 %).

General procedure **GP3** was followed using 0.158 g of 1,4-naphthoquinone, 0.702 g of *p*-chlorobenzaldehyde in 50 mL of acetone and illumination in sunlight for 200 min. Yield: 0.102 g (34 %).

General procedure **GP4** was followed using 0.316 g of 1,4-naphthoquinone, 1.4 g of *p*-chlorobenzaldehyde in 100 mL of acetone and a residence time of 70 min. Yield: 0.310 g (52%).

The crude photoproduct was purified by washing with warm distilled water (~50°C) and filtration, followed by precipitation from cold chloroform and drying in vacuum to give the title compound as a brownish solid.

¹H-NMR: (400 MHz, CDCl₃)

δ (ppm): 13.43 (s, 1H, OH), 9.98 (s, 1H, OH), 8.13 (d, *J* = 8.2 Hz, 1H, CH_{arom}), 8.03 (d, *J* = 8.7 Hz, 1H, CH_{arom}), 7.72 (ddd, *J* = 8.3, 1.3 Hz, 1H, CH_{arom}), 7.66 (d, *J* = 8.6 Hz, 2H, CH_{arom}), 7.62 (ddd, *J* = 8.2, 1.2 Hz, 1H, CH_{arom}), 7.50 (d, *J* = 8.6 Hz, 2H, CH_{arom}), 7.45 (d, *J* = 8.7 Hz, 1H, CH_{arom}), 7.26 (s, 1H, CH_{arom}), 6.82 (s, 1H, CH_{arom}).

¹³C NMR: (100 MHz, CDCl₃)

δ (ppm): 199.5 (s, 1C, C=O), 159.1 (s, 1C, C_{qarom}), 142.9 (s, 1C, C_{qarom}), 138.2 (s, 1C, C_{qarom}), 136.7 (s, 1C, C_{qarom}), 131.7 (s, 1C, C_{qarom}), 130.5 (d, 2C, 2×CH_{arom}), 130.4 (d, 1C, CH_{arom}), 129.7 (s, 1C, C_{qarom}), 129.1 (d, 1C, CH_{arom}), 128.9 (d, 2C, 2×CH_{arom}), 126.9 (d, 1C, CH_{arom}), 126.3 (d, 1C, CH_{arom}), 124.9 (d, 1C, CH_{arom}), 121.9 (d, 1C, CH_{arom}), 111.4 (s, 1C, C_{qarom}), 107.7 (d, 1C, CH_{arom}).

MS (DUIS):

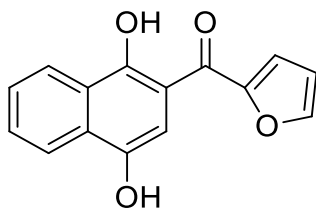
m/z: 299 [M⁺+H]; expected: 298 [M⁺].

IR (neat):

ν (cm⁻¹): 3295, 2554, 1677, 1633, 1580, 1545, 1425, 1398, 1294, 1200, 1110, 1076, 998, 843, 757.

M.P: 207-208°C (lit.:⁴² 189-190°C).

6.3.5.9 Synthesis of (1,4-dihydroxy-2-naphthalenyl) (furan-2-yl) methanone (6h)



General procedure **GP2** was followed using 0.079 g of 1,4-naphthoquinone, 0.24 g of furfural in 25 mL of acetone and a residence time of 70 min. Yield: 0.026 g (20 %).

General procedure **GP3** was followed using 0.158 g of 1,4-naphthoquinone, 0.48 g of furfural in 50 mL of acetone and illumination in sunlight for 200 min. Yield: 0.042 g (16 %).

General procedure **GP4** was followed using 0.36 g of 1,4-naphthoquinone, 1.92 g of furfural in 100 mL of acetone and a residence time of 70 min.

The crude photoproduct was purified by column chromatography using toluene : ethyl acetate (5 : 1) and afforded the title product as an orange solid.

¹H-NMR: (400 MHz, acetone-d₆)

δ (ppm): 13.87 (s, 1H, OH), 8.82 (broad s, 1H, OH), 8.44 (d, J = 7.8 Hz, 1H, CH_{arom}), 8.24 (d, J = 8.3 Hz, 1H, CH_{arom}), 8.02 (dd, J = 1.7, 0.8, 1H, CH_{arom}), 7.81 (s, 1H, CH_{arom}), 7.75 (ddd, J = 8.3, 1.3 Hz, 1H, CH_{arom}), 7.64 (ddd, J = 8.2, 1.2 Hz, 1H, CH_{arom}), 7.56 (dd, J = 3.6, 0.7 Hz, 1H, CH_{arom}), 6.82 (dd, J = 3.6, 1.7, 1H, CH_{arom}).

¹³C NMR: (100 MHz, acetone-d₆)

δ (ppm): 185.1 (s, 1C, C=O), 159.0 (s, 1C, C_q_{arom}), 153.2 (s, 1C, C_q_{arom}), 148.6 (d, 1C, CH_{arom}), 145.7 (s, 1C, C_q_{arom}), 139.9 (s, 1C, C_q_{arom}), 130.6 (d, 1C, CH_{arom}), 127.3 (d, 1C, CH_{arom}), 126.8 (d, 1C, CH_{arom}), 124.9 (d, 1C, CH_{arom}), 123.1 (d, 1C, CH_{arom}), 121.6 (d, 1C, CH_{arom}), 113.5 (d, 1C, CH_{arom}), 112.2 (s, 1C, C_q_{arom}), 106.2 (d, 1C, CH_{arom}).

IR (neat):

ν (cm⁻¹): 3299, 3132, 2852, 1634, 1560, 1459, 1387, 1301, 1275, 1197, 1123, 1076, 1030, 914, 886, 751.

M.P: 188-189°C (lit.:⁴⁴ 188.5-189°C).

6.3.5.10 Attempted synthesis of 1-(1, 3, 4-trihydroxyaphthalen-2-yl)butan-1-one (10)

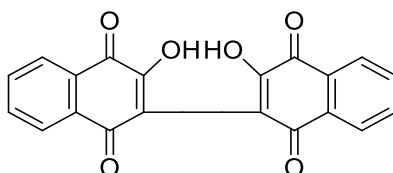
General procedure **GP2** was followed using 0.174 g of 2-hydroxy-1,4-naphthoquinone, 0.36 g of butyraldehyde in 50 mL of acetone and irradiation with visible light for 12 hours.

General procedure **GP2** was followed using 0.174 g of 2-hydroxy-1,4-naphthoquinone, 0.36 g of butyraldehyde in 50 mL of acetone and irradiation with 419 nm light for 28 hours.

¹H-NMR: (400 MHz, acetone-d₆)

No conversion to a detectable photoproduct was observed.

6.3.5.11 Synthesis of 7, 7'-dihydroxy-[2, 2'-binaphthalene]-5, 5', 8, 8'tetraone (11)



¹H-NMR: (400 MHz, acetone-d₆)

δ (ppm): 9.19 (broad s, 2H, 2×OH), 8.16 (dd, $J = 7.4, 2.0$ Hz, 2H, 2×CH_{arom}), 8.11 (dd, $J = 7.3, 1.7$ Hz, 2H, 2×CH_{arom}), 7.92 (ddd, $J = 7.5, 1.6$ Hz, 2H, 2×CH_{arom}), 7.87 (ddd, $J = 7.5, 1.6$ Hz, 2H, 2×CH_{arom}).

¹³C NMR: (100 MHz, DMSO-d₆)

δ (ppm): 182.3 (s, 2C, 2×C=O), 181.0 (s, 2C, 2×C=O), 156.9 (s, 2C, 2×C_{qarom}), 134.9 (d, 2C, 2×CH_{arom}), 133.5 (d, 2C, 2×CH_{arom}), 132.2 (s, 2C, 2×C_{qarom}), 130.3 (s, 2C, 2×C_{qarom}), 126.0 (d, 4C, 4×CH_{arom}), 115.9 (s, 2C, 2×C_{qarom}).

MS (DUIS):

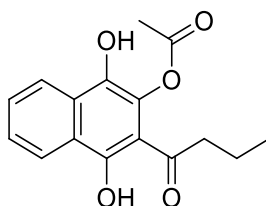
m/z : 345 [$M^+ - H$]; expected: 346 [M^+].

IR (neat): (lit.¹⁷⁶)

ν (cm⁻¹): 3348, 3328, 1672, 1641, 1632, 1588, 1460, 1383, 1350, 1297, 1250, 1217, 1118, 1040, 1000, 891, 721.

M.P: 287-288°C(lit.:⁹³ 280-282°C).

6.3.5.12 Synthesis of 3-butyryl-1,4-dihydroxynaphthalen-2-yl acetate (12)



General procedure **GP1** was followed using 0.216 g of 2-acetoxy-1,4-naphthoquinone, 0.36 g of butyraldehyde in 50 mL of acetone and irradiation with UVB light for 28 hours. Yield: 0.058 g (20%).

General procedure **GP1** was followed using 0.216 g of 2-acetoxy-1,4-naphthoquinone, 0.36 g of butyraldehyde in 50 mL of TFT and irradiation with 419 nm light for 7 hours. Yield: 0.052 g (18%).

The crude photoproduct was purified by washing with warm distilled water (~50°C) and filtration, followed by precipitation from cold TFT and drying in vacuum to give the title product as an orange solid.

¹H-NMR: (400 MHz, CDCl₃)

δ (ppm): 14.93 (s, 1H, OH), 8.40 (d, J = 8.4 Hz, 1H, CH_{arom}), 7.60 (dd, J = 7.6 Hz, 1H, CH_{arom}), 7.48 (d, J = 8.3 Hz, 1H, CH_{arom}), 7.38 (dd, J = 7.6 Hz, 1H, CH_{arom}), 6.10 (broad s, 1H, OH), 3.20 (t, J = 7.3 Hz, 2H, CH₂), 2.53 (s, 3H, CH₃) 1.79 (sxt, J = 7.4 Hz, 2H, CH₂), 1.02 (t, J = 7.4 Hz, 3H, CH₃).

¹³C NMR: (100 MHz, CDCl₃)

δ (ppm): 169.9 (s, 1C, C=O), 163.1 (s, 1C, C=O), 143.8 (s, 1C, C_{qarom}), 131.3 (s, 1C, C_{qarom}), 130.4 (s, 1C, C_{qarom}), 125.2 (d, 1C, CH_{arom}), 124.1 (d, 1C, CH_{arom}), 121.2 (s, 1C, C_{qarom}), 119.5 (d, 1C, CH_{arom}), 107.2 (d, 1C, CH_{arom}), 46.4 (t, 1 C, CH₂), 20.9 (q, 1C, CH₃), 18.2 (t, 1C, CH₂), 14.1 (q, 1C, CH₃).

MS (DUIS):

m/z: 287 [M⁺-H]; expected: 288 [M⁺].

IR (neat):

ν (cm⁻¹): 3329, 2963-2880, 1731, 1622, 1573, 1446, 1362, 1228, 1189, 1136, 1104, 1051, 1039, 1018, 911, 883, 764.

M.P: 124-125°C.

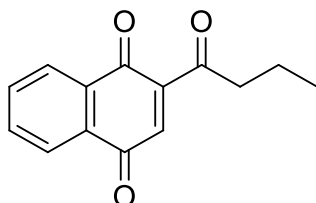
6.3.6 Multistep one-flow reactions

The photochemical-thermal tandem synthesis of model acylated naphthoquinones was performed by combining the photoacylation with a thermal oxidation step in a single flow operation.

General procedure 5 (GP5): A solution of 1,4-naphthoquinone (0.5 mmol) and aldehyde (2.5 mmol) in acetone (25 mL) was degassed with nitrogen for 5 minutes and pumped through the

in-house flow photoreactor equipped with a single 8 W fluorescent tube (UVB). The oxidation was carried out in-line using a plunger cartridge loaded loosely with solid Ag_2O (10 g). A residence time of 70 min was selected for both steps photoacylation and thermal oxidation.

6.3.6.1 Synthesis of 2-Butyryl-1,4-naphthoquinone (9b)



General procedure **GP5** was followed using 0.079 g of 1,4-naphthoquinone, 0.18 g of butyraldehyde in 25 mL of acetone, 10 g of Ag_2O and a residence time of 70 min. The crude photoproduct was purified by precipitation from the cold ether and drying in vacuum to give the title product as a brownish solid.

$^1\text{H-NMR}$: (400 MHz, CDCl_3)

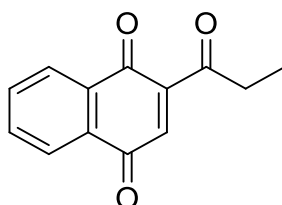
δ (ppm): 8.10 (dd, $J = 8.9$ Hz, 1H, CH_{arom}), 7.83–7.75 (m, 3H, CH_{arom}), 7.07 (s, 1H, CH_{quin}), 2.92 (t, $J = 7.2$ Hz, 2H, CH_2), 1.72 (sxt, $J = 7.6$ Hz, 2H, CH_2), 0.99 (t, $J = 7.4$ Hz, 3H, CH_3).

$^{13}\text{C NMR}$: (100 MHz, CDCl_3)

δ (ppm): 200.9 (s, 1C, C=O), 185.1 (s, 1C, C=O), 183.5 (s, 1C, C=O), 146.2 (s, 1C, C_{qarom}), 136.7 (d, 1C, CH_{arom}), 134.6 (d, 1C, CH_{arom}), 134.5 (d, 1C, CH_{arom}), 131.9 (s, 1C, C_{qarom}), 127.0 (d, 1C, CH_{arom}), 126.4 (d, 1C, CH_{arom}), 45.5 (t, 1C, CH_2), 17.2 (t, 1C, CH_2), 13.8 (q, 1C, CH_3).

M.P: 66-67°C (lit.:¹²⁰ 64-66°C).

6.3.6.2 Synthesis of 2-Propionyl-1,4-naphthoquinone (9a)

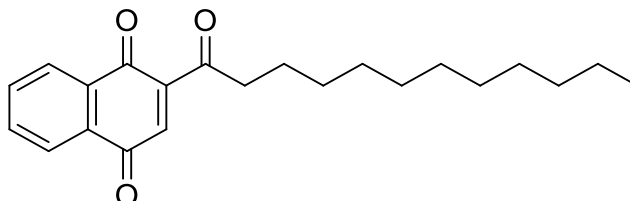


General procedure **GP5** was followed using 0.079 g of 1,4-naphthoquinone, 0.145 g of propionaldehyde in 25 mL of acetone, 10 g of Ag_2O and a residence time of 70 min.

$^1\text{H-NMR}$: (400 MHz, CDCl_3)

δ (ppm): 8.10 (dd, $J = 9.0$ Hz, 1H, CH_{arom}), 7.84–7.73 (m, 3H, CH_{arom}), 7.09 (s, 1H, CH_{quin}), 2.97 (q, $J = 7.2$ Hz, 2H, CH_2), 1.19 (t, $J = 7.2$ Hz, 3H, CH_3).

6.3.6.3 Synthesis of 2-undecanoyl-1,4-naphthoquinone (9d)

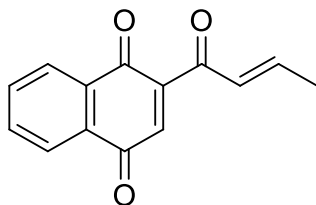


General procedure **GP5** was followed using 0.079 g of 1,4-naphthoquinone, 0.46 g of dodecylaldehyde in 25 mL of acetone, 10 g of Ag_2O and a residence time of 70 min.

$^1\text{H-NMR}$: (400 MHz, CDCl_3)

δ (ppm): 8.12–8.06 (m, 1H, CH_{arom}), 7.78–7.73 (m, 3H, CH_{arom}), 7.05 (s, 1H, CH_{quin}), 2.93 (t, $J = 7.2$ Hz, 2H, CH_2), 2.17 (m, 2H, CH_2), 1.62–1.54 (m, 16H, 8x CH_2), 0.70 (t, $J = 7.4$ Hz, 3H, CH_3).

6.3.6.4 Synthesis of 2-crotonyl-1,4-naphthoquinone (9e)



General procedure **GP5** was followed using 0.079 g of 1,4-naphthoquinone, 0.175 g of crotonaldehyde in 25 mL of acetone, 10 g of Ag_2O and a residence time of 70 min.

$^1\text{H-NMR}$: (400 MHz, CDCl_3)

δ (ppm): 8.15–8.06 (m, 2H, 2x CH_{arom}), 7.82–7.77 (m, 2H, 2x CH_{arom}), 7.01 (s, 1H, CH_{arom}), 7.00–6.91 (m, 1H, $\text{CH}=\text{}$), 6.53 (dd, $J = 15.7$ Hz, 1H, $\text{CH}=\text{}$), 2.05 (dd, $J = 6.9$ Hz, 3H, CH_3).

6.4 [2+2]-Photocycloadditions of naphthoquinones

6.4.1 Photocycloadditions of naphthoquinones under batch conditions

General procedure 6 (GP6): A solution of 1,4-naphthoquinone (1 mmol) and alkene or alkyne (5 mmol) in different organic solvents (50 mL) was degassed with nitrogen for 5 minutes and

irradiated in a Pyrex Schlenk flask (transmission >300 nm) for 10-13 hours using a Rayonet photochemical reactor (RPR-200; Southern New England Ultraviolet Company) equipped with 16×8 W fluorescent tubes.

6.4.2. Photocycloadditions of naphthoquinones under continuous-flow conditions

General procedure 7 (GP7): A solution of 1,4-naphthoquinone (0.5 mmol) and alkene (2.5 mmol) in acetone (25 mL) was degassed with nitrogen for 5 minutes, loaded into a syringe and pumped through the in-house flow photoreactor equipped with a single 8 W fluorescent tube.

6.4.3. Solar photocycloadditions of naphthoquinones under batch conditions

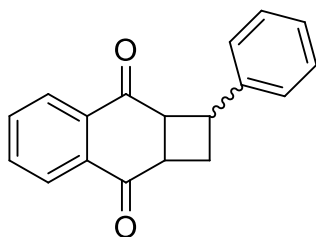
General procedure 8 (GP8): A solution of 1,4-naphthoquinone (1 mmol) and alkene (5 mmol) in acetone (50 mL) was degassed with nitrogen for 5 minutes, split over two test tubes and exposed to sunlight in a solar float for 200 min.

6.4.4. Solar photocycloadditions of naphthoquinones under continuous-flow conditions

General procedure 9 (GP9): A solution of 1,4-naphthoquinone (2 mmol) and alkene (10 mmol) in acetone (100 mL) was degassed with nitrogen for 5 minutes and pumped through the in-house solar flow reactor.

6.4.5. Photochemical transformations

6.4.5.1. Synthesis of 1-phenyl-1, 2, 2a, 8a-tetrahydrocyclobuta[b]naphthal-ene-3,8-dione (15a)



General procedure **GP6** was followed using 0.158 g of 1,4-naphthoquinone, 0.52 g of styrene in 50 mL of acetone and irradiation with UVB light for 10 hours. Yield: 0.182 g (69 %).

General procedure **GP7** was followed using 0.079 g of 1,4-naphthoquinone, 0.26 g of styrene in 25 mL of acetone and a residence time of 45 min. Yield: 0.111 g (84%).

General procedure **GP8** was followed using 0.158 g of 1,4-naphthoquinone, 0.52 g of styrene in 50 mL of acetone and illumination in sunlight for 200 min. Yield: 0.113 g (43 %).

General procedure **GP9** was followed using 0.316 g of 1,4-naphthoquinone, 1.041 g of styrene in 100 mL of acetone and a residence time of 70 min. Yield: 0.340 g (65 %).

The crude photoproduct was purified by automated chromatography using *n*-hexane : ethyl acetate (4 : 1) as the eluent. The main *anti*-adduct was crystalized from methanol as colorless crystals, while the *syn*-isomer was precipitated from cold TFT as a colorless solid.

Main *anti*-isomer:

¹H-NMR: (400 MHz, CDCl₃)

δ (ppm): 8.10 (dd, *J* = 9.3 Hz, 2H, CH_{arom}), 7.73 (dd, *J* = 5.3 Hz, 2H, CH_{arom}), 7.26 (dd, *J* = 5.3 Hz, 4H, CH_{arom}), 7.17 (d, *J* = 6.9 Hz, 1H, CH_{arom}), 3.84–3.67 (m, 2H, CH), 3.56–3.40 (m, 1H, CH), 2.77 (dd, *J* = 10.7 Hz, 1H, CH), 2.68 (ddd, *J* = 12.0, 7.7, 3.3 Hz, 1H, CH).

¹³C NMR: (100 MHz, CDCl₃)

δ (ppm): 198.6 (s, 1C, C=O), 195.4 (s, 1C, C=O), 142.2 (s, 1C, C_{qarom}), 135.6 (s, 1C, C_{qarom}), 135.2 (s, 1C, C_{qarom}), 134.6 (d, 1C, CH_{arom}), 134.4 (d, 1C, CH_{arom}), 128.7 (d, 2C, 2×CH_{arom}), 127.6 (d, 1C, CH_{arom}), 127.4 (d, 1C, CH_{arom}), 126.9 (d, 1C, CH_{arom}), 126.3 (d, 2C, 2×CH_{arom}), 51.3 (d, 1C, CH_{arom}), 44.7 (d, 1C, CH), 41.1 (t, 1C, CH₂), 32.2 (s, 1C, CH).

MS (DUIS):

m/z: 263 [M⁺+H]; expected: 262 [M⁺].

IR (neat):

ν (cm⁻¹): 1671, 1587, 1449, 1283, 1262, 1119, 968, 761.

M.P: 115-116°C (lit.:⁹⁶ 78.5-79.5°C).

Minor *syn*-isomer

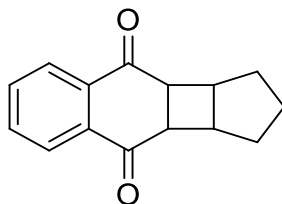
¹H-NMR: (400 MHz, CDCl₃)

δ (ppm): 8.12 (dd, *J* = 7.7, 1.0 Hz, 1H, CH_{arom}), 7.86 (dd, *J* = 7.7, 1.1 Hz, 1H, CH_{arom}), 7.75 (ddd, *J* = 7.6, 1.4 Hz, 1H, CH_{arom}), 7.68 (ddd, *J* = 7.5, 1.4 Hz, 1H, CH_{arom}), 7.23–7.13 (m, 2H, CH_{arom}), 7.03 (d, *J* = 6.9 Hz, 2H, CH_{arom}), 4.24 (dd, *J* = 19.8, 9.2 Hz, 1H, CH), 4.02 (ddd, *J* = 9.0, 8.0, 2.9 Hz, 1H, CH), 3.75 (ddd, *J* = 9.8, 8.0 Hz, 1H, CH), 2.99 (ddd, *J* = 12.0, 10.4, 2.0 Hz, 1H, CH), 2.80 (ddd, *J* = 13.0, 9.2, 0.8 Hz, 1H, CH).

¹³C NMR: (100 MHz, CDCl₃)

δ (ppm): 197.3 (s, 1C, C=O), 195.2 (s, 1C, C=O), 138.4 (s, 1C, C_qarom), 136.8 (s, 1C, C_qarom), 134.9 (s, 1C, C_qarom), 134.4 (d, 1C, CH_{arom}), 134.3 (d, 1C, CH_{arom}), 128.4 (s and d, 2C, C_qarom and CH_{arom}), 128.0 (d, 2C, 2×CH_{arom}), 127.5 (d, 1C, CH_{arom}), 127.2 (d, 2C, 2×CH_{arom}), 50.1 (d, 1C, CH), 42.4 (d, 1C, CH), 40.7 (t, 1C, CH₂), 31.2 (d, 1C, CH).

6.4.5.2. Synthesis of 2,3,3a,3b,9a,9b-hexahydro-1H-cyclopenta[3,4]cyclobuta[1,2-b]naphthaaalene-4,9-dione (15b)



General procedure **GP6** was followed using 0.158 g of 1,4-naphthoquinone, 0.34 g of cyclopentene in 50 mL of acetone and irradiation with UVB light for 13 hours. Yield: 0.114 g (50 %).

General procedure **GP7** was followed using 0.079 g of 1,4-naphthoquinone, 0.17 g of cyclopentene in 25 mL of acetone and a residence time of 60 min. Yield: 0.083 g (73 %).

General procedure **GP8** was followed using 0.158 g of 1,4-naphthoquinone, 0.34 g of cyclopentene in 50 mL of acetone and illumination in sunlight for 200 min. Yield: 0.098 g (43%).

General procedure **GP9** was followed using 0.316 g of 1,4-naphthoquinone, 0.681 g of cyclopentene in 100 mL of acetone and a residence time of 70 min. Yield: 0.254 g (56%).

The crude photoproduct was purified by automated chromatography using *n*-hexane : ethyl acetate (4 : 1) as eluent. The product was crystallized from the eluent as colorless needles.

¹H-NMR: (400 MHz, CDCl₃)

δ (ppm): 8.12 (d, *J* = 9.2 Hz, 2H, CH_{arom}), 7.77 (d, *J* = 9.2 Hz, 2H, CH_{arom}), 3.08 (d, *J* = 3.3 Hz, 2H, CH), 2.90 (d, *J* = 4.4 Hz, 2H, CH), 2.06–1.83 (t, 4H, CH), 1.62 (s, 2H, CH).

¹³C NMR: (100 MHz, CDCl₃)

δ (ppm): 197.6 (s, 2C, 2×C=O), 135.6 (s, 2C, 2×C_qarom), 134.4 (d, 2C, 2×CH_{arom}), 127.5 (d, 2C, 2×CH_{arom}), 47.1 (d, 2C, 2×CH), 43.5 (d, 2C, 2×CH), 33.2 (t, 2C, 2×CH₂), 24.6 (t, 1C, CH₂).

MS (DUIS):

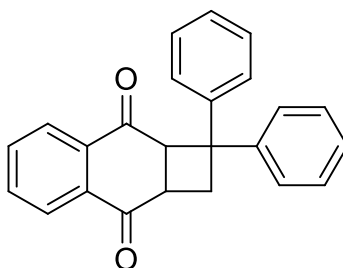
m/z: 227 [M⁺+H]; expected: 226 [M⁺].

IR (neat):

ν (cm⁻¹): 1673, 1583, 1320, 1274, 1262, 1228, 955, 788.

M.P: 123-124°C (lit.:¹²⁰ 106-107°C).

6.4.5.3. Synthesis of 1, 1-diphenyl-1, 2, 8a-tetrahydrocyclobuta[b]naphthalene-3, 8-dione (15c)



General procedure **GP6** was followed using 0.158 g of 1,4-naphthoquinone, 0.901 g of 1,1-diphenylethylene in 50 mL of acetone and irradiation with UVB light for 12 hours. Yield: 0.142 g (42 %).

General procedure **GP7** was followed using 0.079 g of 1,4-naphthoquinone, 0.45 g of 1,1-diphenylethylene in 25 mL of acetone and a residence time of 60 min. Yield: 0.101g (60 %).

General procedure **GP8** was followed using 0.158 g of 1,4-naphthoquinone, 0.901 g of 1,1-diphenylethylene in 50 mL of acetone and illumination in sunlight for 200 min. Yield 0.068 g (20 %).

General procedure **GP9** was followed using 0.316 g of 1,4-naphthoquinone, 1.8 g of 1,1-diphenylethylene in 100 mL of acetone and a residence time of 70 min. Yield: 0.311 g (46 %).

The crude photoproduct was purified by automated chromatography using *n*-hexane : ethyl acetate (4 : 1) as eluent. The product was crystallized from methanol as colorless crystals.

¹H-NMR: (400 MHz, acetone-d₆)

δ (ppm): 7.96 (dd, *J* = 7.7, 1.7 Hz, 1H, CH_{arom}), 7.80 (dd, *J* = 7.6, 1.2 Hz, 1H, CH_{arom}), 7.56 (ddd, *J* = 7.4, 1.5 Hz, 2H, 2×CH_{arom}), 7.48 (dd, *J* = 8.3, 1.2 Hz, 2H, 2×CH_{arom}), 7.37 (dd, *J* = 7.8 Hz, 2H, 2×CH_{arom}), 7.22 (dd, *J* = 7.4 Hz, 1H, CH_{arom}), 7.09 (dd, *J* = 8.5, 1.2 Hz, 2H, 2×CH_{arom}), 6.95 (dd, *J* = 7.7 Hz, 2H, 2×CH_{arom}), 6.84 (dd, *J* = 7.3 Hz, 1H, CH_{arom}), 4.62 (d, *J* = 8.8 Hz, 1H, CH), 3.68 (dd, *J* = 12.5, 2.9 Hz, 1H, CH), 3.56 (ddd, *J* = 10.7, 8.8, 2.9 Hz, 1H, CH), 3.13 (dd, *J* = 12.5, 10.6 Hz, 1H, CH).

¹³C NMR: (100 MHz, acetone-d₆)

δ (ppm): 198.7 (s, 1C, C=O), 195.8 (s, 1C, C=O), 151.2 (s, 1C, C_{qarom}), 142.0 (s, 1C, C_{qarom}), 137.3 (d, 1C, CH_{arom}), 136.8 (d, 1C, CH_{arom}), 134.7 (s, 1C, C_{qarom}), 134.6 (s, 1C, C_{qarom}), 129.3 (d, 4C, 4×CH_{arom}), 128.7 (d, 4C, 4×CH_{arom}), 127.2-127.0 (d, 4C, 4×CH_{arom}), 58.1 (d, 1C, CH), 55.1 (d, 1C, CH), 41.4 (d, 1C, CH), 36.9 (d, 1C, CH).

MS (DUIS):

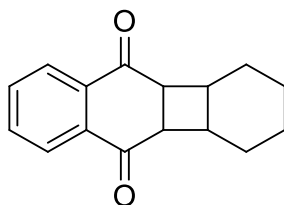
m/z : 338 [M^+]; expected: 338 [M^+].

IR (neat):

ν (cm⁻¹): 1675, 1586, 1494, 1287, 1270, 761, 752.

M.P: 136-137°C.

6.4.5.4. Synthesis of 1,2,3,4,4a,4b,10a,10b-octahydrobenzo[b]biphenylene-5,10-dione (15d)



General procedure **GP6** was followed using 0.158 g of 1,4-naphthoquinone, 0.41 g of cyclohexene in 50 mL of acetone and irradiation with UVB light for 12 hours. Yield: 0.062 g (25 %).

The crude photoproduct was purified by automated chromatography using *n*-hexane : ethyl acetate (4 : 1) as eluent. The product was crystallized from ethanol as colorless crystals.

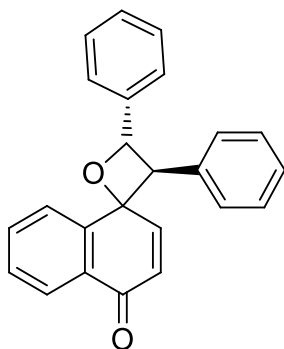
¹H-NMR: (400 MHz, CDCl₃)

δ (ppm): 8.13 (dd, J = 5.8, 3.3 Hz, 2H, 2×CH_{arom}), 7.76 (dd, J = 5.9, 3.3 Hz, 2H, 2×CH_{arom}), 3.35 (dd, J = 3.2, 1.4 Hz, 2H, 2×CH), 2.69 (board s, 2H, 2×CH), 1.84 (board s, 2H, CH₂), 1.61 (board s, 6H, 3×CH₂).

¹³C NMR: (100 MHz, CDCl₃)

δ (ppm): 197.8 (s, 2C, 2×C=O), 135.3 (s, 2C, 2×C_{qarom}), 134.4 (d, 2C, 2×CH_{arom}), 127.4 (d, 2C, 2×CH_{arom}), 47.5 (d, 2C, 2×CH), 39.4 (d, 2C, 2×CH), 27.5 (t, 2C, 2×CH₂), 22.3 (t, 2C, 2×CH₂).

6.4.5.5. Synthesis of 3',4'-diphenyl-4H-spiro[naphthalene-1,2'-oxetan]-4-one (16e)



General procedure **GP6** was followed using 0.158 g of 1,4-naphthoquinone, 0.901 g of *trans*-stilbene in 50 mL of acetone and irradiation with UVB light for 13 hours. Yield: 0.092 g (27 %).

General procedure **GP6** was followed using 0.158 g of 1,4-naphthoquinone, 0.901 g of *trans*-stilbene in 50 mL of acetone and irradiation with 419 nm light for 6 hours. Yield: 0.263 g (78 %). General procedure **GP7** was followed using 0.079 g of 1,4-naphthoquinone, 0.45 g of *trans*-stilbene in 25 mL of acetone and a residence time of 60 min. Yield: 0.079 g (47 %).

General procedure **GP8** was followed using 0.158 g of 1,4-naphthoquinone, 0.901 g of *trans*-stilbene in 50 mL of acetone and illumination in sunlight for 200 min. Yield: 0.095 g (30 %).

General procedure **GP9** was followed using 0.316 g of 1,4-naphthoquinone, 1.802 g of *trans*-stilbene in 100 mL of acetone and a residence time of 70 min.

The crude photoproduct was purified by automated chromatography using *n*-hexane : ethyl acetate (4 : 1) as eluent. The product was crystallized from ethanol as colorless needles.

¹H-NMR: (400 MHz, CDCl₃)

δ (ppm): 8.13 (ddd, *J* = 7.4, 5.1, 1.0 Hz, 2H, CH_{arom}), 7.73 (ddd, *J* = 8.0, 1.6 Hz, 1H, CH_{arom}), 7.62 (d, *J* = 7.6 Hz, 2H, 2×CH_{arom}), 7.55–7.47 (m, 3H, 3×CH_{arom}), 7.44–7.35 (m, 2H, 2×CH_{arom}), 7.33–7.25 (m, 3H, 3×CH_{arom}), 7.03 (d, *J* = 6.9 Hz, 2H, 2×CH_{arom}), 6.48 (d, *J* = 9.2 Hz, 1H, CH_{arom}), 6.27 (d, *J* = 10.4 Hz, 1H, CH), 4.64 (d, *J* = 9.3 Hz, 1H, CH).

¹³C NMR: (100 MHz, CDCl₃)

δ (ppm): 184.2 (s, 1C, C=O), 147.4 (d, 1C, CH_{arom}), 144.3 (s, 1C, C_q_{arom}), 141.2 (s, 1C, C_q_{arom}), 135.2 (s, 1C, C_q_{arom}), 133.7 (d, 1C, CH_{arom}), 130.2 (s, 1C, C_q_{arom}), 129.7 (d, 1C, CH_{arom}), 129.0 (d, 2C, 2×CH_{arom}), 129.0 (d, 1C, CH_{arom}), 128.5 (d, 1C, CH_{arom}), 127.9 (d, 1C, CH_{arom}), 127.7 (d, 1C, CH_{arom}), 127.1 (d, 2C, 2×CH_{arom}), 126.5 (d, 1C,

CH_{arom}), 125.3 (d, 2C, $2\times\text{CH}_{\text{arom}}$), 81.4 (s, 1C, $\text{C}_{\text{qoxetane}}$), 79.0 (d, 1C, $\text{CH}_{\text{oxetane}}$), 62.5 (d, 1C, $\text{CH}_{\text{oxetane}}$).

MS (DUIS):

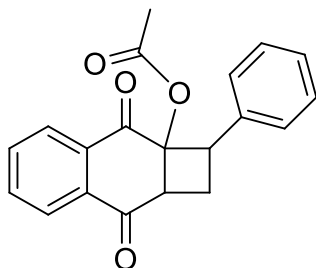
m/z: 339 [M^+H]; expected: 338 [M^+].

IR (neat):

ν (cm^{-1}): 1667, 1599, 1495, 1448, 1297, 1000, 966.

M.P: 142-143°C (lit.:¹²⁰ 138-139°C).

6.4.5.6. Synthesis of 3,8-dioxo-2-phenyl-1,3,8,8a tetrahydrocyclobuta [b]naphthalene-2a(2H)-yl acetate (17a)



General procedure **GP6** was followed using 0.216 g of 2-acetyloxy-1,4-naphthoquinone, 0.520 g of styrene in 50 mL of acetone and irradiation with UVA light for 10 hours. Yield: 0.220 g (69 %).

General procedure **GP7** was followed using 0.108 g of 2-acetyloxy-1,4-naphthoquinone, 0.26 g of styrene in 25 mL of acetone and a residence time of 120 min. Yield: 0.912 g (91 %).

General procedure **GP8** was followed using 0.216 g of 2-acetyloxy-1,4-naphthoquinone, 0.52 g of styrene in 50 mL of acetone and illumination in sunlight for 200 min. Yield: 0.092g (29 %).

General procedure **GP9** was followed using 0.432 g of 2-acetyloxy-1,4-naphthoquinone, 1.041 g of styrene in 100 mL of acetone and a residence time of 70 min. Yield: 0.577 g (90 %).

The crude photoproduct was purified by automated chromatography using *n*-hexane : ethyl acetate (4 : 1) as eluent. The product was crystalized from methanol as colorless crystals.

$^1\text{H-NMR}$: (400 MHz, CDCl_3)

δ (ppm): 8.28 (dd, $J = 5.9, 2.9$ Hz, 1H, CH_{arom}), 8.21 (dd, $J = 6.2, 3.3$ Hz, 1H, CH_{arom}), 7.84 (dd, $J = 5.8, 3.3$ Hz, 2H, $2\times\text{CH}_{\text{arom}}$), 7.41–7.34 (m, 2H, $2\times\text{CH}_{\text{arom}}$), 7.33–7.27 (m, 3H, $3\times\text{CH}_{\text{arom}}$), 3.98 (dd, $J = 9.1$ Hz, 1H, CH), 3.62 (ddd, $J = 11.1, 4.6, 1.2$ Hz, 1H, CH), 3.11 (ddd, $J = 12.0, 11.1, 9.1$ Hz, 1H, CH), 2.59 (ddd, $J = 12.1, 9.3, 4.6$ Hz, 1H, CH).

^{13}C NMR: (100 MHz, CDCl_3)

δ (ppm): 195.9 (s, 1C, C=O), 192.0 (s, 1C, C=O), 170.5 (s, 1C, C=O), 136.1 (s, 1C, C_{qarom}), 135.0 (s, 1C, C_{qarom}), 134.8-134.8 (d, 2C, $2\times\text{CH}$), 133.7 (s, 1C, C_{qarom}), 128.5 (d, 2C, $2\times\text{CH}_{\text{arom}}$), 128.3 (d, 2C, $2\times\text{CH}_{\text{arom}}$), 127.8 (d, 1C, CH_{arom}), 127.5 (d, 1C, CH_{arom}), 81.2 (q, 1C, CH_3), 49.7 (d, 1C, CH), 45.6 (d, 1C, CH), 28.2 (d, 1C, CH), 20.6 (t, 1C, CH_2).

MS (DUIS):

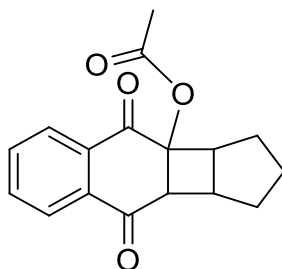
m/z : 321 [$\text{M}^+ + \text{H}$]; expected: 320 [M^+].

IR (neat):

ν (cm^{-1}): 1725, 1687, 1593, 1268, 1214, 1122, 971.

M.P: 147-148°C (lit.:⁸¹ 134-136°C).

6.4.5.7. Synthesis of 4,9-dioxo-1,2,3,3a,4,9,9a,9b-octahydro-3bH-cyclopenta-[3,4]cyclobuta[1,2-b]naphthalen-3b-yl acetate (17b)



General procedure **GP6** was followed using 0.216 g of 2-acetyloxy-1,4-naphthoquinone, 0.34 g of cyclopentene in 50 mL of acetone and irradiation with UVA light for 12 hours. Yield: 0.060 g (21 %).

General procedure **GP7** was followed using 0.108 g of 2-acetyloxy-1,4-naphthoquinone, 0.17 g of cyclopentene in 25 mL of acetone and a residence time of 100 min. Yield: 0.042 g (30 %).

The crude photoproduct was purified by automated chromatography using *n*-hexane : ethyl acetate (4 : 1) as eluent. The product was crystallized from methanol as colorless crystals.

^1H -NMR: (400 MHz, CDCl_3)

δ (ppm): 8.19–8.14 (m, 1H, CH_{arom}), 8.12–8.08 (m, 1H, CH_{arom}), 7.83–7.73 (m, 2H, $2\times\text{CH}_{\text{arom}}$), 3.03 (d, $J = 6.9$ Hz, 1H, CH), 2.90 (t, $J = 8.0$ Hz, 1H, CH), 2.70 (dd, $J = 12.9, 6.3$ Hz, 1H, CH), 2.38 (dd, $J = 13.8, 6.1$ Hz, 1H, CH), 2.11 (s, 3H, CH_3) 2.01–1.78 (m, 3H, $3\times\text{CH}$), 1.75–1.51 (m, 2H, CH_2).

^{13}C NMR: (100 MHz, CDCl_3)

δ (ppm): 194.3 (s, 1C, C=O), 194.2 (s, 1C, C=O), 170.2 (s, 1C, C=O), 134.8 (s, 1C, C_q_{arom}), 134.6 (d, 1C, CH_{arom}), 133.9 (d, 1C, CH_{arom}), 133.4 (s, 1C, C_q_{arom}), 127.9 (d, 1C, CH_{arom}), 127.6 (d, 1C, CH_{arom}), 75.7 (q, 1C, CH₃), 56.2 (d, 1C, CH), 43.8 (d, 1C, CH), 40.2 (d, 1C, CH), 32.9 (d, 1C, CH), 26.8 (d, 1C, CH), 25.5 (d, 1C, CH), 20.3 (d, 1C, CH).

MS (DUIS):

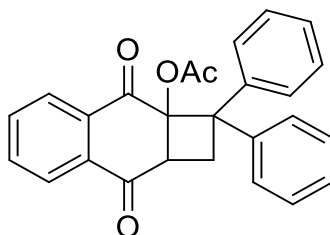
m/z : 285 [$M^+ + H$]; expected: 284 [M^+].

IR (neat):

ν (cm⁻¹): 1730, 1686, 1592, 1243, 1259, 1227, 1062, 997.

M.P: 183-184°C.

6.4.5.8. Synthesis of 3,8-dioxo-2,2-diphenyl-1,3,8,8a-tetrahydrocyclobuta[b]-naphthalen-2a(2H)-yl acetate (17c).



General procedure **GP6** was followed using 0.216 g of 2-acetyloxy-1,4-naphthoquinone, 0.901 g of 1,1-diphenylethylene in 50 mL of acetone and irradiation with UVA light for 20 hours. Yield: 0.196g (50 %).

General procedure **GP7** was followed using 0.108 g of 2-acetyloxy-1,4-naphthoquinone, 0.45 g of 1,1-diphenylethylene in 25 mL of acetone and a residence time of 300 min. Yield: 0.097 g (50 %).

General procedure **GP8** was followed using 0.216 g of 2-acetyloxy-1,4-naphthoquinone, 0.901 g of 1,1-diphenylethylene in 50 mL of acetone and illumination in sunlight for 200 min. Yield: 0.077 g (20 %).

General procedure **GP9** was followed using 0.432 g of 2-acetyloxy-1,4-naphthoquinone, 1.8 g of 1,1-diphenylethylene in 100 mL of acetone and a residence time of 70 min. Yield: 0.286 g (36 %).

The crude photoproduct was purified by automated chromatography using *n*-hexane : ethyl acetate (4 : 1) as eluent. The product was crystallized from methanol as colorless crystals.

¹H-NMR: (400 MHz, CDCl₃)

δ (ppm): 7.94 (dd, $J = 7.8, 1.7$ Hz, 1H, CH_{arom}), 7.79 (dd, $J = 7.4, 1.3$ Hz, 1H, CH_{arom}), 7.58 (ddd, $J = 7.5, 1.5$ Hz, 1H, CH_{arom}), 7.53 (dd, $J = 7.6, 1.5$ Hz, 1H, CH_{arom}), 7.49 (dd, $J = 8.4, 1.2$ Hz, 2H, $2 \times \text{CH}_{\text{arom}}$), 7.34 (dd, $J = 7.7$ Hz, 2H, $2 \times \text{CH}_{\text{arom}}$), 7.22 (dd, $J = 7.4, 1.3$ Hz, 3H, $3 \times \text{CH}_{\text{arom}}$), 6.99 (dd, $J = 7.7$ Hz, 2H, $2 \times \text{CH}_{\text{arom}}$), 6.88 (dd, $J = 6.8$ Hz, 1H, CH_{arom}), 3.57 (dd, $J = 10.6, 4.6$ Hz, 1H, CH), 3.46 (ddd, $J = 12.3, 7.6$ Hz, 2H, CH_2), 2.08 (s, 3H, CH_3).

^{13}C NMR: (100 MHz, CDCl_3)

δ (ppm): 196.0 (s, 1C, $\text{C}=\text{O}$), 192.5 (s, 1C, $\text{C}=\text{O}$), 170.5 (s, 1C, $\text{C}=\text{O}$), 143.8 (d, 1C, CH_{arom}), 139.6 (d, 1C, CH_{arom}), 135.3 (s, 1C, C_{qarom}), 134.9 (s, 1C, C_{qarom}), 134.0-133.9 (s, 2C, $2 \times \text{C}_{\text{qarom}}$), 128.3 (d, 2C, $2 \times \text{CH}_{\text{arom}}$), 128.2 (d, 2C, $2 \times \text{CH}_{\text{arom}}$), 128.1 (d, 2C, $2 \times \text{CH}_{\text{arom}}$), 127.6 (d, 2C, $2 \times \text{CH}_{\text{arom}}$), 127.3 (d, 1C, CH_{arom}), 127.1 (d, 1C, CH_{arom}), 126.8 (d, 1C, CH_{arom}), 126.6 (d, 1C, CH_{arom}), 85.5 (q, 1C, CH_3), 58.7 (s, 1C, Cq), 49.1 (s, 1C, Cq), 34.0 (d, 1C, CH), 20.9 (t, 1C, CH_2).

MS (DUIS): $[\text{M}^+ \text{H}]$: 397 m/z; expected 396 m/z.

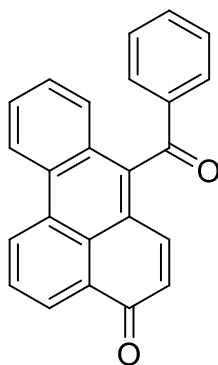
m/z: 397 $[\text{M}^+ + \text{H}]$; expected: 396 $[\text{M}^+]$.

IR (neat):

ν (cm^{-1}): 1723, 1687, 1593, 1293, 1276, 1217, 1085, 784.

M.P: 192-193°C (lit.:⁸¹ 191-192°C).

6.4.5.9. Synthesis of 7-benzoyl-4H-benzo[de]anthracen-4-one (19a)



General procedure **GP6** was followed using 0.158 g of 1,4-naphthoquinone, 0.891 g of diphenylacetylene in 50 mL of acetone and irradiation with UVB light for 12 hours. The crude photoproduct was purified by automated chromatography using *n*-hexane : ethyl acetate (4 : 1) as eluent and afforded the title product as a yellow solid. Yield: 0.253 g (75%).

^1H -NMR: (400 MHz, CDCl_3)

δ (ppm): 9.05 (dd, $J = 8.4, 1.0$ Hz, 1H, H_{arom}), 8.80 (d, $J = 8.4$ Hz, 1H, H_{arom}), 8.71 (dd, $J = 7.5, 1.2$ Hz, 1H, H_{arom}), 8.02–7.95 (m, 1H, H_{arom}), 7.91 (d, $J = 7.1$ Hz, 2H, $2 \times \text{H}_{\text{arom}}$), 7.79

(ddd, $J = 8.3, 7.0, 1.3$ Hz, 1H, H_{arom}), 7.71 (dd, $J = 8.2, 0.7$ Hz, 1H, H_{arom}), 7.67–7.54 (m, 3H, $3 \times H_{\text{arom}}$), 7.48 (dd, $J = 7.9$ Hz, 2H, $2 \times H_{\text{arom}}$), 6.69 (d, $J = 10.0$ Hz, 1H, H_{arom}).

^{13}C NMR: (100 MHz, CDCl_3)

δ (ppm): 198.3 (s, 1C, $\text{C}=\text{O}$), 185.3 (s, 1C, $\text{C}=\text{O}$), 142.0 (s, 1C, C_{qarom}), 141.5 (s, 1C, C_{qarom}), 138.4 (s, 1C, CH_{arom}), 137.6 (s, 1C, C_{qarom}), 134.9 (d, 1C, CH_{arom}), 131.5 (s, 1C, C_{qarom}), 130.6 (s, 1C, C_{qarom}), 130.4 (d, 1C, CH_{arom}), 130.2 (d, 1C, CH_{arom}), 130.0 (d, 1C, CH_{arom}), 129.8 (d, 1C, CH_{arom}), 129.8 (s, 1C, C_{qarom}), 129.3 (d, 2C, $2 \times \text{CH}_{\text{arom}}$), 129.1 (s, 1C, C_{qarom}), 128.6 (d, 1C, CH_{arom}), 128.3 (d, 1C, CH_{arom}), 128.3 (d, 1C, CH_{arom}), 128.1 (d, 1C, CH_{arom}), 126.8 (s, 1C, C_{qarom}), 123.6 (d, 1C, CH_{arom}), 123.4 (s, 1C, C_{qarom}).

MS (DUIS):

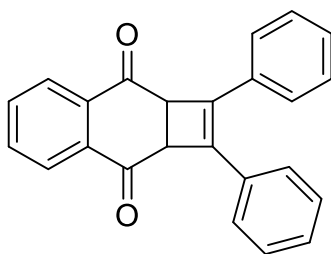
m/z : 336 [$\text{M}^+ + 2\text{H}$]; expected: 334 [M^+].

IR (neat):

ν (cm^{-1}): 1660, 1631, 1579, 1251, 1221, 1174, 707.

M.P: 209–210°C. (lit.:¹⁷² 208°C).

6.4.5.10. Synthesis of 1, 2-diphenylcyclobuta[b]naphthalene-3, 8(2aH, 8aH)-dione (20a).



General procedure **GP6** was followed using 0.158 g of 1,4-naphthoquinone, 0.891 g of diphenylacetylene in 50 mL of acetone and irradiation with UVB light for 12 hours. The crude photoproduct was purified by automated chromatography using *n*-hexane : ethyl acetate (4 : 1) as eluent. The cycloadduct was dried in vacuum to give the title product as a yellow solid. Yield: 0.045 g (13%).

^1H -NMR: (400 MHz, CDCl_3)

δ (ppm): 8.2 (dd, 2H, $2 \times \text{CH}_{\text{arom}}$), 7.72 (dd, 2H, $2 \times \text{CH}_{\text{arom}}$), 7.60 (dd, 4H, $4 \times \text{CH}_{\text{arom}}$), 7.36–7.30 (m, 6H, $6 \times \text{CH}_{\text{arom}}$), 4.47 (s, 2H, $2 \times \text{CH}$).

^{13}C NMR: (100 MHz, CDCl_3)

δ (ppm): 195.9 (s, 2C, 2 \times C=O), 141.1 (s, 2C, 2 \times C_{qarom}), 134.6 (s, 2C, 2 \times C_{qarom}), 134.2 (s, 2C, 2 \times C_{qarom}), 133.4 (d, 2C, 2 \times CH_{arom}), 129.1 (d, 2C, 2 \times CH_{arom}), 128.7 (d, 4C, 4 \times CH_{arom}), 127.7 (d, 4C, 4 \times CH_{arom}), 127.1 (d, 2C, 2 \times CH_{arom}), 50.9 (s, 2C, 2 \times CH).

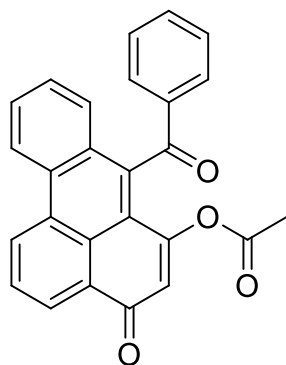
MS (DUIS):

m/z : 337 [$M^+ + H$]; expected: 336 [M^+].

IR (neat):

ν (cm⁻¹): 1640, 1594, 1301, 1252, 1211, 1030, 700.

M.P: 180-181°C (lit.:¹⁷² 170-171°C).

6.4.5.11. Synthesis of 7-benzoyl-4-oxo-4H-benzo[de]anthracen-6-yl-acetate (19b)

General procedure **GP6** was followed using 0.216 g of 2-acetyloxy-1,4-naphthoquinone, 0.891 g of diphenylacetylene in 50 mL of acetone and irradiation with UVA light for 10 hours. The crude photoproduct was purified by automated chromatography using *n*-hexane : ethyl acetate (4 : 1) as the eluent afforded the title product as a yellow solid. Yield: 0.030 g (7 %).

¹H-NMR: (400 MHz, CDCl₃)

δ (ppm): 9.08 (d, J = 7.4 Hz, 1H, CH_{arom}), 8.80 (d, J = 8.4 Hz, 1H, CH_{arom}), 8.74 (d, J = 8.6 Hz, 1H, CH_{arom}), 8.00 (dd, J = 8.0 Hz, 1H, CH_{arom}), 7.91 (d, J = 8.0 Hz, 2H, 2 \times CH_{arom}), 7.79 (dd, J = 8.3 Hz, 1H, CH_{arom}), 7.66 (m, 3H, 3 \times CH_{arom}), 7.61–7.51 (m, 2H, 2 \times CH_{arom}), 7.48 (dd, J = 7.9 Hz, 2H, 2 \times CH_{arom}), 7.37–7.31 (m, 3H, 3 \times CH_{arom}), 4.34 (s, 1H, CH_{arom}), 2.32 (s, 3H, CH₃).

¹³C NMR: (100 MHz, CDCl₃)

δ (ppm): 197.9 (s, 1C, C=O), 178.3 (s, 1C, C=O), 168.5 (s, 1C, C=O), 146.9 (s, 1C, C_{qarom}), 142.5 (s, 1C, C_{qarom}), 137.4 (s, 1C, C_{qarom}), 135.0 (d, 1C, CH_{arom}), 131.8 (s, 1C, C_{qarom}), 130.3 (d, 2C, 2 \times CH_{arom}), 130.1 (d, 1C, CH_{arom}), 129.9 (s, 1C, C_{qarom}), 129.4 (d, 2C, 2 \times CH_{arom}), 129.1 (d, 1C, CH_{arom}), 128.8 (s, 1C, C_{qarom}), 128.7 (d, 1C, CH_{arom}),

128.5 (s, 1C, C_qarom), 128.4 (d, 1C, CH_{arom}), 128.4 (d, 1C, CH_{arom}), 128.1 (d, 1C, CH_{arom}), 127.7 (d, 1C, CH_{arom}), 127.5 (s, 1C, C_qarom), 126.8 (d, 1C, CH_{arom}), 123.6 (d, 1C, CH_{arom}), 122.5 (d, 1C, CH_{arom}), 20.7 (q, 1C, CH₃).

MS (DUIS):

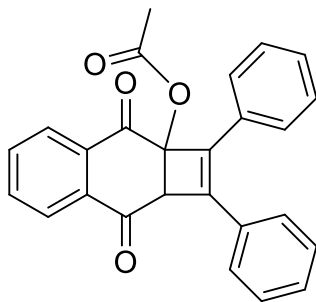
m/z: 392 [M⁺]; expected: 392 [M⁺].

IR (neat):

ν (cm⁻¹): 1765, 1663, 1646, 1577, 1446, 1223, 1228, 1183, 757.

M.P: 196-197°C.

6.4.5.12. Synthesis of 3,8-dioxo-1,2-diphenyl-8,8a dihydrocyclobuta[b]nap-hthalen-2a(3H)-yl acetate (20b)



General procedure **GP6** was followed using 0.216 g of 2-acetyloxy-1,4-naphthoquinone, 0.891 g of diphenylacetylene in 50 mL of acetone and irradiation with UVA light for 10 hours. The crude photoproduct was purified by automated chromatography using *n*-hexane : ethyl acetate (4 : 1) as eluent. The product was crystallized from methanol as pale yellow crystals. Yield: 0.021 g (5 %).

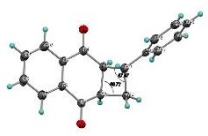
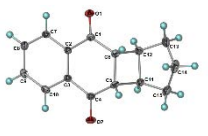
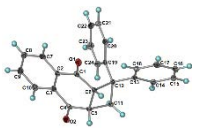
¹H-NMR: (400 MHz, CDCl₃)

δ (ppm): 8.14–8.09 (m, 1H, CH_{arom}), 7.96–7.92 (m, 1H, CH_{arom}), 7.73–7.66 (m, 4H, 4×CH_{arom}), 7.60–7.55 (m, 2H, 2×CH_{arom}), 7.37–7.30 (m, 6H, 6×CH_{arom}), 4.34 (s, 1H, CH), 2.22 (s, 3H, CH₃).

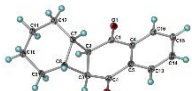
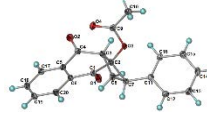
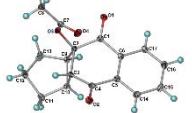
¹³C NMR: (100 MHz, CDCl₃)

δ (ppm): 194.3 (s, 1C, C=O), 192.3 (s, 1C, C=O), 171.0 (s, 1C, C=O), 144.0 (s, 1C, C_qarom), 137.9 (s, 1C, C_qarom), 134.8 (d, 1C, CH_{arom}), 134.4 (d, 1C, CH_{arom}), 133.6 (s, 1C, C_qarom), 132.9 (s, 1C, C_qarom), 132.1 (s, 1C, C_qarom), 131.3 (s, 1C, C_qarom), 130.1 (d, 1C, CH_{arom}), 129.5 (d, 1C, CH_{arom}), 128.8 (d, 2C, CH_{arom}), 128.7 (s, 2C, 2×CH_{arom}), 128.3 (d, 1C, CH_{arom}), 127.7 (d, 2C, 2×CH_{arom}), 127.6 (d, 1C, CH_{arom}), 127.5 (d, 2C, 2×CH), 80.6 (s, 1C, C_q), 60.2 (d, 1C, CH), 20.7 (q, 1C, CH₃).

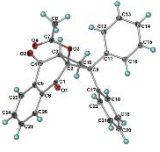
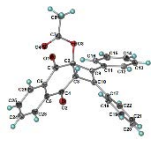
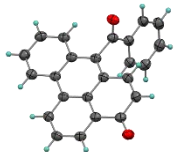
MS (DUIS):m/z: 394 [M⁺]; expected: 394 [M⁺].**IR (neat):** ν (cm⁻¹): 1728, 1682, 1584, 1444, 1278, 1265, 1228, 1138, 1055, 902, 762.**M.P:** 211-212°C (lit.:¹⁶⁹ 209-211°C).**6.5 X-ray crystallographic data**Key crystallographic data is compiled in **Table 6.1****Table 6.1:** Key crystallographic data.

Parameter	18a	18b	18c
			
Formula	C ₁₈ H ₁₄ O ₂	C ₁₅ H ₁₄ O ₂	C ₂₄ H ₁₈ O ₂
M_w (g/mol)	262.29	226.26	338.41
a (Å)	32.872(7)	9.1860(18)	9.1680(18)
b (Å)	9.2550(19)	11.527(2)	16.291(3)
c (Å)	23.836(5)	10.444(2)	11.981(2)
α (°)	90	90	90
β (°)	133.42(3)	90.31(3)	107.89(3)
γ (°)	90	90	90
Volume (Å³)	5267(3)	1105.9(4)	1702.9(6)
Z	16	4	8
δ_{calc} (g/cm³)	1.323	9.1860(18)	1.320
Crystal system	monoclinic	monoclinic	monoclinic
Space group	C 2/c	P2 ₁ /c	P2 ₁ /n
Reflections collected	29573	12793	19262
Reflections unique	4580	1837	2734
R₁	0.1161	0.0413	0.0388

wR₂	0.3159	0.1022	0.0991
Goodness of Fit	0.975	1.057	1.060

Parameter	18d	21a	21b
			
Formula	C ₁₆ H ₁₆ O ₂	C ₂₀ H ₁₆ O ₄	C ₁₇ H ₁₆ O ₄
M_w (g/mol)	240.29	320.33	284.30
a (Å)	9.7000(19)	7.9260(16)	7.9890(16)
b (Å)	11.577(2)	23.600(5)	8.3110(17)
c (Å)	10.597(2)	8.4760(17)	12.192(2)
α (°)	90	90	70.46(3)
β (°)	91.52(3)	100.41(3)	80.96(3)
γ (°)	90	90	65.67(3)
Volume (Å³)	1189.6(4)	1559.4(6)	695.0(3)
Z	4	4	2
δ_{calc} (g/cm³)	1.342	1.364	1.359
Crystal system	monoclinic	monoclinic	triclinic
Space group	P2 ₁ /c	P2 ₁ /c	P-1
Reflections collected	13790	15479	6748
Reflections unique	2074	2716	2217
R₁	0.0452	0.0454	0.0374
wR₂	0.1026	0.0931	0.0933
Goodness of Fit	1.058	1.044	1.062

Parameter	21c	23b	24a
-----------	-----	-----	-----

			
Formula	C ₂₆ H ₂₀ O ₄	C ₂₆ H ₁₈ O ₄	C ₂₄ H ₁₄ O ₂
M_w (g/mol)	396.42	394.40	334.35
a (Å)	7.8830(16)	6.1000(12)	9.980(2)
b (Å)	29.196(6)	14.340(3)	14.490(3)
c (Å)	8.4660(17)	21.601(4)	22.650(5)
α (°)	90	90	90
β (°)	103.49(3)	90	90
γ (°)	90	90	90
Volume (Å³)	1894.7(7)	1889.5(7)	3275.4(11)
Z	4	4	8
δ_{calc} (g/cm³)	1.390	1.386	1.356
Crystal system	monoclinic	orthorhombic	orthorhombic
Space group	P2 ₁ /c	P2 ₁ 2 ₁ 2 ₁	Pbca
Reflections collected	21936	22362	72300
Reflections unique	3099	3335	2877
R₁	0.0390	0.0366	0.0387
wR₂	0.0935	0.0753	0.0971
Goodness of Fit	1.073	1.049	1.061

6.6 References

1. Barbafina, A.; Elisei, F.; Latterini, L.; Milano, F.; Agostiano, A.; Trotta, M., Photophysical properties of quinones and their interaction with the photosynthetic reaction centre. *Photochemical & Photobiological Sciences* **2008**, 7 (8), 973-978.
2. Valderrama, J. A.; Ibacache, A.; Rodriguez, J. A.; Theoduloz, C.; Benites, J., Studies on quinones. Part 47. Synthesis of novel phenylaminophenanthridinequinones as potential antitumor agents. *Eur J Med Chem* **2011**, 46 (8), 3398-409.
3. Abraham, I.; Joshi, R.; Pardasani, P.; Pardasani, R. T., Recent advances in 1,4-benzoquinone chemistry. *Journal of the Brazilian Chemical Society* **2011**, 22 (3), 385-421.
4. Brunmark, A., Redox and addition chemistry of quinoid compounds and its biological implications. *Free radical biology & medicine* 7 (4), 435-477.
5. Pedroza, D. A.; De Leon, F.; Varela-Ramirez, A.; Lema, C.; Aguilera, R. J.; Mito, S., The cytotoxic effect of 2-acylated-1,4-naphthohydroquinones on leukemia/lymphoma cells. *Bioorg Med Chem* **2014**, 22 (2), 842-7.
6. Monks, T. J.; Hanzlik, R. P.; Cohen, G. M.; Ross, D.; Graham, D. G., Quinone chemistry and toxicity. *Toxicology and applied pharmacology* **1992**, 112 (1), 2-16.
7. Roth, H. D., The beginnings of organic photochemistry. *Angewandte Chemie International Edition in English* **1989**, 28 (9), 1193-1207.
8. Klán, P.; Wirz, J., *Photochemistry of organic compounds: from concepts to practice*. John Wiley & Sons: Chichester, 2009; p 5.
9. Rohatgi-Mukherjee, K., *Fundamentals of photochemistry*. New Age International: 1978.
10. Braslavsky, S. E., Glossary of terms used in photochemistry, (IUPAC Recommendations 2006). *Pure and Applied Chemistry* **2007**, 79 (3), 293-465.
11. Albini, A., *Photochemistry*. Springer: Brln, 2016; p 18.
12. Braun, A. M.; Maurette, M.-T.; Oliveros, E., *Photochemical technology*. John Wiley & Son Ltd: Baffins Ln, 1991; p 28, 107.
13. Coyle, J. D., *Introduction to organic photochemistry*. John Wiley & Sons: Britain, 1986; p 2-37.
14. Braun, A. M.; Maurette, M.-T.; Oliveros, E., *Photochemical technology*. John Wiley & Son Ltd: 1991.
15. Pandey, G., Photoinduced electron transfer (PET) in organic synthesis. In *Photoinduced Electron Transfer V*, Mattay, J., Ed. Springer Berlin, Heidelberg, 1993; Vol. 168, pp 175-221.

16. Mukherjee, T., Photo and radiation chemistry of quinones. *Pins* **2000**, *66* (2), 239-265.
17. Patai, S.; Rappaport, Z., *The chemistry of the quinonoid compounds*. Wiley New York: 1974; Vol. 3.
18. Umadevi, M.; Ramasubbu, A.; Vanelle, P.; Ramakrishnan, V., Spectral investigations on 2-methyl-1, 4-naphthoquinone: solvent effects, host–guest interactions and SERS. *Journal of Raman Spectroscopy* **2003**, *34* (2), 112-120.
19. Görner, H., Photoreactions of 1, 4-Naphthoquinones: Effects of Substituents and Water on the Intermediates and Reactivity¶. *Photochemistry and photobiology* **2005**, *81* (2), 376-383.
20. Fisher, G. J.; Land, E. J., Photosensitization of pyrimidines by 2-methylnaphthoquinone in water: a laser flash photolysis study. *Photochemistry and photobiology* **1983**, *37* (1), 27-32.
21. Horspool, W. M.; Song, P. S., *CRC Handbook of Organic Photochemistry and Photobiology*. CRC-Press: Boca Raton, 1995.
22. Schiel, C.; Oelgemöller, M.; Ortner, J.; Mattay, J., Green photochemistry: the solar-chemical 'Photo–Friedel–Crafts acylation' of quinones. *Green Chemistry* **2001**, *3* (5), 224-228.
23. Pacut, R.; Grimm, M. L.; Kraus, G. A.; Tanko, J. M., Photochemistry in supercritical carbon dioxide. The benzophenone-mediated addition of aldehydes to unsaturated carbonyl compounds. *Tetrahedron Letters* **2001**, *42*, 1415–1418.
24. Griesbeck, A. G.; Oelgemöller, M.; Ghetti, F., *CRC Handbook of Organic Photochemistry and Photobiology*. CRC Press: 2012; Vol. 1.
25. Esser, P.; Pohlmann, B.; Scharf, H. D., The photochemical synthesis of fine chemicals with sunlight. *Angewandte Chemie International Edition in English* **1994**, *33* (20), 2009-2023.
26. Schönberg, A.; Moubacher, R., 306. Photo-reactions. Part IV. Photo-reaction between phenanthraquinone and aromatic aldehydes. A new passage from phenanthraquinone to fluorenone. *Journal of the Chemical Society (Resumed)* **1939**, 1430-1432.
27. Moore, R.; Waters, W. A., 48. The photochemical addition of benzaldehyde to quinones. *Journal of the Chemical Society (Resumed)* **1953**, 238-240.
28. Murphy, B.; Goodrich, P.; Hardacre, C.; Oelgemöller, M., Green photochemistry: photo-Friedel–Crafts acylations of 1,4-naphthoquinone in room temperature ionic liquids. *Green Chemistry* **2009**, *11* (11), 1867.
29. Oelgemöller, M.; Mattay, J., The "Photochemical Friedel-Crafts Acylation" of Quinones: From the Beginnings of Organic Photochemistry to Modern Solar Chemical Applications. In *Handbook of Organic Photochemistry and Photobiology*, Third ed.; Griesbeck, A.; Oelgemöller, M.; Ghetti, F., Eds. CRC Press: Boca Raton, 2012; Vol. 2, p 10.

30. Bruce, J. M., Light-induced reactions of quinones. *Quarterly Reviews, Chemical Society* **1967**, *21* (3), 405-428.
31. Maruyama, K.; Osuka, A., Recent advances in the photochemistry of quinones. In *The Chemistry of Quinonoid Compounds*, Patai, S.; Rappoport, Z., Eds. John Wiley & Sons: New York, 1988; Vol. 2, p 759.
32. Maruyama, K.; Otsuki, T.; Naruta, Y., Photochemical reaction of 9, 10-phenanthrenequinone with hydrogen donors. Behavior of radicals in solution as studied by CIDNP. *Bulletin of the Chemical Society of Japan* **1976**, *49* (3), 791-795.
33. Maruyama, K.; Sakurai, H.; Otsuki, T., The addition reaction of acyl radicals to 9, 10-phenanthrenequinone in the presence of the corresponding aldehydes. A support for the in-cage mechanism of the photochemical reaction of 9, 10-phenanthrenequinone with aldehydes. *Bulletin of the Chemical Society of Japan* **1977**, *50* (10), 2777-2779.
34. Kraus, G. A.; Kirihara, M., Quinone photochemistry. A general synthesis of acylhydroquinones. *The Journal of Organic Chemistry* **1992**, *57* (11), 3256-3257.
35. Michael Oelgemöller, C. S., Roland Fröhlich, and Jochen Mattay, The “Photo-Friedel–Crafts Acylation” of 1,4-Naphthoquinones. *Eur. J. Org. Chem* **2002**, 2465–2474.
36. Murphy, B. The photo-Friedel-Crafts acylation of naphthoquinone in alternative “green” media and the photochemical generation of novel biaryl trifluoro phthalonitriles, their condensation to phthalocyanines and evaluation as singlet oxygen sensitizers. Dublin City University, Dublin 2012.
37. Kraus, G. A.; Liu, P., Benzophenone-Mediated Conjugate Additions of Aromatic Aldehydes to Quinones. *Tetrahedron Letters* **1994**, *35* (42), 7723-7726.
38. Friedrichs, F.; Murphy, B.; Nayrat, D.; Ahner, T.; Funke, M.; Ryan, M.; Lex, J.; Mattay, J.; Oelgemöller, M., An Improved Procedure for the Photoacylation of 1,4-Naphthoquinone with Aliphatic Aldehydes. *Synlett* **2008**, (20), 3137-3140.
39. Benites, J.; Rios, D.; Díaz, P.; Valderrama, J. A., The solar-chemical photo-Friedel–Crafts heteroacylation of 1,4-quinones. *Tetrahedron Letters* **2011**, *52* (5), 609-611.
40. Mitchell, L. J.; Lewis, W.; Moody, C. J., Solar photochemistry: optimisation of the photo Friedel–Crafts acylation of naphthoquinones. *Green Chemistry* **2013**, *15* (10), 2830.
41. Musiol, R.; Jampilek, J.; Nycz, J. E.; Pesko, M.; Carroll, J.; Kralova, K.; Vejsova, M.; O'Mahony, J.; Coffey, A.; Mrozek, A., Investigating the activity spectrum for ring-substituted 8-hydroxyquinolines. *Molecules* **2010**, *15* (1), 288-304.
42. Waske, P. A. Radical cation cyclization of cyclopropyl silyl ethers induced by PET: synthetic applications for the construction of polycyclic compounds, and Photoacylation of

- 1, 4-naphthoquinones: a concise access to the biologically active quinonoid compounds. University of Bielefeld, Bielefeld, 2006.
43. Waske, P. A. Radical Cation Cyclization of Cyclopropyl Silyl Ethers Induced by PET Synthetic Applications for the Construction of Polycyclic Compounds and Photoacylation of 1,4-Naphthoquinones A Concise Access to the Biologically Active Quinonoid Compounds. University of Bielefeld, 2006.
44. Julio, B.; Michael, C.; Luis, M.; Cynthia, e.; David, R.; Jorge, A.; Jaime a, V., Green Synthetic approaches to furoylnaphthohydroquinone and juglone. *Journal of the Chilean Chemical Society* **2014**, 59 (2), 2455-2457.
45. De Leon, F.; Kalagara, S.; Navarro, A. A.; Mito, S., Synthesis of 6-acyl-5,8-quinolinediols by photo-Friedel–Crafts acylation using sunlight. *Tetrahedron Letters* **2013**, 54 (24), 3147-3149.
46. Paola Arenas, A. P., David Ríos, Julio Benites, Giulio G. Muccioli, Pedro Buc Calderon, and Jaime A. Valderrama, Eco-friendly synthesis and antiproliferative evaluation of some oxygen substituted diaryl ketones. *Molecules* **2013**, 18 (8), 9818-9832.
47. Nielsen, L. B.; Wege, D., The enantioselective synthesis of elecanacin through an intramolecular naphthoquinone-vinyl ether photochemical cycloaddition. *Organic & biomolecular chemistry* **2006**, 4 (5), 868-876.
48. Chen, X.; Huang, C.; Zhang, W.; Wu, Y.; Chen, X.; Zhang, C.-y.; Zhang, Y., A universal activator of microRNAs identified from photoreaction products. *Chemical communications* **2012**, 48 (51), 6432-6434.
49. Kravina, A. G.; Carreira, E. M., Total Synthesis of Epicolactone. *Angewandte Chemie International Edition* **2018**, 57 (40), 13159-13162.
50. Schoenberg, A.; Mustafa, A., Reactions of ethylenes with 1,2-Diketones in sunlight. *Nature* **1944**, 12, 195.
51. Schönberg, A.; Mustafa, A., Photochemical reactions. Part VIII. Reaction of ethylenes with phenanthraquinone. *Journal of the Chemical Society* **1944**, 387-387.
52. Creed, D., 1,4-Quinone cycloaddition reactions with alkene, alkynes and related compounds. In *CRC Handbook of Organic Photochemistry and Photobiology*, 1st ed.; Horspool, W. M.; Song, P.-s., Eds. CRC Press: Boca Raton, 1995; p 280.
53. Bunce, N. J.; Hadley, M., On the Mechanism of Oxetan Formation in the Photocycloaddition of p-Benzoquinone to Alkenes. *Canadian Journal of Chemistry* **1975**, 53 (21), 3240-3246.
54. Wilson, R. M.; Wunderly, S. W.; Walsh, T. F.; Musser, A. K.; Outcalt, R.; Geiser, F.; Gee, S. K.; Brabender, W.; Yerino Jr, L., Laser photochemistry: Trapping of quinone-olefin

- preoxetane intermediates with molecular oxygen and chemistry of the resulting 1, 2, 4-trioxanes. *Journal of the American Chemical Society* **1982**, *104* (16), 4429-4446.
55. Schnapp, K. A.; Wilson, R. M.; Ho, D. M.; Caldwell, R. A.; Creed, D., Benzoquinone-olefin exciplexes: the observation and chemistry of the p-benzoquinone-tetraphenylallene exciplex. *Journal of the American Chemical Society* **1990**, *112* (9), 3700-3702.
56. Goetz, M.; Frisch, I., Photocycloadditions of quinones with quadricyclane and norbornadiene. A mechanistic study. *Journal of the American Chemical Society* **1995**, *117* (42), 10486-10502.
57. Maruyama, K.; Imahori, H., Photoreactions of halogeno-1, 4-naphthoquinones with electron-rich alkenes. *Journal of the Chemical Society, Perkin Transactions 2* **1990**, (2), 257-265.
58. Takahashi, Y.; Endoh, F.; Ohaku, H.; Wakamatsu, K.; Miyashi, T., Triplet-state electron-transfer reactions of phenylcyclopropane with quinones. *Journal of the Chemical Society, Chemical Communications* **1994**, (9), 1127-1128.
59. Eckert, G.; Goetz, M., Photoinduced electron-transfer reactions of aryl olefins. 1. Investigation of the Paterno-Buechi reaction between quinones and anetholes in polar solvents. *Journal of the American Chemical Society* **1994**, *116* (26), 11999-12009.
60. Bunce, N. J.; Ridley, J. E.; Zerner, M. C., On the excited states of p-quinones and an interpretation of the photocycloaddition of p-quinones to alkenes. *Theoretica chimica acta* **1977**, *45* (4), 283-300.
61. Griesbeck, A. G., *Handbook of Synthetic Photochemistry*. Edited by Angelo Albini and Maurizio Fagnoni. 2010; Vol. 49, p 5033-5033.
62. Gilbert, A., 1, 4-Quinone Cycloaddition Reactions with Alkenes, Alkynes, and Related Compounds. In *CRC Handbook of Organic Photochemistry and Photobiology*, 2nd ed.; Horspool, W.; Lenci, F., Eds. CRC press: Boca Raton, 2004; Vol. 35, pp 1-16.
63. Krauch, C. H.; Farid, S., Competition between cyclobutane and oxetane formation in the photoaddition of 1,4-Naphthoquinone to benzocyclic olefins. *Tetrahedron Letters* **1966**, *7* (39), 4783-4788.
64. Barltrop, J.; Hesp, B., Organic photochemistry. Part V. The illumination of some quinones in the presence of conjugated dienes and other olefinic systems. *Journal of the Chemical Society* **1967**, 1625-1635.
65. Maruyama, K.; Otsuki, T.; Takuwa, A.; Kako, S., Photochemical Reaction of 1, 4-Naphthoquinone with Olefins. *Bulletin of the Institute for Chemical Research, Kyoto University* **1972**, *50* (4), 344-347.

-
66. Maruyama, K.; Otsuki, T.; Naruta, Y., photocycloaddition of 1,4-naphthoquinone with 2-norbornene-a novel type of photocycloaddition. *Chemistry Letters* **1973**, 2 (7), 641-644.
67. Maruyama, K.; Naruta, Y.; Otsuki, T., Photo-addition Reaction of 1, 4-Naphthoquinone with Olefins. Formation of 2: 1 Addition Compounds. *Bulletin of the Chemical Society of Japan* **1975**, 48 (5), 1553-1558.
68. Bryce-Smith, D.; Evans, E. H.; Gilbert, A.; McNeill, H. S., Photoaddition of ethenes to 1, 4-naphthoquinone: factors influencing the site of reaction. *Journal of the Chemical Society, Perkin Transactions 1* **1992**, (4), 485-489.
69. Christl, M.; Braun, M., [2+ 2] Photocycloadditions of Homobenzvalene. *Liebigs Annalen* **1997**, (6), 1135-1141.
70. Kim, S. S.; Lim, S. J.; Lee, J. M.; Shim, S. C., Photochemical Formation of 1, 5-Diketones from Dibenzoylmethane and Some Quinones. *Bulletin of the Korean Chemical Society* **1999**, 20 (5), 531-534.
71. Liu, H.-J.; Chan, W. H., Photocycloaddition of 2-methyl-1, 4-naphthoquinone to enol esters. A photochemical approach to benzofuran derivatives. *Canadian Journal of Chemistry* **1980**, 58 (20), 2196-2198.
72. Maruyama, K.; Narita, N., Photocycloaddition Reaction of Alkyl-substituted 1, 4-Naphthoquinones with Olefins. Substituent Effects on Controlling the Orientation of Cycloaddition Reaction. *Bulletin of the Chemical Society of Japan* **1980**, 53 (3), 757-763.
73. Maruyama, K.; Otsuki, T.; Tai, S., Photoinduced electron-transfer-initiated aromatic cyclization. *The Journal of Organic Chemistry* **1985**, 50 (1), 52-60.
74. Wang, W.; Zhang, W.-J.; Wang, L.; Quah, C. K.; Fun, H.-K.; Xu, J.-H.; Zhang, Y., Photoinduced reactions of para-quinones with bicyclopropylidene leading to diverse polycyclic compounds with spirocyclopropanes. *The Journal of organic chemistry* **2013**, 78 (12), 6211-6222.
75. Maruyama, K.; Otsuki, T., A Novel Photocycloaddition Reaction Of 2-Alkoxy-1,4-naphthoquinones With olefinns. *Chemistry Letters* **1974**, 3 (2), 129-130.
76. Otsuki, T., The Photochemical Reaction of 2-Alkoxy-1, 4-naphthoquinones with Olefins. II. The Formation of Tetrahydropyran-ring Compounds. *Bulletin of the Chemical Society of Japan* **1974**, 47 (12), 3089-3093.
77. Otsuki, T., The Photochemical Reaction of 2-Alkoxy-1, 4-naphthoquinones with Olefins. III. The Re-examination of the Structures of the Photo-addition Compounds and the Reaction Mechanism. *Bulletin of the Chemical Society of Japan* **1976**, 49 (9), 2596-2605.

78. Cleridou, S.; Covell, C.; Gadhia, A.; Gilbert, A.; Kamonnawin, P., Photocycloaddition of arylenes to 2-substituted-1, 4-naphthoquinones and reactions of the cyclobutane adduct isomers. *Journal of the Chemical Society, Perkin Transactions 1* **2000**, (7), 1149-1155.
79. Kraus, G. A.; Shi, J.; Reynolds, D., A Reinvestigation of the Photochemistry of 2-Alkoxy-1, 4-naphthoquinones. *Synthetic Communications* **1990**, 20 (12), 1837-1841.
80. Senboku, H.; Kajizuka, Y.; Kobayashi, K.; Tokuda, M.; Sugimoto, H., Photoinduced molecular transformations. Part 160. Furan annelation of 2-hydroxynaphthoquinone involving photochemical addition and radical fragmentation: exclusion of the intermediacy of [2+ 2] cycloadduct in a one-pot formation of furanoquinones by the regioselective 3+ 2 photoaddition of hydroxyquinones with alkenes. *Heterocycles* **1997**, 1 (44), 341-348.
81. Covell, C.; Gilbert, A.; Richter, C., Sunlight-induced Regio-and Stereo-specific ($2\pi + 2\pi$) Cycloaddition of Arylenes to 2-Substituted-1, 4-naphthoquinones. *Journal of Chemical Research, Synopses* **1998**, (6), 316-317.
82. Clark, N. G., The fungicidal activity of substituted 1, 4-naphthoquinones. Part II: Alkoxy, phenoxy and acyloxy derivatives. *Pesticide science* **1984**, 15 (3), 235-240.
83. Friedrichs, F.; Murphy, B.; Nayrat, D.; Ahner, T.; Funke, M.; Ryan, M.; Lex, J.; Mattay, J.; Oelgemöller, M., An improved procedure for the photoacylation of 1, 4-Naphthoquinone with aliphatic aldehydes. *Synlett* **2008**, 2008 (20), 3137-3140.
84. Leshina, T.; Polyakov, N., The mechanism of photoreduction of quinones by alcohols from proton CIDNP data in high and low magnetic fields. *Journal of Physical Chemistry* **1990**, 94 (11), 4379-4382.
85. Griesbeck, A. G.; Mattay, J., *Photochemical Key Steps in Organic Synthesis: An Experimental Course Book*. VCH: Weinheim, 1994; p 5-10.
86. Schenck, G., Photosensitization. *Industrial & Engineering Chemistry* **1963**, 55 (6), 40-43.
87. Murphy, B. The photo-Friedel-Crafts acylation of naphthoquinone in alternative “Green” Media. Dublin City University, Dublin, 2012.
88. Mitchell, L. J.; Lewis, W.; Moody, C. J., Solar photochemistry: optimisation of the photo Friedel–Crafts acylation of naphthoquinones. *Green Chemistry* **2013**, 15 (10), 2830-2842.
89. Kraus, G. A.; Liu, P., Benzophenone-mediated conjugate additions of aromatic aldehydes to quinones. *Tetrahedron letters* **1994**, 35 (42), 7723-7726.
90. Webb, D.; Jamison, T. F., Continuous flow multi-step organic synthesis. *Chemical Science* **2010**, 1 (6), 675-680.

91. Hase, J.; Nishimura, T., Antibacterial properties of naphthoquinones. I. Syntheses and antibacterial properties of acynaphthoquinones. . *Journal of the Pharmaceutical Society of Japan* **1955**, 75 (2), 203-207.
92. Lamoureux, G.; Perez, A. L.; Araya, M.; Agüero, C., Reactivity and structure of derivatives of 2-hydroxy-1, 4-naphthoquinone (lawsone). *Journal of Physical Organic Chemistry* **2008**, 21 (12), 1022-1028.
93. Hazra, B.; Acharya, S.; Ghosh, R.; Patra, A.; Banerjee, A., Vanadium (V) in perchloric acid: A novel use of the reagent for dimerisation of some naphthalene derivatives. *Synthetic communications* **1999**, 29 (9), 1571-1576.
94. Maruyama, K.; Otsuki, T.; Takuwa, A.; Kako, S., Photochemical reaction of 1, 4-Naphthoquinone with olefins *Bulletin of the Institute for chemical Research, Kyoto university* **1972**, 50 (4), 344-347.
95. Harbour, J. R.; Tollin, G., ESR studies of solvent radicals formed upon photoreduction of quinones in alcohols. *Photochemistry and Photobiology* **1974**, 20 (4), 387-391.
96. Bryce-Smith, D.; Evans, E. H.; Gilbert, A.; McNeill, H. S., Photoaddition of ethenes to 1,4-naphthoquinone: factors influencing the site of reaction. *Journal of the Chemical Society, Perkin Transactions 1* **1992**, (4), 485-489.
97. Dragojlovic, V., Conformational analysis of cycloalkanes. *ChemTexts* **2015**, 1 (3), 14.
98. Cotton, F. A.; Frenz, B. A., Conformations of cyclobutane. *Tetrahedron* **1974**, 30 (12), 1587-1594.
99. Moore, W. M.; Morgan, D. D.; Stermitz, F. R., The photochemical conversion of stilbene to phenanthrene. The nature of the intermediate. *Journal of the American Chemical Society* **1963**, 85 (6), 829-830.
100. Sun, D.; Hubig, S. M.; Kochi, J. K., Oxetanes from [2+ 2] cycloaddition of stilbenes to quinone via photoinduced electron transfer. *The Journal of Organic Chemistry* **1999**, 64 (7), 2250-2258.
101. Pedroza, D. A.; De Leon, F.; Varela-Ramirez, A.; Lema, C.; Aguilera, R. J.; Mito, S., The cytotoxic effect of 2-acylated-1, 4-naphthohydroquinones on leukemia/lymphoma cells. *Bioorganic & medicinal chemistry* **2014**, 22 (2), 842-847.
102. Murphy, B.; Goodrich, P.; Hardacre, C.; Oelgemöller, M., Green photochemistry: Photo-Friedel–Crafts acylations of 1, 4-naphthoquinone in room temperature ionic liquids. *Green Chemistry* **2009**, 11 (11), 1867-1870.

103. Pacut, R.; Grimm, M. L.; Kraus, G. A.; Tanko, J. M., Photochemistry in supercritical carbon dioxide. The benzophenone-mediated addition of aldehydes to α , β -unsaturated carbonyl compounds. *Tetrahedron Letters* **2001**, 42 (8), 1415-1418.
104. Görner, H., Photoprocesses of p-naphthoquinones and vitamin K 1: effects of alcohols and amines on the reactivity in solution. *Photochemical & Photobiological Sciences* **2004**, 3 (1), 71-78.
105. Lymar, S. V.; Schwarz, H. A., Hydrogen atom reactivity toward aqueous tert-butyl alcohol. *The Journal of Physical Chemistry A* **2012**, 116 (5), 1383-1389.
106. Borkman, R. F.; Kearns, D. R., Electronic-relaxation processes in acetone. *The Journal of Chemical Physics* **1966**, 44 (3), 945-949.
107. Montalti, M.; Credi, A.; Prodi, L.; Gandolfi, M. T., *Handbook of photochemistry*. Third ed.; CRC press: Boca Raton, 2006.
108. Choudhry, G. G.; Roof, A. A. M.; Hutzinger, O., Mechanisms in sensitized photochemistry of environmental chemicals. *Toxicological & Environmental Chemistry Reviews* **1979**, 2 (4), 259-302.
109. Maruyama, K.; Miyagi, Y., Photo-induced condensation reaction of p-quinones with aldehydes. *Bulletin of the Chemical Society of Japan* **1974**, 47 (5), 1303-1304.
110. Lamola, A. A.; Sharp, L. J., Environmental effects on the excited states of o-hydroxy aromatic carbonyl compounds. *The Journal of Physical Chemistry* **1966**, 70 (8), 2634-2638.
111. Elliot, A. J.; Wan, J. K., A CIDEP study of the photoreduction of quinones in the presence of phenols and 2-propanol. *The Journal of Physical Chemistry* **1978**, 82 (4), 444-452.
112. Rennert, J.; Ginsburg, P., Sensitization and quenching of naphthoquinone photoreduction. *Journal of Photochemistry* **1975**, 4 (3), 171-178.
113. Rennert, J.; Japar, S.; Guttman, M., Photo-dimerization and photo-reduction of alpha-naphthoquinone in different solvent media. *Photochemistry and Photobiology* **1967**, 6 (7), 485-490.
114. Schiel, C.; Oelgemöller, M.; Ortner, J.; Mattay, J., Green photochemistry: the solar-chemical 'Photo-Friedel-Crafts acylation' of quinones. *Green chemistry* **2001**, 3 (5), 224-228.
115. Henderson, R. K.; Jiménez-González, C.; Constable, D. J.; Alston, S. R.; Inglis, G. G.; Fisher, G.; Sherwood, J.; Binks, S. P.; Curzons, A. D., Expanding GSK's solvent selection guide—embedding sustainability into solvent selection starting at medicinal chemistry. *Green Chemistry* **2011**, 13 (4), 854-862.
116. Horspool, W.; Lenci, F., The "Photochemical Friedel-Crafts Acylation" of Quinones: From the Beginnings of Organic Photochemistry to Modern Solar Chemical Applications. In *CRC*

- hand book of organic Photochemistry and Photobiology*, 2nd ed.; Oelgemöller, M.; Mattay, J., Eds. CRC Press:: Boca Raton, 2004; p 88.
117. Bruce, J. M., Photochemistry of quinones. In *The Chemistry of the Quinonoid Compounds*, Patai, S., Ed. John Wiley & Sons: Bristol, 1974; Vol. 1, pp 465-538.
118. Mukherjee, T., Photo and radiation chemistry of quinones. *Proceedings-Indian National Science Academy Part A* **2000**, 66 (2), 239-266.
119. Fabian, J., Zur Natur des 1, 4-Naphthochinonchromophors. *Zeitschrift für Chemie* **1980**, 20 (8), 299-300.
120. Oelgemöller, M.; Schiel, C.; Fröhlich, R.; Mattay, J., The photo-Friedel– Crafts acylation of 1, 4-naphthoquinones. *European Journal of Organic Chemistry* **2002**, 2002 (15), 2465-2474.
121. Martin, R., Uses of the Fries rearrangement for the preparation of hydroxyarylktones. A review. *Organic preparations and procedures international* **1992**, 24 (4), 369-435.
122. Coyle, E. E.; Oelgemöller, M., Micro-photochemistry: photochemistry in microstructured reactors. The new photochemistry of the future? *Photochemical & Photobiological Sciences* **2008**, 7 (11), 1313-1322.
123. Sugimoto, A.; Fukuyama, T.; Sumino, Y.; Takagi, M.; Ryu, I., Microflow photo-radical reaction using a compact light source: application to the Barton reaction leading to a key intermediate for myriceric acid A. *Tetrahedron* **2009**, 65 (8), 1593-1598.
124. Mumtaz, S. Photochemical Synthesis in Batch and Micro Flow Reactors. James cook, Townsville, 2016.
125. Glaser, J. A., Multistep organic synthesis using flow chemistry. *Clean Technologies and Environmental Policy* **2013**, 15 (2), 205-211.
126. McQuade, D. T.; Seeberger, P. H., Applying flow chemistry: methods, materials, and multistep synthesis. *The Journal of organic chemistry* **2013**, 78 (13), 6384-6389.
127. Fuse, S.; Mifune, Y.; Tanabe, N.; Takahashi, T., Continuous-flow synthesis of activated vitamin D 3 and its analogues. *Organic & biomolecular chemistry* **2012**, 10 (27), 5205-5211.
128. Pinho, V. D.; Gutmann, B.; Kappe, C. O., Continuous flow synthesis of β -amino acids from α -amino acids via Arndt–Eistert homologation. *RSC Advances* **2014**, 4 (70), 37419-37422.
129. Otake, Y.; Nakamura, H.; Fuse, S., Recent advances in the integrated micro-flow synthesis containing photochemical reactions. *Tetrahedron letters* **2018**, 59 (18), 1691-1697.
130. Thomson, R., Naturally Occurring Quinones IV, Recent Advances, 4th. Chapman & Hall: London, 1997.

- 131.Dhar, S.; Mattu, S., Anti-implantation activity of 2 derivatives of o-hydroxy naphthaquinones in rats. *Zhongguo yao li xue bao= Acta pharmacologica Sinica* **1995**, *16* (5), 471-472.
- 132.Khadtare, S. S.; Ware, A. P.; Salunke-Gawali, S.; Jadkar, S. R.; Pingale, S. S.; Pathan, H. M., Dye sensitized solar cell with lawsone dye using a ZnO photoanode: experimental and TD-DFT study. *RSC Advances* **2015**, *5* (23), 17647-17652.
- 133.Singh, I.; Ogata, R.; Moore, R.; Chang, C.; Scheuer, P., Electronic spectra of substituted naphthoquinones. *Tetrahedron* **1968**, *24* (18), 6053-6073.
- 134.Palit, D. K.; Pal, H.; Mukherjee, T.; Mittal, J. P., Photodynamics of the S1 state of some hydroxy-and amino-substituted naphthoquinones and anthraquinones. *Journal of the Chemical Society, Faraday Transactions* **1990**, *86* (23), 3861-3869.
- 135.Idriss, K.; Sedaira, H.; Hashem, E.; Saleh, M.; Soliman, S., The visible absorbance maximum of 2-hydroxy-1, 4-naphthoquinone as a novel probe for the hydrogen bond donor abilities of solvents and solvent mixtures. *Monatshefte für Chemie/Chemical Monthly* **1996**, *127* (1), 29-42.
- 136.Padhye, S.; Kulkarni, B., Hydrogen bonding interaction of some naturally occurring isomeric juglones with dioxane. *The Journal of Physical Chemistry* **1975**, *79* (9), 927-928.
- 137.Fieser, L. F., The tautomerism of hydroxy quinones. *Journal of the American Chemical Society* **1928**, *50* (2), 439-465.
- 138.Rostkowska, H.; Nowak, M. J.; Lapinski, L.; Adamowicz, L., Molecular structure and infrared spectra of 2-hydroxy-1, 4-naphthoquinone; experimental matrix isolation and theoretical Hartree–Fock and post Hartree–Fock study. *Spectrochimica Acta Part A: Molecular and Biomolecular Spectroscopy* **1998**, *54* (8), 1091-1103.
- 139.Hashimoto, S.; Takaka, Y., The Photochemical Reaction of 2-hydroxy-1,4-naphthoquinone and 2-methoxy-1,4-naphthoquinone in water. *Engineering Review of Doshisha University* **1979**, *20* (1).
- 140.Hooker, S. C., The Action of Light on β -Hydroxy- α -naphthoquinone1, 2. *Journal of the American Chemical Society* **1936**, *58* (7), 1212-1216.
- 141.Chandrasenan, K.; Thomson, R., Biquinones—III: The dimerisation of 1, 4-naphthaquinones. *Tetrahedron* **1971**, *27* (12), 2529-2539.
- 142.Suginome, H.; Konishi, A.; Sakurai, H.; Minakawa, H.; Takeda, T.; Senboku, H.; Tokuda, M.; Kobayashi, K., Photoinduced molecular transformations. Part 156. New photoadditions of 2-hydroxy-1, 4-naphthoquinones with naphthols and their derivatives. *Tetrahedron* **1995**, *51* (5), 1377-1386.

143. Kobayashi, K.; Shimizu, H.; Sasaki, A.; Suginome, H., Photoinduced molecular transformations. 140. New one-step general synthesis of naphtho [2, 3-b] furan-4, 9-diones and their 2, 3-dihydro derivatives by the regioselective [3+ 2] photoaddition of 2-hydroxy-1, 4-naphthoquinones with various alkynes and alkenes: Application of the photoaddition to a two-step synthesis of maturinone. *The Journal of Organic Chemistry* **1993**, 58 (17), 4614-4618.
144. Sharma, G.; Vasanth Kumar, S.; Wahab, H. A., Molecular docking, synthesis, and biological evaluation of naphthoquinone as potential novel scaffold for H5N1 neuraminidase inhibition. *Journal of Biomolecular Structure and Dynamics* **2018**, 36 (1), 233-242.
145. Pearson, M. S.; Jensky, B. J.; Greer, F. X.; Hagstrom, J. P.; Wells, N. M., Substituent effects in the keto-enol tautomerism of fused 1, 4-naphthalenediols. *The Journal of Organic Chemistry* **1978**, 43 (24), 4617-4622.
146. Couladouros, E. A.; Plyta, Z. F.; Papageorgiou, V. P., A general procedure for the efficient synthesis of (alkylamino) naphthoquinones. *The Journal of organic chemistry* **1996**, 61 (9), 3031-3033.
147. Oelgemoller, M., Solar photochemical synthesis: from the beginnings of organic photochemistry to the solar manufacturing of commodity chemicals. *Chemical reviews* **2016**, 116 (17), 9664-9682.
148. Protti, S.; Fagnoni, M., The sunny side of chemistry: green synthesis by solar light. *Photochemical & Photobiological Sciences* **2009**, 8 (11), 1499-1516.
149. Shvydkiv, O.; Gallagher, S.; Nolan, K.; Oelgemöller, M., From conventional to microphotochemistry: Photodecarboxylation reactions involving phthalimides. *Organic letters* **2010**, 12 (22), 5170-5173.
150. Fernández-García, A.; Zarza, E.; Valenzuela, L.; Pérez, M., Parabolic-trough solar collectors and their applications. *Renewable and Sustainable Energy Reviews* **2010**, 14 (7), 1695-1721.
151. Bryce-Smith, D.; Evans, E. H.; Gilbert, A.; McNeill, H. S., Factors influencing the regiochemistry of spiro-oxetane formation from the photocycloaddition of ethenes to 1, 4-benzoquinone. *Journal of the Chemical Society, Perkin Transactions 2* **1991**, (10), 1587-1593.
152. Barltrop, J. A.; Hesp, B., Organic photochemistry. Part V. The illumination of some quinones in the presence of conjugated dienes and other olefinic systems. *Journal of the Chemical Society* **1967**, 1625-1635.

153. Crimmins, M. T.; Reinhold, T. L., Enone Olefin [2+2] Photochemistry cycloaddition. In *Organic Reactions*, Paquette, L. A., Ed. John Wiley & Sons, Inc.: New York, 1993; Vol. 44, pp 298-579.
154. Glass, D. C.; Gray, C. N.; Jolley, D. J.; Gibbons, C.; Sim, M. R.; Fritschi, L.; Adams, G. G.; Bisby, J. A.; Manuell, R., Leukemia risk associated with low-level benzene exposure. *Epidemiology* **2003**, *14* (5), 569-577.
155. Mattay, J.; Griesbeck, A., *Photochemical Key Steps in Organic Synthesis*. VCH: Weinheim, 1994.
156. Albini, A.; Fagnoni, M., *Handbook of synthetic photochemistry*. Wiley-VCH: Weinheim, 2010; p 7,181.
157. Cucarull-González, J.; Hernando, J.; Alibés, R.; Figueredo, M.; Font, J.; Rodríguez-Santiago, L.; Sodupe, M., [2+ 2] Photocycloaddition of 2 (5 H)-Furanone to Unsaturated Compounds. Insights from First Principles Calculations and Transient-Absorption Measurements. *The Journal of organic chemistry* **2010**, *75* (13), 4392-4401.
158. Vargas, F.; Rivas, C.; Fuentes, A.; Carbonell, K.; Rodríguez, R., Photosensitized (2+ 2) cycloadditions of 2, 3-dimethylmaleic anhydride to 3, 4-dimethyl-1-phenylphosphole. *Journal of Photochemistry and Photobiology A: Chemistry* **2004**, *162* (1), 63-66.
159. Wexler, A. J.; Balchunis, R. J.; Swenton, J. S., Product studies of the photocycloaddition reactions of 5-chloro-and 5-fluorouracil derivatives and olefins. An interesting and useful effect of fluorine on regioselectivity. *The Journal of Organic Chemistry* **1984**, *49* (15), 2733-2738.
160. Bruce, J. M., Photochemistry of quinones In *The chemistry of quinonoid compounds*, Patai, S., Ed. Wiley: New York, 1974; Vol. 1, pp 469-537.
161. Gilbert, A., 1, 4-Quinone Cycloaddition Reactions with Alkenes, Alkynes, and Related Compounds. In *CRC Handbook of Organic Photochemistry and Photobiology*, 2nd edn ed.; Horspool, W.; Lenci, F., Eds. CRC Press LLC: Boca Raton, 2004; pp pp. 1–16.
162. Wong, S. K., Electron transfer versus hydrogen abstraction in photoreduction of quinones. An application of chemically induced dynamic electron polarization. *Journal of the American Chemical Society* **1978**, *100* (17), 5488-5490.
163. Tedaldi, L. M.; Baker, J. R., In situ reduction in photocycloadditions: a method to prevent secondary photoreactions. *Organic letters* **2009**, *11* (4), 811-814.
164. Barltrop, J.; Hesp, B., Organic photochemistry. Part V. The illumination of some quinones in the presence of conjugated dienes and other olefinic systems. *Journal of the Chemical Society C: Organic* **1967**, 1625-1635.

165. Albin, A.; Fagnoni, M., *Handbook of Synthetic Photochemistry*. WILEY-VCH Verlag GmbH & Co. KGaA: Weinheim, 2010; Vol. 49, p 5033-5033.
166. Horspool, W. M., *Synthetic Organic Photochemistry*. 1st ed.; Plenum Press: New York, 1984.
167. Taniguchi, M.; Du, H.; Lindsey, J. S., PhotochemCAD 3: Diverse Modules for Photophysical Calculations with Multiple Spectral Databases. *Photochemistry and photobiology* **2018**, *94* (2), 277-289.
168. Matsushima, T.; Kobayashi, S.; Watanabe, S., Air-driven potassium iodide-mediated oxidative photocyclization of stilbene derivatives. *The Journal of organic chemistry* **2016**, *81* (17), 7799-7806.
169. Pappas, S.; Portnoy, N. A., Substituent effects on the photoaddition of diphenylacetylene to 1, 4-naphthoquinones. *The Journal of Organic Chemistry* **1968**, *33* (6), 2200-2203.
170. Farid, S.; Kothe, W.; Pfundt, G., Competitive photoadditions of acetylenes to the C=C and C=O bonds of p-quinones. *Tetrahedron Letters* **1968**, *9* (39), 4147-4150.
171. Pappas, S. P.; Portnoy, N. A., Substituent effects on the different modes of alkyne photoaddition to quinones. *Journal of the Chemical Society D: Chemical Communications* **1970**, (17), 1126b-1127.
172. Chen, X.; Huang, C.; Zhang, W.; Wu, Y.; Chen, X.; Zhang, C.-y.; Zhang, Y., A universal activator of micro RNAs identified from photoreaction products. *Chemical communications* **2012**, *48* (51), 6432-6434.
173. Bosch, E.; Hubig, S.; Kochi, J., Paterno–Büchi coupling of (diaryl) acetylenes and quinone via photoinduced electron transfer. *Journal of the American Chemical Society* **1998**, *120* (2), 386-395.
174. Schönberg, A.; Mustafa, A., 103. Photochemical reactions. Part VIII. Reaction of ethylenes with phenanthraquinone. *Journal of the Chemical Society* **1944**, 387-387.
175. Fulmer, G. R.; Miller, A. J.; Sherden, N. H.; Gottlieb, H. E.; Nudelman, A.; Stoltz, B. M.; Bercaw, J. E.; Goldberg, K. I., NMR chemical shifts of trace impurities: common laboratory solvents, organics, and gases in deuterated solvents relevant to the organometallic chemist. *Organometallics* **2010**, *29* (9), 2176-2179.
176. de Lima, C. G.; DuFresne, A., Ligand dimerization during complex formation—the iron (III)-2-hydroxy-1, 4-naphthoquinone system. *Inorganic and Nuclear Chemistry Letters* **1971**, *7* (9), 843-846.